



N8127619

HIGH-PRESSURE LOX/HYDROCARBON PREBURNERS AND GAS GENERATORS

1. Report No. NASA CR-161814		2. Government Accession No.		3. Recipient's Catalog No.	
4. Title and Subtitle HIGH-PRESSURE LOX/HYDROCARBON PREBURNERS AND GAS GENERATORS FINAL REPORT				5. Report Date April 1981	
				6. Performing Organization Code	
7. Author(s) A. W. Huebner				8. Performing Organization Report No. RI/RD81-129	
9. Performing Organization Name and Address Rocketdyne Division Rockwell International 6633 Canoga Avenue Canoga Park, CA 91304				10. Work Unit No.	
				11. Contract or Grant No. NAS8-33243	
12. Sponsoring Agency Name and Address National Aeronautics and Space Administration George C. Marshall Space Flight Center AL 35812				13. Type of Report and Period Covered Final (December, 1978- April, 1981)	
				14. Sponsoring Agency Code	
15. Supplementary Notes					
16. Abstract The objective of the program was to conduct a small-scale hardware test program to establish the technology base required for LOX/hydrocarbon preburners and gas generators. The program consisted of six major tasks; Task I reviewed and assessed the performance prediction models and defined a subscale test program. Task II designed and fabricated this subscale hardware. Task III tested and analyzed the data from this hardware. Task IV analyzed the hot-fire results and formulated a preliminary design for 40K preburner assemblies. Task V took the preliminary design and detailed and fabricated three 40K size preburner assemblies, one each fuel-rich LOX/CH ₄ and LOX/RP-1, and one oxidizer-rich LOX/CH ₄ . Task VI delivered these preburner assemblies to MSFC for subsequent evaluation.					
17. Key Words (Suggested by Author(s)) LOX/Methane High Chamber Pressure Preburner Injectors Performance Predictions Injector Fabrication LOX/RP-1			18. Distribution Statement		
19. Security Classif. (of this report) Unclassified		20. Security Classif. (of this page) Unclassified		21. No. of Pages 192	22. Price*

* For sale by the National Technical Information Service, Springfield, Virginia 22151



FOREWORD

This final report is submitted for the High-Pressure LOX/Hydrocarbon Preburners and Gas Generators program per the requirements of Contract NAS8-33243. This program was performed by the Rocketdyne Division of Rockwell International for the NASA-Marshall Space Flight Center (MSFC) under Contract NAS8-33243.

The objective of the program was to conduct a small-scale hardware test program to establish the technology base required for LOX/hydrocarbon preburners and gas generators, and to use this technology to determine the design characteristics required to fabricate oxidizer- and fuel-rich LOX/hydrocarbon 40K size preburners for subsequent test fire evaluation at MSFC.

The NASA/MSFC Project Manager was C. R. Bailey. The Rocketdyne Program Manager was F. M. Kirby; Project Engineer was A. W. Huebner, and Test Engineer was R. J. Metzner.

Principal Rocketdyne personnel contributing to the technical effort of the program were: I. Kaith and J. W. Heine, Design; V. W. Jaqua, Injector Technology; W. W. Wang, Stability; E. E. Fryk, Structural Analysis; and R. T. Cook, Thermal Analysis.

The period of performance for the program was December 1978 to April 1981.



CONTENTS

Introduction	1
Program Objective	2
Program Summary	2
Discussion	5
Task I: Performance Prediction	5
Subtask 01100 - Review and Assessment	5
Subtask 01200 - Define Subscale Testing	31
Task II: Small-Scale Hardware Design and Fabrication	33
Subtask 02100 - Analysis and Detail Design	33
Subtask 02200 - Fabrication	38
Task III: Small-Scale Hardware Testing	49
Subtask 03100 - Testing	49
Subtask 03200 - Data Analysis	55
Subtask 03300 - Models Modification	136
Task IV: Preburner Analysis and Preliminary Design	141
Subtask 04100 - Analysis	141
Subtask 04200 - Preliminary Design	146
Task V: Preburner Detail Design and Fabrication	155
Subtask 05100 - Detail Design	155
Subtask 05200 - Fabrication	171
Task VI: Hardware Delivery	179



ILLUSTRATIONS

1. LOX/CH ₄ Ambient Gas Theoretical Performance	6
2. LOX/CH ₄ Ambient Gas Theoretical Combustor Temperature	6
3. Theoretical Performance, LOX/RP-1	7
4. Theoretical Combustor Temperature, LOX/RP-1	8
5. Theoretical Performance, LOX/RP-1	10
6. Theoretical Combustor Temperature, LOX/RP-1	11
7. Theoretical Performance, LOX/CH ₄ amb gas	12
8. Theoretical Combustor Temperature, LOX/CH ₄ amb gas	13
9. LOX/RP-1 Partial-Combustion Products	14
10. LOX/CH ₄ Ambient Gas Partial-Combustion Products	14
11. Percent Vaporization	22
12. Percent Vaporization	23
13. Chamber Axial Temperature Profile	24
14. LOX/CH ₄ High-Pressure Preburner Vaporization Efficiency	27
15. LOX/RP-1 High-Pressure Preburner Vaporization Efficiency	28
16. LOX Median Dropsize (\bar{D}) Effect on Vaporization Efficiency	30
17. Percent Vaporization	32
18. Chamber Axial Temperature Profile	32
19. Oxidizer-Rich LOX/CH ₄ Pentad Injector	39
20. Fuel-Rich LOX/CH ₄ Triplet-Injector	41
21. Oxidizer-Rich LOX/RP-1 Like-Doublet/Showerhead	42
22. Fuel-Rich LOX/RP-1 Like-Doublet	43
23. 2-Inch Preburner Test Hardware	44
24. Slotted Carbon Deposition Insert	45
25. Combustion Gas Uniformity Measurement Segments	46
26. APTF High-Pressure LOX/Hydrocarbon Flow Diagram	50
27. LOX/Hc High-Pressure Test Position	51
28. Fuel-Rich LOX/CH ₄ Test Firing	56
29. Fuel-Rich LOX/RP-1 Test Firing	57
30. Test 004 High-Frequency Data Record	69
31. PSD Plot of Injector End P _c High-Frequency Transducer	69

32.	Frequency vs Time Plot	70
33.	Test 004 - Combustor Pressure vs Time	71
34.	PSD Plot of Test With Quarter-Wave Absorber	75
35.	PSD Plot of Test With a Helmholtz Resonator	76
36.	LOX/CH ₄ Triplet Helmholtz Absorber Degradation	77
37.	Turbine Blade Coking Fixture	78
38.	LOX/CH ₄ Chamber Temperature Profile	79
39.	Damaged Nozzle	81
40.	Theoretical Combustor Temperature LOX/CH ₄ amb gas	82
41.	Oxidizer-Rich Pentad Injector Face	83
42.	Carbon Streaks - Pentad Injector Element	84
43.	Modified Oxidizer-Rich LOX/CH ₄ Pentad Injector	85
44.	RP-1 Fuel Tank Pressure, Test 004	86
45.	Fuel-Rich LOX/RP-1 Chamber Pressure, Test 004	87
46.	RP-1 Tank Pressure, Test 005	89
47.	LOX/RP-1 Like-Doublet Injector	90
48.	High-Frequency A-C Trace, Test 005	91
49.	High-Frequency A-C Status Plot, Test 006	92
50.	Carbon Deposition Fixture	93
51.	Alternate Design Turbine Blade Simulator Used for Carbon Checking Evaluation	94
52.	High-Frequency A-C Status Plot, Test 008	96
53.	Chamber Pressure Trace, Test 008	97
54.	LOX/RP-1 Chamber Temperature Profile	99
55.	Oxidizer-Rich Combustor Failure	100
56.	Oxidizer-Rich Preburner Failure	101
57.	Chamber Pressure vs Time	103
58.	LOX Injection Pressure vs Time	104
59.	Fuel Injection Pressure vs Time	105
60.	LOX Line Pressure vs Time	106
61.	Schematic of Typical Sample Bottle System	122
62.	Theoretical Performance, LOX/RP-1	124
63.	Theoretical Combustion Temperature, LOX/RP-1	125
64.	Theoretical Performance, LOX/CH ₄ amb gas	128

65.	Theoretical Combustor Temperature, LOX/CH ₄ amb gas	129
66.	Theoretical Performance, LOX/CH ₄	134
67.	Theoretical Combustor Temperature, LOX/CH ₄	135
68.	Material Operating Conditions	142
69.	Injector Test Configuration	147
70.	Injector Face Average Temperature	152
71.	12-Inch Combustion Chamber Section	156
72.	4-Inch Combustion Chamber Section	157
73.	Propellant Manifold - Fuel/Oxidizer	158
74.	Nozzle	159
75.	Igniter Assembly	160
76.	Pressure Test Plate	161
77.	Propellant Dome - Fuel/Oxidizer	162
78.	Fuel-Rich LOX/RP-1 Triplet Injector	163
79.	Fuel-Rich LOX/CH ₄ Coaxial Injector	164
80.	Oxidizer-Rich LOX/CH ₄ Pentad Injector	165
81.	Preburner Assembly	166
82.	LOX/RP-1 Acoustic Cavity	167
83.	L-Shaped Acoustic Cavity	169
84.	Cavity Design Damping Coefficient	170
85.	Oxidizer-Rich Pentad Cold Flow	172
86.	Preburner Assembly Pressure Check	173
87.	Preburner Assembly	175
88.	Triplet Injector/Fuel Manifold Assembly	176
89.	Rear View -Triplet Injector Assembly	177



TABLES

1.	High-Pressure LOX/Hydrocarbon Injector Performance	21
2.	Selected Contract Injectors	25
3.	Injector Candidates Performance Prediction	27
4.	Injector Candidates	34
5.	Injector Operating Conditions Contract and Independent Research and Development	34
6.	LOX/Hydrocarbon High-Pressure Preburner Data Summary	58
7.	Chemical Analysis Report (Test 014-010)	111
8.	Chemical Analysis Report (Test 014-014).	112
9.	Chemical Analysis Report (Test 014-015).	113
10.	Chemical Analysis Report (Test 014-023).	114
11.	Chemical Analysis Report (Test 014-024).	115
12.	Chemical Analysis Report (Test 014-025).	116
13.	Chemical Analysis Report (Test 014-010).	117
14.	Chemical Analysis Report (Test 014-010).	118
15.	Chemical Analysis Report (Test 014-010).	119
16.	Chemical Analysis Report (Test 014-025).	120
17.	Chemical Analysis Report (Test 014-025).	121
18.	Fuel-Rich LOX/RP-1. Gas Properties and Composition, Experimental and Theoretical	126
19.	Fuel-Rich LOX/CH ₄ . Gas Properties and Composition, Experimental and Theoretical	127
20.	Summary of Model Features for LOX/RP-1 and LOX/CH ₄ Gas Generators	137
21.	Preburner Assembly - Minimum Structural Summary	144
22.	Injector Injection Parameters	148
23.	40K Preburner Injector Design Criteria	149
24.	Mass Flux Density	149
25.	Preburner Component Drawing Identification	155
26.	Flow Coefficient	171



INTRODUCTION

Recent advanced booster studies have been concentrating on LOX/hydrocarbon propellants for a wide variety of future launch vehicle applications. Engine system studies are addressing both gas generator and stage-combustion, turbine-drive power cycles. These studies require a capability of predicting turbine-drive fluid gas properties and the use of combustor design models to evaluate the various design concepts. High main chamber combustion pressures (3000 to 7000 psia) are common to these preburner/gas generator designs. During the course of these studies, it has been found that there is very little experience or technical information available pertaining to the design and operation of the preburners or gas generators at high pressures. Specifically, it was found that the information that is available for fuel-rich LOX/RP-1 from past engine programs is at low chamber pressures (approximately 1000 psia). In addition, poor agreement was found between experimental measurements of gas properties and theoretical predictions. Little or no experience was available pertaining to LOX-rich LOX/RP-1, and LOX or fuel-rich LOX/methane high-pressure turbine drive combustor operation. Therefore, it was difficult to determine the accuracy of the gas property and design/performance prediction techniques in these cases. These findings clearly showed the need for a technology program to investigate high-pressure LOX/hydrocarbon turbine-drive combustor design and operation prior to any engine development programs. This information was needed for future engine system design and application studies, before these studies could narrow down to a specific engine configuration. It is these areas of technology, and basic design information to which this program was focused.

A 28-month program to furnish a high-pressure LOX/hydrocarbon turbine-drive combustor technology base for future booster engine programs has been completed. The program began by evaluating LOX/RP-1 and LOX/methane preburner and gas generator performance and gas property prediction methods for fuel-rich and oxidizer-rich operating conditions. A small-scale hardware test program was conducted to supply the information necessary to reduce the uncertainties in the prediction techniques to an acceptable level. The data obtained from the

testing was used to improve the existing design and performance models. Three 40K size preburners (LOX/RP-1 fuel-rich, and LOX/methane fuel- and oxidizer-rich) were designed, fabricated, and delivered to NASA/MSFC.

PROGRAM OBJECTIVE

The basic objective of the program was to furnish a high-pressure LOX/hydrocarbon preburner and gas generator technology base for future booster engine programs.

PROGRAM SUMMARY

To fulfill the program objective, establishing a technology base for LOX/hydrocarbon preburners and gas generators, the NAS8-33243 program was undertaken.

The program was divided into five major tasks, plus hardware and drawing delivery, and reporting tasks. Task I was devoted to evaluating existing preburner combustion gas and design/performance prediction techniques for their applicability to LOX/RP-1 and LOX/methane propellants operating either fuel- or oxidizer-rich at chamber pressures of 3000 to 7000 psia. The task began by evaluating the hydrocarbon propellants for preburner and gas generator performance and gas property prediction methods for fuel-rich and oxidizer-rich operating conditions. The adequacy of these techniques was evaluated and a small-scale hardware hot-fire test program was designed to provide empirical data to improve the analytical prediction methods. The results of Task I models assessment and the small-scale test plan were presented to NASA/MSFC for approval. With NASA/MSFC concurrence, the small-scale hardware injector designs were initiated.

The detailed design of the small-scale hardware was completed and fabrication of the hardware was conducted in Task II. A small-scale hardware test program was conducted in Task III along with the verification or modification of the prediction methods based on the test results. The test program has resulted in hot-fire testing of fuel-rich LOX/CH₄, oxidizer-rich LOX/CH₄, fuel-rich LOX/RP-1, and several unsuccessful attempts at oxidizer-rich LOX/RP-1 testing.

A preliminary design effort was completed in Task IV for three 40K size preburners (fuel-rich LOX/RP-1 and LOX/methane and oxidizer-rich LOX/methane). Supporting analyses were conducted in the areas of performance, stability, heat transfer, and stress to ensure a high-performing, reliable preburner capable of continued operation through a comprehensive hot-fire test program at MSFC. In support of the preliminary design effort, thrust chamber sizes were selected, coax and triplet fuel-rich injectors and an oxidizer-rich LOX/methane pentad injector were selected. These preliminary injector designs were presented for approval prior to the detailed designs of Task V. The Task V effort was devoted to the detailed design and fabrication of the selected 40K preburner assembly configurations. The fabricated fuel-rich hardware was subjected to a proof pressure test of 6300 psig to demonstrate overall engine integrity. All three fabricated injectors were H₂O flow-calibrated to establish flow characteristics.

The three 40K preburner assemblies were delivered to NASA/MSFC at the end of the program for subsequent hot-fire evaluation at MSFC.



DISCUSSION

TASK I: PERFORMANCE PREDICTION

Subtask 01100 - Review and Assessment

The program began with a review of existing Rocketdyne design models for injectors and combustors to assess the adequacy of the available models for designing oxidizer-rich and fuel-rich combustors operating at high pressures with oxygen-hydrocarbon propellants. A review was made of the procedures and models used for predicting combustion efficiency, gas temperature distribution, and carbon deposition. This review considered the range of applicability of each technique with particular emphasis on injector element operation, where the mass flow of one reactant was greatly different from the other.

The Rocketdyne Thermochemical Program (RTP) is the primary model used at Rocketdyne to predict reaction products and define the thermodynamic properties of the gases generated. This program solves for equilibrium reaction products and final gas properties by a method of minimization of free energy.

The obvious source of error using this type of program for preburner analysis is that preburner reactions seldom go to chemical equilibrium. One source of error is the assumption that all reactants are mixed completely. Incomplete mixing would, of course, account for a reduction in temperature and could occur if injection mixing parameters, generally developed for significantly different operating mixture ratios, are not valid at preburner conditions.

With the oxidizer-rich LOX/CH₄ and LOX/RP-1 preburner analysis, the RTP program was used for the analysis. By running RTP over the mixture ratio range required for the desired pressure the curves illustrated in Fig. 1 through 4 represent the anticipated theoretical properties.

To use this program (RTP) in analysis of fuel-rich preburners, some modifications in the equilibrium chemistry were made. Modifications to the equilibrium chemistry

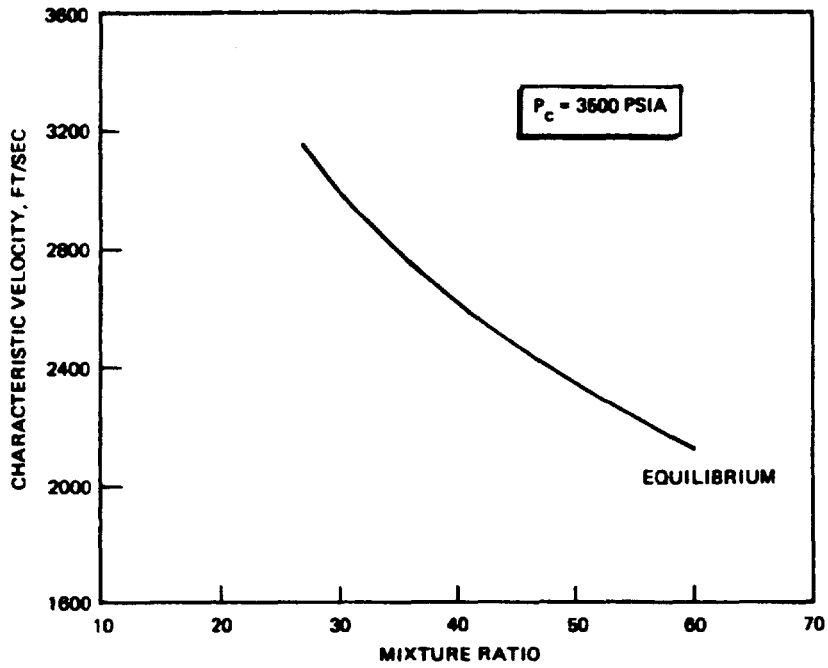


Figure 1. LOX/CH₄ Ambient Gas Theoretical Performance

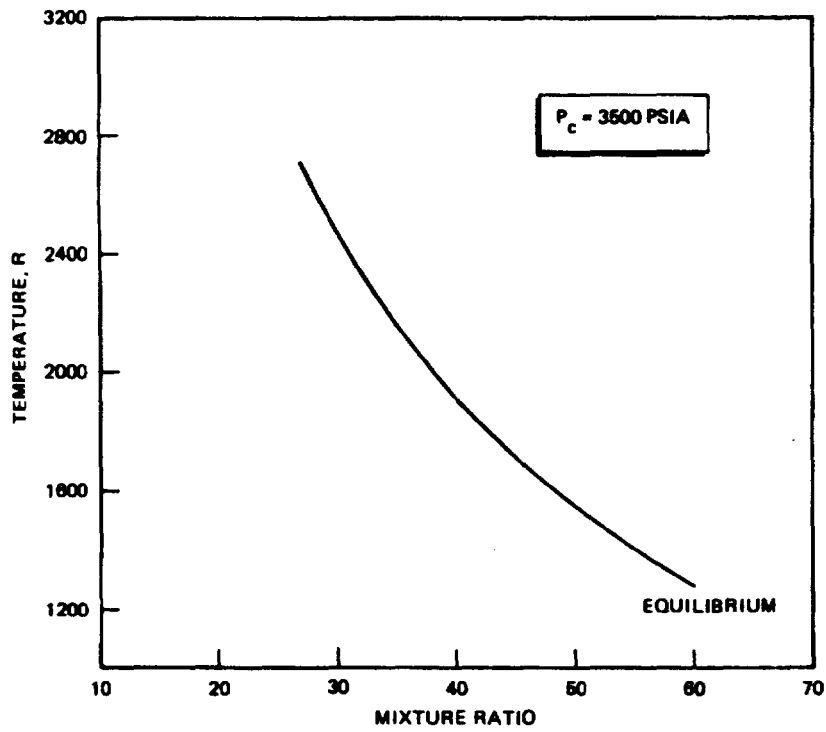


Figure 2. LOX/CH₄ Ambient Gas Theoretical Combustor Temperature

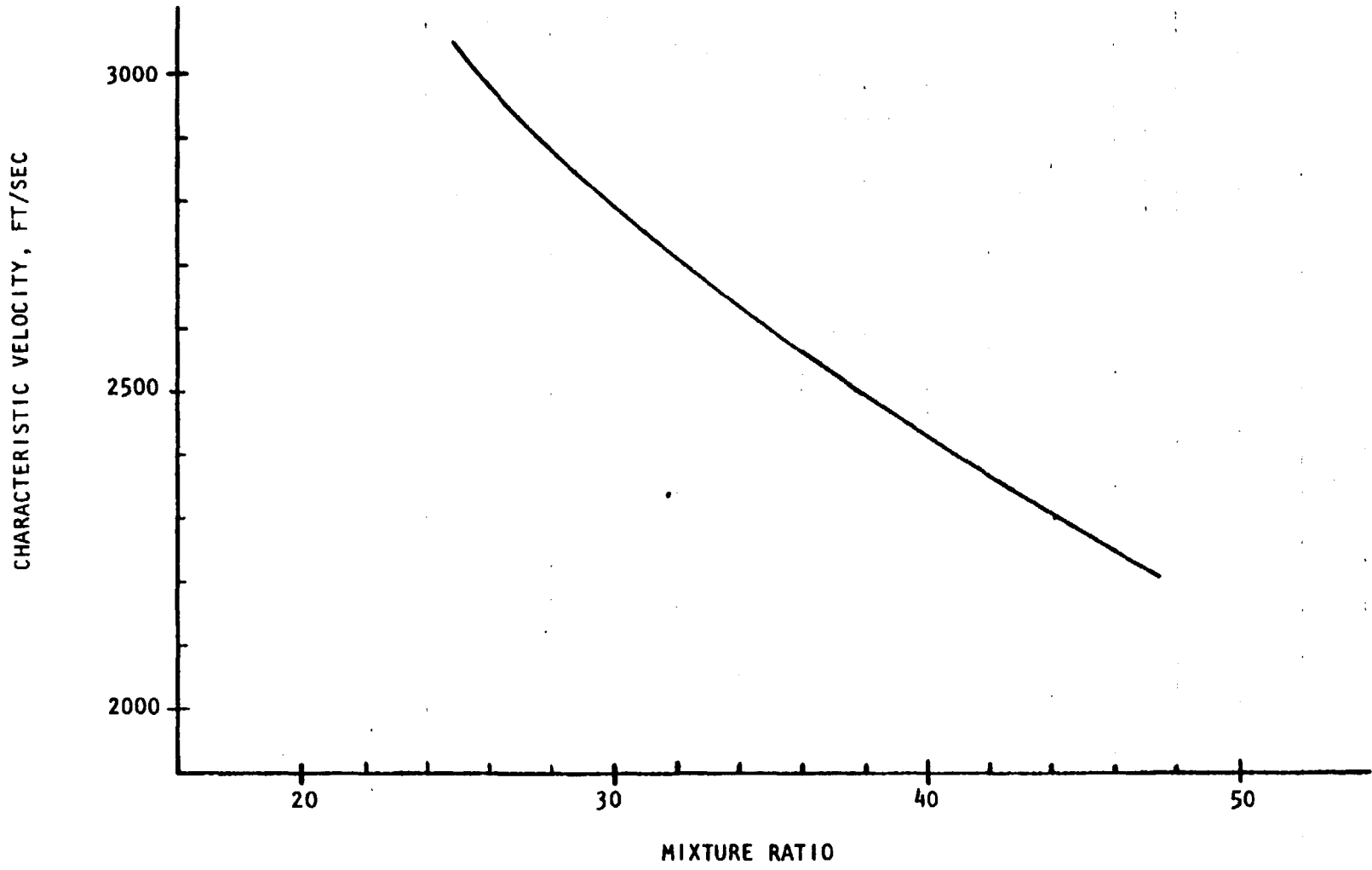


Figure 3. Theoretical Performance, LOX/RP-1

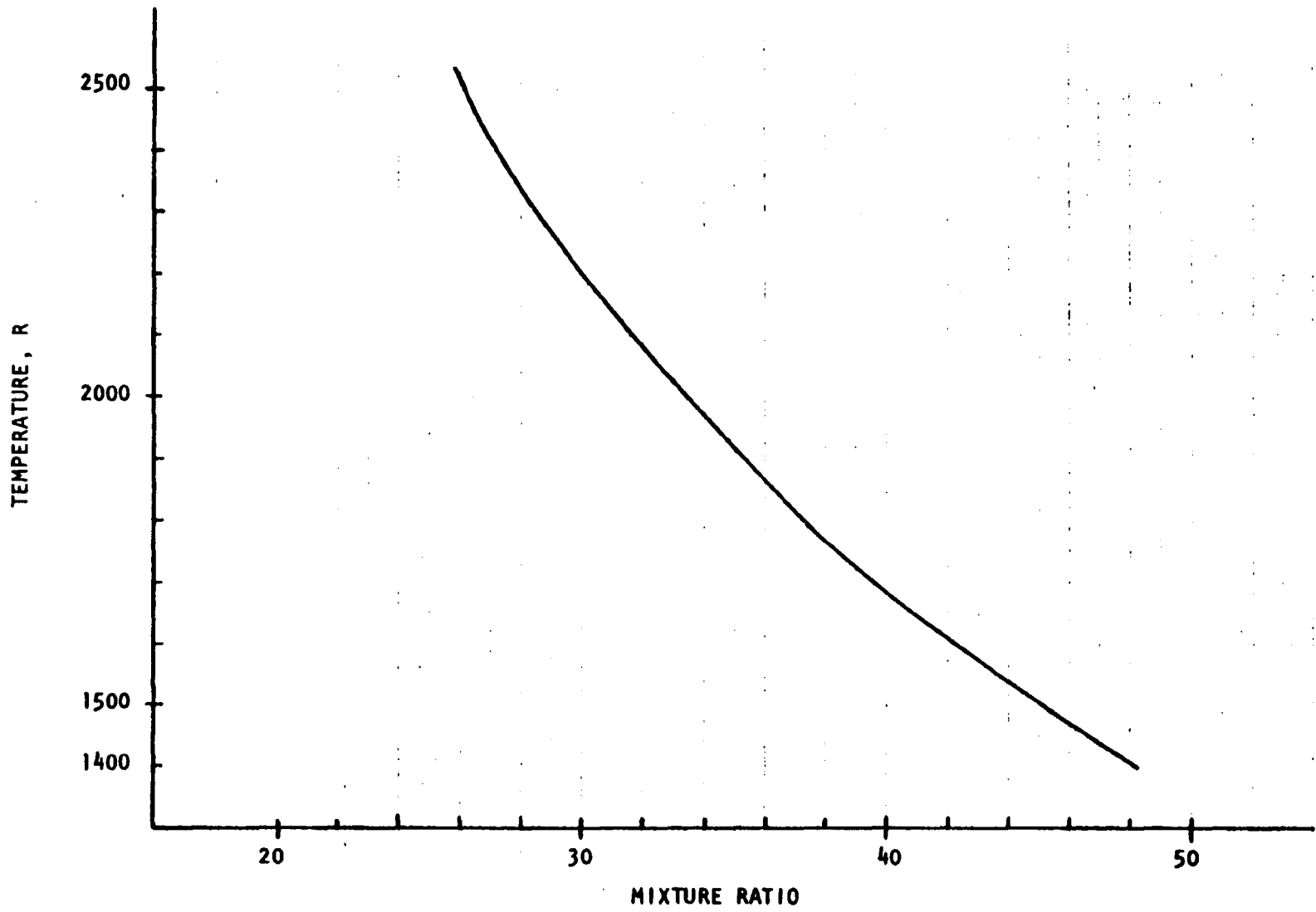


Figure 4. Theoretical Combustor Temperature, LOX/RP-1

were made to better correlate the output with data realized during the review and assessment period. Using experimental data realized from the Atlas gas generator tests, an experimental data curve fit was realized, as illustrated in Fig. 5 and 6. To correlate the RTP output with the experimental data for the fuel-rich LOX/RP-1 low mixture ratios, it was assumed that (1) no free carbon was formed during the combustion process as determined by gas samples taken in the free stream of the gas generator tests, and (2) various quantities of oxygen were withheld.

Applying the same analogy to the low mixture ratio LOX/methane data, (1) no solid free-stream carbon formation is permitted because of the short residence time, and (2) unreacted oxygen increases as mixture ratio decreases below 0.5, and assuming none of the higher hydrocarbon molecules are formed because of the low thermal environment, the model was run and resulted in the characteristic velocity and theoretical combustor temperatures illustrated in Fig. 7 and 8. The species expected to be formed in the preburner combustion reaction was then identified by running RTP over the range of mixture ratios and pressures required. This output then determines those constituents that must be identified during the analyses of the combustor gas samples.

Also as a result of the modified RTP output, the products of combustion are predicted. Figures 9 and 10 show partial combustion products realized from both equilibrium and modified reaction conditions. These plots were useful in establishing the validity of the modifications when the gas samples taken during the hot-fire test program were analyzed. Figure 9 shows the LOX/RP-1 primary combustion products of interest, while Fig. 10 shows the primary combustion products of LOX/CH₄, both curves illustrating the changes realized as mixture ratio variations are realized.

The performance predictions review showed the following programs to be available for preburner analysis and subsequent upgrading using hot-fire data. To predict the combustion efficiency, the Coaxial Injector Combustor Model (CICM), the Standardized Energy Release (SDER), and the General Kinetics Analyses Program (GKAP) were used. The CICM program, which predicts performance of a coax element

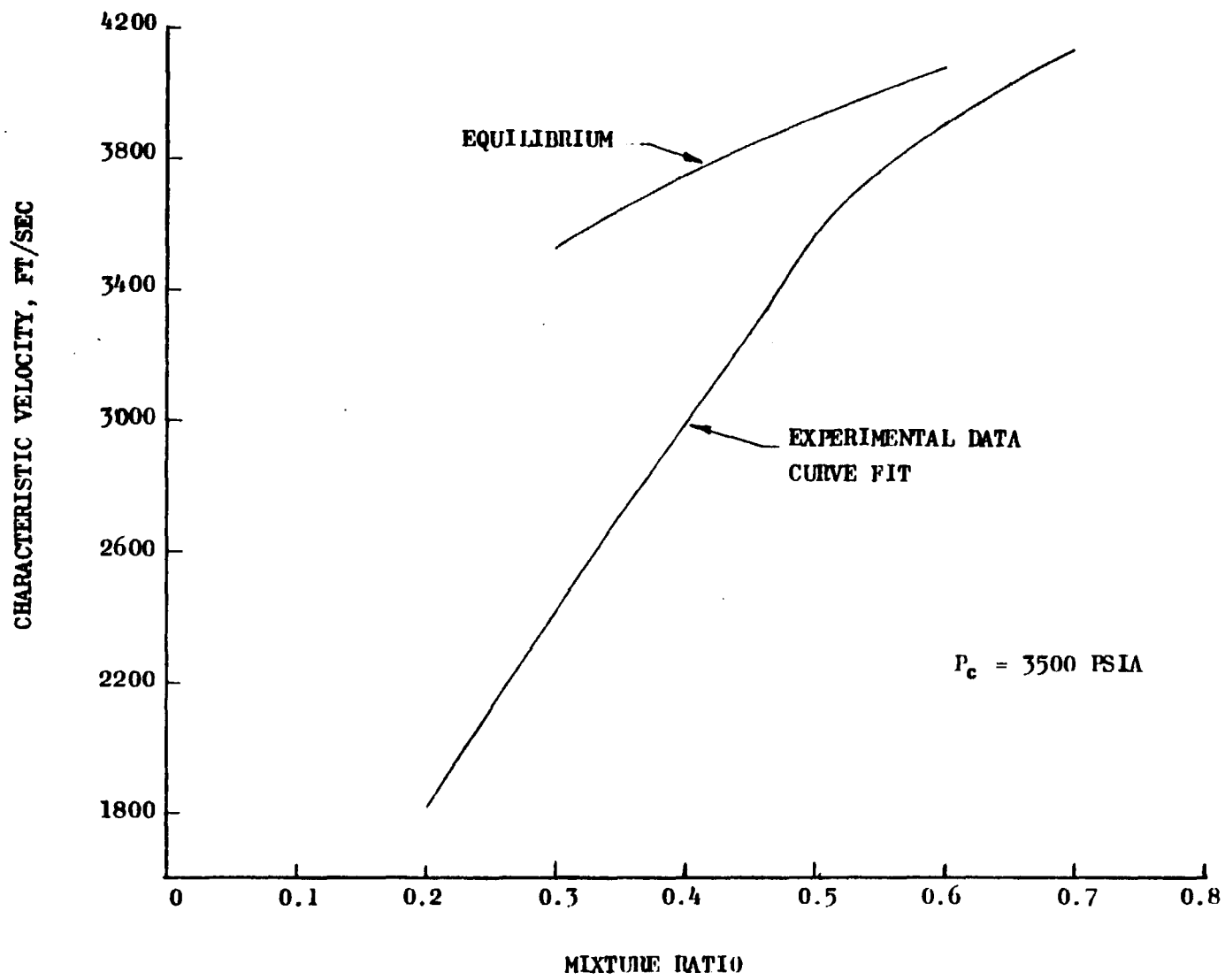


Figure 5. Theoretical Performance, LOX/RP-1

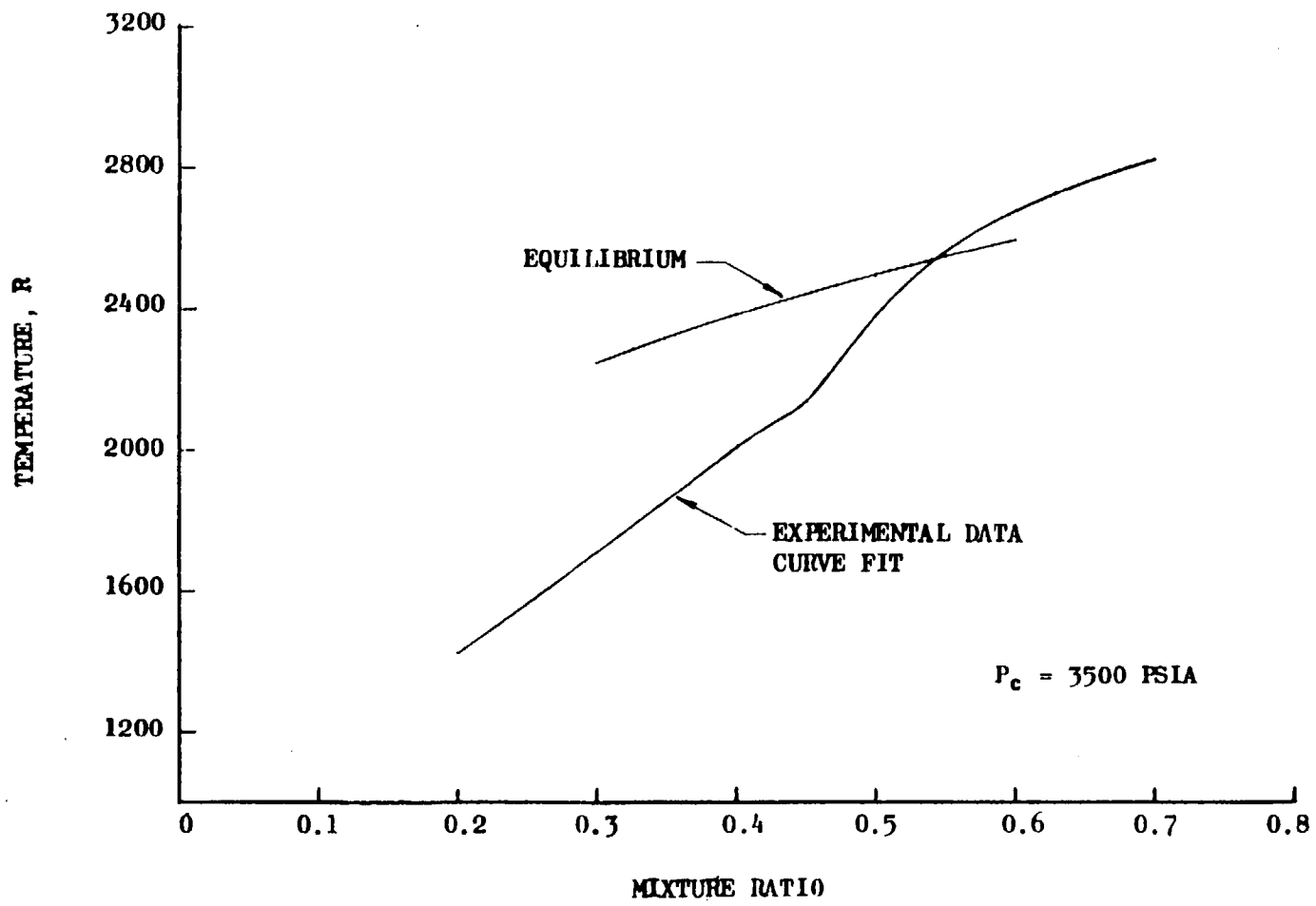


Figure 6. Theoretical Combustor Temperature, LOX/RP-1

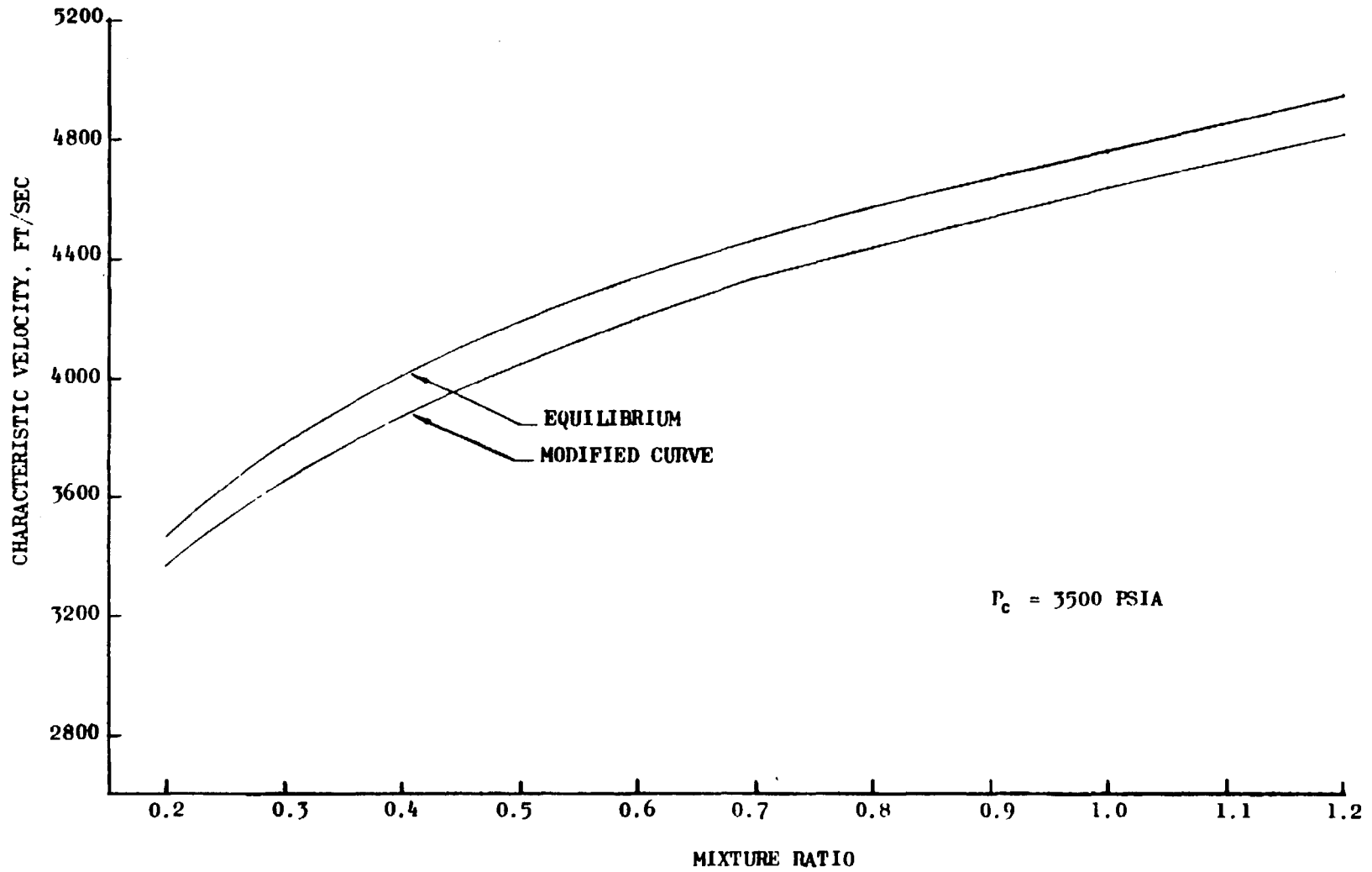


Figure 7. Theoretical Performance, LOX/CH₄ amb gas

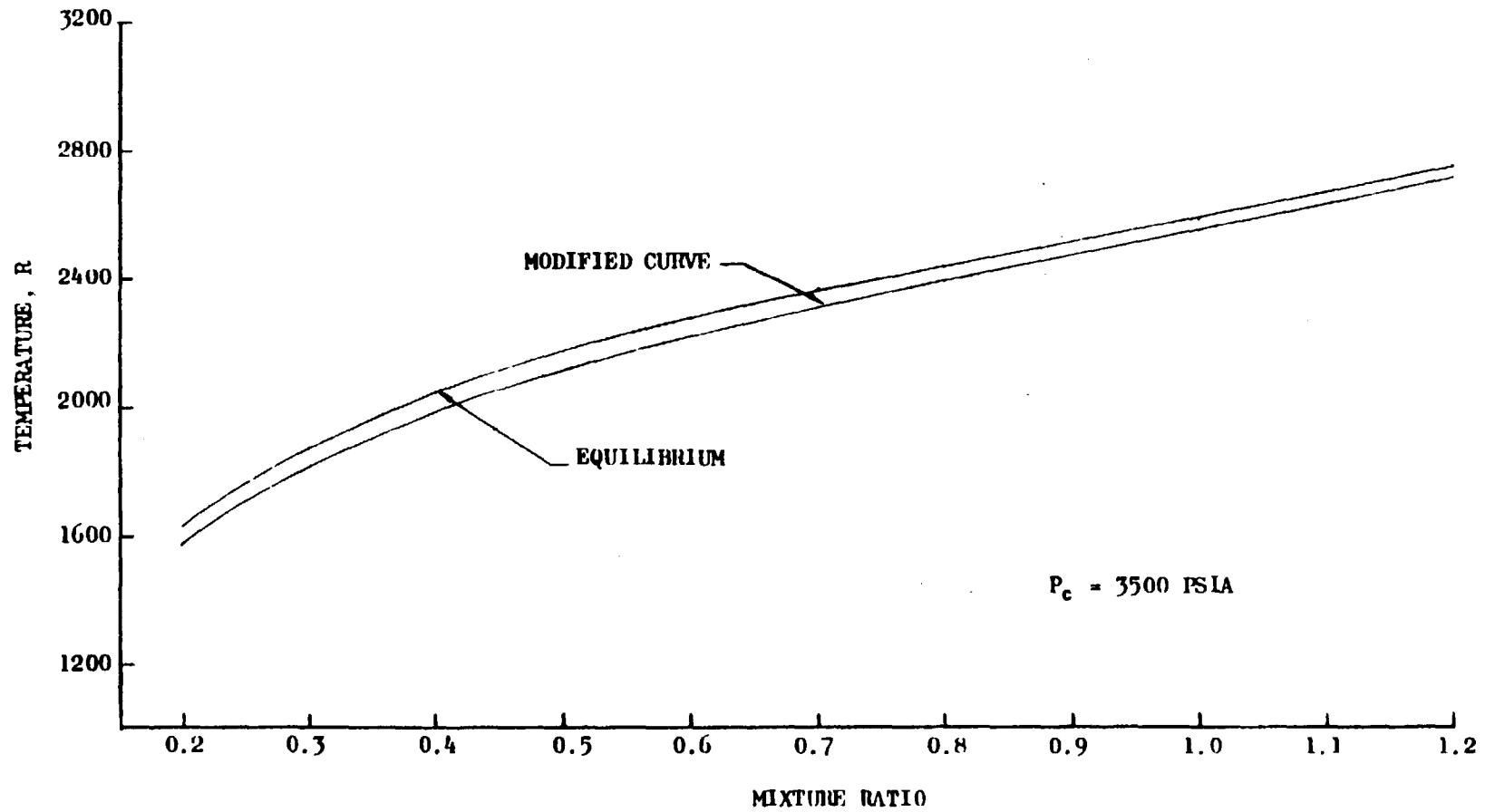


Figure 8. Theoretical Combustor Temperature, LOX/CH₄ amb gas

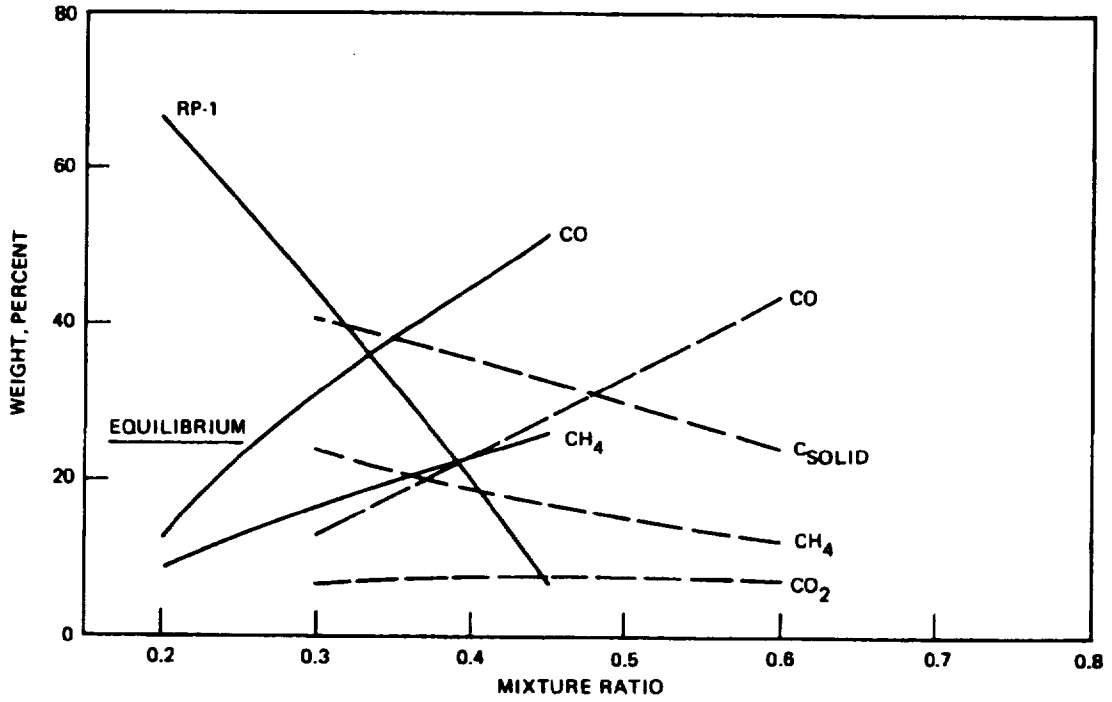


Figure 9. LOX/RP-1 Partial-Combustion Products

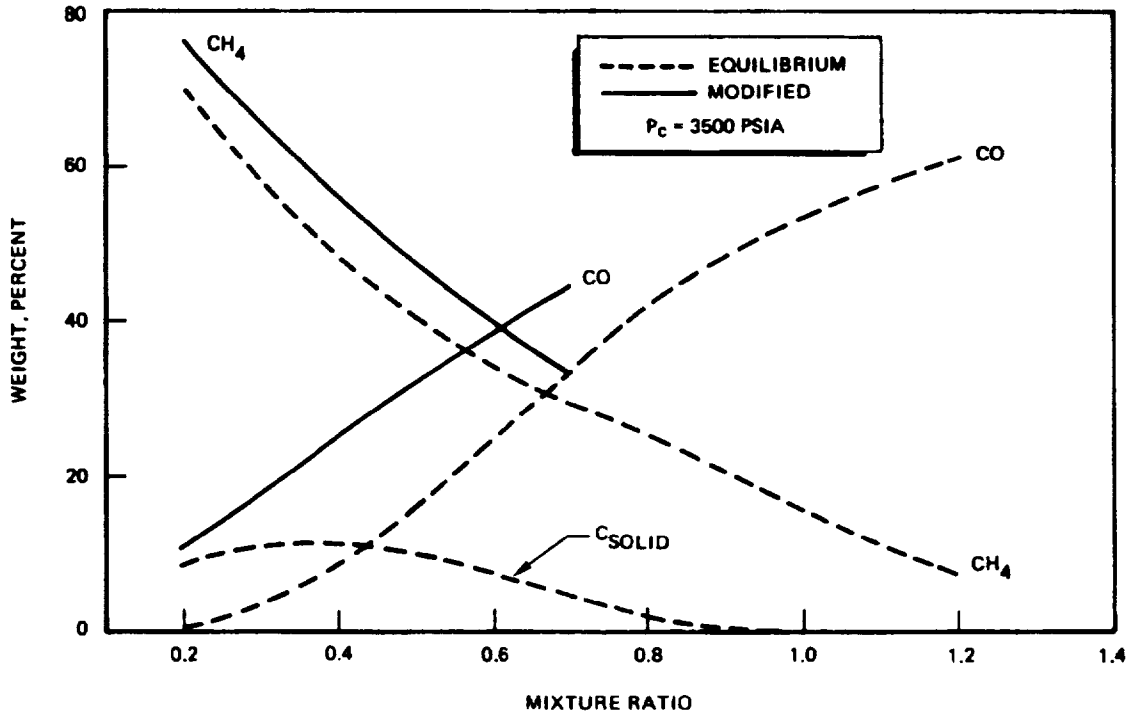


Figure 10. LOX/CH₄ Ambient Gas Partial-Combustion Products

using any propellant combination, includes effect of spray droplet atomization heating, burning, and droplet drag. This program has been substantiated for LOX/GH₂ coax injectors. To provide realistic data, the program required good combustion gas properties at gas generator conditions, liquid jet atomization characteristics, and shear layer mixing characteristics. The SDER Program which calculates spray mass flux, velocity vectors of injected streams, droplet diameters, and energy release in increments from the injector face to the throat relies also on combustion gas properties and initial combustion characteristics. This model has been used primarily for liquid-liquid injectors such as doublet, triplet, and pentads at main chamber operating conditions. The GKAP program which allows mass, energy, and momentum addition rates to be controlled as input data, provides analysis of nonequilibrium reactions. This model requires vaporization rates and combustion gas reaction rates as inputs. The model was developed initially for oil burner emission studies and laser reaction kinetics. For propellant mixing, the Liquid Injector Spray Program (LISP) is used. To determine vaporization, the Stream Tube Combustion (STC) model is used; it computes the vaporization process of injected reactants, uses simultaneous heat and mass transfer, includes real gas effects, solubility effect, and supercritical pressure ranges.

The combustion stability model used is a version of the Priem model, which predicts the occurrence of high-frequency acoustic modes of instability in liquid/liquid or gas/liquid combustors. With the input of actual gas property conditions, as established from the hot-fire tests, the model will result in adequate predictions.

Combustion Modeling. The technique to simulate rocket engine combustion can be separated easily into two categories. The first involves the characterization of the mixing and atomization processes of the injector. Secondly, the droplets formed by the injector are being heated and vaporized, as computed by the transport processes of heat and mass in a stream tube. Infinite kinetic rates are assumed, and the propellants once vaporized will react in the bulk gas. Thus, the performance is represented by the mixing efficiency and the vaporization efficiency.

The difference between rocket combustion chamber and preburner combustion is the temperature of the combustion gas. The low preburner exit temperature (1200 - 2200 F) is required due to the turbine design limit. Consequently, the mixture ratio in the preburner has to be such that the excess propellants can serve as diluents. However, because of the low gas temperature, the reaction rates are reduced substantially. Thus, thermodynamic equilibrium cannot be reached within the stay time provided in the preburner. As a result, gas equilibrium, assumed in the combustion model, is not valid. The effect of reaction kinetics must be included in the analysis. The kinetics will be discussed following descriptions of the mixing and vaporization processes.

Mixing. Proper mixing is achieved by distributing the fuel and the oxidizer uniformly across the injector. The preburner injector designs consist primarily of impinging elements which enhance mixing by forming spray fans of fuel and oxidizer next to each other. Depending on the relative jet moments, the included angle among the jets, and the physical properties of the propellants, the spray fan can be characterized by the propellant flux distribution.

Experimental data have been obtained by collecting simulants downstream of the impingement points. Results from the correlated data are contained in the computer model subprogram, Liquid Injector Spray Pattern (LISP).

The mixing characteristic velocity efficiency (c^*_{mix}) is defined as:

$$\eta_{c^*, mix} = \frac{\sum_i c^*(MR_i)X_i}{c^*(MR_{inj})} \times 100\% \quad (1)$$

where

X_i = local mass fraction

MR_i = local mixture ratio

and

MR_{inj} = injector mixture ratio

The result is then the ratio of the summation of local mass weighted characteristic velocity to the overall value based on the total injected mixture ratio. Although secondary diffusion mixing does occur, the effect is insignificant due to the short stay time. For the preburner, the contribution by the diffusion process should be further diminished because the gas flow is dominated by the extra propellants. Therefore, the analysis technique should be applicable for the preburner injectors. It should be noted that, for the same reason, the existence of extra propellants tends to result in good mixing performance. However, deficiency may develop if uniform mixture ratio cannot be achieved due to the flammability problem. In that case, some stoichiometric combustion zones must be maintained and thus degrade the mixing performance.

Vaporization. The droplets formed by the jet impingement then undergo the heating and vaporization phases. The dropsize and its distribution have been characterized by wax flow experiments. The molten wax was used as the propellant simulant. The atomized drops are frozen and collected for classification. The results from the wax flow tests are then correlated with the injector design and operation expressions; then, the calibrated expressions can be applied to other propellants based on the propellant properties. The computation for the dropsize group is made in the computer subprogram LISP. The ensuing heating and vaporization processes are analyzed in the Stream Tube Combustion (STC) subprogram.

The droplet heating model in STC was used to analyze the vaporization processes. The model is formulated for supercritical chamber conditions (chamber pressure exceeds the propellants' critical pressure). Under such a condition, there is no heat of vaporization. Hence, for the conventional wet-bulb model, a singularity will exist as the droplet is heated through the critical temperature and, as a result, the vaporization rate is optimistically predicted.

The supercritical model assumes a moving control volume for computing the mass diffusion into and out of the volume. This control volume (or "pocket") undergoes changes in size due to the heating as well as the diffusion process. Thus,

it actually contains both raw propellant and the combustion gas which diffuses in to replace the gasified vapor. The "pocket" can be heated through the critical temperature and avoid the singularity. This method of analysis provides a more realistic description of the high-pressure combustion and, in addition, the real gas effect under high pressure is easily included. The results have been correlated well with engines that operate under supercritical chamber conditions.

The vaporization efficiency is defined as:

$$\eta_{VAP} = \left(F_{VAP} \frac{1}{MR+1} + O_{VAP} \frac{MR}{MR+1} \right) 100\% \quad (2)$$

where

F_{VAP} is fuel fraction vaporized

and

O_{VAP} is oxidizer fraction vaporized

The computed value is essentially the overall percent propellant vaporized.

In liquid rocket engines, once the droplet is vaporized, the vaporized propellant is assumed to react instantaneously. The instantaneous reaction rate is realistic due to the high gas temperature ($\sim 4000-7000$ F) which is characterized as vaporization rate limited. On the other hand, it is a well known fact that gas generator (preburner) gas products do not react instantaneously and are far from equilibrium. Therefore, for the preburner analysis, the kinetics effects were considered.

Chemical Reaction Kinetics. If accurate reaction rates are known, the kinetics can be computed for the gas flow. Unfortunately, only limited methane oxidation rates are available and essentially none for RP-1. Furthermore, the gas flow in

a preburner is not truly one dimensional due to the large contraction ratio. Therefore, the interaction between the gas flow and the chemical reactions become a very complicated process, especially if the vaporization rate and the reaction rate are the same order of magnitude.

A simplistic approach was to utilize the previous gas generator data to compute the gas properties. If they could be treated as the quasi-equilibrium, meaning a typical preburner or gas generator design would experience only the limited reactions, the effect on the vaporization could then be calculated. This approach essentially linearizes the kinetics effect on the preburner performance. As more data are available, an iterative computation can be effected to fully analyze the off-stoichiometric combustion processes.

Currently, the gas equilibrium model is modified so that specific species of reactions are not allowed if they were not evident from previous gas generator data. The analysis is for mixture ratios below 0.6 for both propellant combinations. Since the results can be considered as kinetics limited, the computed gas properties, which were used in the heating model, provided a first estimate of the kinetics effects on the vaporization.

Basically, if the mixing, vaporization, and kinetics are all linear influences on the performance, they can be studied independently. So, when compared with the rocket engine performance analysis technique, this approach is tenable as a reasonable extrapolation.

Analysis. The LOX/CH₄ cases assume the gaseous methane as a dense fluid for mixing computation and revert to gas in STC modeling. All cases were analyzed assuming a 12-inch-long chamber and 700-psia pressure drop across the injector. The chamber contraction starts at 10 inches from the injector.

Currently, LISP contains the cold-flow mass flux correlation for the impinging-type elements, including the doublets (like and unlike), the triplet, and the pentad. Therefore, no new cold-flow data are needed. The pseudo-collection

plane is divided into radial and angular mesh systems to compute the local mass flux for each propellant. Equation 1 is then used for computing the mixing efficiency.

In the same subprogram, the mass median diameter (\bar{D}) is also calculated for each type of injection element. This information is then supplied to the STC subprogram as the initial condition for the marching calculation. The chamber axial length is divided into increments. At each station, the equations of continuity, momentum, and energy are solved and the boundary conditions must be satisfied. The results are tabulated at each station and consist of the states of the gas and droplets. The total percentages of propellant vaporization at the throat are then obtained as the vaporization efficiency.

Results. Table 1 is a summary of the results from the analysis. It shows the mixing efficiency, the predicted \bar{D} , and the respective vaporization efficiency for each injector design. The results indicate that the mixing efficiencies are all near 100%. The reason is simply because of the extreme mixture ratio: the mass flux distribution in any stream tube is dominated by the extra propellants as diluents.

It is interesting to note that the preburner injector can still have excellent mixing characteristic velocity efficiency, even if the design may include some stoichiometric combustion zones. According to the definition, such zones will have significantly higher characteristic velocities and thus improve the overall efficiency value. In general, experience has shown that preburners or gas generators all have good mixing performance.

The vaporization efficiency obviously depends heavily on the initial dropsize and the total mass to be vaporized. Injector designs produce various droplets and can improve the performance by generating very fine sprays. The drop sizes are represented by mass mean diameters which are shown in Table 1.

The two LOX/CH₄ cases are shown to be 100% vaporized; obviously this is because the methane is introduced as a gas resulting in less mass to be vaporized.

TABLE 1. HIGH-PRESSURE LOX/HYDROCARBON INJECTOR PERFORMANCE

P _c = 3500 PSIA; ΔP _{inj} = 700 PSI; 12-INCH CHAMBER					
INJECTOR TYPE	$\dot{\omega}_{TOTAL}$, LB/SEC	MR	\bar{D} [μ]	η_{c^*} (MIX), %	η_{c^*} (VAP), %
TRIPLET (36 ELEMENTS) LOX: ϕ 0.035 INCH CH ₄ : ϕ 0.063 INCH	16.9	0.345	LOX=50	97	100
18 PENTAD LOX: ϕ 0.057 INCH CH ₄ : ϕ 0.027 INCH	23.13	40.1	LOX=30	100	100
LIKE DOUBLET 18 RP-1 ELEMENTS (ϕ 0.074 INCH) 18 LOX ELEMENTS (ϕ 0.041 INCH)	21.92	0.363	LOX=70 RP-1=300	100	81
LIKE DOUBLET + SHOWERHEAD 12 RP-1 DOUBLET (ϕ 0.019 INCH) 12 LOX DOUBLET (ϕ 0.035 INCH) 48 LOX SHOWER (ϕ 0.068 INCH)	23.52	35.3	LOX=300 RP-1=100	100	98

The liquid oxygen in general has a high vaporization rate and very fine droplets as a result of its physical properties. Figures 11 and 12 show the percentage of vaporization for LOX in the 12-inch-long chamber. As noted, methane is 100% vaporized at the start. The figures also show that the oxidizer-rich case requires more chamber distance for complete vaporization due to the higher LOX mass.

In the LOX/RP-1 cases, the process is limited by RP-1. The figures show the percent vaporized by each propellant as functions of the chamber length. Liquid oxygen vaporizes relatively fast when compared with the RP-1. The poor performance of the fuel-rich case is a direct result of the RP-1 injection element design. Modifications such as smaller injection orifices and higher injection velocity should improve the vaporization efficiency.

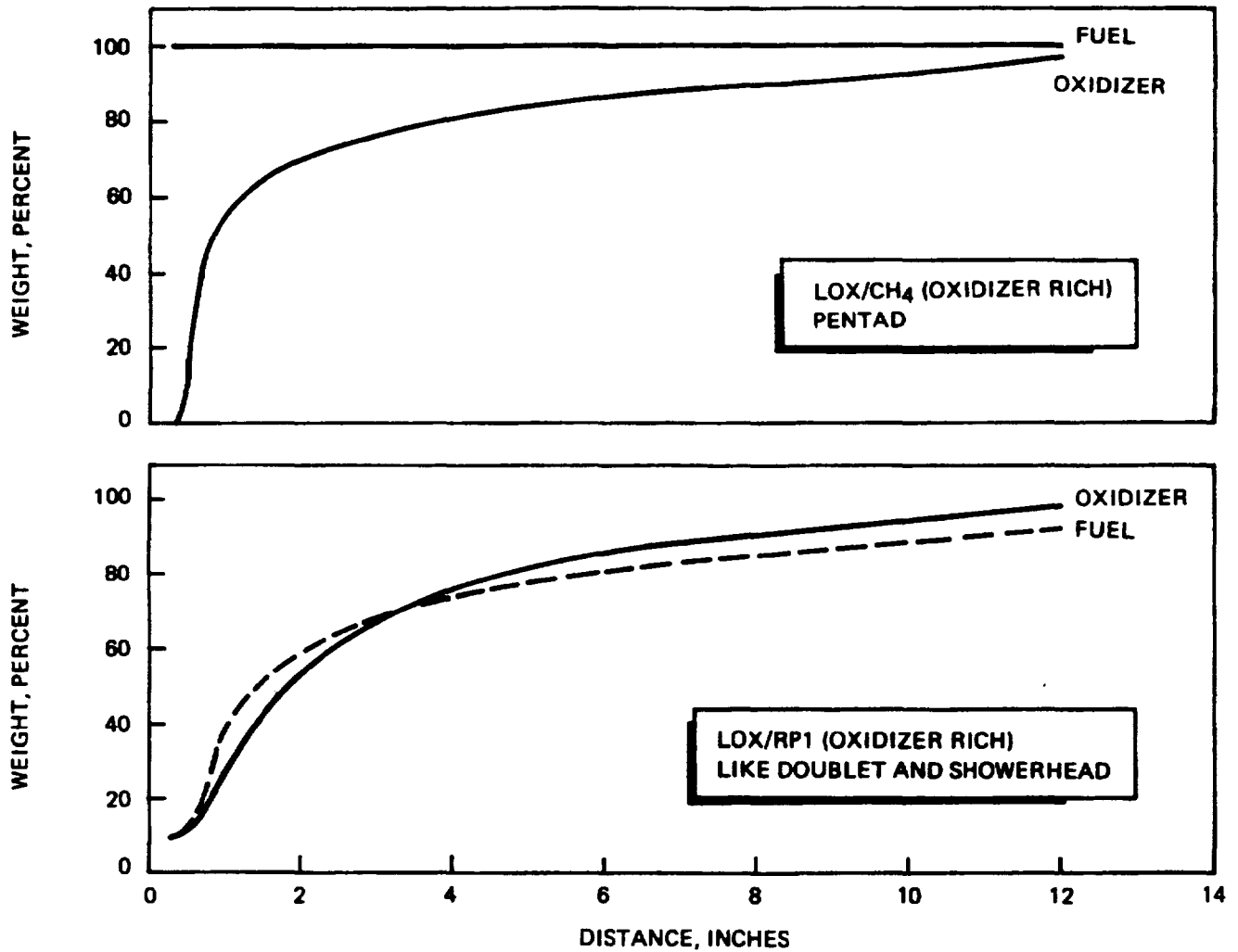


Figure 11. Percent Vaporization

It should be noted that, due to the relative ease for LOX to vaporize, a problem may develop for the oxidizer-rich case. In the model there will be insufficient energy generated from the limited combustion to sustain the vaporization process due to the large mass of liquid oxygen that rapidly vaporized. The condition can be interpreted as "flameout" with LOX serving as the heat sink. The solution is to moderate the LOX vaporization rate. The result shown on Table 1 reflects a larger \bar{D}_{LOX} . In actuality, the showerhead elements for the LOX may be effective in that the liquid jets tend to remain as jets for at least a few inches into the chamber. The vaporization rate will then be moderated.

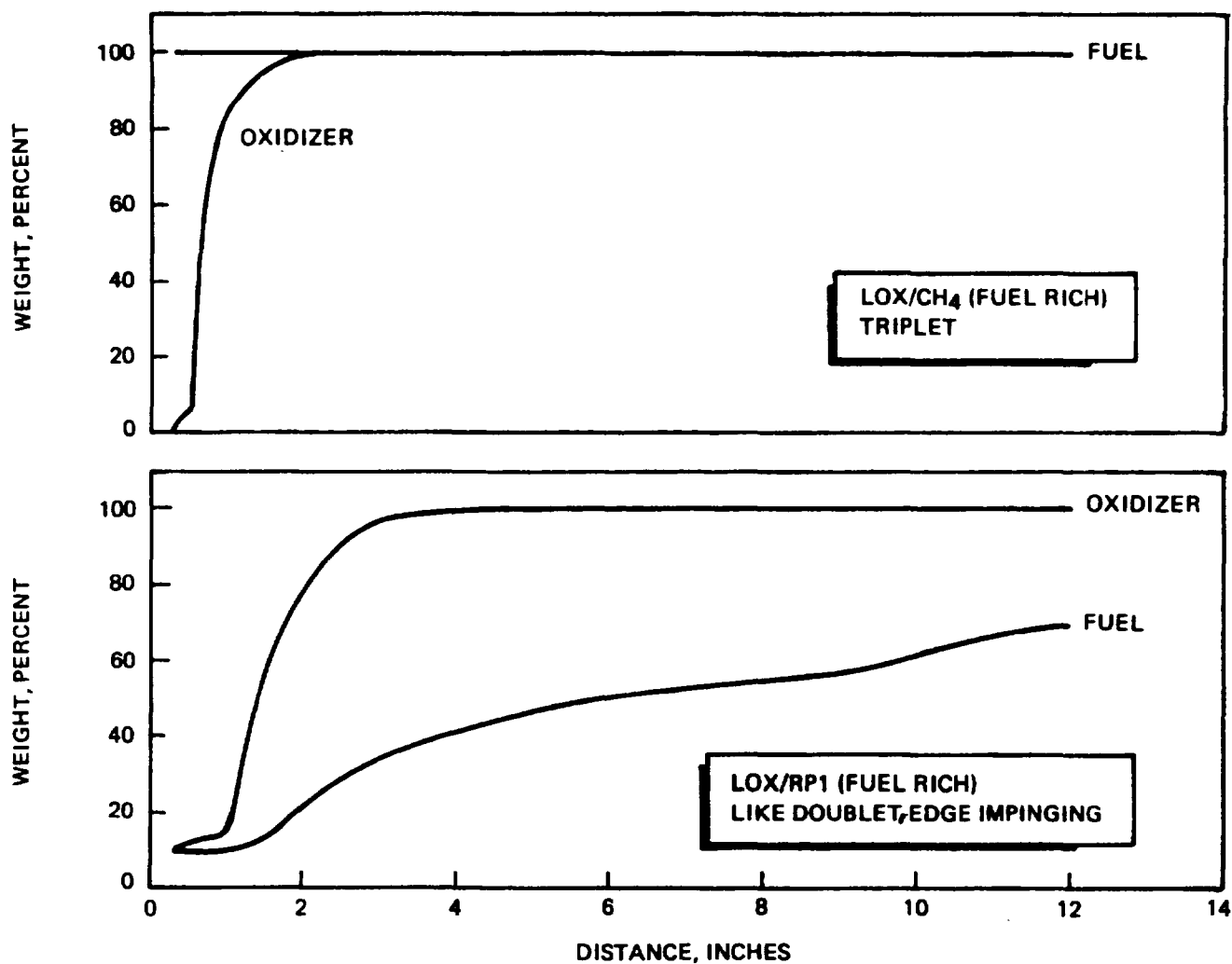


Figure 12. Percent Vaporization

Figure 13 contains the axial gas temperature profile along the chamber by assuming, instantaneously, reactions of the vaporized propellants. It shows that, in all but one case, a high-temperature gas zone exists near the injector. The reason is due to the different vaporization rates. There is a region where the mixture ratio in the bulk gas is stoichiometric. This can be interpreted as the "flame front." The exception is the fuel-rich LOX/methane case. The fact that methane is already a gas causes the bulk gas to be methane rich at all times. The gas temperature is therefore suppressed. The model prediction of the temperature profile can be correlated with experimental data. The drops near the throat are due to the contraction and compressibility effects.

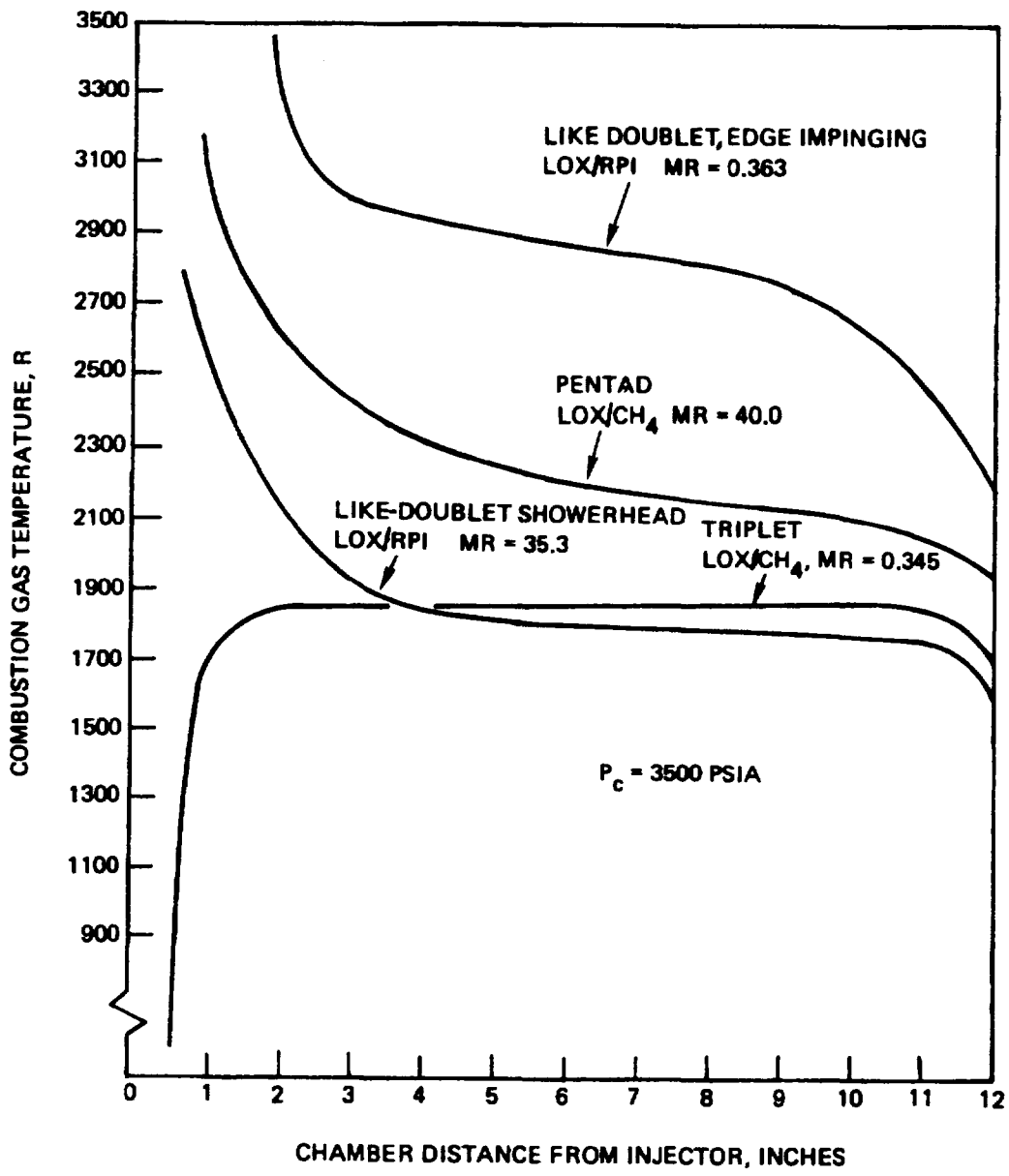


Figure 13. Chamber Axial Temperature Profile

The gas temperature may also be used to illustrate the reaction kinetics. The existence of the high-temperature zone indicates that the kinetics may not be seriously limited. The result itself actually includes the first-order effects by using the modified gas "equilibrium" properties. The kinetic rate-limited performance can be directly calculated by dividing the equilibrium characteristic velocity into the value obtained by the model. The exception of the low temperature profile for the fuel-rich LOX/CH₄ case would raise the question whether

there will be any reaction. A one-dimensional kinetic calculation, utilizing existing reaction rates data, shows no reaction for gas temperature below 2200 F. However, due to the one-dimensional nature of the models, it is difficult to show any localized combustion. The question was resolved by actual testing.

Four injector concepts were selected for evaluation in the LOX/hydrocarbon pre-burner. Table 2 lists the injector type and the respective design mixture ratio. The performance of each injector was analyzed, assuming the same chamber pressure (3500 psia) and pressure drop across the injector (700 psi). The chamber diameter was 2 inches with a 12-inch length.

TABLE 2. SELECTED CONTRACT INJECTORS

PROPELLANT	INJECTOR	M/R
LOX/RP-1	FUEL-RICH/LIKE DOUBLET	0.363
	OXIDIZER-RICH/LIKE DOUBLET + OXIDIZER SHOWER HEAD	35.3
LOX/CH ₄	FUEL-RICH/TRIPLET	0.345
	OXIDIZER-RICH/PENTAD	40.1

The injector performance is generally a product of its mixing and vaporization efficiency. The mixing is primarily a function of the propellant distribution and is associated with the injection pattern and the injection element characteristics. Most injection characterization for the impinging-type elements was obtained from past cold-flow mixing studies. They were correlated with the hot-fire test results and were included in the Liquid Injector Spray Pattern (LISTP) subprogram in the Standardized Distributed Energy Release (SDER) computer program.

The vaporization process depends heavily on the size of the droplet formed by the atomization process which was characterized by past wax cold-flow experiments. The correlations for the impinging elements are included in the LISP. The propellant droplet sizes are computed and input in the Stream Tube Combustion

(STC) model. The model then uses the droplet heating model in a one-dimensional flow formulation to calculate the vaporization. The vaporization efficiency is expressed as the percentage of propellants vaporized at the throat. Real gas effect as well as the combustion gas velocity effect on the vaporization process are included in the model.

Table 3 is a summary of results for the four injectors. The two LOX/CH₄ injectors both have very high performance. It can be attributed to the fact that methane is a gas and the liquid oxygen vaporizes with relative ease. Figure 14 compares the vaporization process for the two operating extremes. The initial lower vaporization rate for the oxidizer-rich case is due to the higher LOX mass. It is evident from Fig. 14 that both injectors complete vaporization in a relatively short chamber distance. A longer combustor length was used to ensure gas temperature uniformity. During the evaluation it was demonstrated the fuel-rich LOX/CH₄ triplet was violently unstable, and the oxidizer-rich LOX/CH₄ pentad performance was lower than anticipated.

The chemical reaction kinetics for fuel-rich LOX/CH₄ were analyzed. The technique assumed both propellants are gaseous in a 12-inch-long chamber. As evident in Fig. 14, this is a valid assumption since complete vaporization is achieved in the first few inches. The gases are allowed to flow with an initial velocity of 60 ft/sec which approximates the calculation from the continuity equation assuming a 2-inch-diameter chamber. The gases are also assumed to be well mixed. The reactions among the different chemical species are computed by including all possible chemical reaction rates. The species production rate as well as the energy are then computed algebraically into the gas flow equations. The purpose of this analysis is to determine if the kinetics effects can limit the gas generator performance due to the lower gas temperature.

The results indicate that to initiate and sustain a fast and complete reaction, an energy level corresponding to 1700 F gas temperature is needed as an initial condition. In a real system, this energy can be provided by the ignition source. At that energy level, appreciable radicals would be produced and proceed to complete oxidation. At 10 inches, approximately 20% of the total methane, which

TABLE 3. INJECTOR CANDIDATES PERFORMANCE PREDICTION

CASE	E_m (%)	$\eta_{c* \text{ mix}}$ (%)	$\eta_{c* \text{ VAP}}$ (%)
1 LOX/CH ₄ FUEL-RICH	80.0	97.0	100.0
2 LOX/CH ₄ OXIDIZER-RICH	90.0	100.0	100.0
3 LOX/RP-1 FUEL-RICH	92.0	100.0	81.0
4 LOX/RP-1 OXIDIZER-RICH	91.0	100.0	98.0

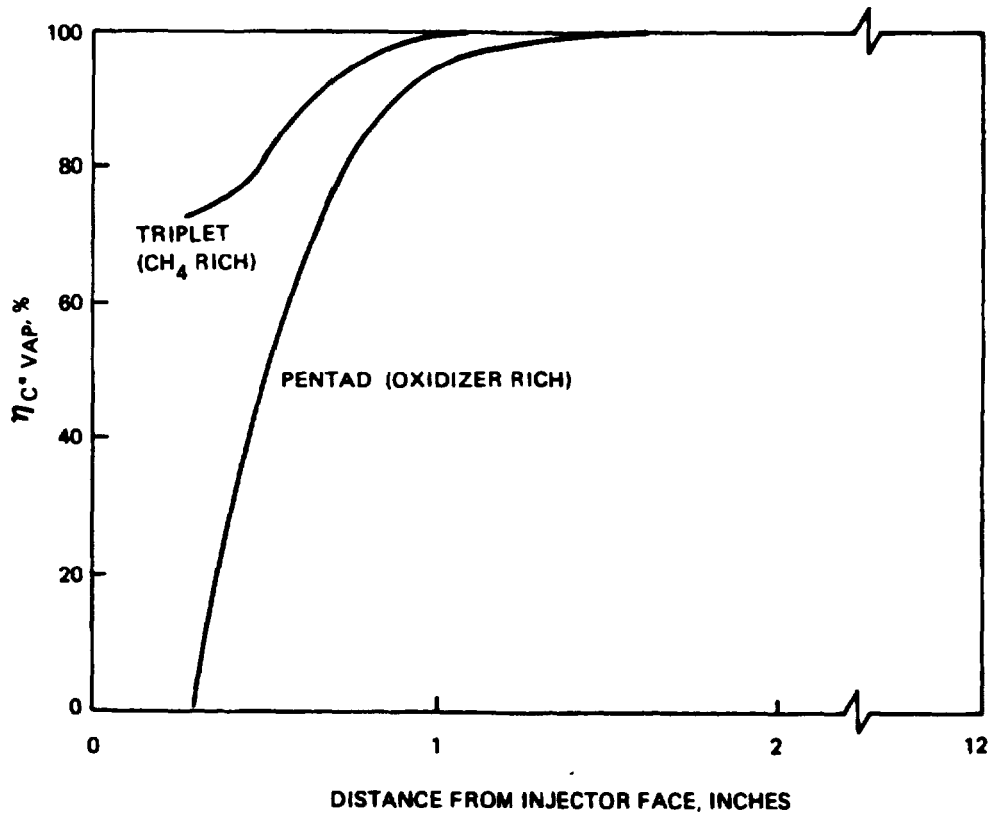


Figure 14. LOX/CH₄ High-Pressure Preburner Vaporization Efficiency

is 8% more than required for stoichiometric combustion, would be converted. The results tend to support the postulation that only part of the methane will combust and the energy release will simply heat up the excess methane. Consequently, the gas generator performance is not affected by the kinetic processes due to the lower combustion gas temperature.

The LOX/RP-1 injectors have the disadvantage that injected RP-1 is a liquid and needs to be atomized and vaporized. Also, due to its lower vaporization rate than the liquid oxygen, a significant difference may develop in the chamber condition when compared with the LOX/CH₄ case; e.g., RP-1 has to compete with the liquid oxygen for the thermal energy for vaporization. Figure 15 shows the percent of total propellants vaporized along the chamber.

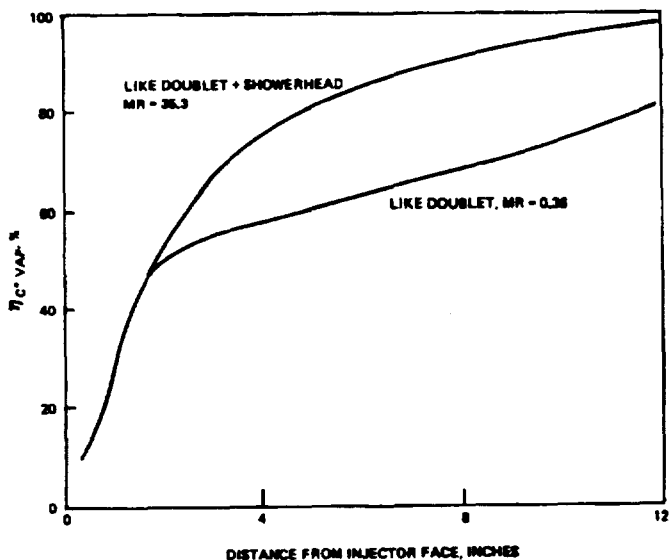


Figure 15. LOX/RP-1 High-Pressure Preburner Vaporization Efficiency

In the oxidizer-rich LOX/RP-1 case, the liquid oxygen can cause the combustion gas temperature to be too low to sustain the vaporization process. Physically, it can be viewed as "flame quenching." The problem lies with the large mass of liquid oxygen which utilizes all the heat for its vaporization and insufficient RP-1 vapor is present to combust. When no additional heat is released through the combustion processes, the gas temperature drops to the extinguishing point.

To circumvent the problem, the LOX droplets have to assume a larger size so that its vaporization rate can be moderated. Figure 16 is a plot of the percent of total vaporization as a function of the initial LOX median droplet size (\bar{D}). The \bar{D}_{RP-1} values are also shown. A Rosin-Rammler* distribution function is assumed for all the droplets. A maximum of 98% is achieved before "quenching" occurs. The corresponding \bar{D} for the LOX and RP-1 are 250 and 100 μ , respectively. The calculation based on the cold-flow data and the preliminary design layout indicates that 100 μ size RP-1 can be produced. However, the LOX droplets may have to be modified to produce larger droplets.

The performance of the fuel-rich LOX/RP-1 case ($MR = 0.363$) is only 81%. The primary reason is significantly larger RP-1 drops. Therefore, it was recommended that both smaller injection elements for the RP-1 and a longer chamber to increase the resident time, would be required for the fuel-rich LOX/RP-1 injector.

The kinetics analysis was performed for the LOX/RP-1. It was believed that if RP-1 could be vaporized sufficiently fast, the reaction kinetics would be similar to LOX/ CH_4 .

Having reviewed the injector designs and the performance realized from these injector configurations presented previously, it was decided to review the LOX/RP-1 fuel-rich low performer. The injector element packaging was reviewed and it was shown that 27 elements could be packaged satisfactorily. This revised configuration resulted in a vaporization efficiency of 87%, a considerable improvement over the 81% previously quoted. The change in the vaporization efficiency is a result of increasing the total number of elements and consequently decreasing the individual orifice diameters. The efficiency obviously depends heavily on the initial droplet size and the total mass to be vaporized. Generally, specific injector configurations produce various droplets, and a performance improvement can be realized by generating finer sprays. Reducing the orifice diameters therefore results in a finer spray.

*Correlation of Spray Droplet Size Distribution and Injector Variables (1969)
L. J. Zajac, R-8455, NAS7-726 contract.

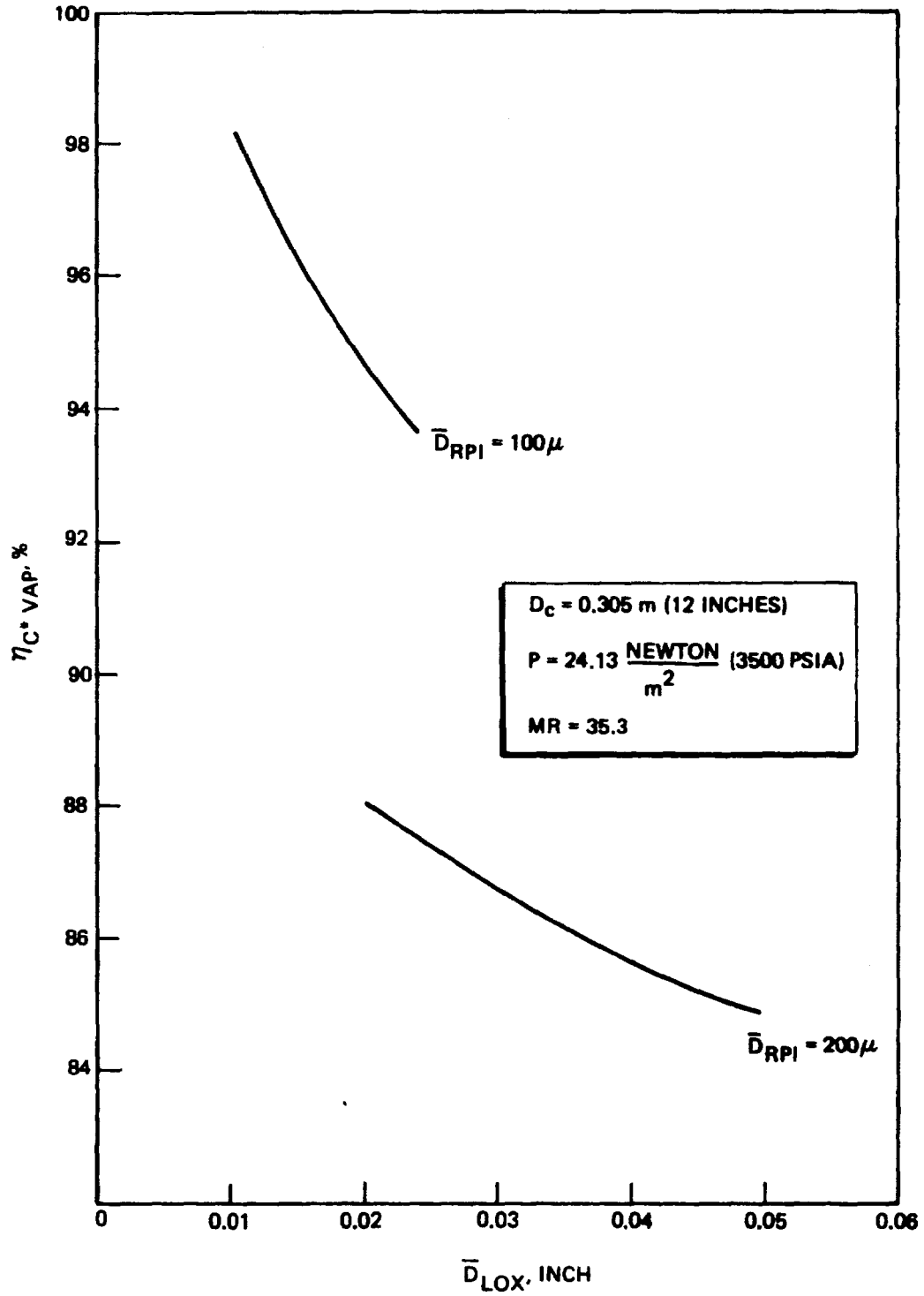


Figure 16. LOX Medium Dropsizes (\bar{D}) Effect on Vaporization Efficiency

Figure 17 shows the percent vaporized by each propellant as a function of chamber length for the revised LOX/RP-1 doublet injector. Liquid oxygen in general has a high vaporization rate and very fine droplets as a result of its physical properties. As shown in Fig. 17, the vaporization process is limited by RP-1; the liquid oxygen vaporized relatively fast compared to the RP-1. Poor performance of the fuel-rich LOX/RP-1 injector is a direct result of the fuel injection element design, therefore the smaller injection orifices and higher injection velocities result in improved vaporization efficiency.

Figure 18 shows the axial gas temperature profile along the chamber, comparing the effects of reducing the orifice sizes and the results of the reactions of the vaporized propellants.

Subtask 01200 - Define Subscale Testing

In March 1979, the "Santa Susana Field Laboratory Small-Scale Test Plan" was issued. This plan defined the test requirements for a small-scale (2-inch diameter) high pressure (3500 psia nominal) fuel-rich and oxidizer-rich LOX/RP-1 and LOX/CH₄ combustor, together with the data acquisition requirements and the ancillary hardware needed to meet these requirements. This plan was used to establish the operational characteristics of the different injection concepts associated with each of the four operating regimes.

Per the original test plan, oxidizer-rich LOX/CH₄ and LOX/RP-1 tests were scheduled to be conducted, using CTF as an ignition source. Two test attempts were made in an oxidizer-rich environment, one for each propellant combination.

Both tests resulted in considerable hardware damage primarily due to excessive combustion temperatures and resultant material oxidation. To prevent this high combustion temperature during the transient start phase, a "TEA" ignition system was incorporated that permitted a continuously controlled oxidizer-rich transition. This change provided for a continuous low combustion bulk temperature and resultant successful operation.

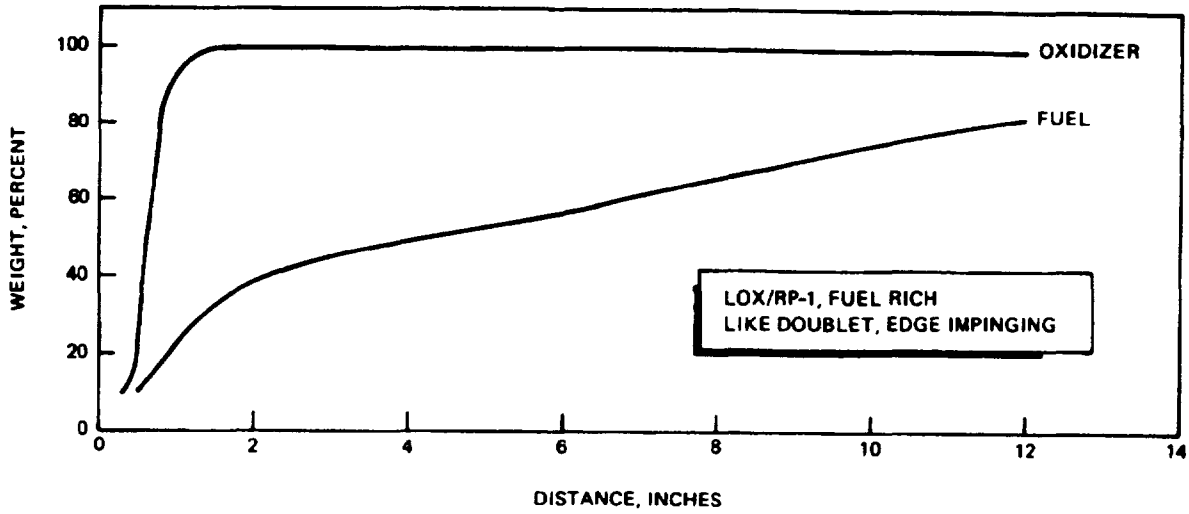


Figure 17. Percent Vaporization

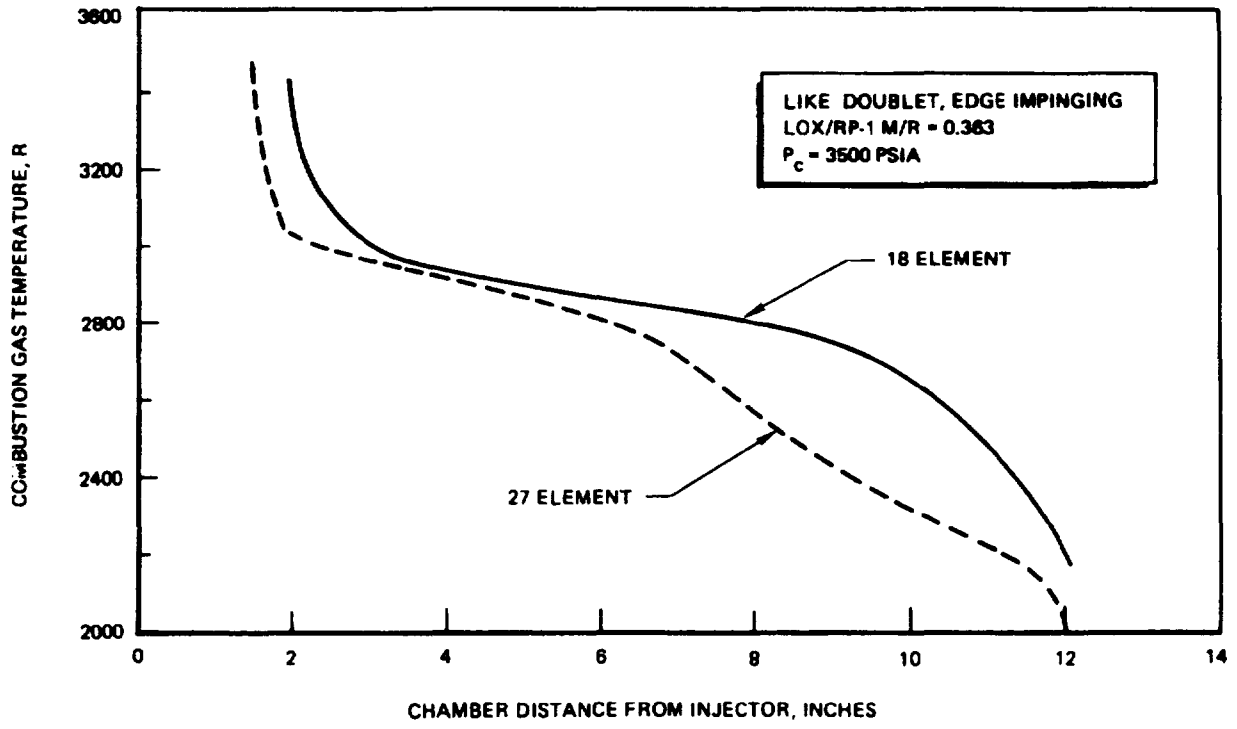


Figure 18. Chamber Axial Temperature Profile

TASK II: SMALL-SCALE HARDWARE DESIGN AND FABRICATION

Subtask 02100 - Analysis and Detail Design

Throughout Task I the approach to and the analysis of the selected injectors was covered briefly. During this concurrent effort, the injector candidates listed in Table 4 were reviewed. This table lists the injector configurations deemed satisfactory for acceptable preburner operation. One each injector was selected to support the contract subscale test effort. Concurrent with this contract effort a Rocketdyne Independent Research and Development (IR&D) effort was in work. Four fuel-rich injector configurations designed for a higher operating combustion gas temperature were being developed. Table 5 lists the eight injectors selected from the candidates in Table 4 and the design conditions. With these eight configurations, numerous variables were determined during the hot-fire evaluation.

The analytical analysis conducted on the injectors used the nominal design point of 3500-psia chamber pressure and 1900 R for the contract injectors and 2100 R for the Rocketdyne injectors.

The primary objective of this subtask was to provide the detailed drawings and analysis of the small-scale hardware identified previously. At the conclusion of Task I effort, the selected injector concepts were presented to the NASA/MSFC program monitor for approval. The preburner design concepts and operating ranges were reviewed.

The detailed designs were completed to produce drawings of each piece of hardware required to manufacture all the component parts and ancillary hardware. This task effort included supporting analysis in the areas of stress, combustion performance and stability, heat transfer, hydraulic flow calculations, materials and manufacturing processes. The component drawings produced included injectors, combustion chambers and all ancillary hardware for the thermodynamic property measurement techniques and carbon deposition evaluation. A slotted nozzle

TABLE 4. INJECTOR CANDIDATES

LOX/RP-1 (OXIDIZER RICH)	LOX/CH ₄ (OXIDIZER RICH)
LIKE DOUBLET + SHOWERHEAD*	PENTAD*
LIKE DOUBLET IMPINGING	LIKE DOUBLET + SHOWERHEAD
FAN FORMER	LIKE DOUBLET
INLINE LIKE DOUBLET 2 + 2	TRIPLET
LOX/RP-1 (FUEL RICH)	LOX/CH ₄ (FUEL RICH)
LIKE DOUBLET, EDGE IMPINGING*	TRIPLET
TRIPLET*	PENTAD
FAN FORMER*	COAX*
PENTAD	FAN FORMER
	LIKE DOUBLET
*INJECTORS ANALYTICALLY EVALUATED	

TABLE 5. INJECTOR OPERATING CONDITIONS CONTRACT AND INDEPENDENT RESEARCH AND DEVELOPMENT

PROPELLANT	OPERATION	PATTERN	P _c , PSIG	T _c , R	MIXTURE RATIO (NOMINAL)
LOX/CH ₄	FUEL RICH	PENTAD	2500 TO 3500	2000 TO 2400	0.49
LOX/CH ₄	FUEL RICH	COAX	2500 TO 3500	2000 TO 2400	0.49
LOX/CH ₄	FUEL RICH	TRIPLET	2500 TO 3500	1800 TO 2000	0.345
LOX/CH ₄	OXIDIZER RICH	PENTAD	2500 TO 3500	1600 TO 2000	40.1
LOX/RP-1	FUEL RICH	LIKE DOUBLET	2500 TO 3500	1800 TO 2000	0.363
LOX/RP-1	FUEL RICH	TRIPLET	2500 TO 3500	2000 TO 2400	0.44
LOX/RP-1	FUEL RICH	FAN FORMER	2500 TO 3500	2000 TO 2400	0.44
LOX/RP-1	OXIDIZER RICH	LIKE DOUBLET + SHOWERHEAD	2500 TO 3500	1600 TO 2000	35.3

configuration to be used for carbon deposition screening also was designed to provide data on carbon formation and deposition in the subsonic flow regime.

Injector Design Rationale.

Fuel-Rich LOX/Methane Triplet. The triplet injection element is well suited for systems involving pro-reactant density ratio and mixture ratio significantly differing from unity. The basic symmetry of the element and the use of two orifices for one reactant to a single orifice for the other reactant provides good mixing and atomization over wide ranges of operating conditions. Atomization and mixing are dependent on the penetration and dispersal of the center liquid stream by the outer gaseous oxidizer jets. The triplet has been applied successfully to liquid/liquid, gas/liquid, and gas/gas reactant systems over a wide range of mixture ratios, and density ratios. Problems are occasionally encountered in controlling mass distribution for chamber compatibility, and there is evidence that triplets are more sensitive to stability disturbances than some other common injector configurations.

The triplet element selected for this application utilized two gaseous fuel streams 0.063 inch in diameter impinging on a central liquid oxidizer stream of 0.045 inch in diameter. There were 36 elements in the selected triplet configuration.

Fuel-Rich LOX/Methane Pentad. Many of the same principles used in selection of the triplet element were also applied to the pentad element. The spray fans have symmetry and axial resultants regardless of mixture ratio and density unbalance. The mass dispersal is even less than for the triplet. The four elements of fuel impinging on the central liquid oxidizer can balance a significant density mismatch in gas/liquid injectors. The pentad injector selected had 19 elements with four 0.027-inch-diameter fuel streams impinging on a 0.056-inch-diameter oxidizer stream.

The pentad element also has a history of sensitivity to combustion pressure oscillations; the small diameter of the test section to be used and the low

mixture ratio operating points were felt to offer significant resistance to stability problems.

Fuel-Rich LOX/Methane Coaxial. The coaxial or concentric-element injector has been used with a great deal of success in gas/liquid rocket systems, primarily with hydrogen and liquid oxygen. In this element, an outer concentric flow of high-velocity gas strips droplets from, and mixes with, the low-velocity liquid in the center. Performance in mixing and atomization is characterized as a function of velocity ratio, or velocity difference, between the gas and the liquid reactants. The higher density of the methane gas, as compared to hydrogen or hot gas as on the SSME, reduces the available velocity ratio of the fuel, and there was some concern as to whether the mixing and atomization would be limited by these conditions. A porous material was used for the faceplate of the injector, between elements, to provide face cooling flow with some of the fuel.

In the coax injector configuration selected, there were 19 elements in the 2-inch face diameter. The 19 fuel annuli represent an area of 0.1752 in.^2 , i.e., a 0.019-inch annular gap. The oxidizer posts have a metering orifice of 0.0455-inch diameter with a 0.0955-inch-diameter exit.

Fuel-Rich LOX/RP-1 Triplet. The triplet element was selected for the liquid/liquid fuel-rich LOX/RP-1 gas generator for many of the same reasons as in the gas/liquid cases, i.e., the basic symmetry of the triplet element and its demonstrated ability to provide good atomization and mixing. Normally, unlike impinging elements are discouraged in systems using liquid oxygen and liquid hydrocarbons because of the infamous "detonable gels." Liquid oxygen freezes most common liquid hydrocarbons resulting in a "gel" or slush of premixed oxygen and fuel. This mixture does not appear to require vaporization in the reaction and, in many cases, is impact sensitive, resulting in a high explosive reaction.

Experience with unlike triplets in gas generator applications indicated that this should not be a serious problem. Two factors seem to preclude the gel problem: the low mixture ratio in which the thermal mass of the fuel is high enough to

resist the gel phenomena, and the smaller elements that will limit the accumulation of any large single masses of premixed propellants. This configuration was considered a high risk, but a high potential gain would be realized if the element selection performed satisfactorily.

The configuration selected had 27 elements, with fuel orifices of 0.055-inch diameter and 0.0447-inch-diameter oxidizer orifices.

Fuel-Rich LOX/RP-1 Like Doublet. The like-impinging doublet has become the traditional injector element for liquid oxygen/liquid hydrocarbon designs. Numerous engine and gas generator applications seemed to indicate that this was the most conservative approach to the liquid oxygen/RP-1 fuel-rich gas generator.

The injector element configuration was patterned after numerous high-performance like-doublet configurations. Radial elements provided circumferential "fans" (flat side to the combustor wall), and fan edge impingement was used to provide mixing. Fan radial offset was used in the outer row to provide a fuel-rich outer zone to enhance combustor wall compatibility. The 27-element injector had impinging fuel streams of 0.061-inch diameter and oxidizer streams of 0.034-inch diameter.

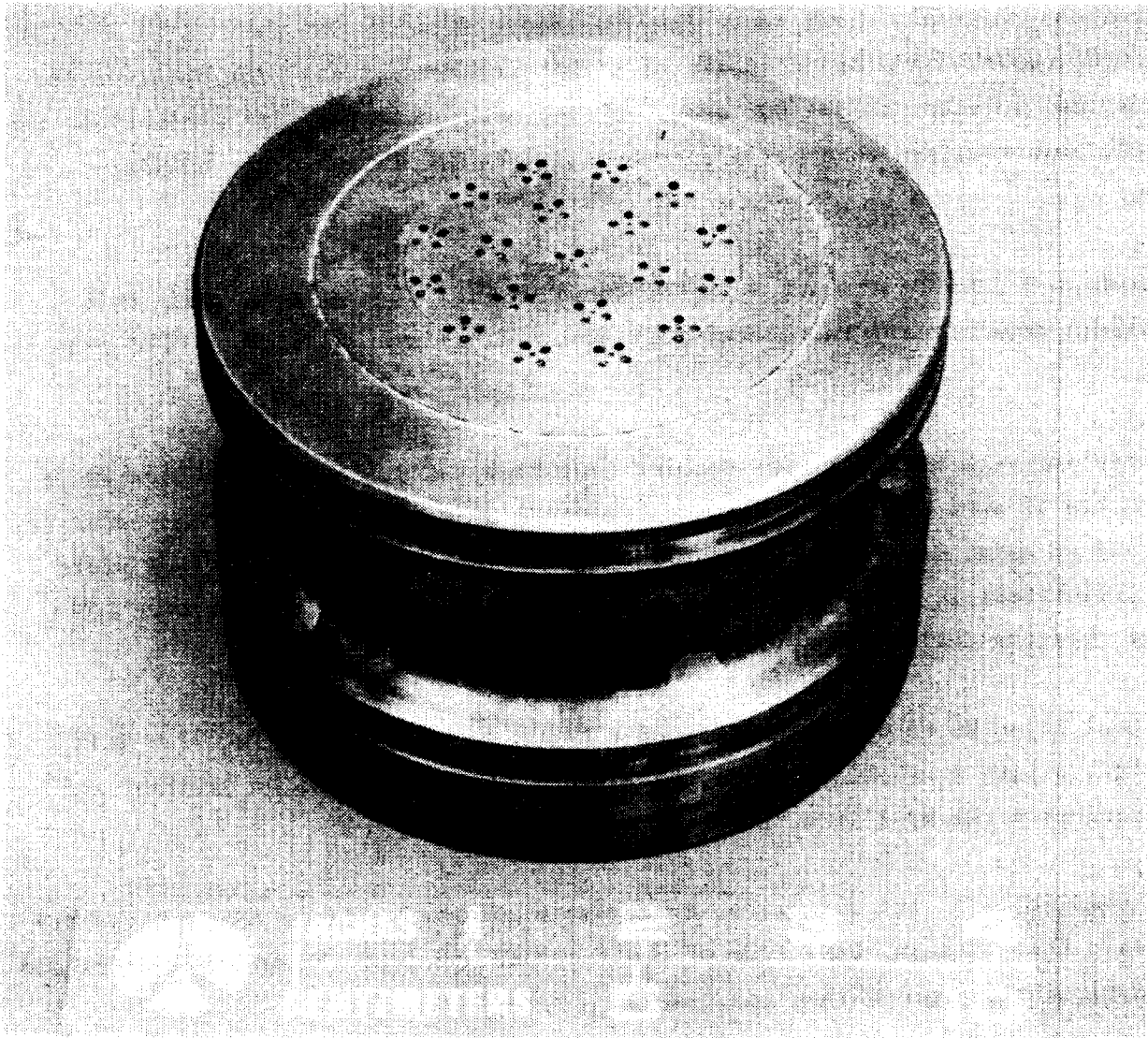
Fuel-Rich LOX/RP-1 Fan Former. The fan former injector was an outgrowth of several Rocketdyne studies of unconventional injection elements. Various injector configurations had been tested which would utilize the intersection of an exit slot with a manifold groove or feed hole to provide a spray "fan" similar to that produced by a like-impinging doublet element. The geometry utilized momentum exchange within the element geometry to produce this spray "fan" with a single-orifice element, which appeared to offer significant "packaging" advantages over a conventional like-doublet pattern. These individual elements were not well suited to quantity fabrication, so a configuration of intersecting slots and grooves was devised, which appeared to satisfy all the momentum relationships. Practical fabrication constraints limited this injector to only two rows of each propellant, and resulted in rather large slots and grooves. The total fuel slot area was 0.09734 in.²; the oxidizer slot area was 0.03672 in.²

Oxidizer-Rich LOX/Methane Pentad. The oxidizer-rich injectors presented a severe design challenge, with the extremely high mixture ratio at design point and operating conditions significantly different from the usual range. The pentad element was chosen for the liquid oxygen/gaseous methane operating conditions because it provided the best match in element sizing. Four liquid oxygen streams (0.056-inch diameter), impinge on a central gaseous methane system (0.027-inch diameter) for each of the 19 elements. The oxidizer streams would easily penetrate the central gas flow, and each combustion core would be expected to be encased in a cooler, oxygen-rich zone. The gross mismatch in both mass flow and volume flow ratio would seem to rule out any other impinging-type elements that did not similarly impinge several oxidizer flows on a single fuel stream. The liquid oxygen gel phenomena was not anticipated with a gaseous fuel, so a direct impinging pattern was selected to maximize mixing and atomization.

Oxidizer-Rich LOX/RP-1 Like Doublet/Showerhead. The oxidizer-rich operation with liquid oxygen and liquid RP-1 was acknowledged to be a very challenging task. The potential for the formation of a detonable gel was very high. The liquid oxygen flowrate was easily in excess of the amount required to gel all available fuel, and an ignition delay under these circumstances would be almost certain disaster. The injector design was contrived in an effort to counteract these problems by deliberately delaying the participation of part of the liquid oxygen from the initial reaction. The mechanism for providing this delay was to establish an injector face pattern of like-impinging doublets utilizing all of the fuel, and a portion of the oxidizer to result in a near stoichiometric local combustion condition (12 elements, fuel orifices of 0.018-inch diameter, and oxidizer orifices of 0.0336-inch diameter). The balance of the liquid oxygen was injected in relatively large (0.0666-inch diameter, 48 places) axial "showerhead" streams which would delay atomization and vaporization to downstream of the primary flame front.

Subtask 02200- Fabrication

During this subtask, all the component support hardware and the preburner assemblies were fabricated. Figure 19 illustrates the oxidizer-rich LOX/CH₄ pentad



1XX42-7/17/79-C1B

Figure 19. Oxidizer-Rich LOX/CH₄ Pentad Injector

ORIGINAL PAGE IS
UNCLASSIFIED

injector as originally designed. The 19-element injector was fabricated entirely from OFHC copper with the exception of a 304L stainless-steel ring required for sealing the injector to the LOX dome. During subsequent hot-fire evaluation, the injector was modified to provide a combustion chamber film coolant boundary layer.

The fuel-rich LOX/CH₄ triplet injector shown in Fig. 20 was fabricated. This 36-element injector was fabricated from 304L stainless steel with an OFHC face plate.

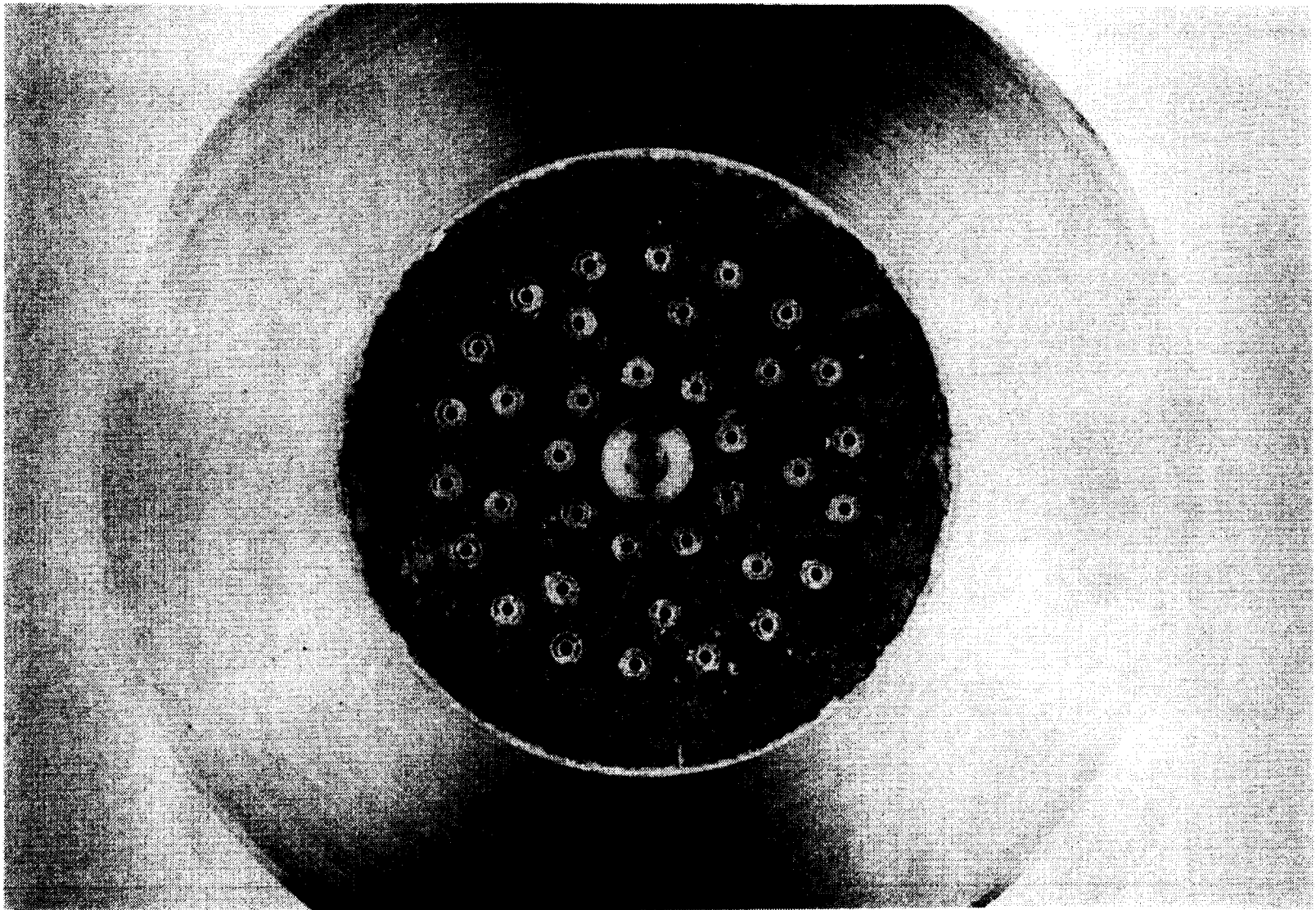
The oxidizer-rich LOX/RP-1 like-doublet plus showerhead injector illustrated in Fig. 21 has 12 sets of doublet elements designed to operate just slightly oxidizer-rich and 48 axial oxidizer orifices. The doublet elements were sized to yield near stoichiometric conditions just off the injector face with subsequent LOX deluge changing the overall bulk mixture ratio to 35.3:1.

The final injector to be fabricated under contract is shown in Fig. 22. This injector, a like doublet, has 54 doublet elements, 27 fuel and 27 oxidizer for operation with LOX/RP-1 in a fuel-rich environment.

After completion of the injectors, appropriate cold-flow checks were implemented to verify that passages were free of obstructions and that the pressure drops and flow distribution were within tolerances.

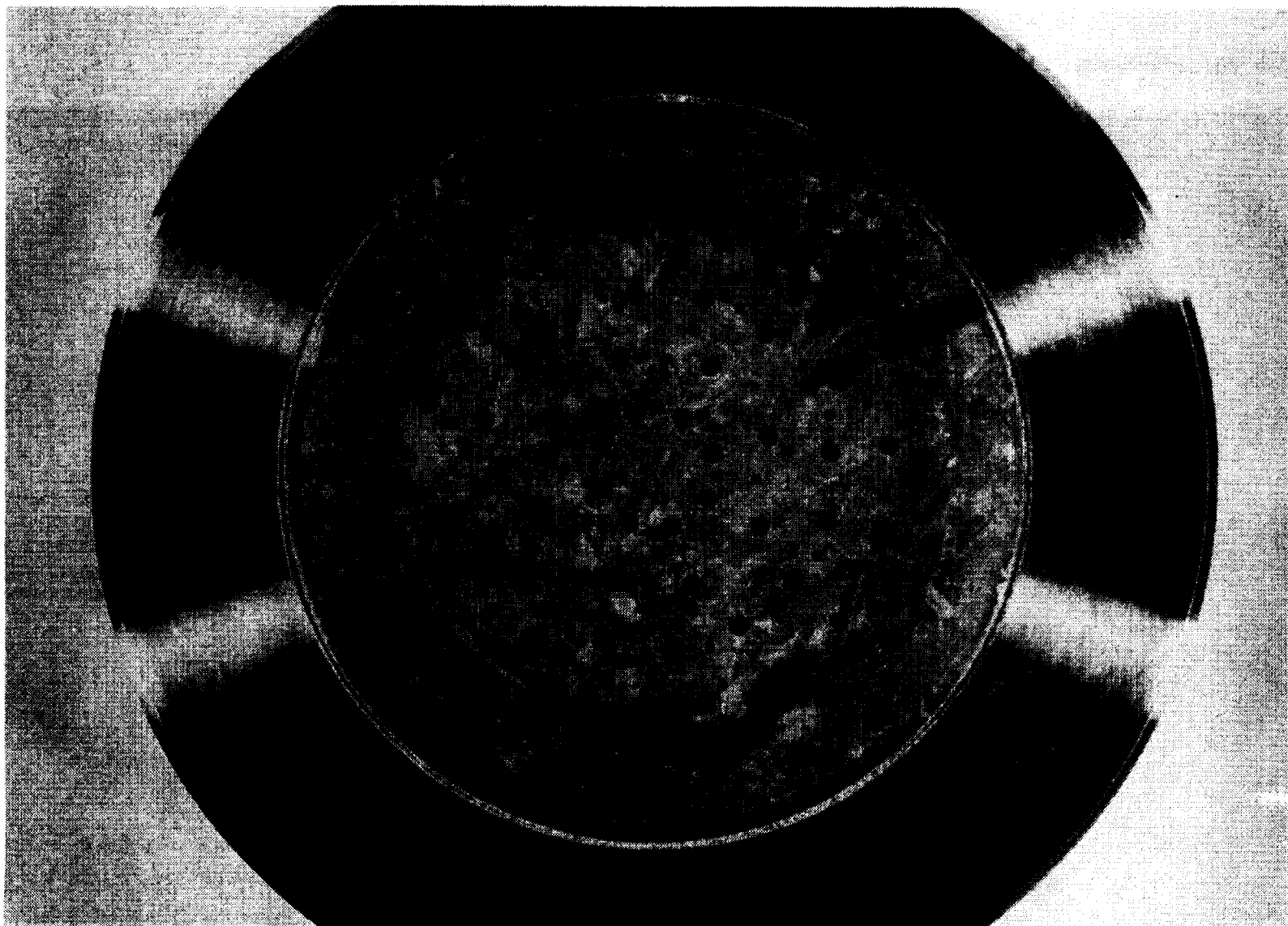
The ancillary hardware fabricated to support the injector evaluation is illustrated in Fig. 23. Three combustor lengths were fabricated: 4-, 6-, and 8-inch sections. These sections permitted a wide range of combustor lengths for performance evaluation. The nozzle illustrated was used for all injector configurations. The slotted nozzle shown in Fig. 24 was used in one test and was consumed immediately due to an injector instability. The thermocouple rake and the gas sampling sections shown in Fig. 25 were used throughout the program.

Some of the support hardware that was going to be subjected to oxidizing environments were plated with a protective coating of gold or nickel to resist the tendency of the stainless steel to oxidize and consume the hot hardware.



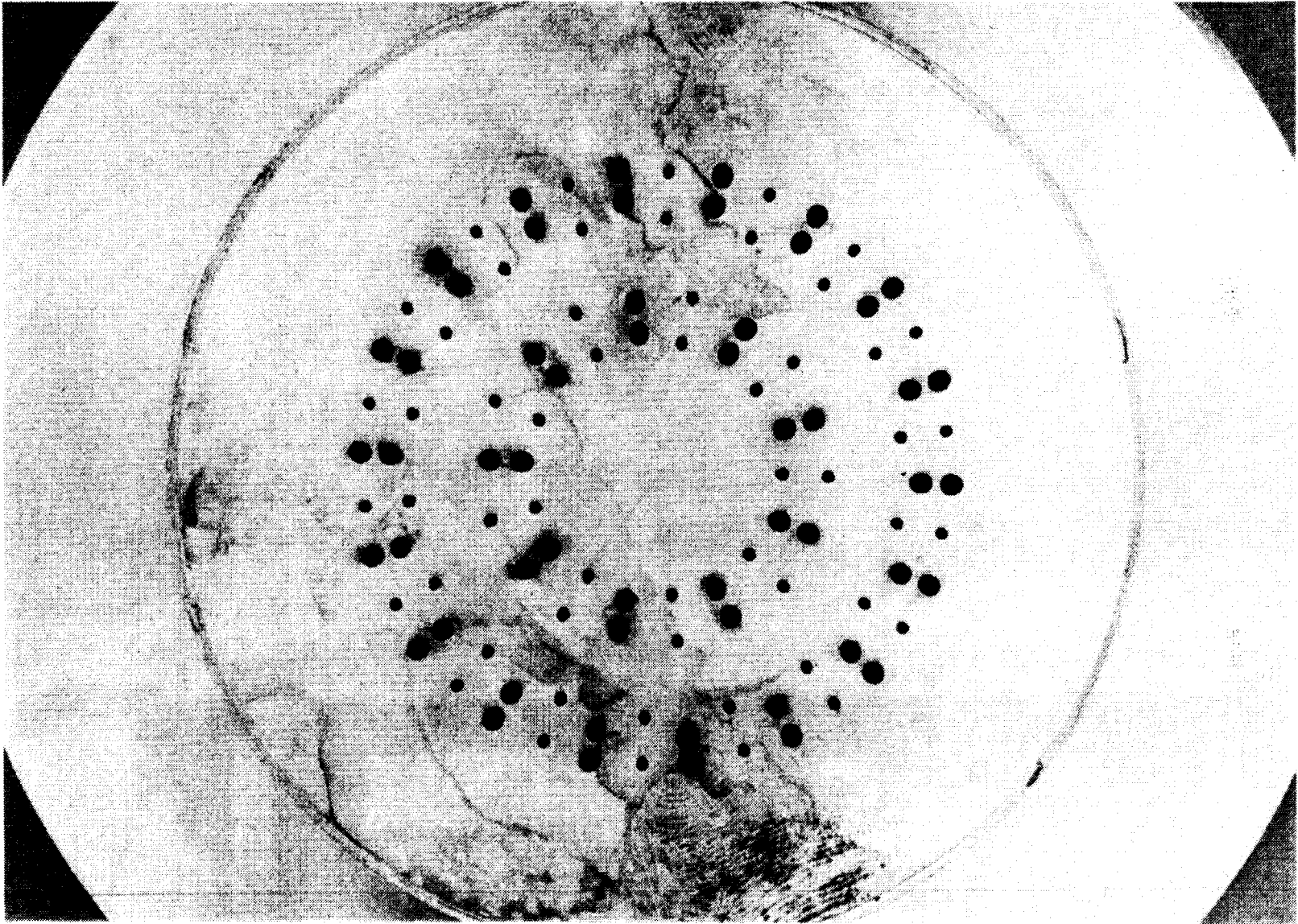
IHS31-8/27/79-C1D

Figure 20. Fuel-Rich LOX/CH₄ Triplet-Injector



IHS31-8/27/79-C1F

Figure 21. Oxidizer-Rich LOX/RP-1 Like-Doublet/Showerhead



1XX35-9/27/79-C1C

Figure 22. Fuel-Rich LOX/RP-1 Like-Doublet

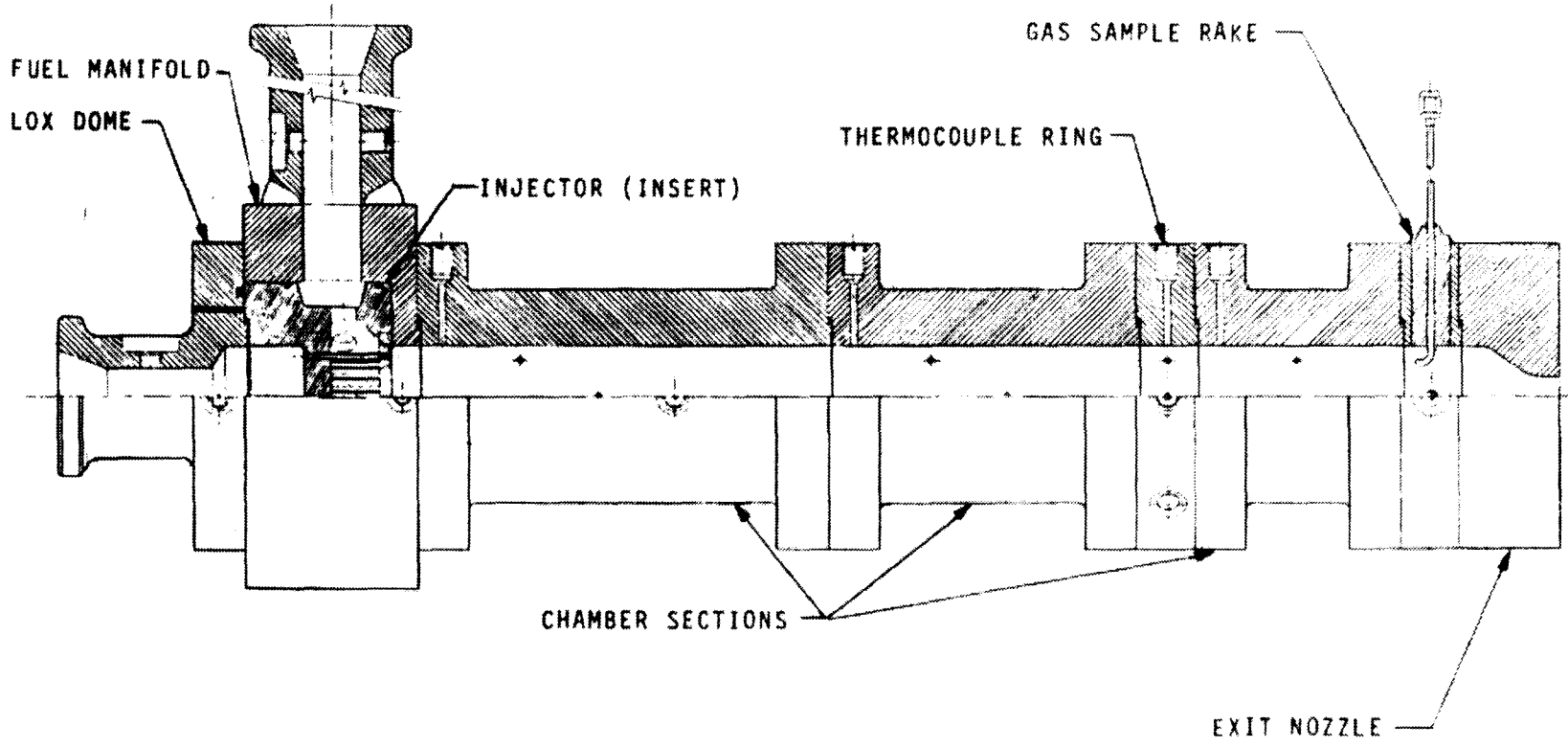
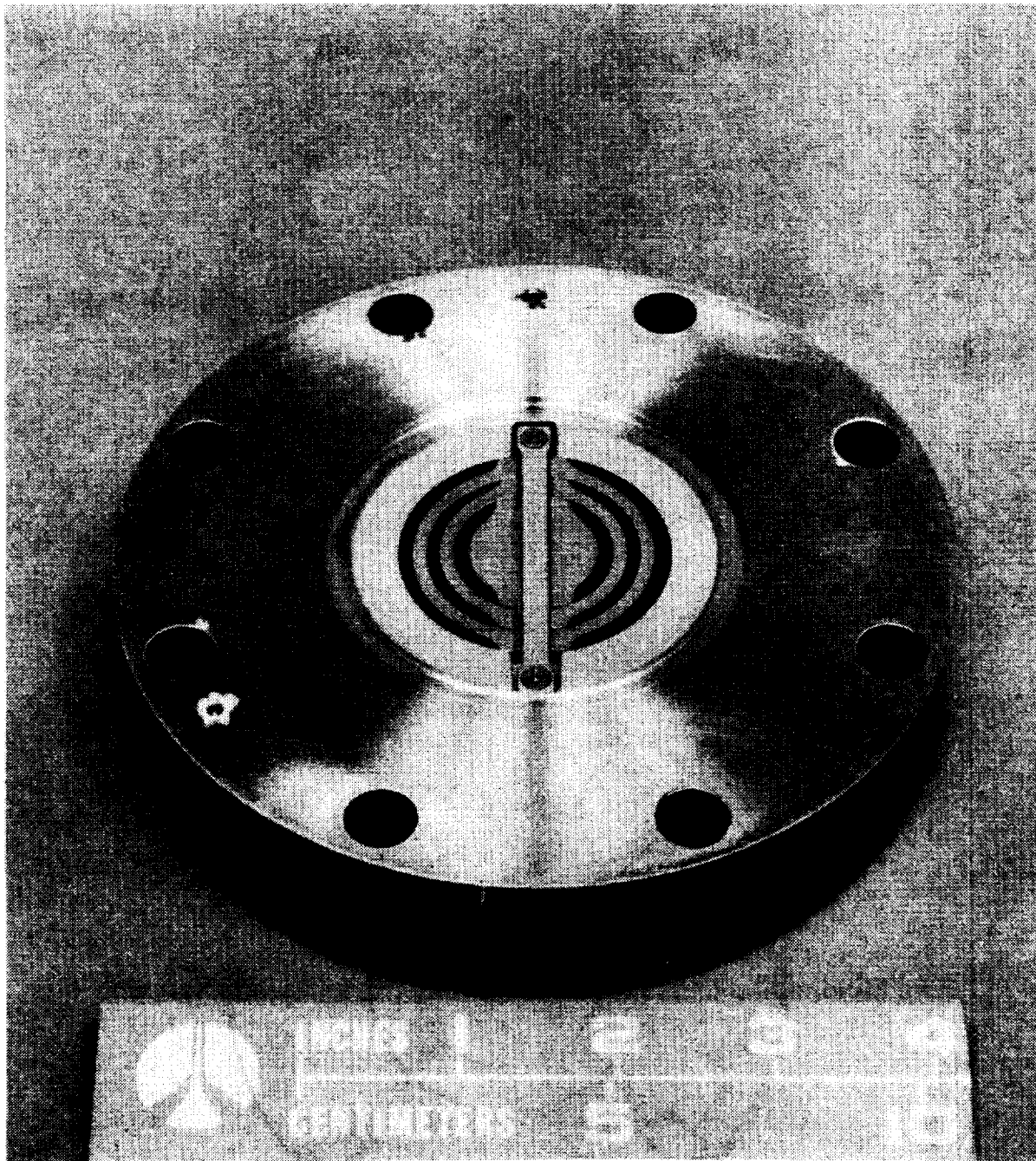


Figure 23. 2-Inch Preburner Test Hardware



1XX32-7/27/79-C1B

Figure 24. Slotted Carbon Deposition Insert

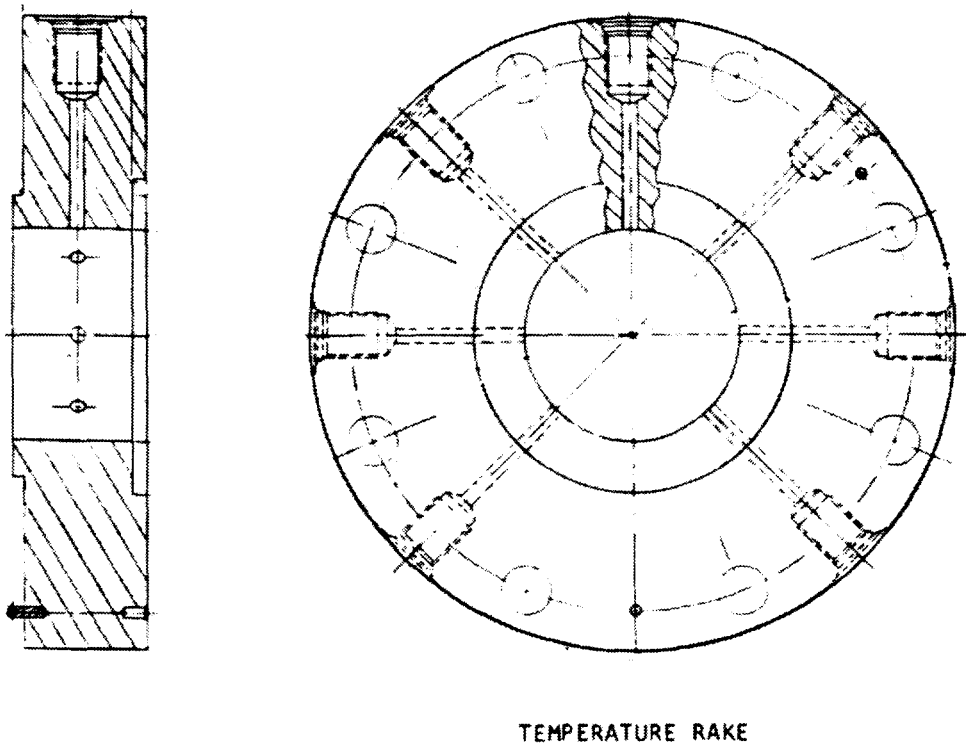
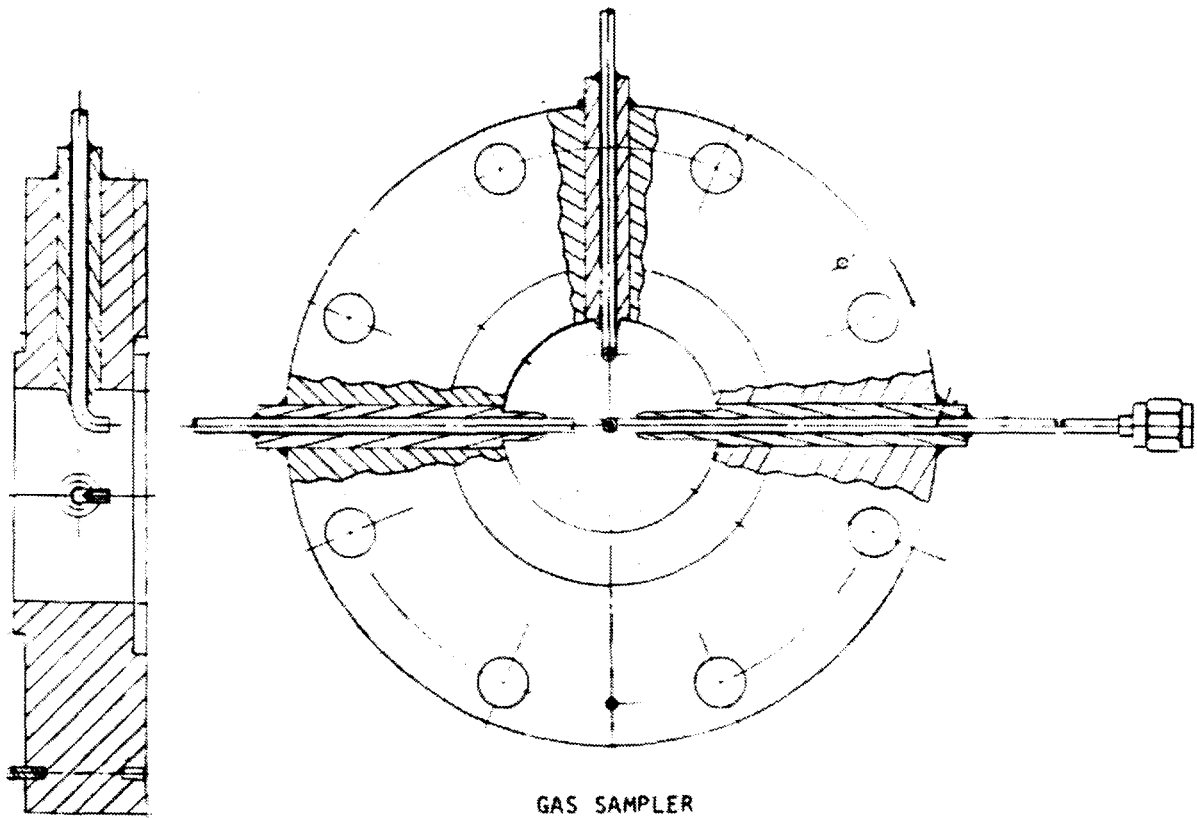


Figure 25. Combustion Gas Uniformity Measurement Segments

The nickel plate was used on the combustion chamber inner diameters because it has a higher melting point than the gold. The gold having superior oxidation resistance was used in areas such as the nozzle where oxidation at higher heat flux would be realized. Hot-fire test evaluation revealed poor adhesion of the nickel plating, resulting in spalling of the coating. The gold plating was eroded after a series of tests.



TASK III: SMALL-SCALE HARDWARE TESTING

Subtask 03100 - Testing

Santa-Susana Test Facility and Operations. The test effort in support of this contract was carried out in the Advanced Propulsion Test Facility (APTF), located at the Santa Susana Field Laboratory (SSFL). This test facility is capable of LOX/CH₄ and LOX/RP-1 preburner firings at chamber pressures up to 3500 psia. All major test stand fluid system components were sized to operate at chamber pressures up to 3500 psia. CTF/TEAB systems were used for engine ignition. Testing at the APTF complex is directed from a central blockhouse that houses control consoles, data recording systems, viewing TV screens, and automatic timers which control test functions with a 1-msec resolution capability.

The subscale preburner testing was conducting at Pit 2 in APTF. The existing capability of the test stand and related systems are described in the subsequent sections. Figure 26 is a flow diagram showing the major elements of the LOX and fuel systems. Figure 27 is the high-pressure test facility showing a LOX/RP-1 configuration and the three gas sample valves.

The test stand is equipped with an existing 40,000-pound-thrust mount for test firing. All test hardware propellant and pressurant systems are capable of providing a minimum of 20 seconds hot-fire duration without replenishment.

Propellant and Pressurant Systems.

LOX System. LOX was supplied to the test hardware from a 5000-psig-rated system. The system includes a 100-gallon-capacity, LN₂-jacketed tank and all the necessary components for operation. The main oxidizer valve is a hydraulically controlled servovalve capable of providing rapid shutdown-opening, adjustable ramp times, or discrete levels.

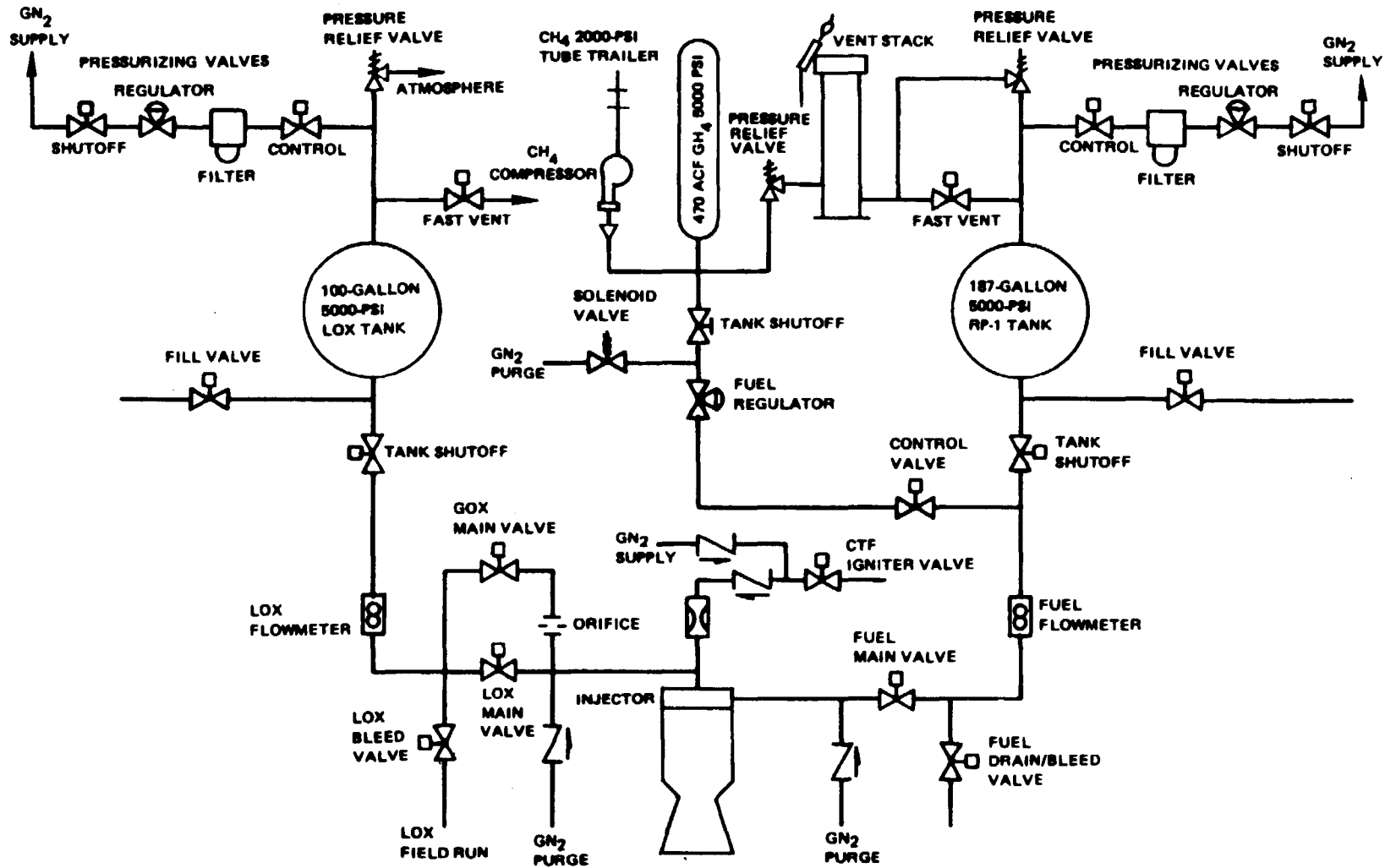
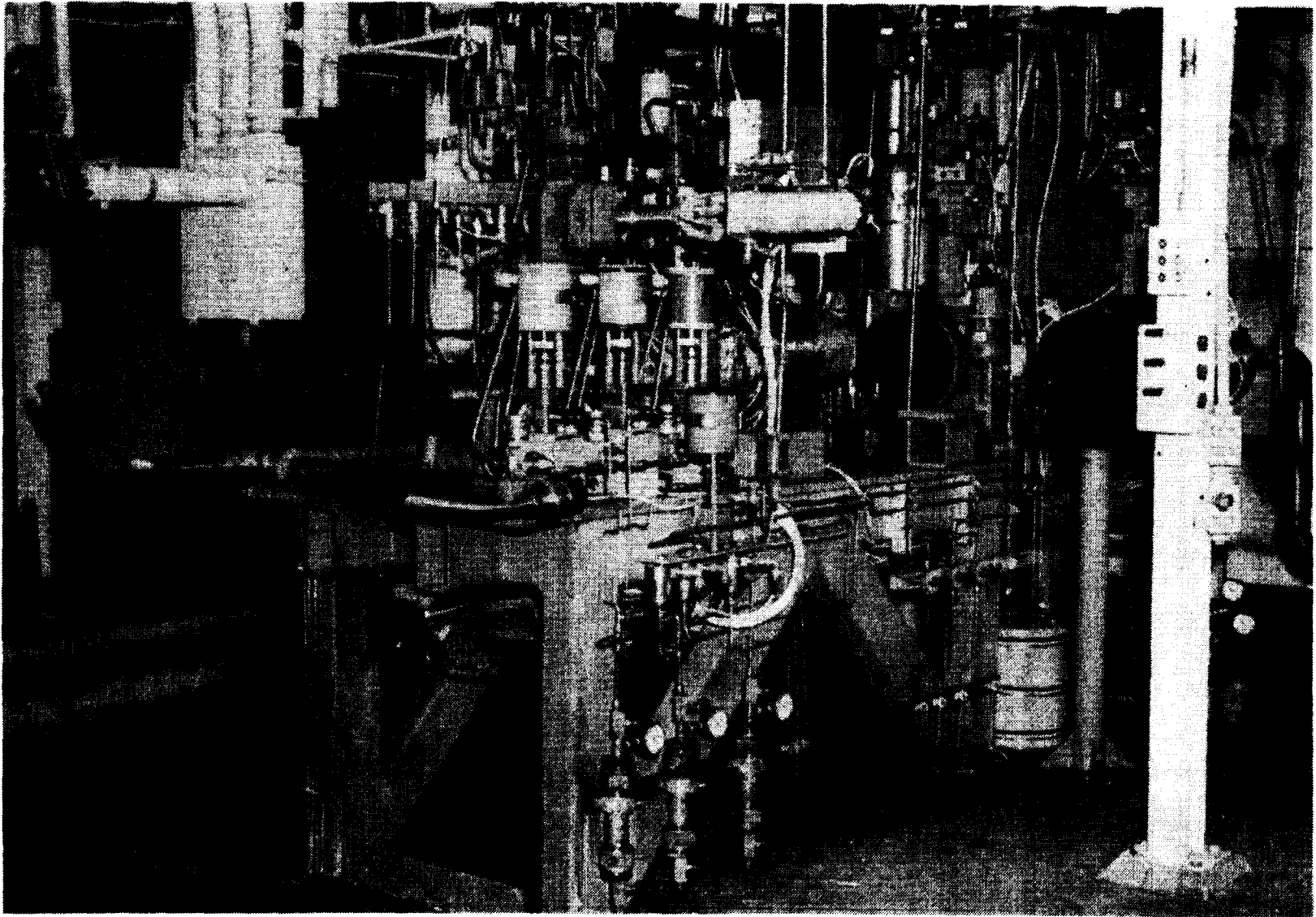


Figure 26. APTF High-Pressure LOX/Hydrocarbon Flow Diagram

51



50P36-4/3/80-S1A*

Figure 27. LOX/Hc High-Pressure Test Position

ALL INFORMATION CONTAINED
HEREIN IS UNCLASSIFIED
DATE 08-23-2011 BY 60322/UCBAW/STP

Gaseous CH₄ System. Methane was supplied to the test hardware as ambient gas, from a 470-acf storage bottle and facility piping system rated at 5000 psi. Methane was supplied from commercial gas transport trailers and boosted up to a maximum of 5000 psi by on-site gas compressors. The main fuel valve is also a hydraulically controlled servovalve capable of various functions.

Ignition System. CTF/TEAB systems were used successfully in this program and provided smooth ignition-to-mainstage transitions.

GN₂ Storage and Distribution. The GN₂ storage system includes two 470-ft³ gas bottles rated at 3000 psig and one existing 470-ft³ gas bottle rated at 5000 psig.

Control and Instrumentation. Rocketdyne has instrumentation and control systems at the APTF control center consisting of digital display capacity (24 displays) for on-line readout of pressure and temperature, and the analog system. Basic instrumentation for this program was used.

Digital Data Acquisition System. Rocketdyne used an existing 100-channel data system at APTF. This system ensured adequate capacity and data sampling rate for the program. The recorded data were processed on the Rocketdyne Canoga-based IBM 360/50, which is a high-speed terminal for the Western Computing Center.

Analog Data System. Data inputs were recorded on FM magnetic tape and on direct-print oscillographs. The magnetic tape was replayed into an oscillograph for "quick-look" data reduction, and was sent to the analog laboratory for further processing.

Data Measurements. All measurements were made with instrumentation evolved over years of research and development of high-performance rocket propulsion components and systems.

Test Operations and Sequencing. All test operations at APTF were performed under the direction of the test engineer. Operational sequences were used similar to those employed successfully on other test programs at APTF and modified per engineering requirements.

Activation of APTF at SSFL was realized using a fuel-rich LOX/CH₄ pentad injector from a Rocketdyne Independent Research and Development (IR&D) program. After system characterization and injector evaluation, the fuel-rich LOX/CH₄ triplet contract injector was installed. The first contract test was conducted 27 November 1979, and the objective was to demonstrate mainstage ignition and stable steady-state operation. This test had a scheduled 1-second mainstage, but demonstrated a tangential instability mode. The injector was removed and replaced with a Rocketdyne-funded coaxial configuration.

On 19 December 1979, the fuel-rich LOX/CH₄ triplet injector testing continued using acoustic absorbers. Three additional tests were conducted using first a quarter-wave followed by tuned Helmholtz absorbers. The test objective was the same with both absorbers--to demonstrate stable mainstage steady-state operation. These tests were unsatisfactory, being terminated in less than 1 second. Combustion instabilities were encountered during the triplet evaluation, even when a quarter-wave Helmholtz acoustic absorber was used.

Subsequent to these tests, the facility was modified to provide an oxidizer-rich LOX/CH₄ environment. A pentad injector with a Helmholtz absorber was tested in this environment on 23 January 1980. The test was terminated by a redline cutoff and resulted in severe hardware damage. A facility malfunction caused the LOX tank pressure to collapse at start, permitting combustion temperatures to exceed the autoignition temperature of the combustor/nozzle material.

The facility was converted to LOX/RP-1, and the contract impinging like-doublet injector was evaluated with and without an absorber. Five hot-fire tests were conducted with facility malfunctions resulting in the loss of some data. During the first test (004), severe degradation of the RP-1 tank pressure was realized.

Test 005 resulted in a premature cutoff due to an excessive chamber pressure. Both tests were targeted for performance and stability evaluation at 1900 R chamber conditions. Combustion oscillations encountered during test were within contractual specified limits. During test 006, severe degradation of the carbon deposition checking device was realized. Test 007 resulted in a premature cutoff due to a faulty thermocouple cut circuit. Both tests were targeted for performance, carbon, and stability evaluation at 1900 F chamber conditions. Combustion oscillations encountered during these tests were out of contractual specified limits. Test 008 resulted in combustion oscillations exceeding the $\pm 10\%$ level after 4 seconds of mainstage. Gas sampling was the test objective, but was not realized because of the premature cutoff.

The facility was converted to an oxidizer-rich LOX/RP-1 test configuration after completing an evaluation of a company-funded triplet injector. The oxidizer-rich, like-doublet/showerhead injector test was terminated prematurely with hardware degradation. Analysis of the two oxidizer-rich injector configurations showed considerable mixture ratio deviation during the ignition/mainstage transition using a oxidizer hypergolic propellant. Sequencing of the facility valves dictated a fuel hypergol would assist in the safe transition to an oxidizer-rich mainstage. A review of ignition systems showed a TEA (triethyl aluminum) system would permit an oxidizer-rich engine start. A TEA system was installed in the facility, permitting a "slug" of TEA to be injected or pushed ahead of the RP-1 or CH_4 . This system was used for all subsequent oxidizer-rich testing.

During this interim period, two fuel-rich LOX/ CH_4 injectors were evaluated under Rocketdyne's IR&D funds.

From 1 August through 18 November 1980, 14 hot-fire tests were attempted, 11 evaluating an oxidizer-rich LOX/ CH_4 pentad and 3 evaluating an oxidizer-rich LOX/RP-1 like doublet and showerhead. The modified pentad injector was evaluated with some facility difficulty. The like-doublet/showerhead injector configuration was tested unsuccessfully, even with substantial facility and hardware modifications. With the repeated hardware damage realized, the program objectives were reviewed and all subsequent small-scale hardware evaluations were terminated.

During the hot-fire test evaluation of the fuel-rich preburner assemblies, a substantial difference was noted in the exhaust plume between LOX/CH₄ and LOX/RP-1. Figures 28 and 29 show the respective exhaust plume from the same vantage point. It is evident from the photos obtained from a movie camera frame that the LOX/RP-1 configuration results in a high carbon gas content while the LOX/CH₄ exhaust is transparent.

Subtask 03200 - Data Analysis

In support of the data analyses of the small-scale test effort, a data reduction program was written. This program, in conjunction with the scaling data program for the high-pressure LOX/hydrocarbon preburner test series, resulted in a compilation of all the critical parameters and calculations of various relationships. This data reduction program was hooked up to the scaling program and resulted in an overall printout summarizing the individual tests. The data reduction program can be used for LOX/gaseous CH₄ or LOX/room-temperature RP-1 simply by flagging a code at a specified vector location. The program is set up to provide reduced performance data for 11 consecutive data slices for a predetermined duration. Each instrumentation parameter has an identification number and this number/vector is used throughout the program computations. With the aid of this program and the FM tape analysis, the following observations are reported and data summarized.

A summary of all the tests conducted to date under NASA contract and Rocketdyne IR&D on the High-Pressure LOX/Hydrocarbon program is shown in Table 6. The gas sampling experiments have resulted in numerous data which are reported in a subsequent section.

Model Analysis Assessment. The technique used to analyze the performance of the preburner injectors assumes that the kinetic effect of the gases is independent of the injector design. The standard mixing and vaporization analysis then determines the injector performance. In preburner chambers, a pseudoequilibrium, correlated with gas generator experience, is assumed. It has been postulated that if the gas sampling data realized during previous test activities are available and realistic an interaction with the kinetic model could eventually lead to a more accurate and

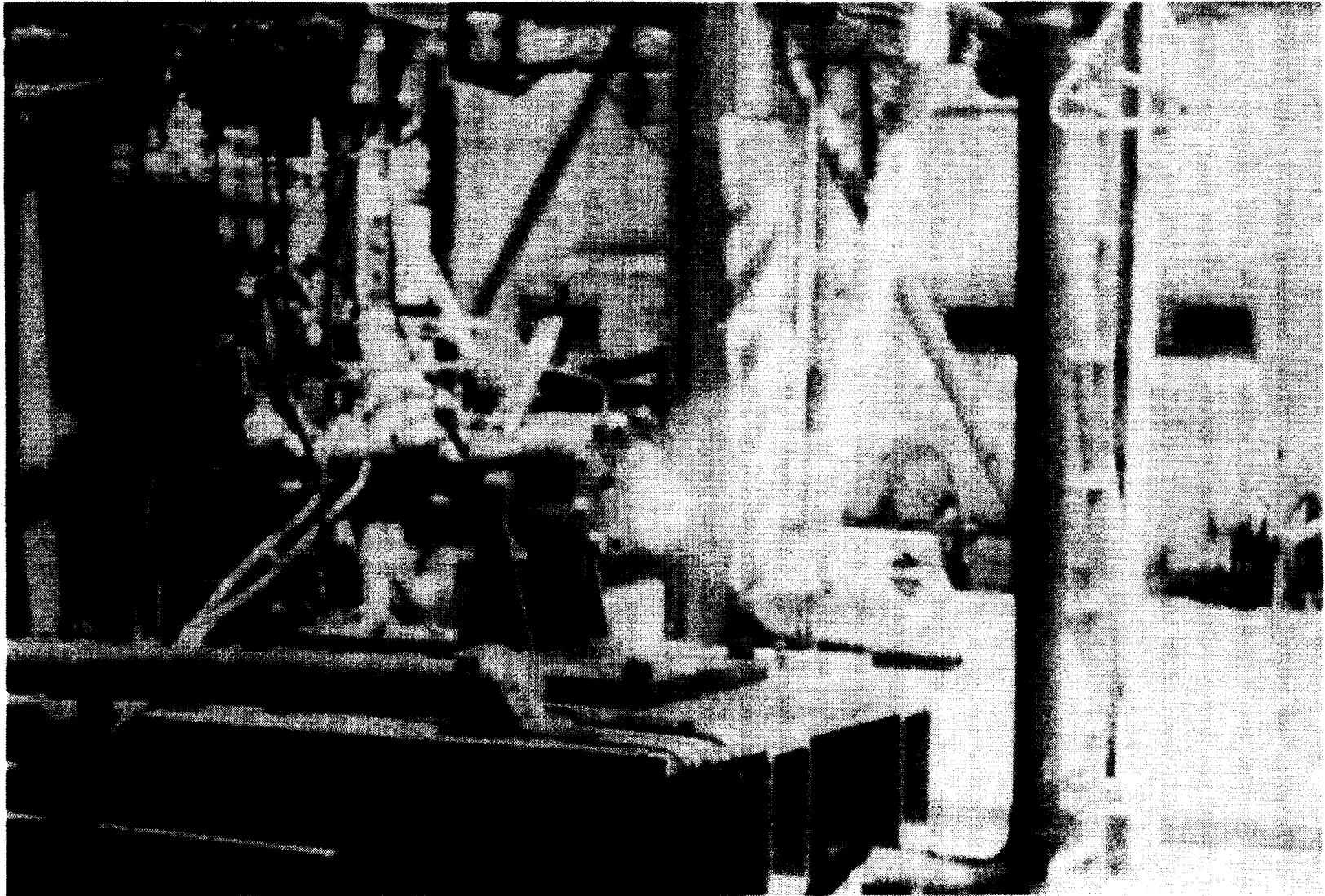


Figure 28. Fuel-Rich LOX/CH₄ Test Firing

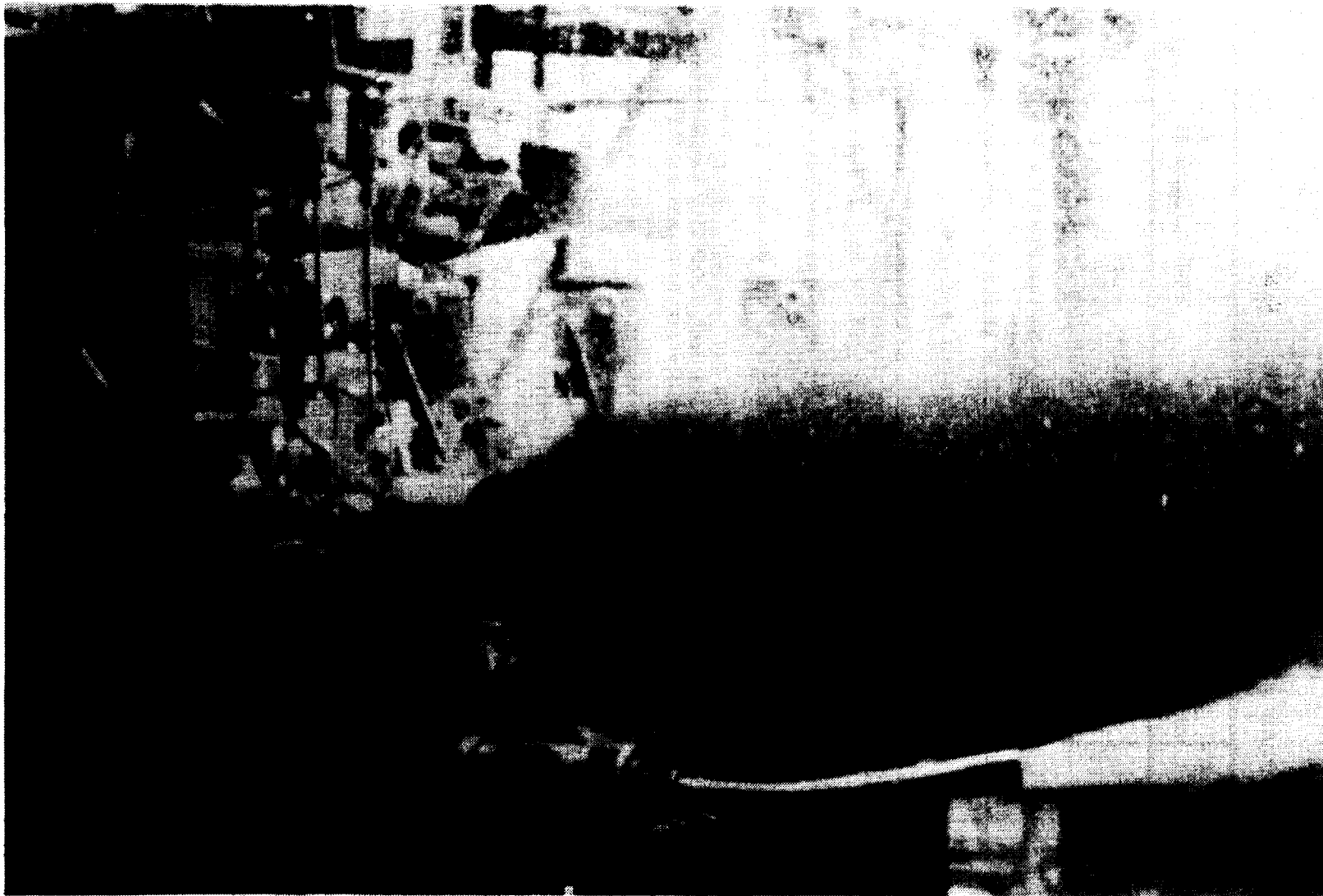


Figure 29. Fuel-Rich LOX/RP-1 Test Firing

TABLE 6. LOX/HYDROCARBON HIGH-PRESSURE PREBURNER DATA SUMMARY

TEST NO.	TEST DATE	INJECTOR	PROPELLANT	CHAMBER LENGTH INCHES	P _c , PSIA	OXIDIZER INJECTOR PRESSURE, PSI	FUEL INJECTOR PRESSURE, PSI	\dot{W} , NO/SEC.	T _c , R	O/F	c* _{act}	DURATION, SEC	RESULTS/COMMENTS
001-9	10-30	Pentad	LOX/CH ₄ fu	17"	-	-	-	-	-	-	-	-	CTF ignition only.
002	11-2	"	"	"	3450	-	-	-	-	-	-	.33	Facility malfunction - LOX inj. pressure low cutoff.
003	11-16	"	"	"	3391	4216	4183	15.2	2239	.537	4033	5.5	Unstable - no absorbers ~ ± 9% oscillations - nozzle damage.
004	11-27	Triplet	"	"	3406	4160	4226	16.9	1747	.373	3652	1.3	Unstable ~ 14,000 Hz - no absorber.
005	12-5	Coax .5D	"	"	3382	4158	4239	15.2	2116	.523	4022	1.4	Stable - no absorbers.
006	12-12	Coax 1.0D	"	"	3570	4185	4260	17.6	1747	.368	3660	5.2	Stable - no absorbers - over pressure on face - damaged injector
007	12-19	Triplet	"	"	3280	-	-	-	-	-	-	.25	Unstable ~ 13,000 Hz 1/4 wave absorber
001-0	1-8	Triplet	"	"	2450	-	-	-	-	-	-	.25	Unstable Helmholtz absorber - facility abort.
002	1-8	"	"	"	3522	4189	4210	14.6	1850	.427	3993	1.4	Unstable ~ 11,000 Hz Helmholtz absorber.
003	1-23	Pentad	LOX/CH ₄ ox	18"	3650	-	-	-	-	-	-	.50	LOX low inj. pressure cutoff-CTF ignition-hardware damage-facility malfunction.
004	2-29	Like Double	LOX/RP-1 fu	19"	3559	4246	4176	19.8	2084	.481	3232	5.20	Marginally stable-no absorber ± 5% oscillations
005	3-20	"	"	"	3557	4188	4132	18.6	2270	.475	3471	2.00	Marginally stable-no absorber ± 5% oscillations PSC cutoff.
006	4-1	"	"	"	3583	-	-	-	-	-	-	.50	Unstable ~ 1850 Hz longitudinal mode-Helmholtz absorber-hardware damage.
007	4-3	"	"	"	-	-	-	-	-	-	-	-	Erroneous skin temp cutoff-abort facility malfunction.
008	4-9	"	"	"	3641	4223	4220	18.6	2071	.453	3319	4.00	Sampling unstable ~ 14,000 Hz - Helmholtz absorber-PSC cutoff.
009	4-17	Triplet	"	"	3562	4207	4201	17.7	2182	.456	3423	5.00	Stable ~ ± 2% 7 cavity Helmholtz absorbers.
010	4-18	"	"	"	3620	4212	4276	17.7	2155	.430	3469	5.10	Sampling-stable ~ ± 2% Helmholtz absorbers.
011	4-24	"	"	14"	3678	4184	4338	15.6	2132	.381	3902	1.50	Coking-Stable ~ ± 2% Helmholtz absorber-Turbine simulator overpressure c/o
012	4-29	"	"	"	3670	4114	4252	15.8	2107	.389	3852	7.80	Coking-Stable ~ ± 2% Helmholtz absorber-Turbine simulator overpressure PSC cutoff.
013	5-13	"	"	9"	3421	-	4252	19.4	2054	.385	2994	12.35	Performance - absorber.
014	5-15	"	"	"	3381	3953	4259	20.0	2030	.366	2876	5.35	Sampling - absorber.
015	5-15	"	"	"	3353	3940	4311	20.6	1856	.356	2771	5.35	Sampling - absorber.
016	5-16	"	"	"	3672	4101	4359	17.0	1910	.352	3665	1.09	Material investigation - absorber.
017	5-20	"	"	13"	3401	4040	4250	19.8	1973	.394	2922	5.35	Performance - absorber.
018	5-22	Fan Former	"	"	3850	-	-	-	-	-	-	.33	Unstable - injector burnout - PSC cutoff.

59

BOLDOUT FRAME

2

58-a

BOLDOUT FRAME

TABLE 6. (Concluded)

TEST NO.	TEST DATE	INJECTOR	PROPELLANT	CHAMBER LENGTH INCHES	P _c , PSIA	OXIDIZER INJECTOR PRESSURE, PSI	FUEL INJECTOR PRESSURE, PSI	\dot{W} , NO/SEC.	T _c , R	U/F	c* _{act}	DURATION, SEC	RESULTS/COMMENTS
019	6-3	Like Double Showerhead	LOX/RP-1 ox	19"	-	-	-	-	-	-	-	.15	LOX low inj. pressure cutoff-CIF ignition-hardware burnout.
020	6-17	Solid Coax	LOX/CH ₄ fu	12"	2000	-	-	-	-	-	-	.67	Fuel low inj. pressure continue cutoff.
021	6-17	"	"	"	3500	-	-	-	-	-	-	.65	Fuel high inj. pressure cutoff.
022	6-25	"	"	"	3430	4198	4232	13.1	2398	.752	4353	5.46	Performance successful-no acoustic device.
023	6-27	"	"	13"	3508	4231	4213	12.2	2360	.805	4766	5.45	Sampling - successful.
024	7-1	"	"	9"	3472	4187	4196	12.8	2347	.759	4459	5.46	Sampling - successful.
025	7-3	"	"	19"	3458	4164	4233	13.0	2377	.735	4360	5.46	Sampling - successful.
026	7-16	Rigimesh	"	12"	3554	4110	4296	13.8	2127	.535	4262	5.48	Successful.
027	7-16	Coax	"	"	3541	4140	4190	13.3	2242	.599	4420	5.48	Successful.
028	7-18	"	"	9"	3420	4006	4286	14.8	2251	.501	3841	5.57	Sampling - successful.
029	8-1	Mod Pentad	LOX/CH ₄ ox	12"	3347	3783	4168	18.0	2109	31.1	3079	1.90	CH ₄ line pressure high cutoff-facility malif. timer caused fu rich shutdown.
030	8-6	"	"	14"	2425	2831	2864	17.3	1480	43.1	2330	5.14	Successful.
031	8-6	"	"	"	3275	4165	3940	26.3	1268	50.9	2061	5.16	Successful.
032	8-8	"	"	"	3423	4215	4258	24.7	1503	42.1	2293	5.15	Successful.
033	8-8	"	"	"	3520	-	-	-	-	-	-	.69	LOX low inj. pressure cutoff-data shows restricted flow thru flowmeter.
034	9-4	"	"	12"	3459	4206	4155	24.1	1676	44.0	2380	5.15	Successful.
035	9-4	"	"	"	~3500	-	-	-	-	-	-	.30	LOX low inj. pressure cutoff-LOX tank cycling.
036	9-11	"	"	8"	~3500	-	-	-	-	-	-	.36	LOX low inj. pressure cutoff-data shows restricted pressure transducer.
037	9-16	"	"	"	3540	4298	4201	23.0	1737	43.0	2554	.92	PSC cutoff-data showed erroneous cut.
038	9-18	"	"	"	3560	-	-	-	-	-	-	.69	LOX high inj. pressure cutoff.
039	9-18	"	"	"	3446	4189	4112	24.3	1516	44.9	2355	5.15	Successful.
040	9-30	Like Double Showerhead	LOX/RP-1 ox	12"	2478	-	-	-	-	-	-	.69	PSC cutoff-longitudinal instability bursts-LOX tank cycling.
041	10-25	"	"	"	3520	-	-	-	-	-	-	.65	LOX inj. pressure low cutoff hardware damaged.
042	11-16	"	"	"	3440	-	-	-	-	-	-	.64	LOX inj. pressure low cutoff hardware damaged. Extensive facility mods pretest.

59
FOLDOUT FRAME59-0
FOLDOUT FRAME

validated model to predict the overall performance of the LOX/hydrocarbon pre-burner. As can be shown in the following paragraph and the results of the gas sampling analysis, the performance prediction for the LOX/CH₄ preburner is very close to the experimental values. The collected CH₄ in the gas sample also correlates well with the kinetic model prediction. Some discussion of the measured c* values will help to evaluate the analysis and provide for future improvement.

The hot-fire tests have basically two persistent results: (1) the measured LOX/RP-1 preburner c* is equal to or less than the characteristic velocity efficiency based on the combustion model results, and (2) the measurement for the LOX/CH₄ is as predicted. Both preburners were operating in a fuel-rich environment. Of the LOX/CH₄ cases, it is shown that the chamber length has no effect on the measured c*; vaporization is complete. Although the impinging-type injectors were unstable, the average measured c* seems to be independent of the injection type, suggesting the mixing is complete. The remaining variable is the kinetics. Gas sample analyses has shown that between 24 to 35% CH₄ has dissociated or reacted depending on the mixture ratio. The kinetic model has predicted that approximately 20% CH₄ will be converted in a 10-inch distance and at a mixture ratio of 0.35.

The analytical model has predicted excellent mixing for all the injector types primarily due to the off-mixture ratio and the high injection element density. Hot-fire test has verified the excellent mixing for the LOX/CH₄ candidates. Since the LOX/CH₄ injectors have only one cryogenic propellant to be vaporized, they are not considered to be vaporization limited. The gas sample analysis has shown only traces of hydrocarbon condensate. Thus, the results are representative of the injector mixing performance. The overall performance has achieved the modified equilibrium as shown by the measured c* value. Although the triplet and the pentad designs are both unstable, it is believed their performance are superior to the coaxial injector.

For LOX/RP-1, the unlike triplet has demonstrated good performance as correlated by the modified equilibrium model. However, from the gas sample analysis and the results with turbulator added, the tests tend to indicate that both the mixing and the vaporization would not be as predicted. The results are questionable since the

addition of the turbulator improved the measured c^* above the theoretical equilibrium, but did not substantially increase the measured combustion temperature. Unfortunately, gas sample data were not available to substantiate the results. The collected gas samples showed a higher-than-expected liquid hydrocarbon. The results can be biased as liquid droplets traversed the chamber slower and represent a higher mass concentration. The data show a wide variation in the collected weight percentage. Hence, it is reasonable to conclude that the LOX/RP-1 preburner also performs as predicted.

It should be noted that there is always uncertainty in the analytical model (LISP). The empirical model is based on cold-flow data. The mass flux distribution and droplet sizes as a result of atomization are in the thrust chamber operation regime. Consequently, the extrapolation for the off-mixture ratio preburner condition should have additional cold-flow validation. Both the mass flux and the droplet distribution are dominant factors in determining the performance of any combustion device.

The condition has changed substantially when excess oxidizer exists in the gas generator. The liquid oxygen is relatively easy to vaporize. Therefore, the injector performance is only mixing limited. The LOX/CH₄ injector has performed as the model predicted near the design mixture ratio. Some performance degradation can be seen at the higher mixture ratio. It is very likely that the mixing is less effective because the higher LOX jets may separate the CH₄ gas stream. Therefore, less mixing surface is available as the CH₄ gas zones are separated. To corroborate this, one can use only the result for the lower-than-design mixture ratio case which has a measured c^* value above the theoretical equilibrium.

The oxidizer-rich LOX/RP-1 condition is more complicated. Unfortunately, the facility problems during the start transients caused chamber failure. No data are available for analysis.

Further analysis and additional experimental data on the chemical reaction rates of these LOX/hydrocarbon propellants are required for improving the kinetic assumptions. This information would influence the vaporization model because the energy available for droplet vaporization and the droplet heat flux are dependent on the surrounding environment. This is especially important for liquid/liquid injection. The vaporization process and the kinetic reaction process are difficult to decouple and analyze separately. Empirical data and the results from this program show that simple experimental correlation suffices.

Because preburner injectors are inherently more stable than main injectors, due to the low energy release of partial combustion, only a cursory investigation was made of the stability ratings for the tested injector configurations. The instabilities realized during hot-fire testing of the 2-inch hardware were not anticipated. The damage sustained by the hardware showed localized combustion temperatures were in excess of those anticipated based on predictions.

Subsequent high-frequency data showed a 13K to 14K Hz pressure oscillation had occurred. The pressure phase relationship and the damage indicated a tangential mode even though the wave frequency calculation using the equilibrium gas temperature could not correlate with the data. From the chamber damage, higher-than-expected gas temperature could be assumed. It was theorized that mixture ratio has changed in the chamber due to the injector response. To prevent its future occurrence, some analyses should be done to find both the triggering mechanism and a suitable fix.

The instability realized generally appeared during start and persisted until cut-off, indicating the injector is inherently unstable. Both the triplet and the pentad are very high-performance injectors and, thorough mixing, LOX atomization and subsequent vaporization (combustion) are rapidly achieved. If the rate of energy release is such that a strong pressure wave is formed and matches the chamber mode, the burning process would be influenced by the chamber acoustics. Assuming the overpressure does not affect the combustion process because the propellants are mixed and burned rapidly, the only variable left which can be affected would be the injection process. The injectors should have been examined

more thoroughly as the possibility exists that its hydraulics were coupling with the chamber mode. The results could be extensive injector mixture ratio excursions. This may help to explain the higher-than-expected gas temperature. This phenomenon should be limited only to the injector end. The bulk gas temperature in the chamber will remain constant as the oscillation can not affect the bulk chamber condition. The oscillating component of the mixture ratio diminishes as it progresses down the combustion chamber.

Injector Test Summary.

Fuel-Rich LOX/CH₄. Hot-fire testing of the 19-element pentad injector indicated stability problems, and excessive thermal damage to the head end of the combustion chamber. Helmholtz chambers were not successful in damping the chamber pressure oscillations. It is not clear whether the instability was connected to the hardware damage, or if two separate problems existed. Indications are that a relatively oxidizer-rich zone exists near the injector face, and recirculation drives the mixture to the head end of the chamber. The addition of fuel film cooling probably would cure the physical problem of head end heating and burning, but it is doubtful that this change would have a stabilizing influence.

The hot-fire testing of the 36-element triplet injector produced similar results to the fuel-rich LOX/CH₄ pentad. Severe chamber pressure oscillations were encountered, which could not be damped with acoustic absorbers. Head end overheating was also noted with this injector configuration, and it also would benefit from film cooling.

A 19-element coax injector provided the most satisfactory operation of all the fuel-rich LOX/CH₄ testing. Stable combustion and high performance characterized the testing. An overpressure in the fuel supply system mechanically failed the first porous face plate, requiring a rework to the injector hardware. In addition to this hardware, another version of the coax injector was fabricated using a solid copper plate instead of the porous (Rigimesh) face plate. This injector performed equally well as the initial coax, showing no indication of face heating nor any increase in stability sensitivity.

This injector configuration was selected as the baseline design for the full-scale 40K fuel-rich LOX/CH₄ preburner/gas generator.

The acoustic stability problem encountered with the impinging injectors was not anticipated, and presented serious problems in conducting this evaluation test series. The fact that these pressure oscillations did not respond satisfactorily to the acoustic absorbers was a further disturbing aspect of this phenomena. The marked difference in stability between impinging injector patterns, and the coaxial element was only partially expected. Coaxial elements have long been acknowledged as less sensitive to stability problems, but the degree of this difference was not anticipated. The effect of the diffused fuel flow through the coaxial injector porous face plate was partially evaluated by running an identical coax injector with solid copper face plate. No significant difference in stability sensitivity, performance, or even face heating was noted.

The impinging injectors were characterized by the recirculation of higher mixture ratio products near the injector face, which contributed to the head end heating and burning of the chamber wall. This is undoubtedly the result of the more vigorous local mixing and atomization, which is typical of impinging streams. The coaxial pattern sheaths the oxidizer in a "shell" of high-velocity gaseous fuel, which would tend to result in only fuel-rich recirculation products. It may be that this difference in mixing phenomena is responsible for the stability differences between the injector types (in addition to the acknowledged impact on wall heating). The proposed reworks to the triplet and the pentad injectors addressed this possibility, in addition to providing cooling protection to the wall. These reworks would add fuel flow area between the injector elements for two primary purposes: to add fuel to the relatively oxidizer-rich recirculating flow, and to reduce the momentum of the fuel streams in the impinging elements. The intent of this revision would be to minimize the overpowering fuel momentum to reduce the oxidizer "overspray," and to dilute any overspray which would still exist by adding the remainder of the fuel adjacent to the impinging elements. Program limitations did not permit testing of the modified injectors.

Fuel-Rich LOX/RP-1. Hot-fire testing of the 27-element, like-impinging doublet injector indicated satisfactory performance, but marginal resistance to stability problems. No chamber overheating occurred, but discrete chamber pressure oscillations were noted at unacceptable levels at several operating points.

Hot-fire testing of the 27-element triplet injector showed performance to be higher than the impinging doublet and a substantial stability margin. This triplet injector was considered a high-stability-risk configuration for the preburner/gas generator program, but hot-fire testing showed the element selection to be very gratifying.

During water flow calibration, the fan former injector configuration showed a disturbing lack of atomization and a high concentration of mass flow in the central zone. The visual evidence suggested that satisfactory performance in hot fire was relatively unlikely. The central element was reworked to provide some outward deflection of the flow and restriction to some of the central core flow. However, the subsequent water calibration tests did not show any encouraging improvement in either mass distribution or apparent atomization.

Hot-fire testing with this injector was even more discouraging, with significant instability and severe damage to the injector face in spite of early test cutoff. The multiplicity of sharp edges and corners on this injector undoubtedly contributed to the rapid face burning. The mechanisms of the instability are not known, and the stability undoubtedly contributed to the early failure. The test was too short to evaluate any performance characteristics.

Oxidizer Rich LOX/CH₄. Hot-fire experience with this 19-element pentad injector indicated basically good operation, although there was some evidence of head-end heating. Carbon deposition on the injector face indicated recirculation of fuel-rich (relative to overall mixture ratio) combustion products near the injector face. Liquid oxygen film-cooling orifices were added to the injector perimeter to protect the walls from potentially damaging heat loads. The massive oxidizer flows in the outer streams undoubtedly were overpenetrating the central fuel stream and apparently dispersing a relatively fuel-rich mixture in the

recirculation zone. Relative to overall flow, this recirculating flow was small but, at the high injection mass flux of high chamber pressure, this low percentage of flow was a rather high actual value. The film cooling provided a satisfactory resolution to this problem. Facility and operational problems resulted in several aborted tests, but the injector configuration appeared to be quite satisfactory for oxidizer-rich liquid oxygen/gaseous CH₄ operation.

Oxidizer-Rich LOX/RP-1. Four hot-fire tests were made with the like-doublet/showerhead injector without obtaining successful data. A combination of facility and operational problems made it difficult to determine if the injector design was the primary cause of early shutdown and hardware damage. Posttest investigations indicated that this injector probably requires liquid oxygen film-cooling provisions similar to those used on the oxidizer rich, LOX/gaseous CH₄ injector. Program limitations precluded further investigation of this injector.

Test Discussion.

Fuel-Rich LOX/CH₄. After system characterization, the fuel-rich LOX/CH₄ triplet injector was tested. The test objective was to demonstrate mainstage ignition and stable steady-state operation. The test was completed satisfactorily and had a scheduled cutoff resulting in 1 second of mainstage operation.

The test conditions realized during mainstage were:

LOX flowrate, lb/sec	4.59
Fuel flowrate, lb/sec	12.31
Mixture ratio	0.373
P _c Nozzle, psia	3421
Average combustor temperature	1750 R

Posttest data analysis showed a high-frequency oscillation was realized in the combustor, as shown in Fig. 30. It is evident from the "Statos" record, a portion of which is shown, that the feed systems are stable and divorced from the chamber pressure fluctuations. Power spectral density (PSD) plots were made of the 1-second mainstage run portion. The results from the injector end chamber pressure high-frequency transducer are shown in Fig. 31. It is evident that 14,000 Hz is the predominant frequency realized with respect to time. A shift of frequencies is seen during the latter portion of the test. Figure 32 shows a frequency/time plot, and it is evident that the frequency shifts as the LOX quality increases.

Several influencing items could cause the frequency shift. The engine start transition goes through liquid CTF/GOX/LOX transition into mainstage. The chamber pressure plot shown in Fig. 33 illustrates this engine phenomena. Changes in local combustion temperature change the acoustic velocity and, subsequently, the frequency. Degradation of the combustion chamber/injector spacer ring tends to damp discrete frequencies.

An analysis of the combustion phenomena that occurs shows that the acoustic velocity cannot be estimated accurately because of the unknown amount of CH_4 decomposition. An estimate of the gas properties based on burning a portion of the CH_4 to water and carbon monoxide, and heating the remainder of the CH_4 unchanged resulted in the following properties:

Temperature	- 1894 R
Molecular weight	- 16.2
Specific heat ratio	- 1.144

Therefore, the acoustic velocity is approximately 2830 ft/sec, and the predominant acoustic modes are:

First tangential	~ 9056 Hz
Second tangential	~ 15,021 Hz
Third tangential	~ 20,708 Hz
First radial	~ 18,853 Hz

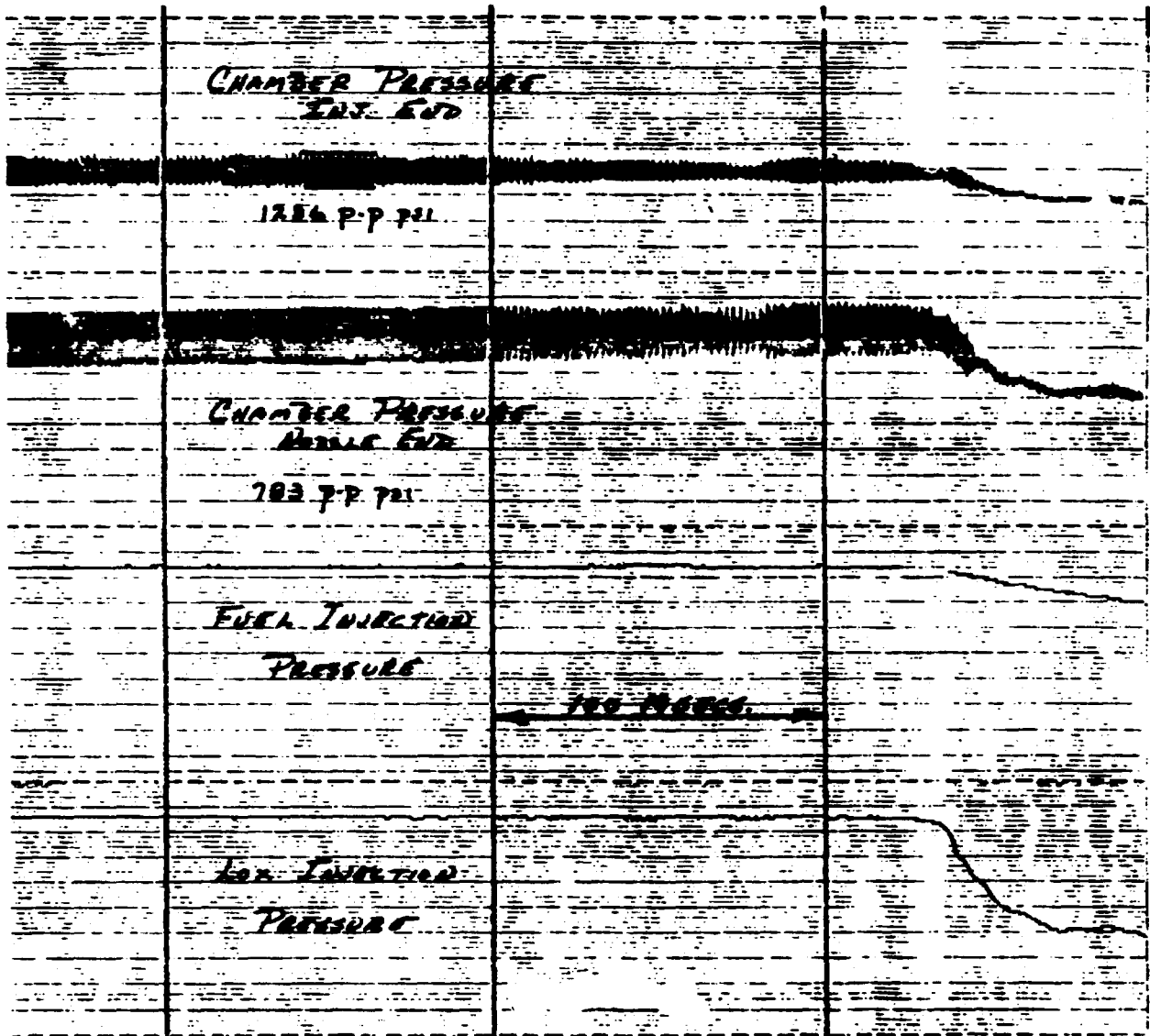


Figure 30. Test 004 High-Frequency Data Record

ORIGINAL MADE IN
OF HIGH QUALITY

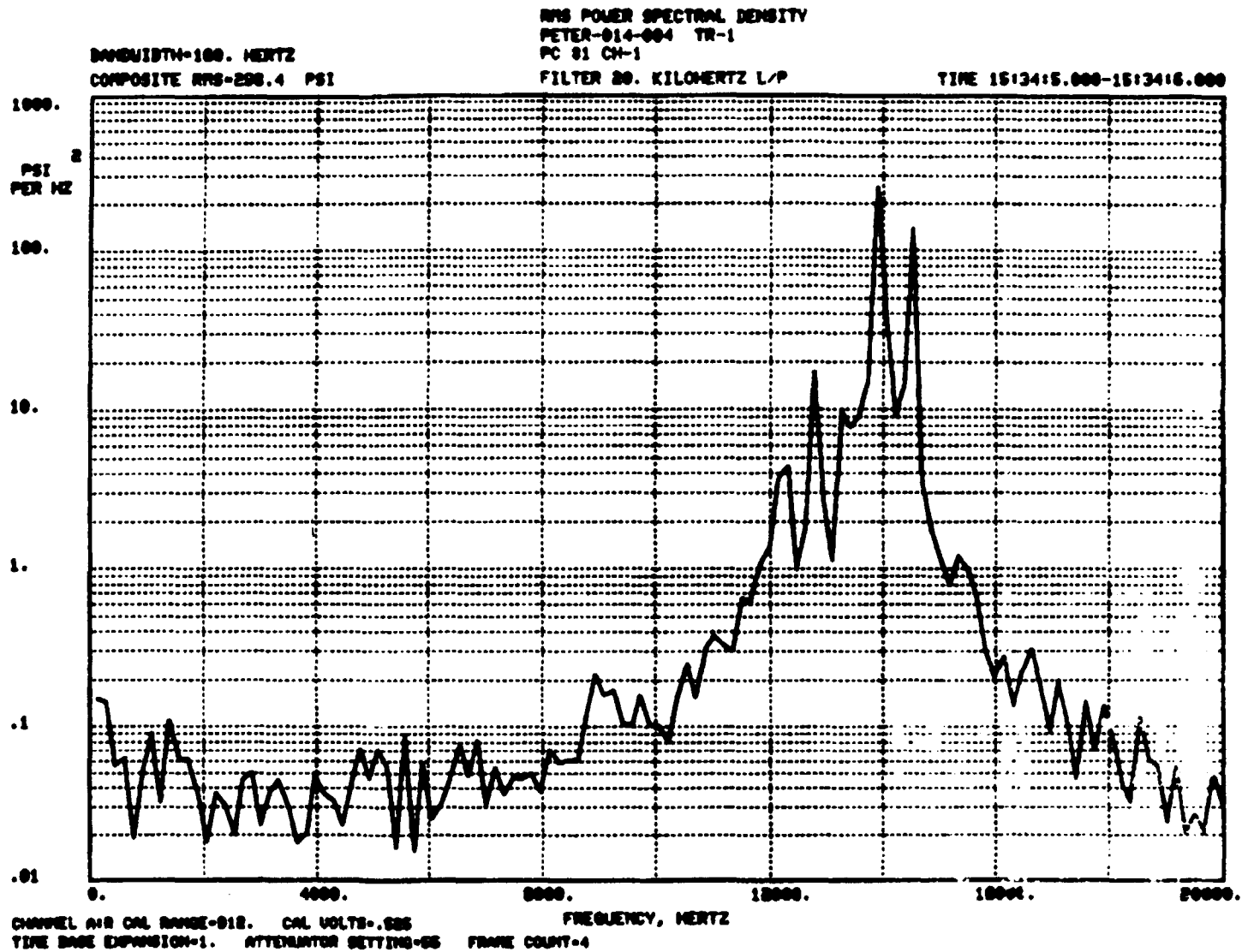


Figure 31. PSD Plot of Injector End P_c High-Frequency Transducer

PETER STANG TEST 0014-004 TR0 1
PC 01 CH0 1
START TIME 15:34:51.000

DURATION-1. SECONDS
BANDWIDTH-100. HERTZ
FILTER 80. KILOHERTZ L/P

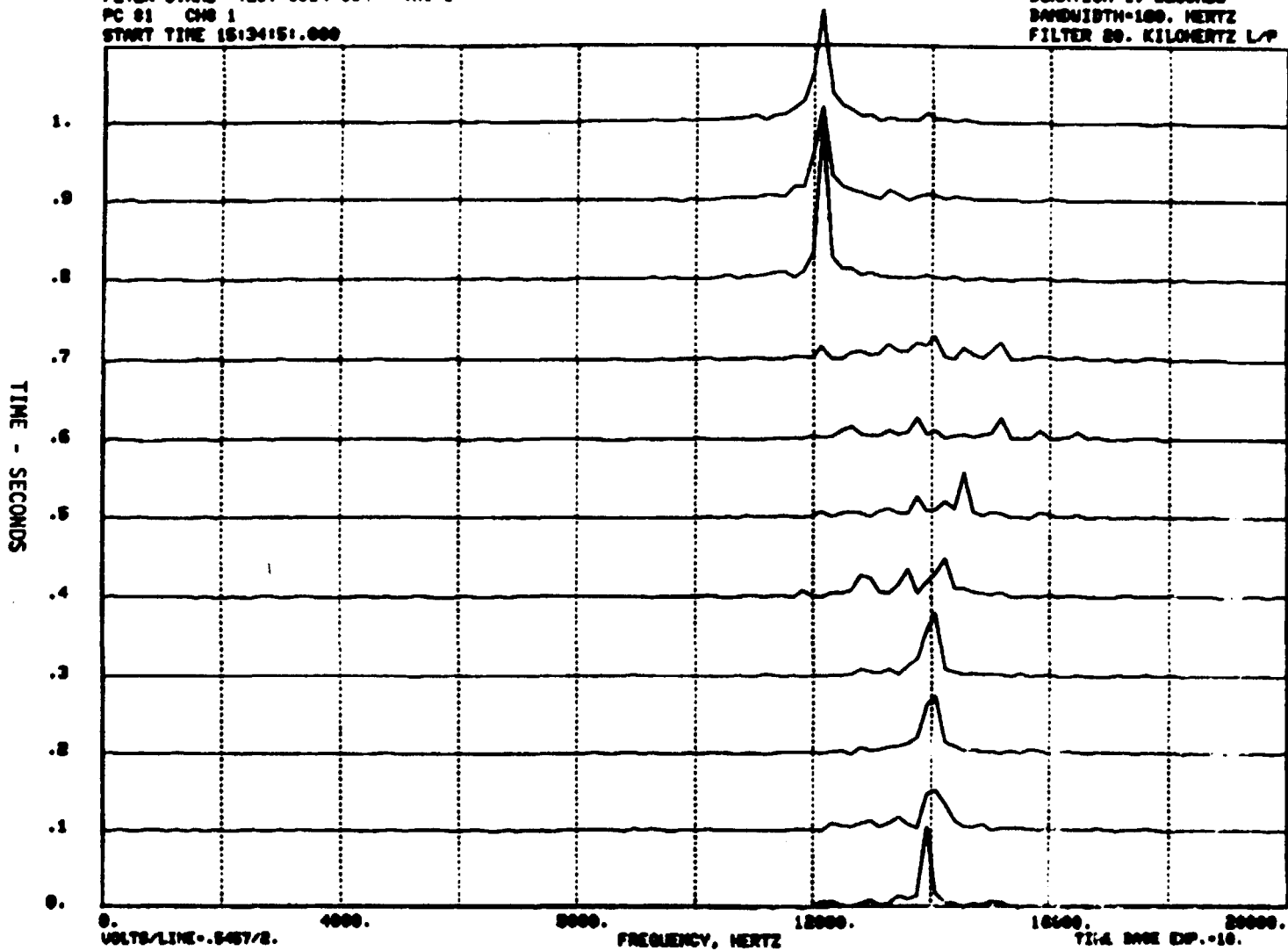


Figure 32. Frequency vs Time Plot

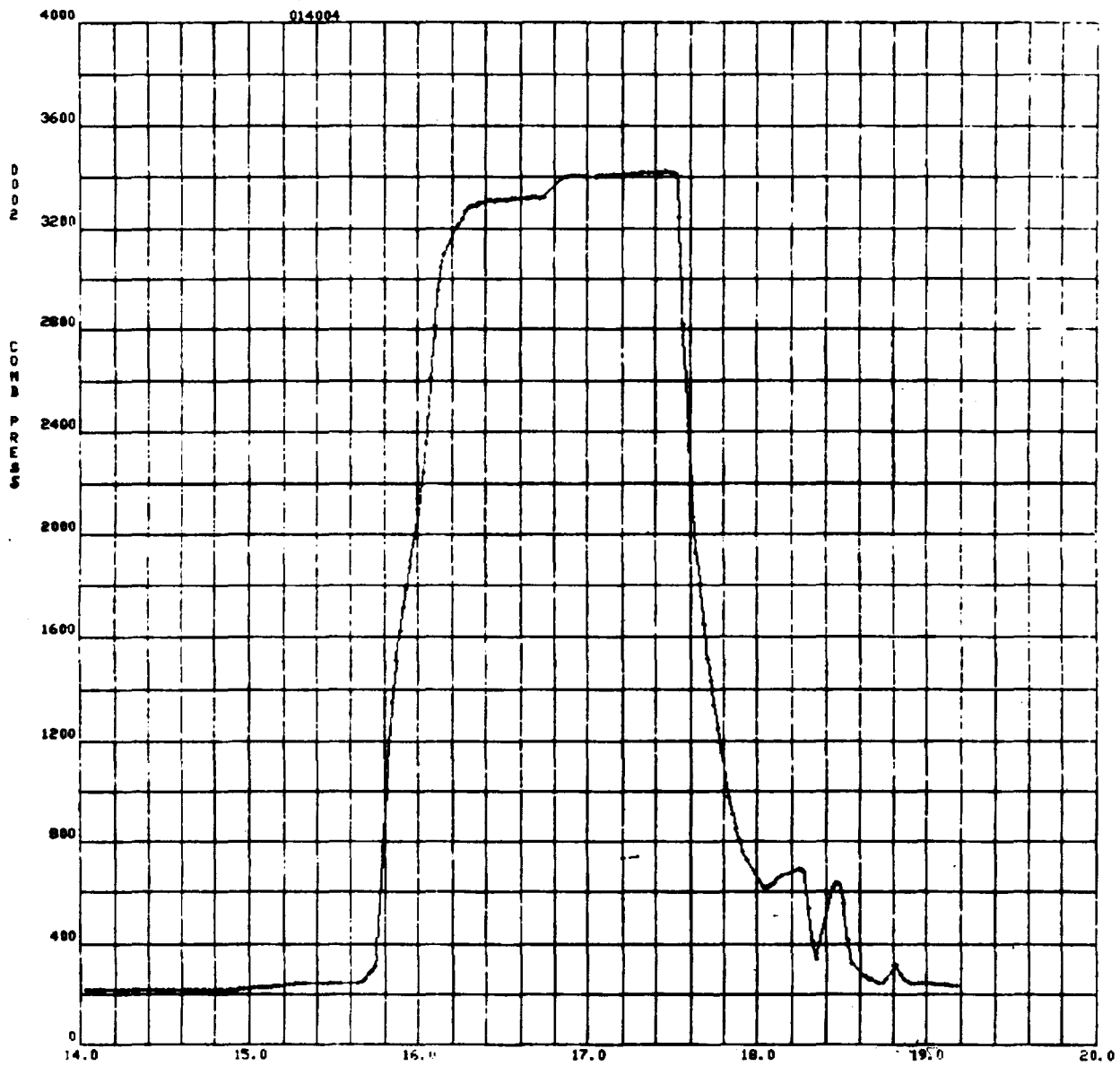


Figure 33. Test 004 - Combustor Pressure vs Time

Since the combustor experienced oscillations of approximately 14,000 Hz, it is expected the dominant mode was not a classic acoustic tangential mode but a hybrid mode possibly coupled with the LOX post acoustic mode. To stabilize the combustor, acoustic absorbers capable of damping both the first and second tangential mode were designed and fabricated. These absorbers were made as quarter-wave pipes tuned to several different modes and as Helmholtz resonators tuned to the first tangential mode and still effective for the higher-order modes.

Designs were established and fabricated for both configurations. The quarter-wave absorber was evaluated first, because of simplicity in accommodating the device. A Helmholtz absorber configuration also was evaluated. It should be noted that the ultimate purpose of the contract was to establish a technology base for future injector configuration predictions and not to rate stability or conduct a stability development program. A simple absorber overkill concept did not permit the program to continue with subsequent objective fulfillment.

During these hot-fire tests, oscillations resulted in burn damage to the combustion spacer section on the front of the fuel manifold. The rework of this section permitted incorporation of the absorber--a copper heat-sink piece. A pentad injector evaluated on company funds with fuel-rich LOX/CH₄ demonstrated instability also. The magnitude of the oscillations, although less than the triplet, were twice the acceptable value. Testing of this injector configuration was terminated when it was realized that the basic element relationship would have to be modified, or stability aids would have to be evaluated to successfully conduct further tests.

Review of the test data from the high-pressure LOX/CH₄ gas generator tests definitely appeared to be related to injector characteristics. The combustion stability problems associated with the impinging injector designs were unexpected, and the resulting hardware damage was difficult to understand. The small diameter of the combustion chamber, and the low mixture ratio operating point, supported a prediction of stable operation. Both the frequency of the disturbance, and the melting of the chamber hardware reflected temperatures much higher than could be predicted from either equilibrium computations or conventional combustion modeling. The mixture ratio of the operating condition, and the relative vaporization rates of the propellants would both predict fuel-rich, low-temperature products which would predict lower resonant frequencies and low potential for hardware damage.

The most reasonable theory explaining the observed phenomena would seem to relate to the "back spray" frequently encountered in impinging elements. The amount of propellant directed back against the injector face is somewhat a function of momentum relationship and the physical configuration of the element, but some back spray is almost always present. At most operating conditions, this back spray is only a minor nuisance, impacting injector face heating in some cases, and providing some problems in chamber head-end heating in the presence of "radial winds." The percentage of total mass flux in this area usually does not represent sufficient potential energy to become a major problem. However, operation at the higher chamber pressure (i.e., over 3000 psi) means that even a 10% mass flux in this zone is equivalent to the average mass flux in a 300-psi chamber, and represents a significant source of energy. The local mixture ratio in this zone, behind the normal flame front is apparently significantly closer to stoichiometric than the average mixture ratio. This zone probably provides both the higher temperature (for the higher frequency, and the hardware damage) and the energy to support the instability.

This theory, that back spray is involved in the instability, is somewhat supported by test experience with coax injectors at similar operating conditions. This unit had both the encircled spray pattern of a coaxial element, and additional "base" flow from a rigimesh porous face plate. The coax injector was tested numerous times, demonstrating very stable operation $<\pm 3\%$.

This experience would suggest that additional fuel added to the injector face zone would be beneficial for both chamber compatibility and combustion stability. Subsequent testing of a solid-face coaxial injector demonstrated comparable stability, suggesting that the element configuration and not the face bleed attributed to the injector stability. Film cooling flow on the chamber wall, or at least outboard of the outer elements, would certainly aid in protecting the upper end of the combustion chamber, and would reduce the energy release potential near the perimeter of the chamber where first tangential activity is most severe.

Posttest data analysis showed high-frequency pressure oscillations were realized with both absorbers. As illustrated previously, the power spectral density (PSD) curve showed maximum energy at 14,000 Hz without an absorbing device. When the quarter-wave absorber was used, the pressure oscillation amplitude was decreased approximately 30%. The predominant frequency that was now evident shifted to 13,000 Hz, as shown in Fig. 34. This change/variation in frequency is no doubt caused by the change in the absorber cavity operating temperature.

When a Helmholtz resonator was installed, the pressure oscillations were decreased by 50%. Figure 35 shows that a shift in frequency has again been realized. As the injector is made to operate more stably, the operating frequency approaches that of the classic acoustic modes. It is evident in this figure that the primary frequency is somewhat less than 12,000 Hz. Figure 36 illustrates the damage sustained by the Helmholtz absorber after a relatively short exposure to oscillations that exceeded $\pm 10\%$ of chamber pressure. The continual increase in pressure oscillations may be attributed to the degradation of the absorber. Fifty milliseconds of oscillations in excess of $\pm 10\% P_c$ automatically initiates the cutoff signal for test termination.

During the LOX/CH₄ injector evaluation, several tests were conducted under company-sponsored activities to evaluate candidate turbine blade materials. The device used is shown in Fig. 37. The temperature profile resulting from these tests is illustrated in Fig. 38. It is evident that the combustion gases when disrupted in the combustor transition zones, prior to entering the test area, realize a substantial change in bulk temperature. This device also was used for carbon deposition checking. Posttest, only a slight discoloration of the surfaces were noted. There was no significant carbon deposition as occurred during the LOX/RP-1 tests.

Oxidizer-Rich LOX/CH₄. Twelve tests/attempts were made with the oxidizer-rich pentad injector. The first test using the basic pentad design was terminated prematurely by a low LOX injection pressure cutoff signal. Visual posttest observation showed considerable hardware degradation was realized.

RMS POWER SPECTRAL DENSITY
PETER-014-007
PC 001 CH 01
BANDWIDTH-100. HERTZ
COMPOSITE RMS-873.1 PSI
FILTER 80. KILOHERTZ L/P
TIME 14:29:30.35-14:29:30.000

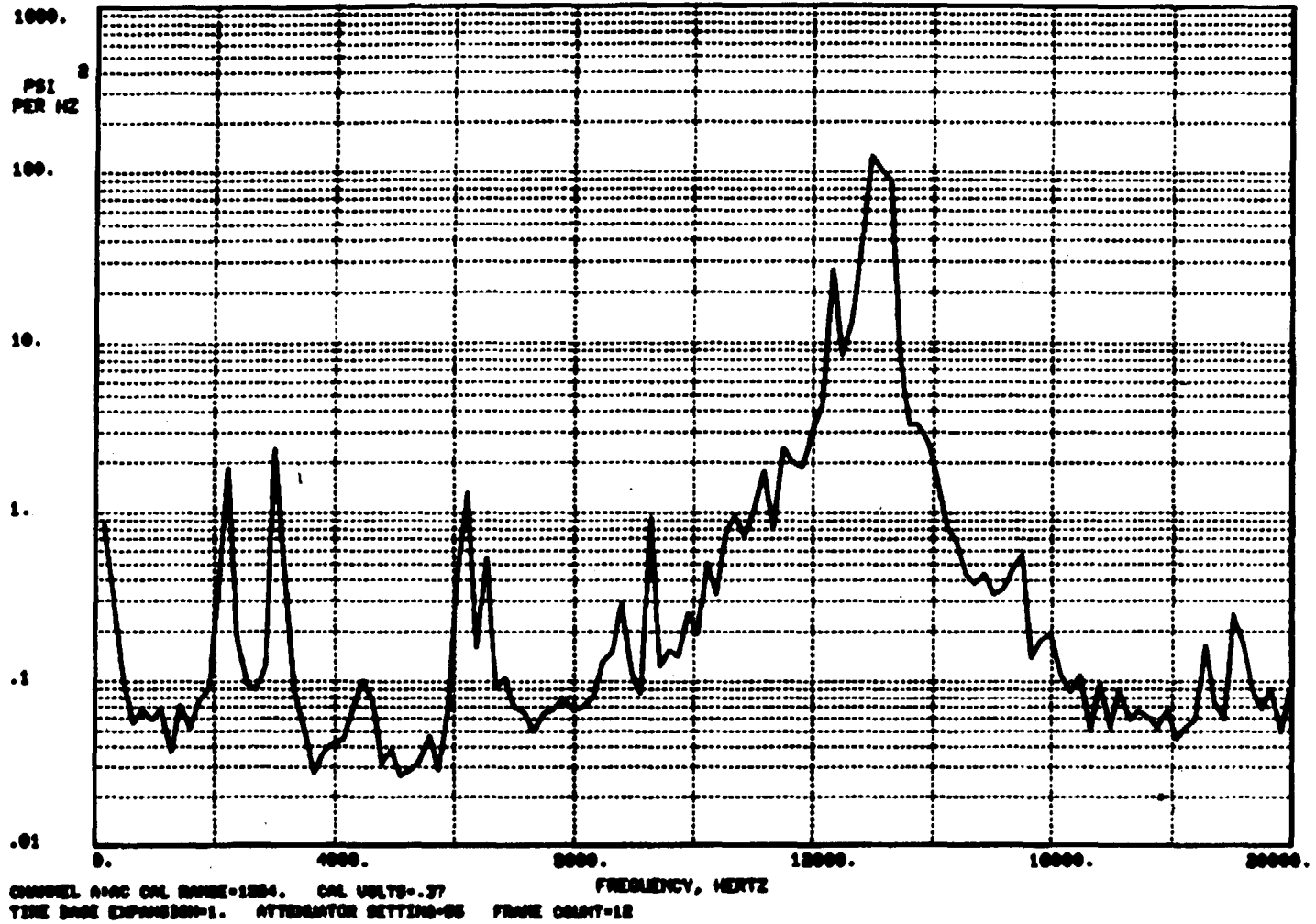
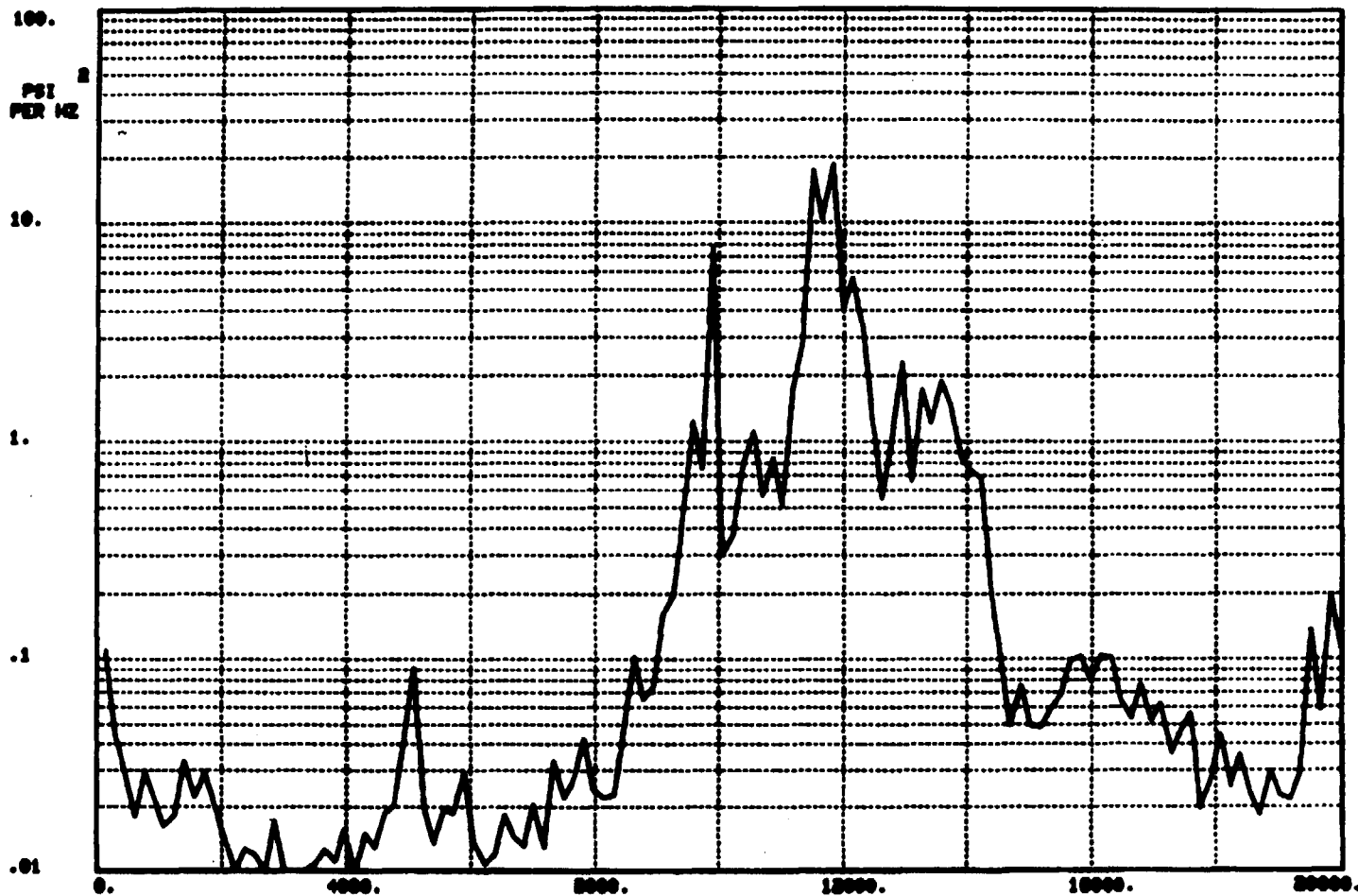


Figure 34. PSD Plot of Test With Quarter-Wave Absorber

BANDWIDTH-100. HERTZ
COMPOSITE RMS-125.3 PSI

RMS POWER SPECTRAL DENSITY
PETER-014-002
PC 901
FILTER 20. KILOHERTZ L/P

TIME 14:18:50.000-14:18:51.2

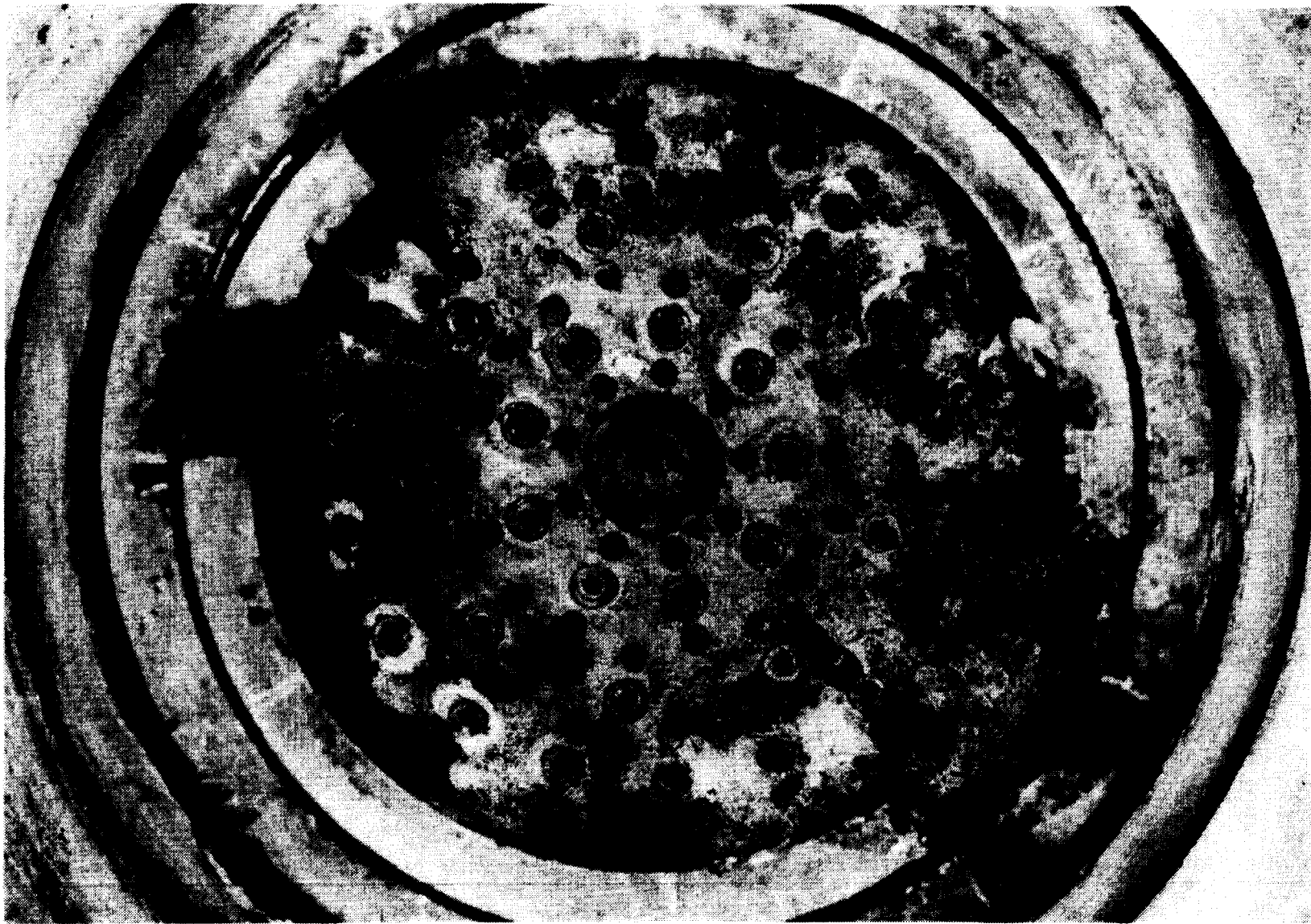


CHANNEL A14C CAL RANGE-1004. CAL VOLTS-.348
TIME BASE EXPANSION-1. ATTENUATOR SETTINGS-55 FRAME COUNT-82

Figure 35. PSD Plot of Test With a Helmholtz Resonator

ORIGINAL PAGE IS
OF POOR QUALITY

77



1XX45-1/11/80-C1B

Figure 36. LOX/CH₄ Triplet Helmholtz Absorber Degradation

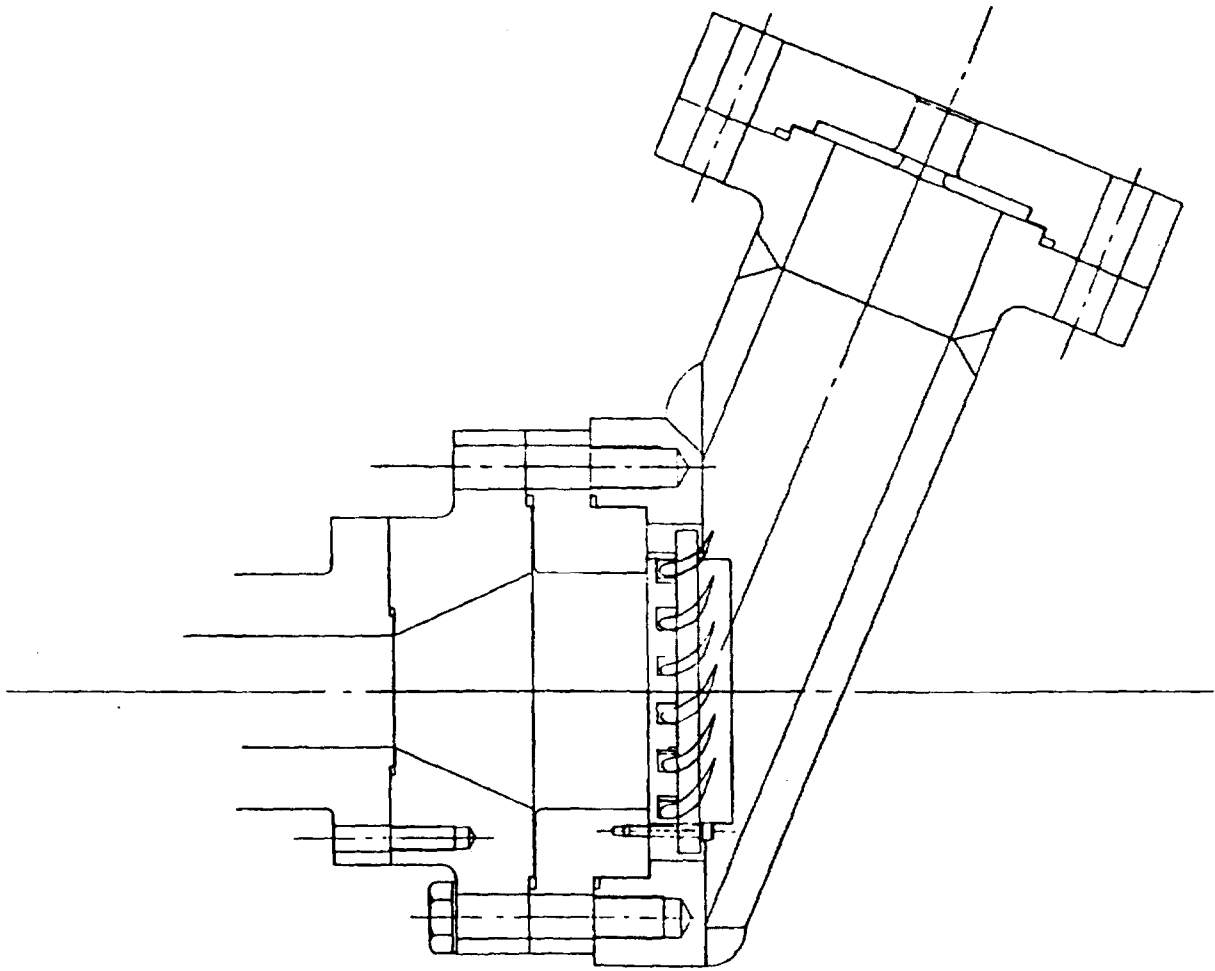


Figure 37. Turbine Blade Coking Fixture

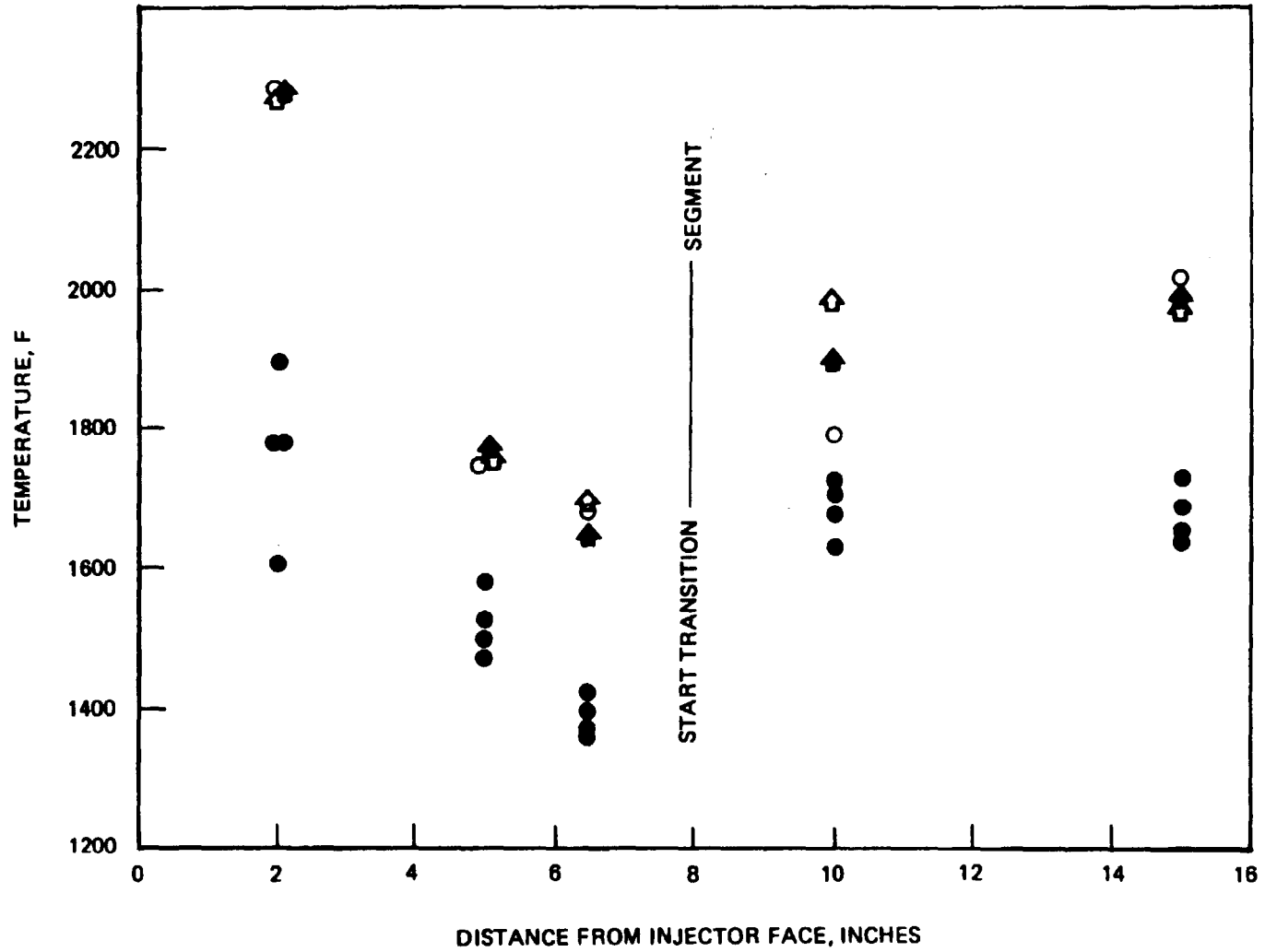


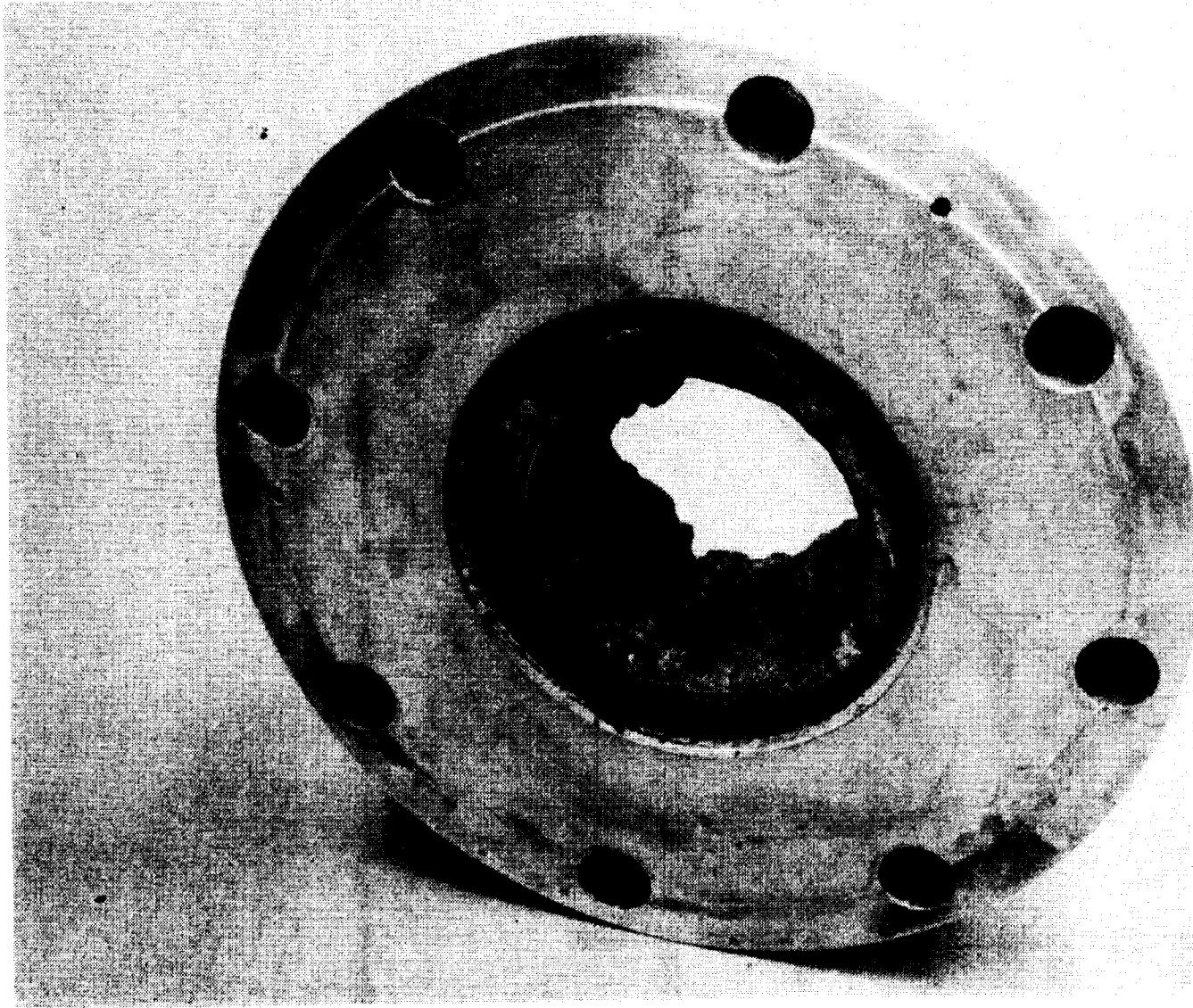
Figure 38. LOX/CH₄ Chamber Temperature Profile

Posttest analysis showed that considerable damage to the combustor and nozzle were experienced during the test cutoff transition. Figure 39 illustrates the damage realized to the nozzle section as a result of the off-mixture ratio operation. The inability of the LOX tank pressurizing system to maintain the required set pressure resulted in the LOX injection pressure falling off. This reduced oxidizer injection pressure resulted in the bulk mixture ratio being lower than the nominal 40:1 targeted. Figure 40 illustrates the rapid change in theoretical combustion temperature as the mixture ratio is decreased.

Figure 41 shows the injector face and the Helmholtz absorber. It is evident that no degradation of these components was realized. Although it is not obvious from the figure, a considerable amount of carbon was evident on the injector face and in streaks across the copper absorber ring. It is theorized that the high oxidizer momentum restricted the penetration of the gas fuel stream, forcing the fuel between the oxidizer streams, as evident in the flow streaks in the carbon shown in Fig. 42.

Evidence suggested that because of the damage realized to the combustor and nozzle, this injector pattern provided insufficient protection for the combustor wall. The back spray phenomena of impinging injector patterns also was suspect in this case, although no combustion instability was evident in the test. The massive mixture ratio unbalance in both fuel-rich and oxidizer-rich systems is difficult to optimize in impinging patterns. Adding a film-cooling flow of liquid oxygen as shown in Fig. 43 significantly improved the combustor wall protection, even during the critical start and shutdown periods. The use of a hypergolic oxidizer injected through the manifold prevents a LOX-rich start, adding to the risk during the start sequence of an oxidizer-rich system. However, the added oxidizer film coolant in the wall zone provided improved protection against excursions of the overall mixture ratio toward stoichiometric.

In conjunction with the added film coolant holes, the ignition system was also modified. A TEA system was installed to aid in providing an oxidizer-rich start. Because the injector had a face delta pressure limitation and the hypergol was introduced through the injector manifold by the incoming propellant, a positive oxidizer lead was difficult to attain.



1XY25-1/30/80-C1A

Figure 39. Damaged Nozzle

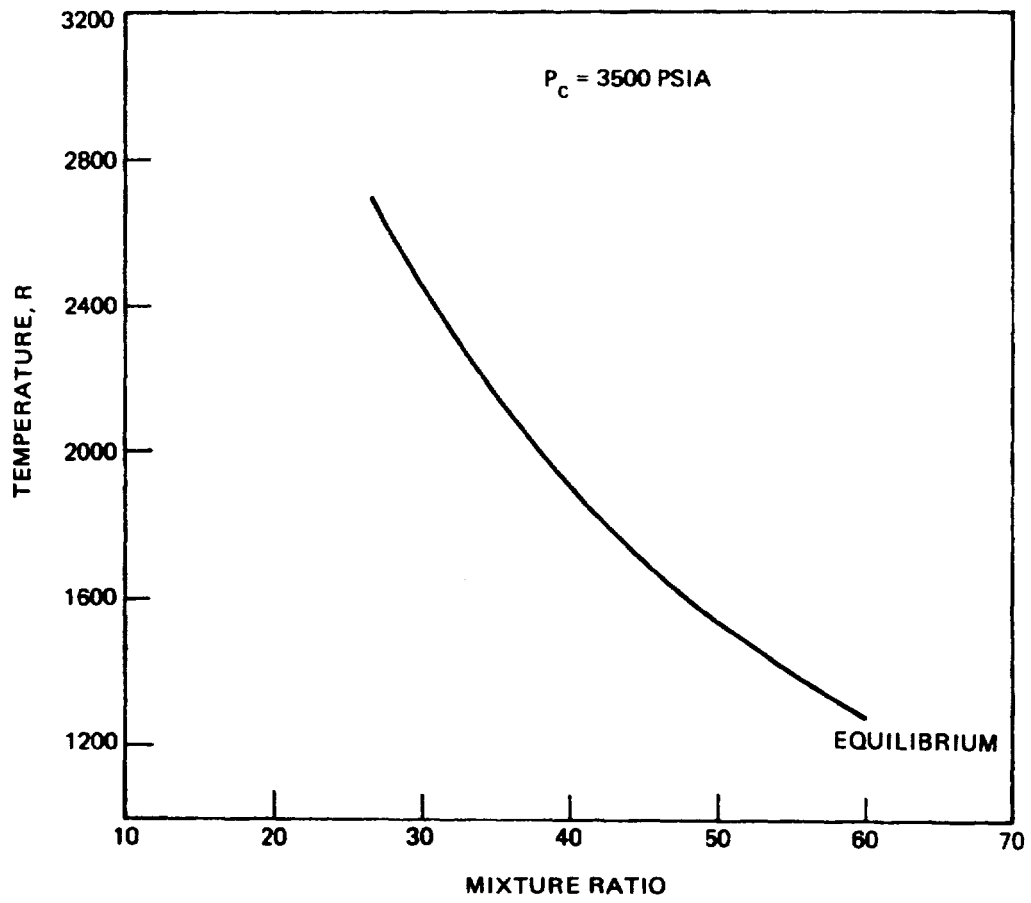


Figure 40. Theoretical Combustor Temperature LOX/CH₄ amb gas

ORIGINAL PAGE IS
OF POOR QUALITY

83



1XZ46-1/31/80-C1B

Figure 41. Oxidizer-Rich Pentad Injector Face

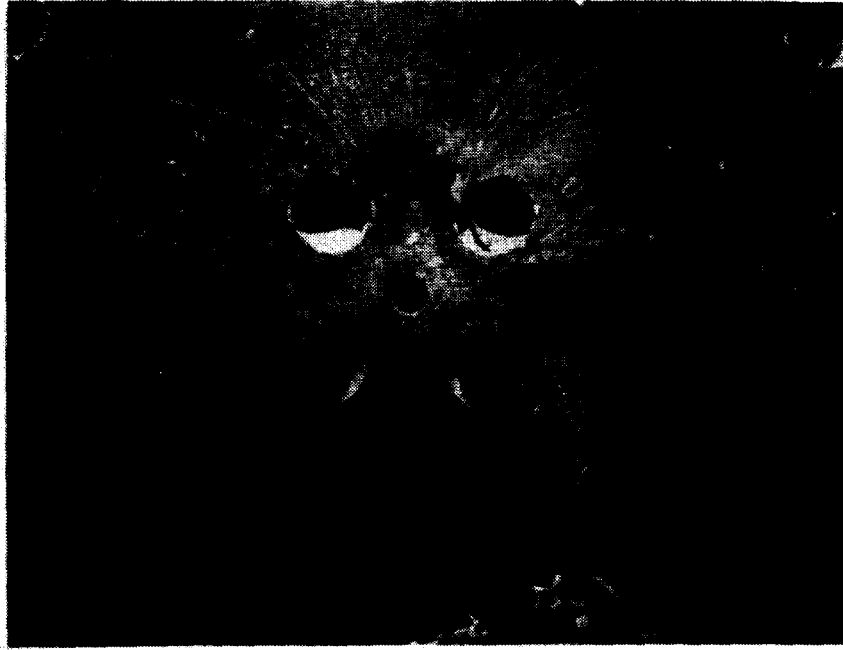
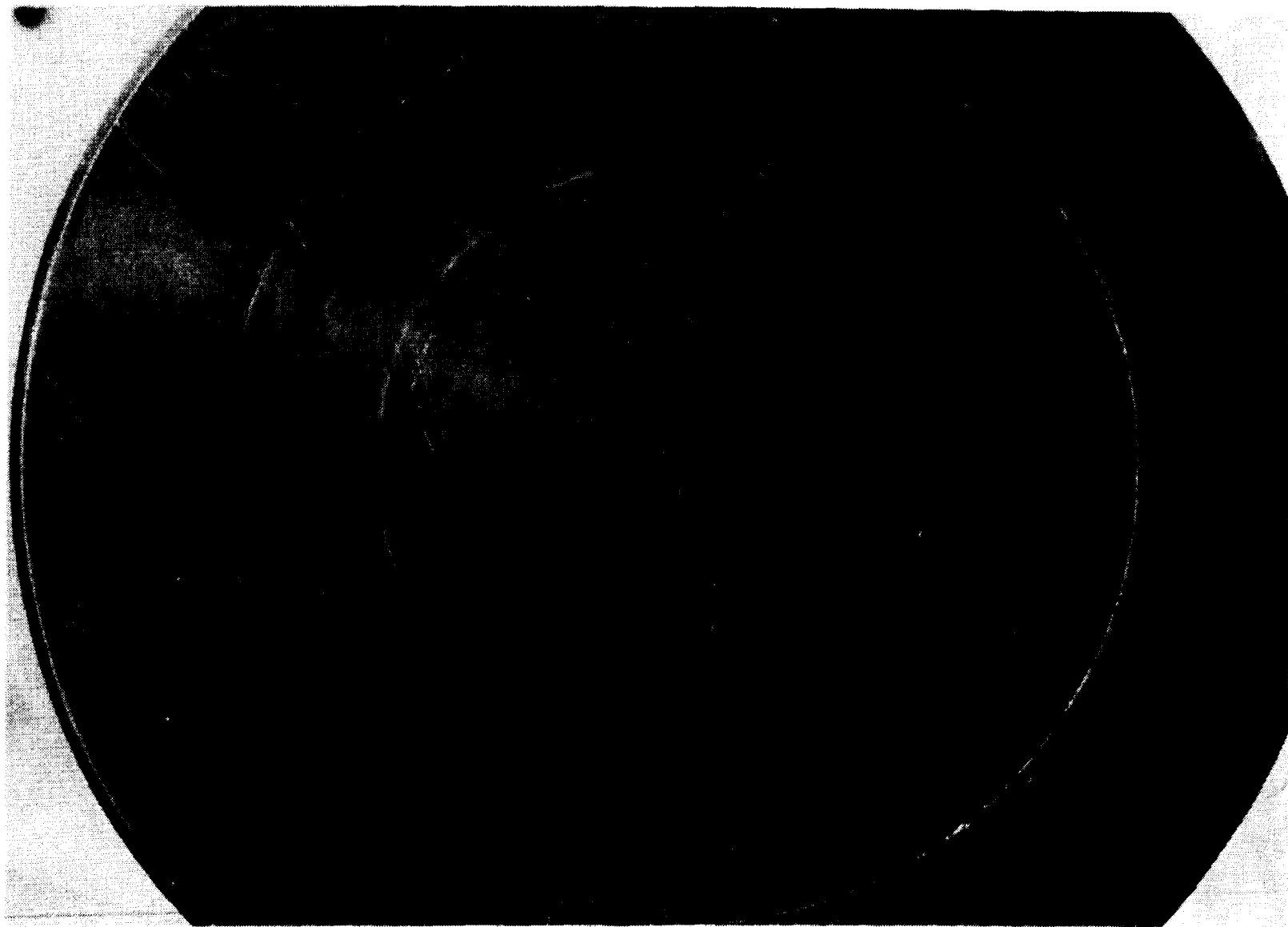


Figure 42. Carbon Streaks - Pentad Injector Element

Several tests conducted during this series were plagued by facility problems. A facility malfunction at shutdown caused a fuel-rich cutoff, restricted flow through the flowmeter caused by icing resulted in a more fuel-rich operation, and an unstable LOX tank pressurizing valve all caused premature cutoffs and resultant hardware damage. Instrumentation malfunction caused another test abort. In the successful tests, oxidizer-rich LOX/CH₄ operation appeared satisfactory with a clear exhaust flame and an acceptable performance.

Fuel-Rich LOX/RP-1. Five tests were conducted under contract on the like-doublet injector in a fuel-rich LOX/RP-1 environment. Due to improper gain setting of the RP-1 tank pressurizing system, a substantial degradation and gradual recovery of the tank pressure on the first test was realized. Figure 44, a CRT taken from the RP-1 tank pressure transducer, shows this anomaly. The marks on the time line abscissa identify the main valve opening and closing time. Figure 45 illustrates the combustor chamber pressure and the rapid rise and decay of pressure realized. The pressure level attained is shown to be in excess of 3500 psi at a mixture ratio of approximately 0.373. Because of the variation in tank pressure, an excursion in mixture ratio was realized.



50P36-7/24/80-S1B

Figure 43. Modified Oxidizer-Rich LOX/CH₄ Pentad Injector

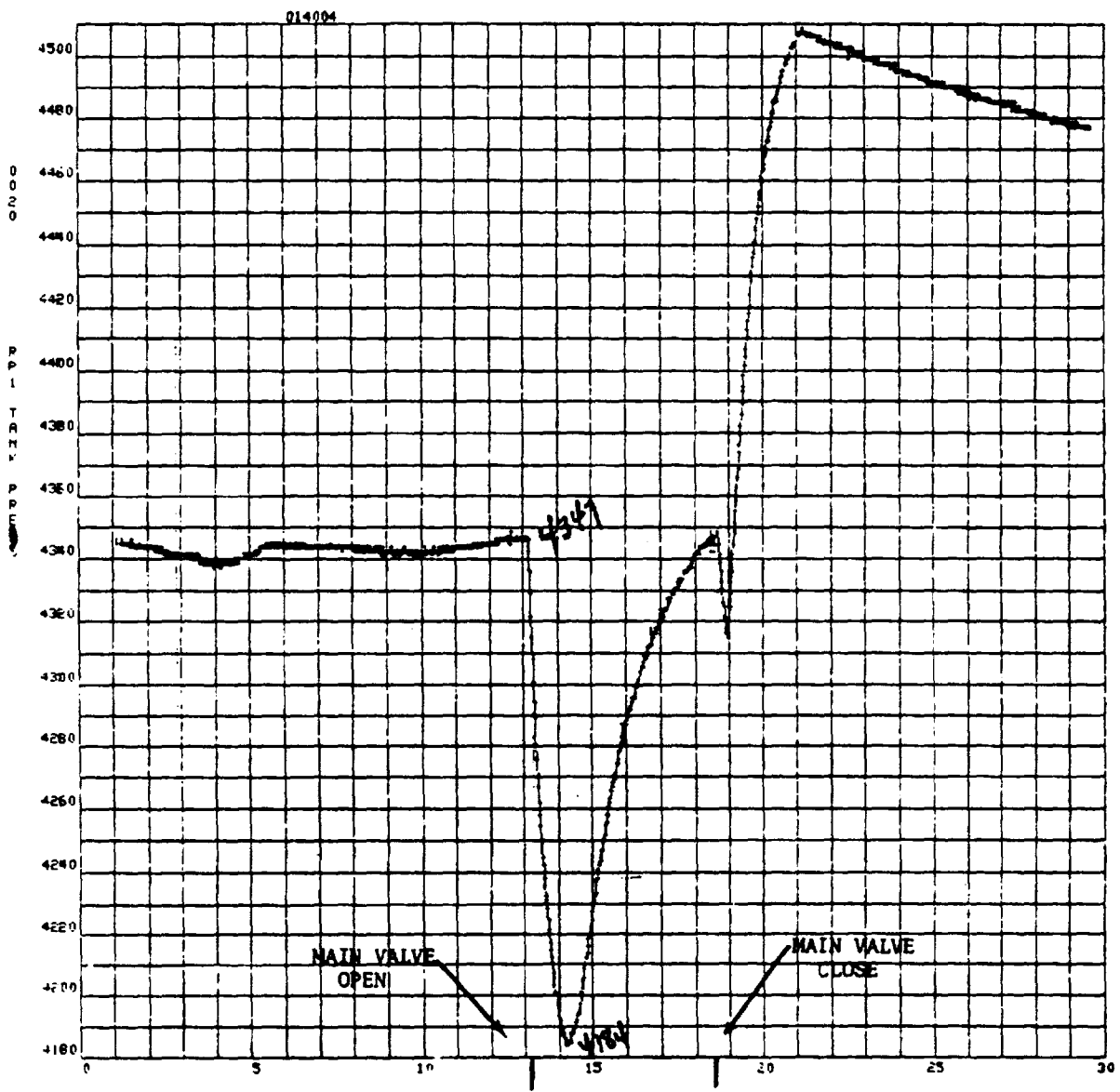


Figure 44. RP-1 Tank Pressure, Test 004

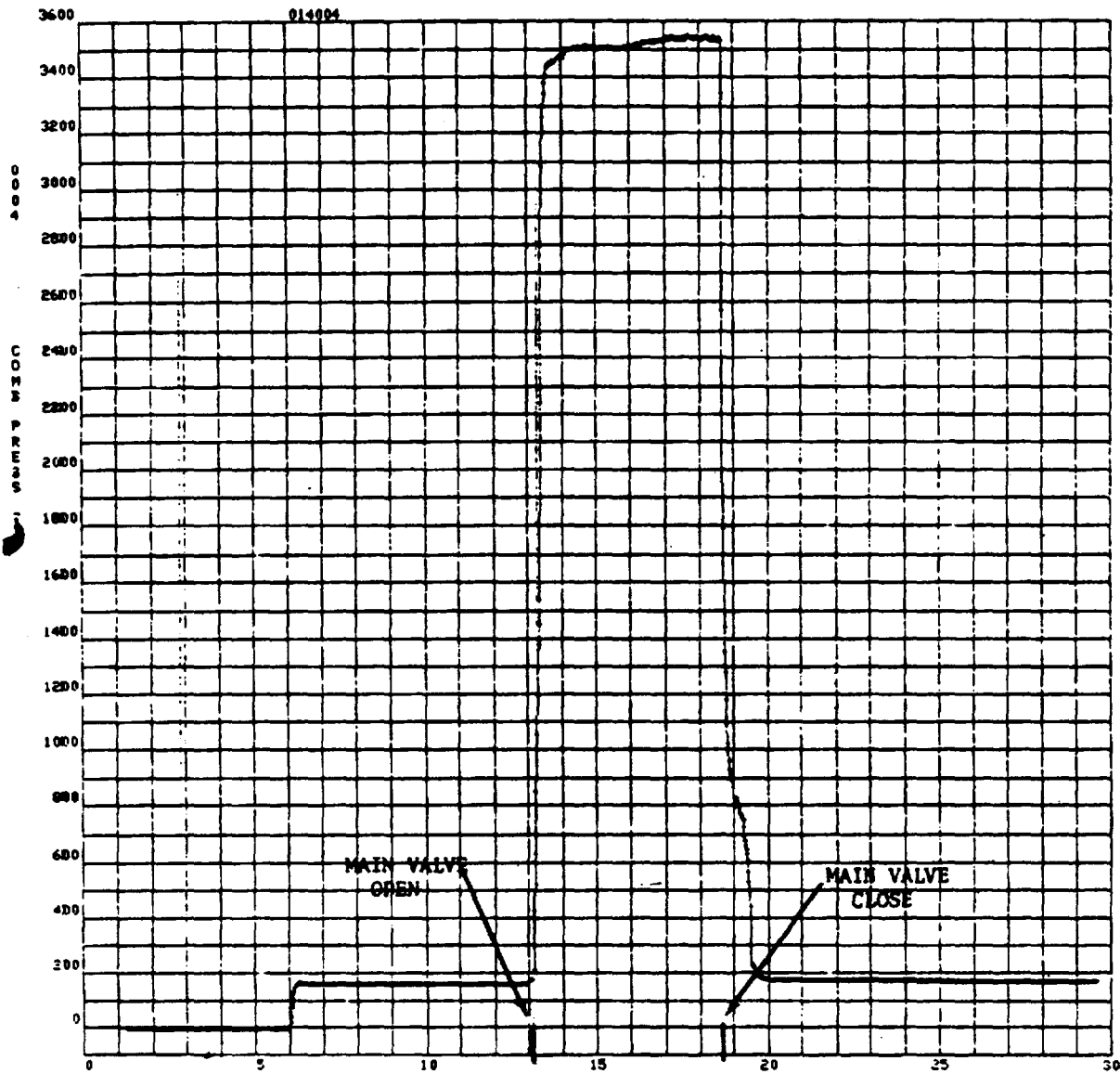


Figure 45. Fuel-Rich LOX/RP-1 Chamber Pressure, Test 004

A small change in mixture ratio results in a sizeable variation of theoretical characteristic velocity and combustion temperature at these mixture ratios.

Figure 46 shows the test 005 RP-1 tank pressure plot. During this test sequence, a faulty seat in the pressurizing valve permitted the tank pressure to creep from 4340 to 4400 psi immediately prior to test. Therefore, when the main valve opened as indicated on the trace, the pressure had to decay a significant amount before the system sensed the loss of pressure. Again, this resulted in a mixture ratio excursion, and a premature cutoff by exceeding a redline parameter.

Figure 47 shows the frontal view of the like-doublet injector. This injector was hot-fire-tested without an acoustic absorber. The stability realized during these tests is illustrated in Fig. 48. Figure 48, a high-frequency trace, shows the frequencies realized during the test. The combustor pressure adjacent to the injector face has pressure oscillations of 340 psi peak-to-peak, marginally stable as defined in the contract. This amplitude is made up of two predominant oscillations as shown in Fig. 48. A 1400 Hz frequency realized in the fuel manifold is superimposed on the 9000 Hz first tangential acoustic mode. Although this injector configuration was deemed stable, future testing incorporated a Helmholtz absorber device to permit gas sampling in a more representative environment.

Test 006 was conducted in an attempt to hot-fire demonstrate 20-second mainstage carbon deposition of a fuel-rich LOX/RP-1 like-doublet injector at 1900 R combustion temperature with a Helmholtz acoustic absorber. The test was terminated prematurely at approximately 0.5 second due to severe longitudinal instability. Figure 49 shows the instability as it occurred after the start transition. This is an a-c trace, and the oscillations realized at cutoff are in excess of +700 psi peak-to-peak. The first tangential acoustic mode has coupled with the longitudinal mode to create a hybrid mode capable of damaging hardware. The carbon deposition device shown in Fig. 50 was consumed as was the exit nozzle. This carbon device was not replaced. An alternate design turbine blade simulator designed for Rocket-dyne IR&D effort was used for future carbon checking evaluations. This configuration is illustrated in Fig. 51.

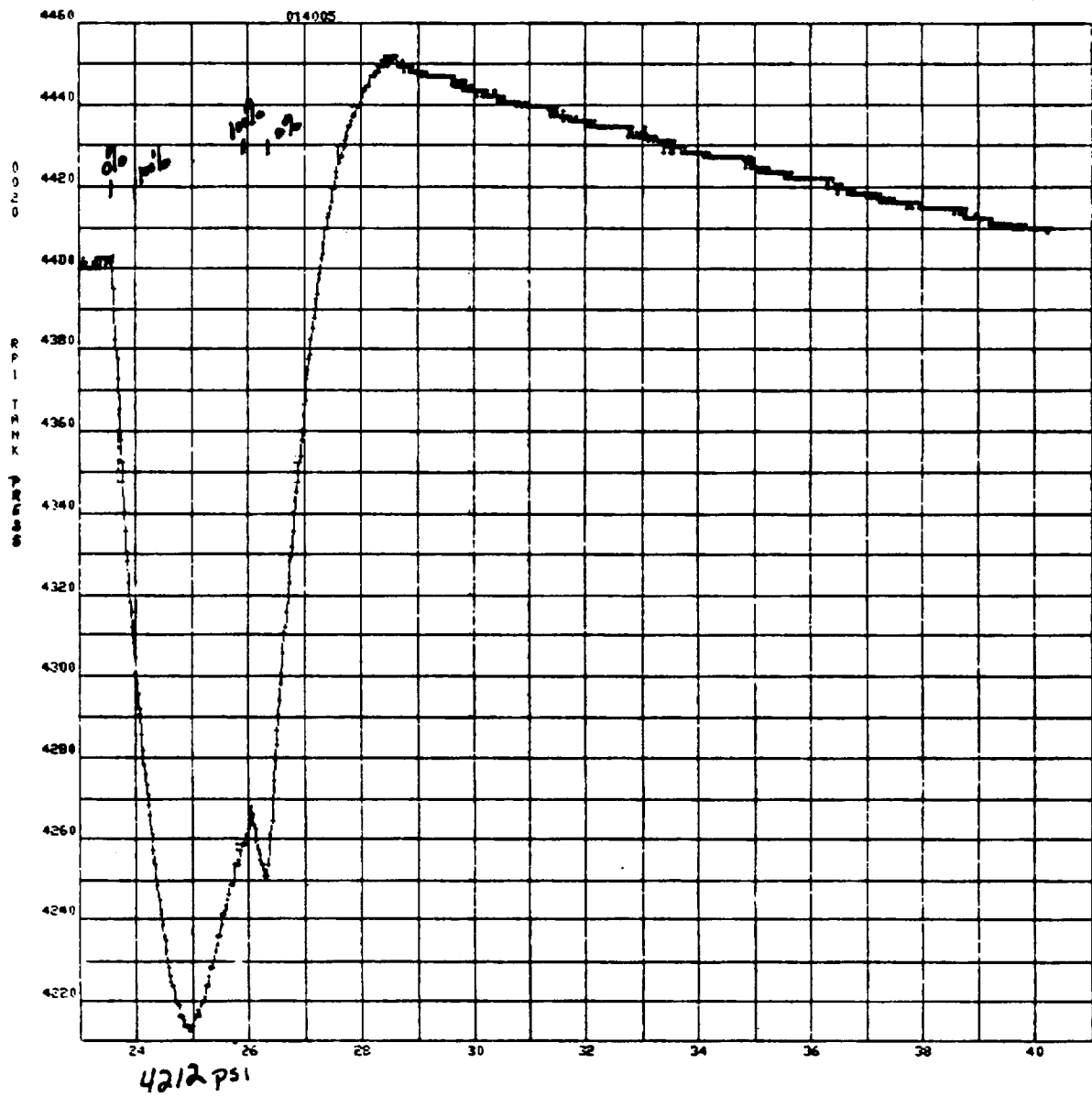
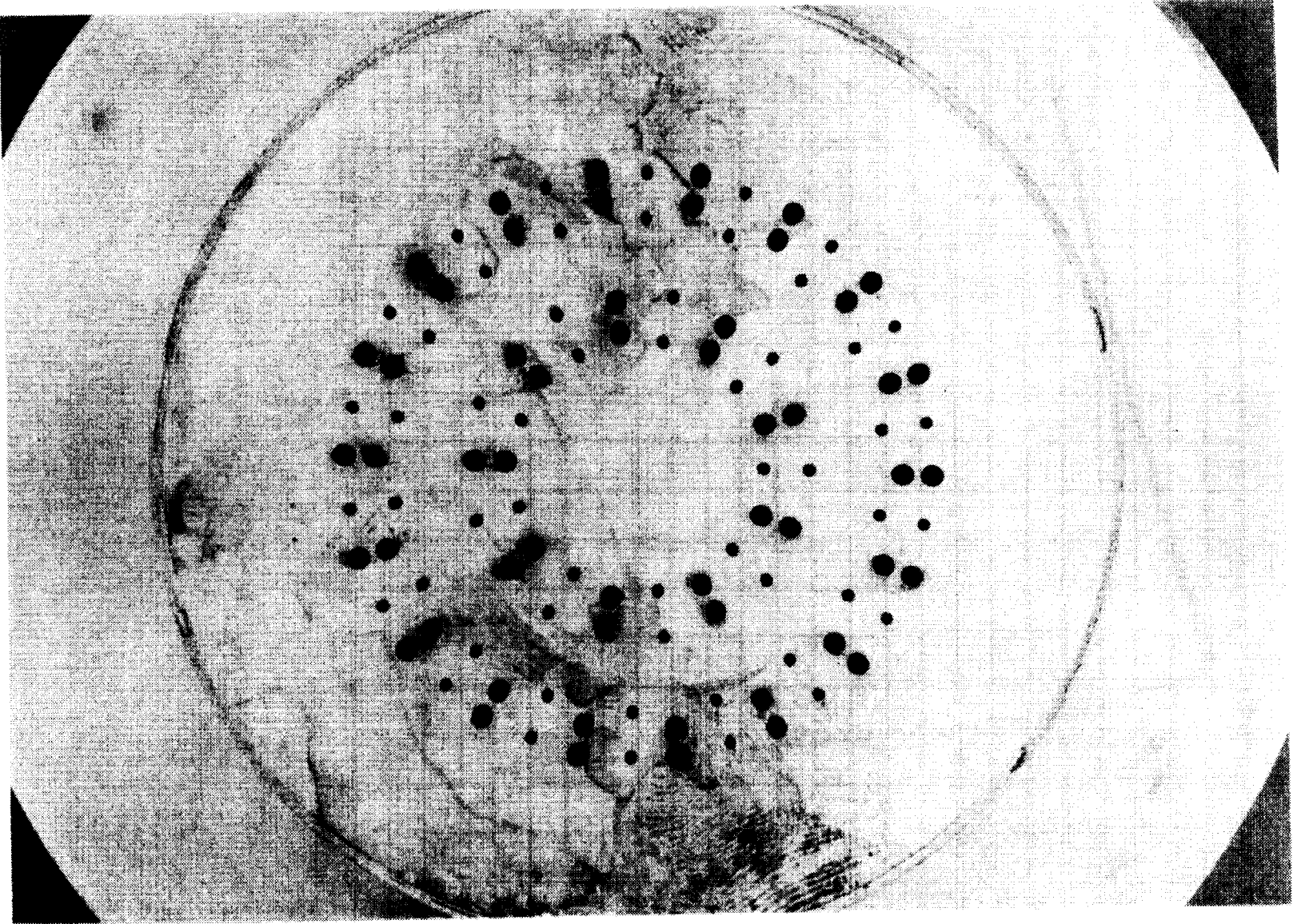


Figure 46. RP-1 Tank Pressure, Test 005



1XX35-9/27/79-C1C

Figure 47. LOX/RP-1 Like-Doublet Injector

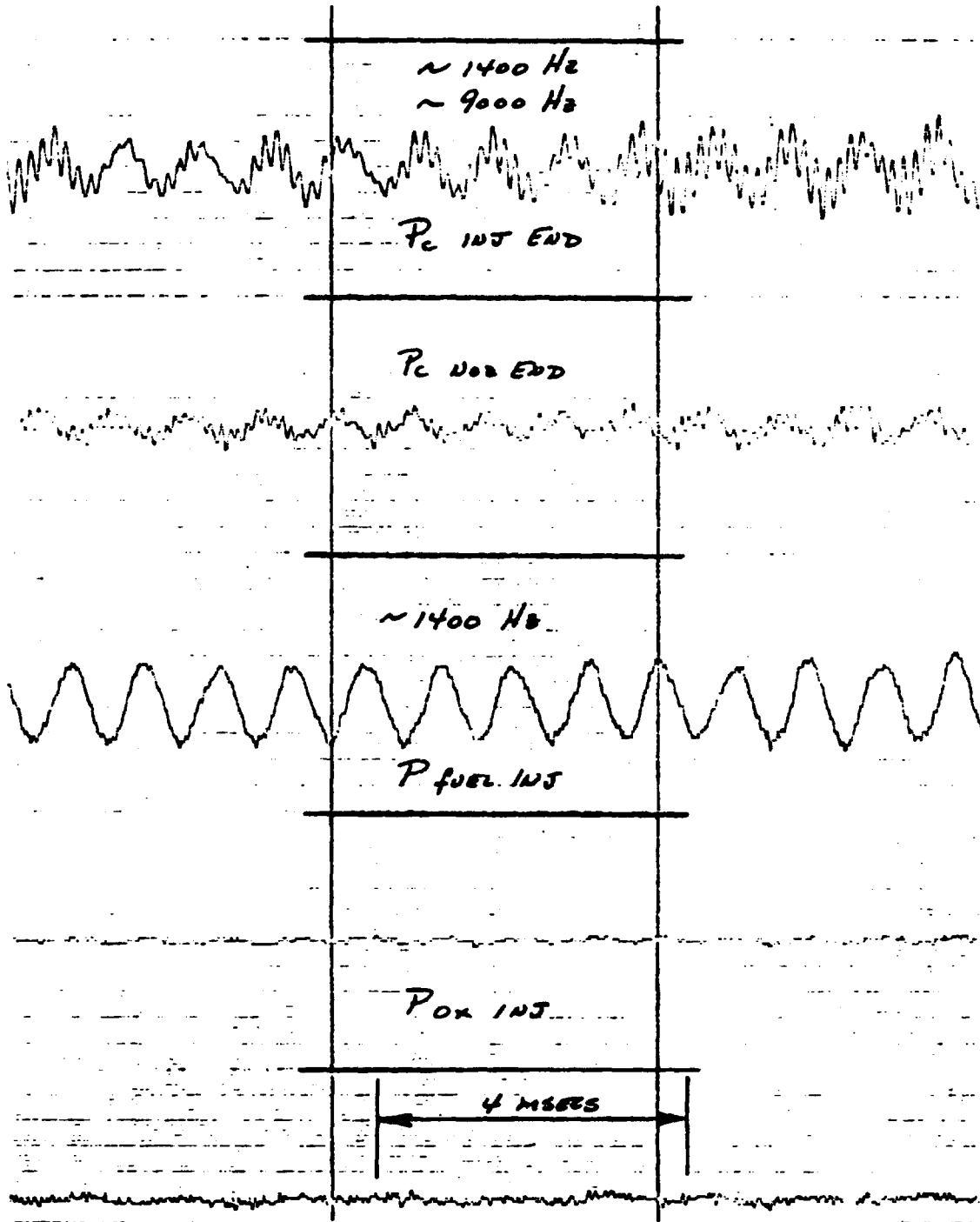


Figure 48. High-Frequency A-C Trace, Test 005

C-2

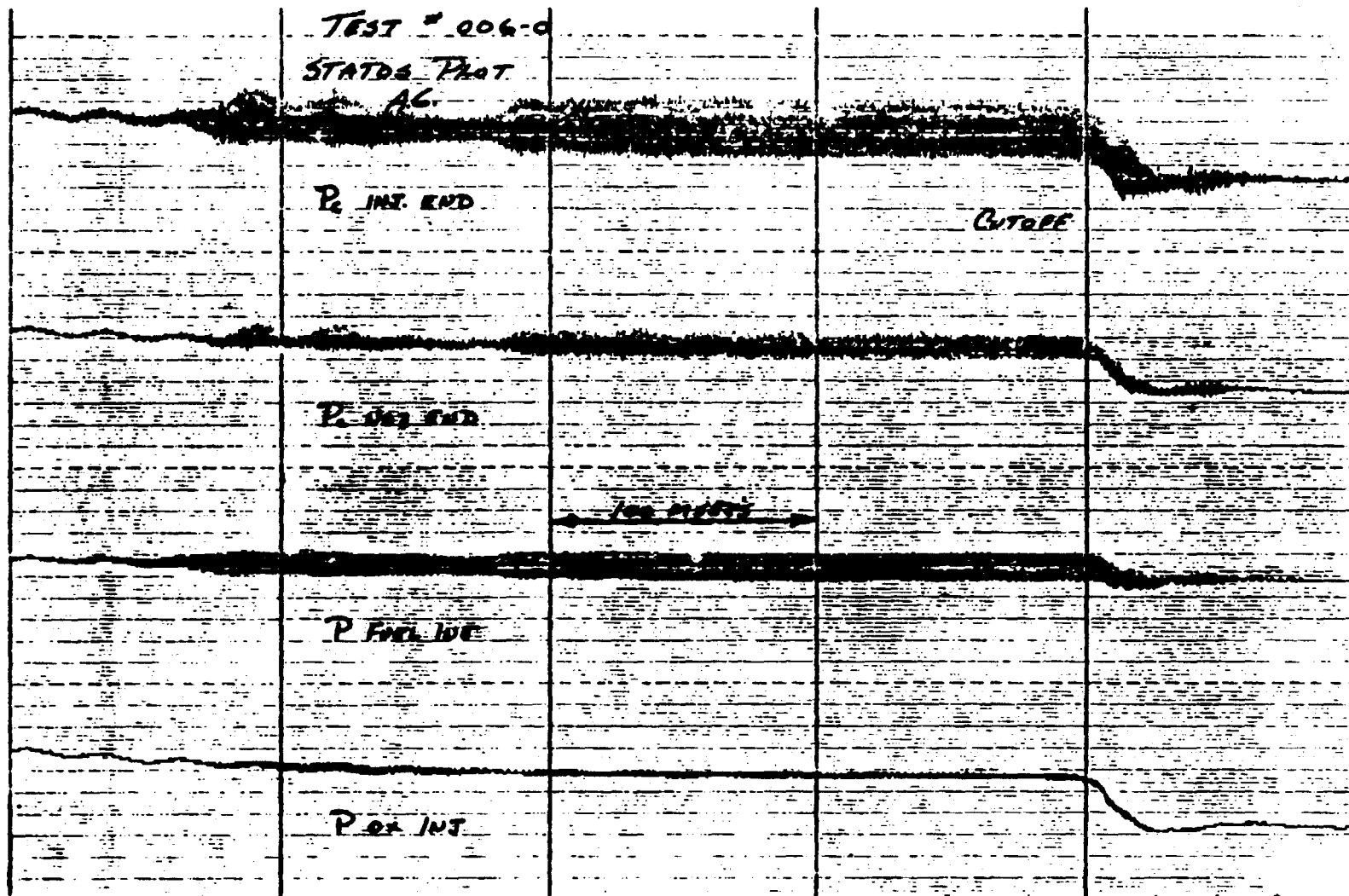
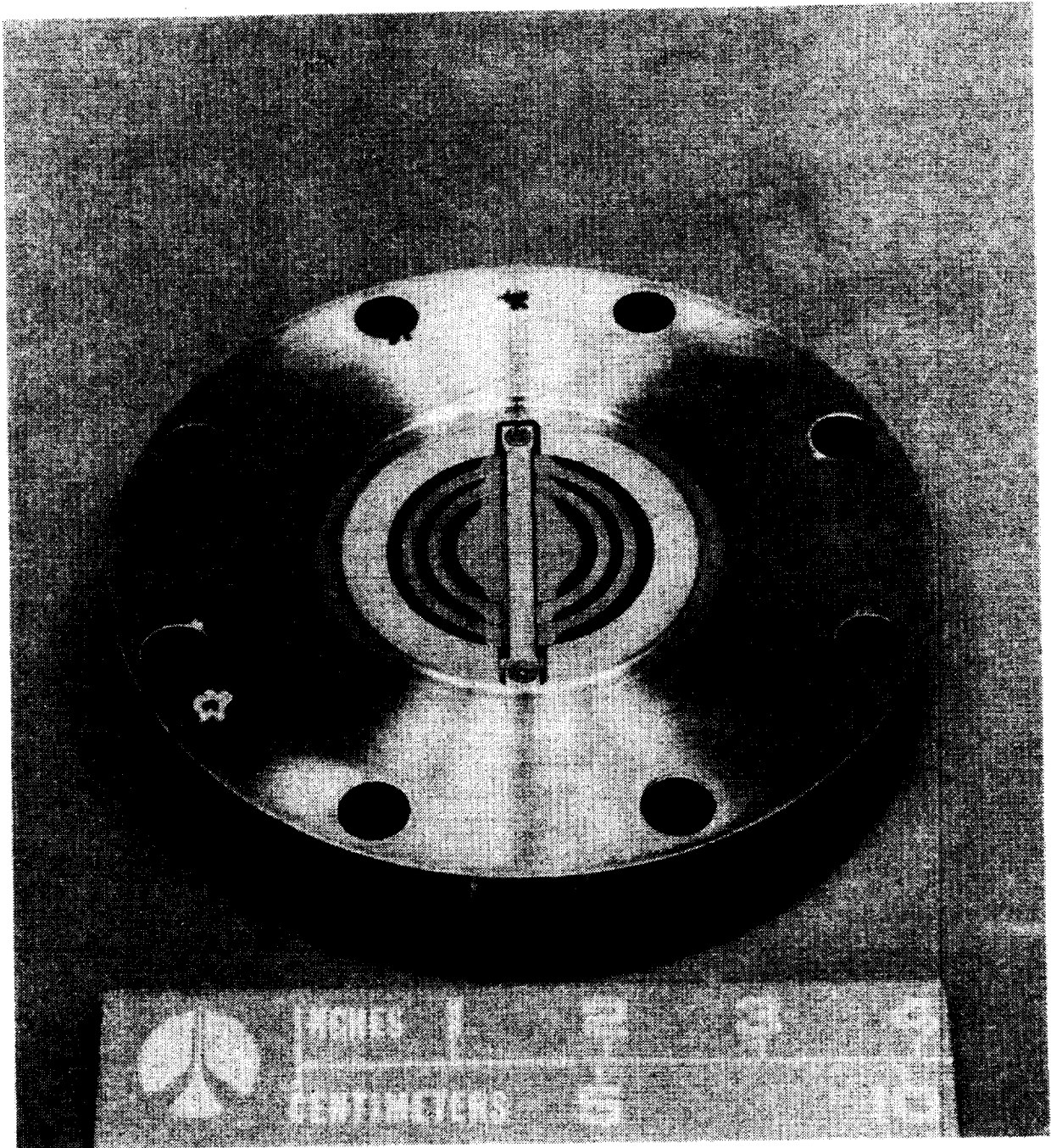


Figure 49. High-Frequency A-C Status Plot, Test 006



LXX32-7/27/79-C1B

Figure 50. Carbon Deposition Fixture

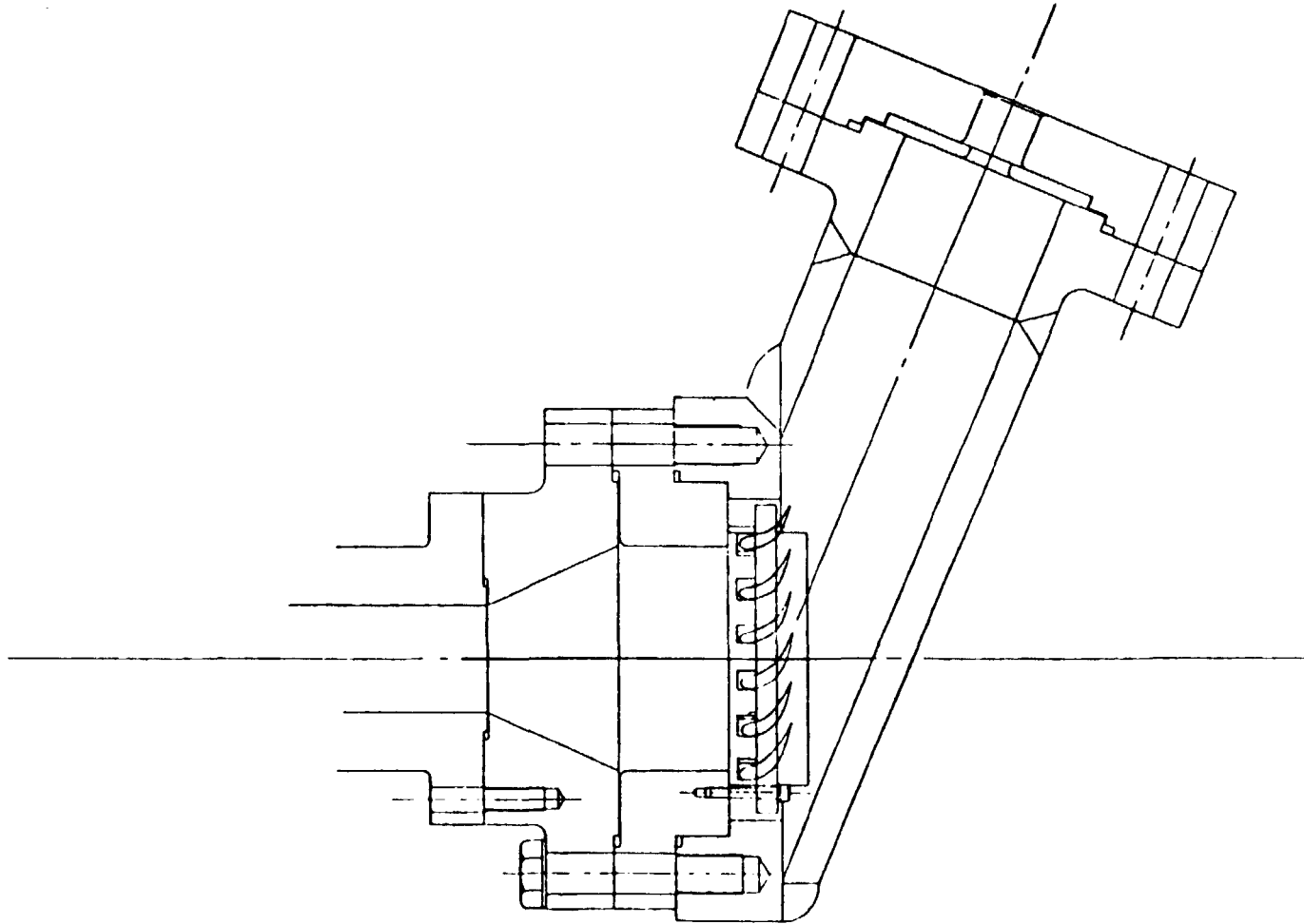


Figure 51. Alternate Design Turbine Blade Simulator Used for Carbon Checking Evaluation

Test 007 was a hot-fire attempt to provide gas sampling of LOX/RP-1 combustion gases at 1900R combustion temperature and 3500-psia chamber pressure. This test was terminated prematurely due to a facility malfunction. A high-temperature thermocouple cutoff circuit was energized due to an erroneous signal, terminating the test. No ignition was realized.

Test 008 was a repeat attempt of 007 and realized 4 seconds of the 5 seconds scheduled. Gas sampling was scheduled for the 4- to 5-second period but was not realized. The test was terminated prematurely 4 seconds into the test due to pressure oscillations exceeding the ± 700 -psi peak-to-peak cutoff point. Figure 52 illustrates the oscillations as they progressed to the cutoff point. This is an a-c "Statos" trace and represents the composite oscillation.

A blowup of this time section shows the oscillations start at a relatively low level and gradually increase until an unacceptable level is attained. This increase is brought about by coupling with the fuel feed system and slowly reinforcing the energy available in the combustor.

Figure 53 illustrates the chamber pressure buildup and the level attained. At this pressure reading, the propellant mixture ratio was 0.453, and the characteristic velocity efficiency attained was 87.4%. This efficiency is based on the equilibrium thermochemical LOX/RP-1 model. To determine the carbon deposition rate, a device shown in Fig. 50 was fabricated under contract. This device was a series of annular rings with spacing comparable to a turbine blade assembly, with a turning surface similar to an air foil section. This device was used to determine the carbon deposition rate during hot-fire tests by providing a delta pressure change versus time plot. In addition to the quantitative relationship, a visual inspection would result in a qualitative evaluation. Due to unanticipated events, the combustion process realized a longitudinal instability and consumed the deposition device before it could be utilized. In lieu of this event, a turbine blade evaluation fixture (shown in Fig. 37) was designed and fabricated with company funds. This device was used in demonstrating the deposition of carbon in a qualitative manner. Test durations were not of significant duration to adequately define the carbon deposition rate. Figures 28 and 29 illustrate the

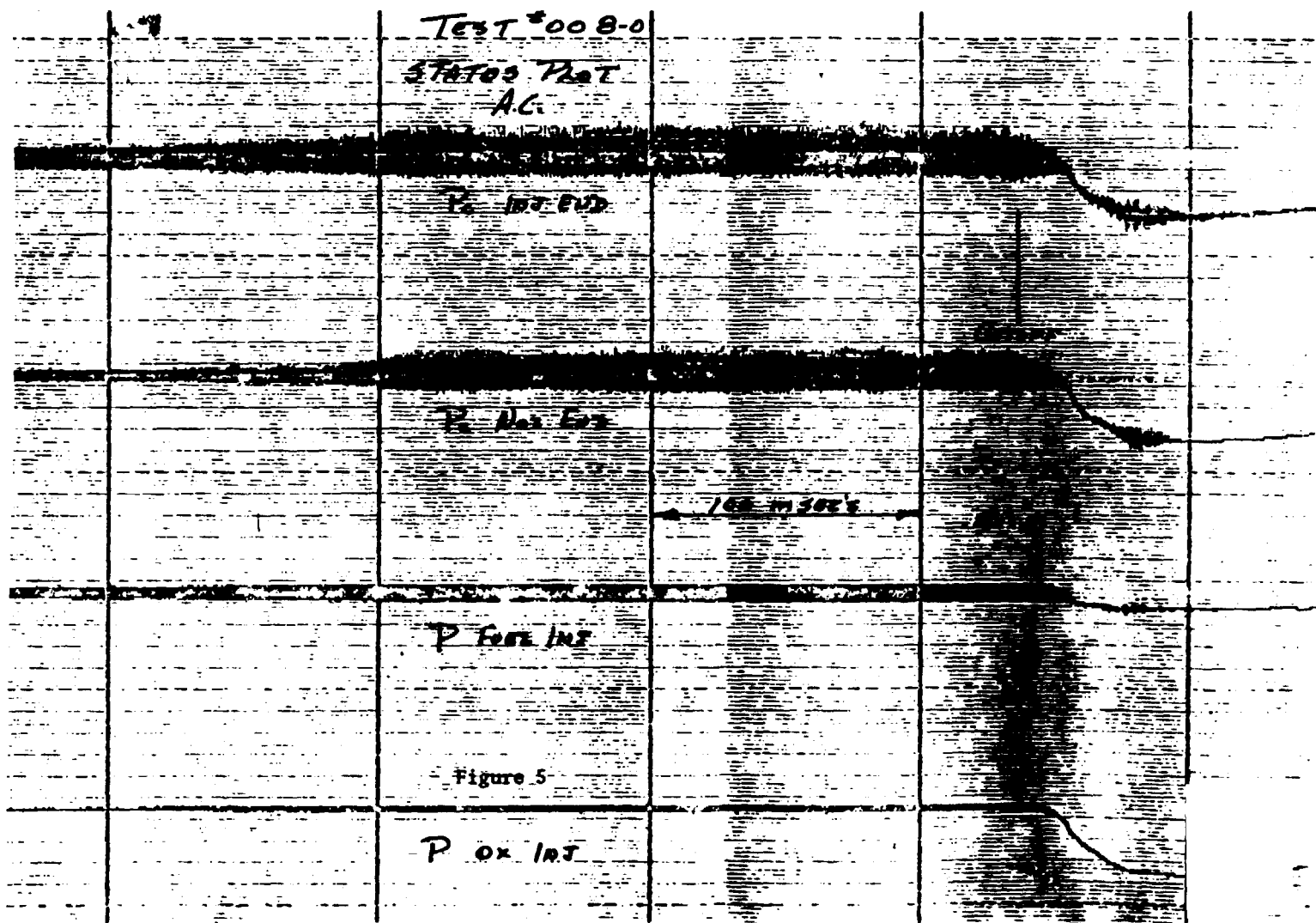


Figure 52. High-Frequency A-C States Plot, Test 008

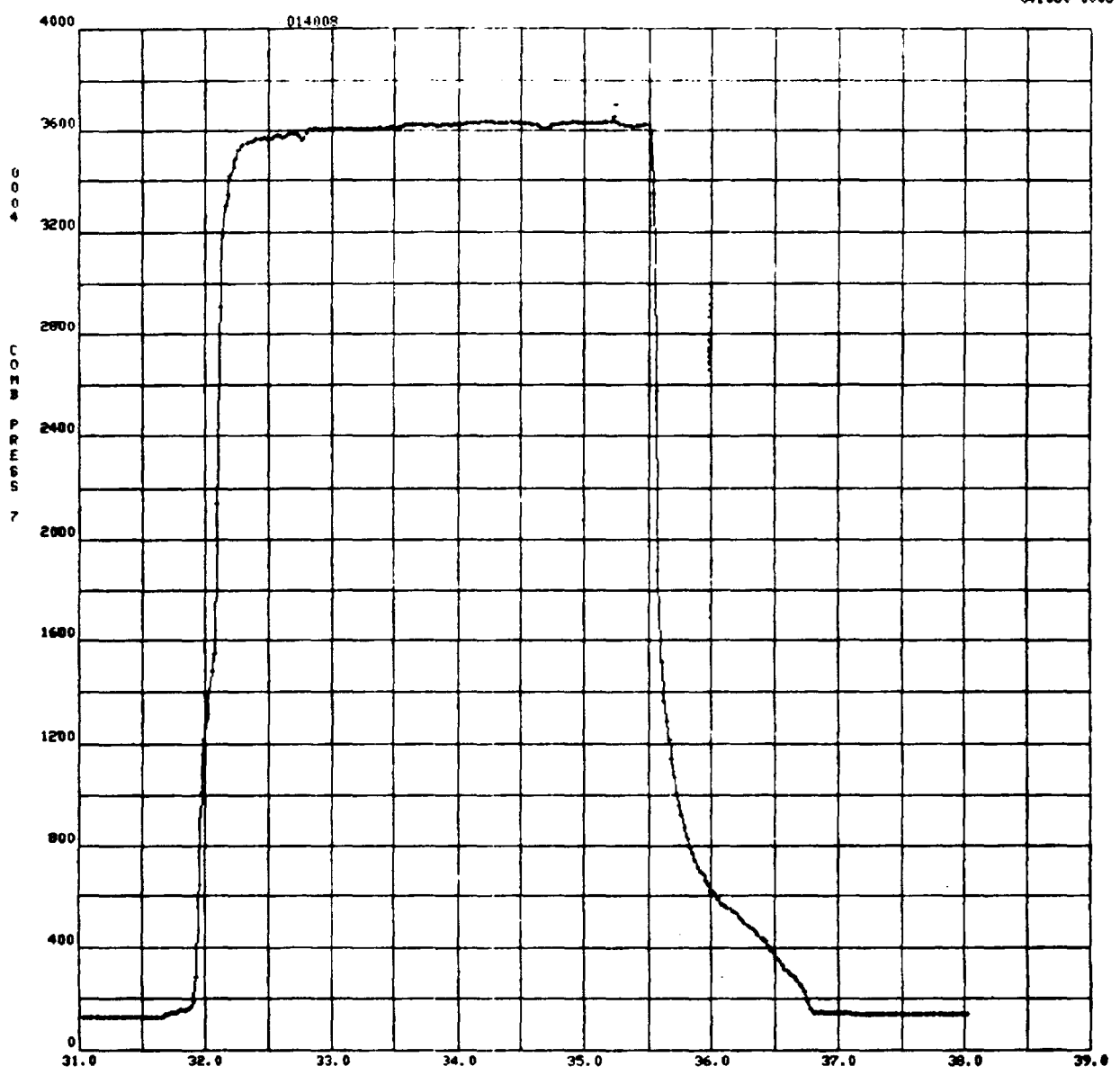


Figure 53. Chamber Pressure Trace, Test 008

visual appearance of the exhaust plumes. These figures show the gross difference in the free carbon available in the combustion products, and this visual observation is substantiated by the combustion product samples that were taken and reported in this section.

This turbine blade coking fixture also was the device used to create the combustion gas turbulence resulting in the combustion gas characteristic velocity increase. The three tests conducted for carbon evaluation resulted in the temperature profile shown in Fig. 54. The profile shows the temperature increase as the combustion gases enter the transition zones.

Oxidizer-Rich LOX/RP-1. Four oxidizer-rich LOX/RP-1 test attempts failed to demonstrate injector performance and stability using a like doublet with oxidizer showerhead injection. The tests were terminated within 600 msec due to overheating and resultant degradation of the combustor hardware. Figures 55 and 56 illustrate the typical post-hardware condition. Various combustor sections were damaged, along with the thermocouple rake, nozzles, and acoustic absorber rings. Minimal damage was done to the injector face.

Analysis of the posttest data as the tests were conducted lead to erroneous conclusions. After the first test, the failure was attributed to the oxidizer hypergol preventing the injector from starting in a true oxidizer-rich mode. The second test utilized a new ignition system--a fuel hypergol. This system, realizing the injector face delta pressure limitations, could provide an oxidizer-rich start and transition to the desired mixture ratio. This test attempt also resulted in hardware degradation, this time caused by a cycling (3 cycles/second) oxidizer tank pressurizing system. During the low periods of the cycle, it was theorized the mixture ratio limits were exceeded causing hardware failure. An extensive check-out of the oxidizer system resulted in modification to the pressurizing system. The third test was attempted and terminated due to low LOX injection pressure. Again, the combustor hardware was damaged.

In preparation for the fourth test, a high-pressure head was installed on the fuel main valve, the valve plug was modified to a linear configuration, the fuel manifold volume was decreased substantially, and a venturi was inserted in the LOX inlet

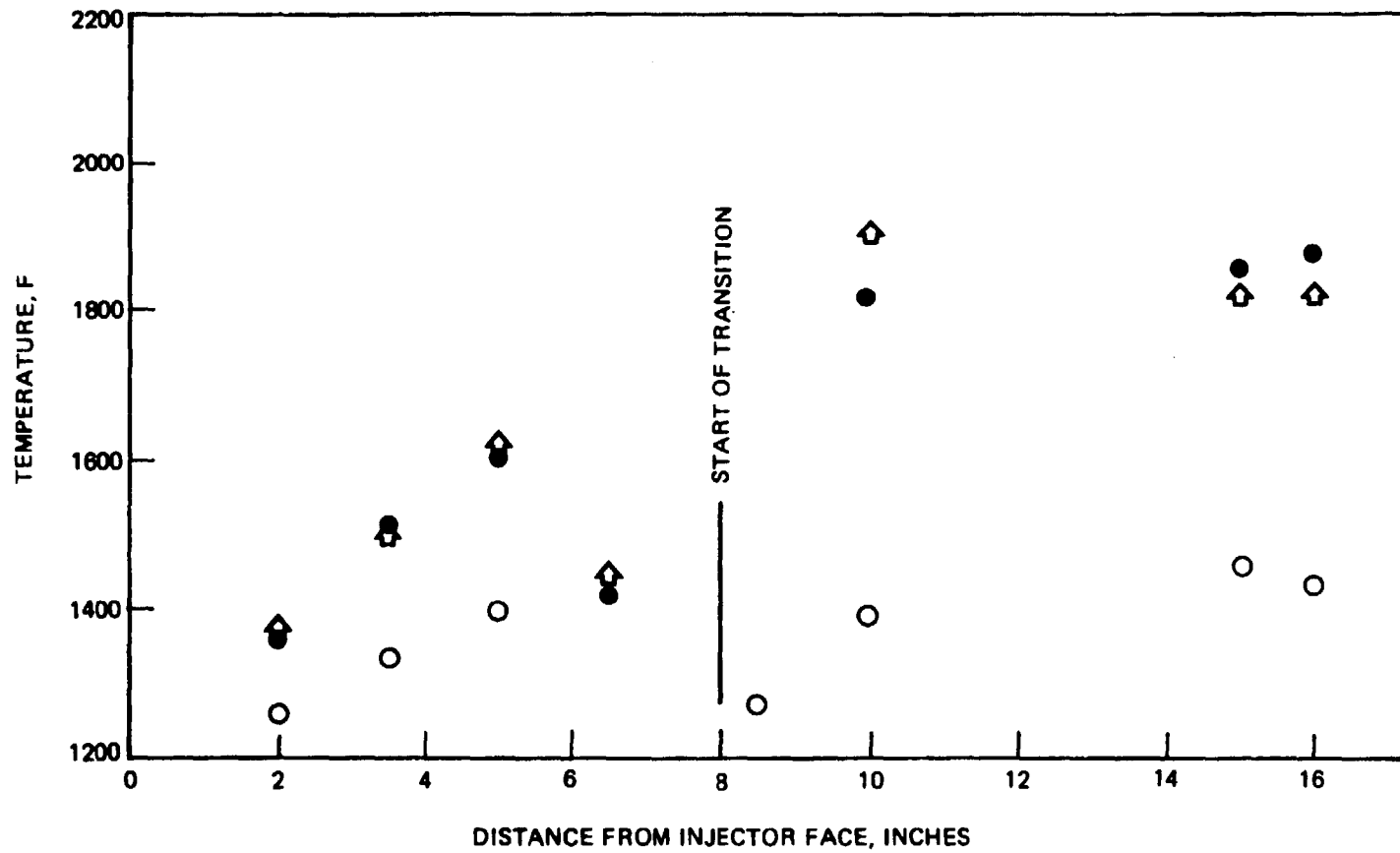
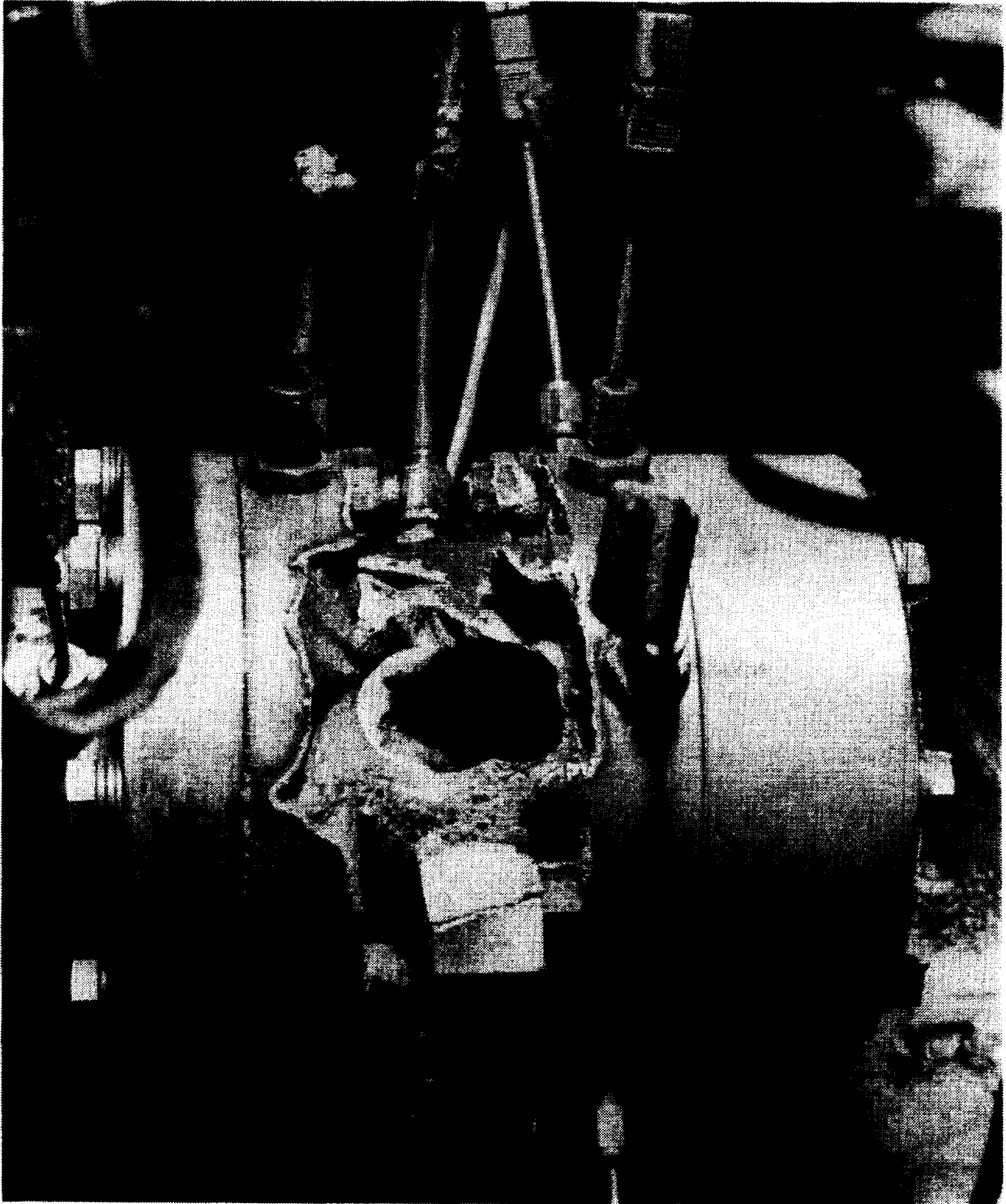


Figure 54. LOX/RP-1 Chamber Temperature Profile

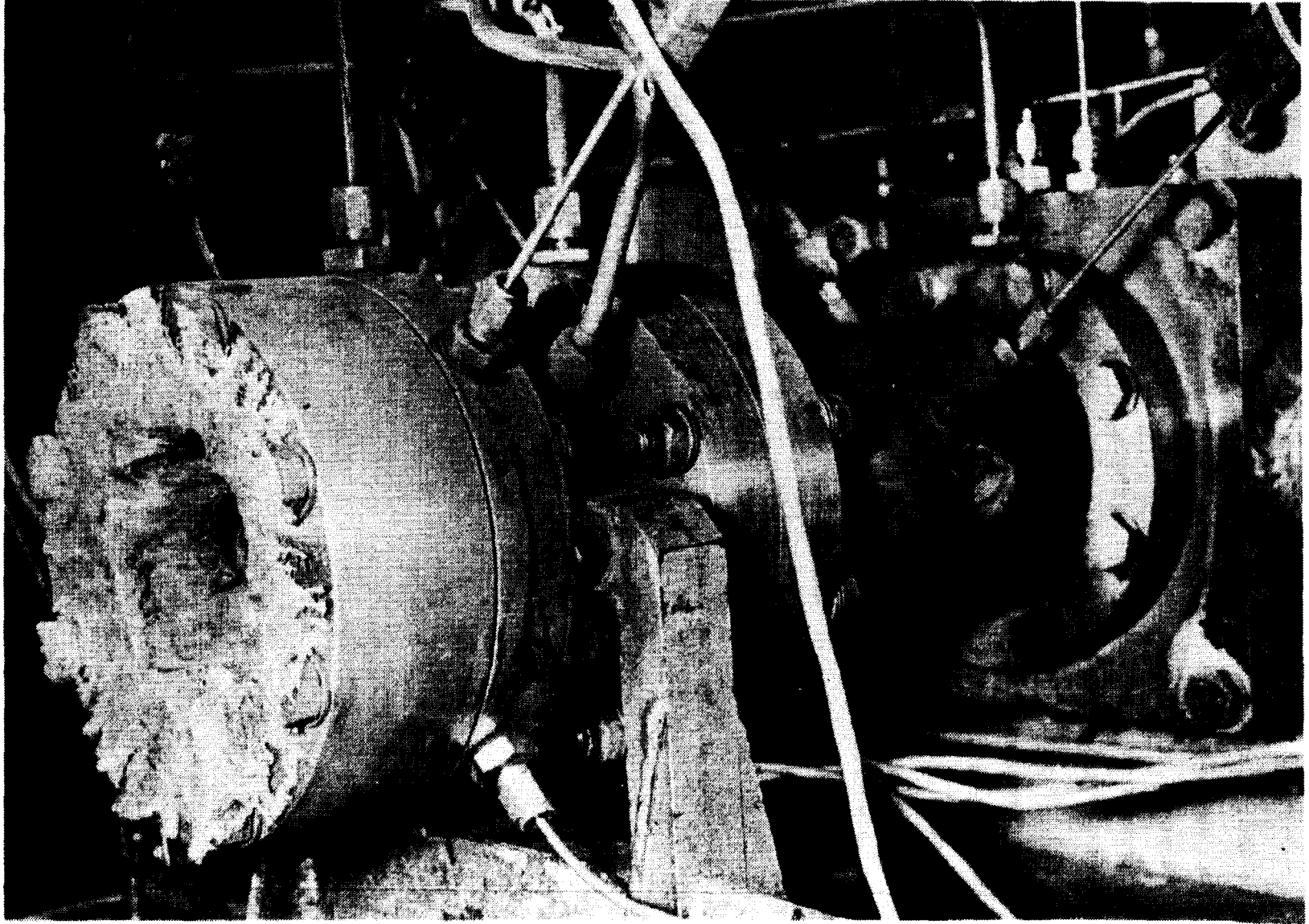


50P36-9/4/80-S1C

Figure 55. Oxidizer-Rich Combustor Failure

ORIGINAL PAGE IS
OF POOR QUALITY

101



50P36-9/4/80-S1A*

Figure 56. Oxidizer-Rich Preburner Failure

manifold to limit flow when injector back pressure was low to prevent exceeding the injector face delta pressure limitations. With these facility modifications and sequencing changes, the fourth and last test attempt was made. This test also resulted in premature termination and hardware degradation. Again, the cutoff was initiated by low LOX injection pressure. Figures 57 through 60 show the test as it occurred. Figure 57 illustrates the combustion chamber pressure cutoff signal was initiated at 16.65 seconds. This shows that cutoff was initiated prior to full chamber pressure and at CTF/RP-1 ignition. Figure 58 shows an oxidizer injection pressure plateau of 2900 psi, this is the CTF in the manifold. Figure 57 shows the fuel injection pressure rise initiation at 16.4 seconds corresponding to the oxidizer injection pressure rise. In Figure 60, the LOX line pressure decay is illustrated. Although the line pressure is cycling, the hardware degradation has been realized before fuel injection pressure is up to specified value. It was concluded that the like-doublet/showerhead injector was realizing no protection from the showerheads at the start of the combustor. The like doublets, sized to operate just over stoichiometric, had a localized gas temperature in excess of the 300 series stainless-steel ignition temperature. The addition of the excess oxidizer rapidly oxidized the stainless combustor.

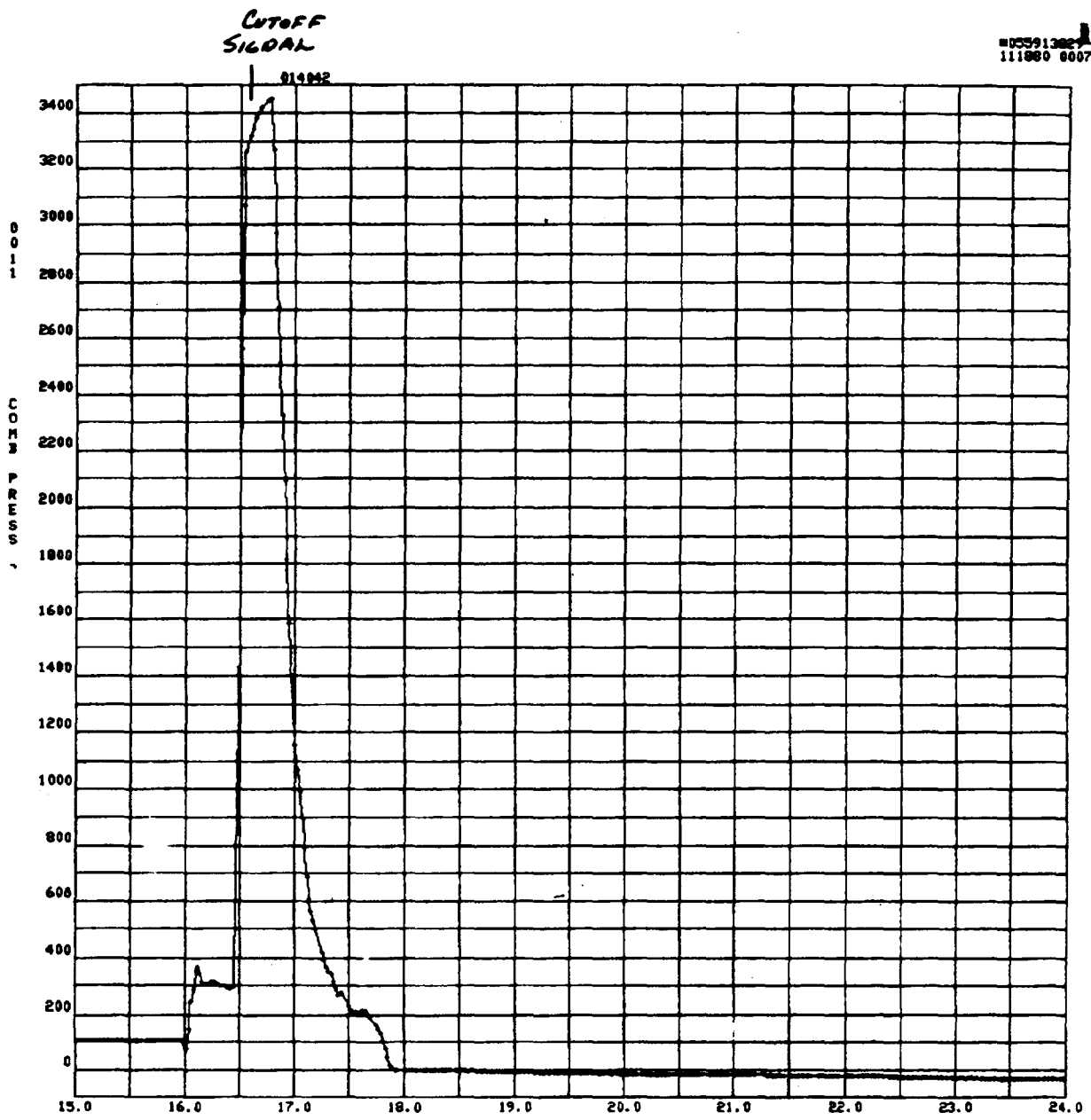


Figure 57. Chamber Pressure vs Time

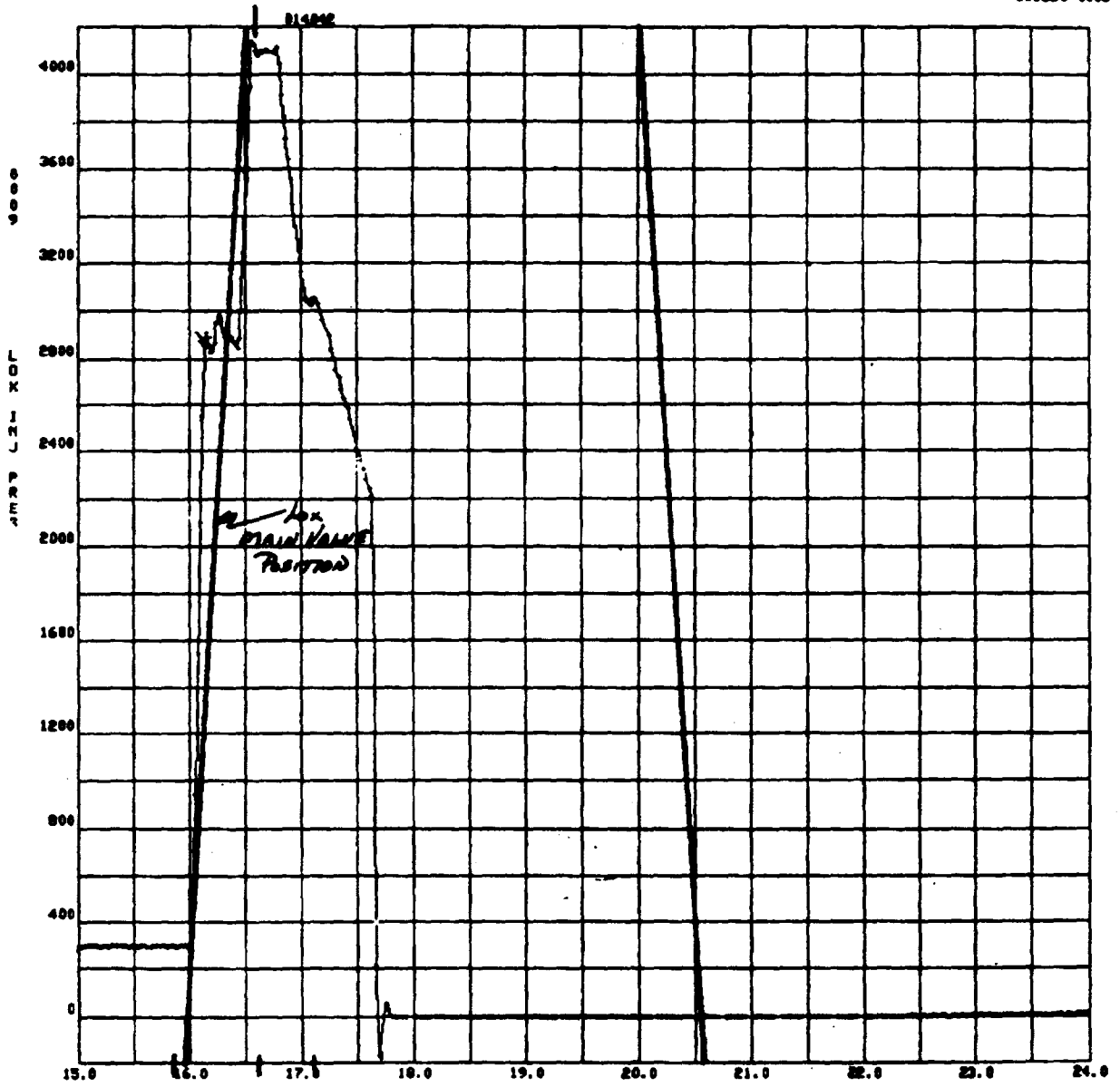


Figure 58. LOX Injection Pressure vs Time

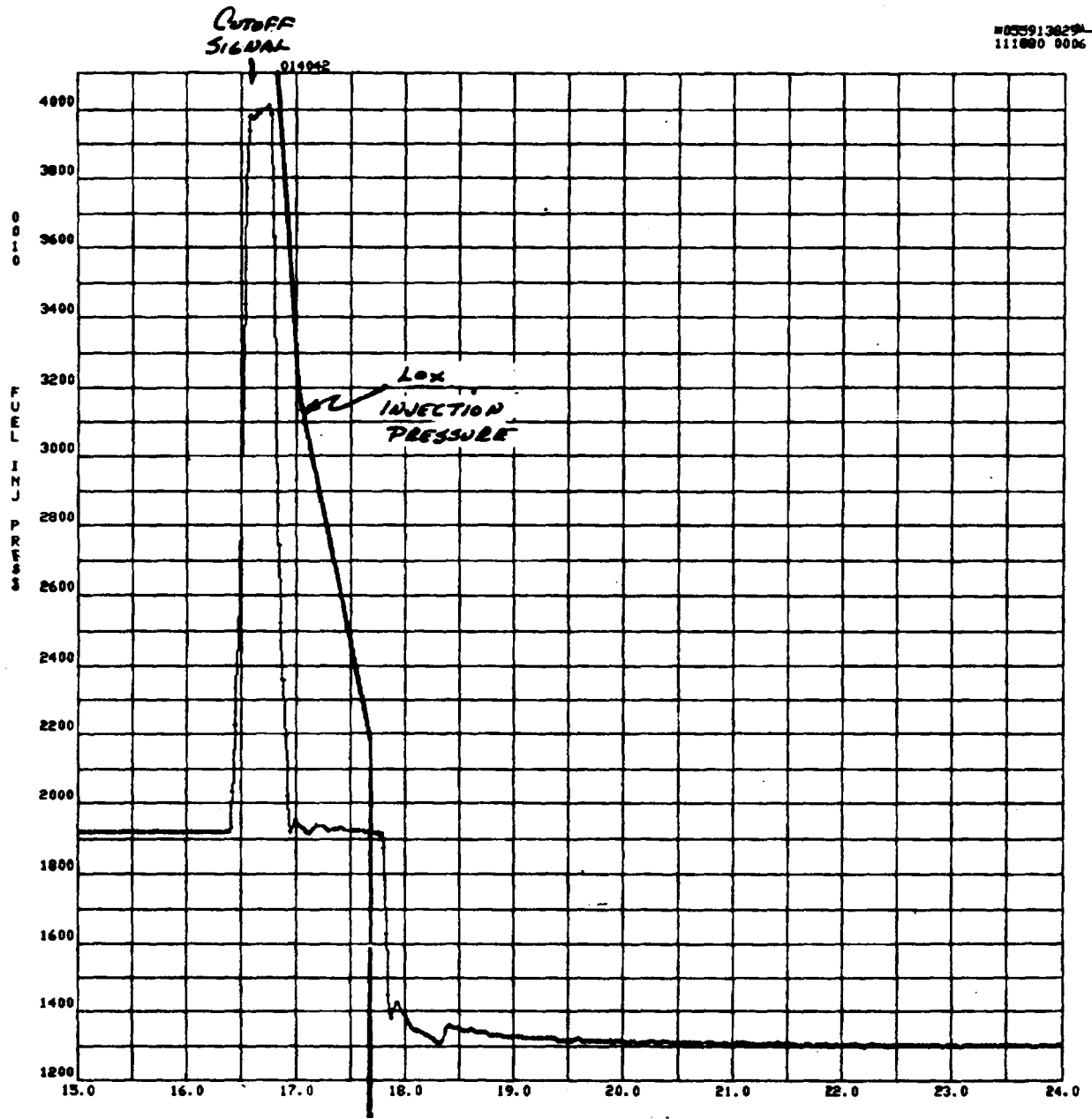


Figure 59. Fuel Injection Pressure vs Time

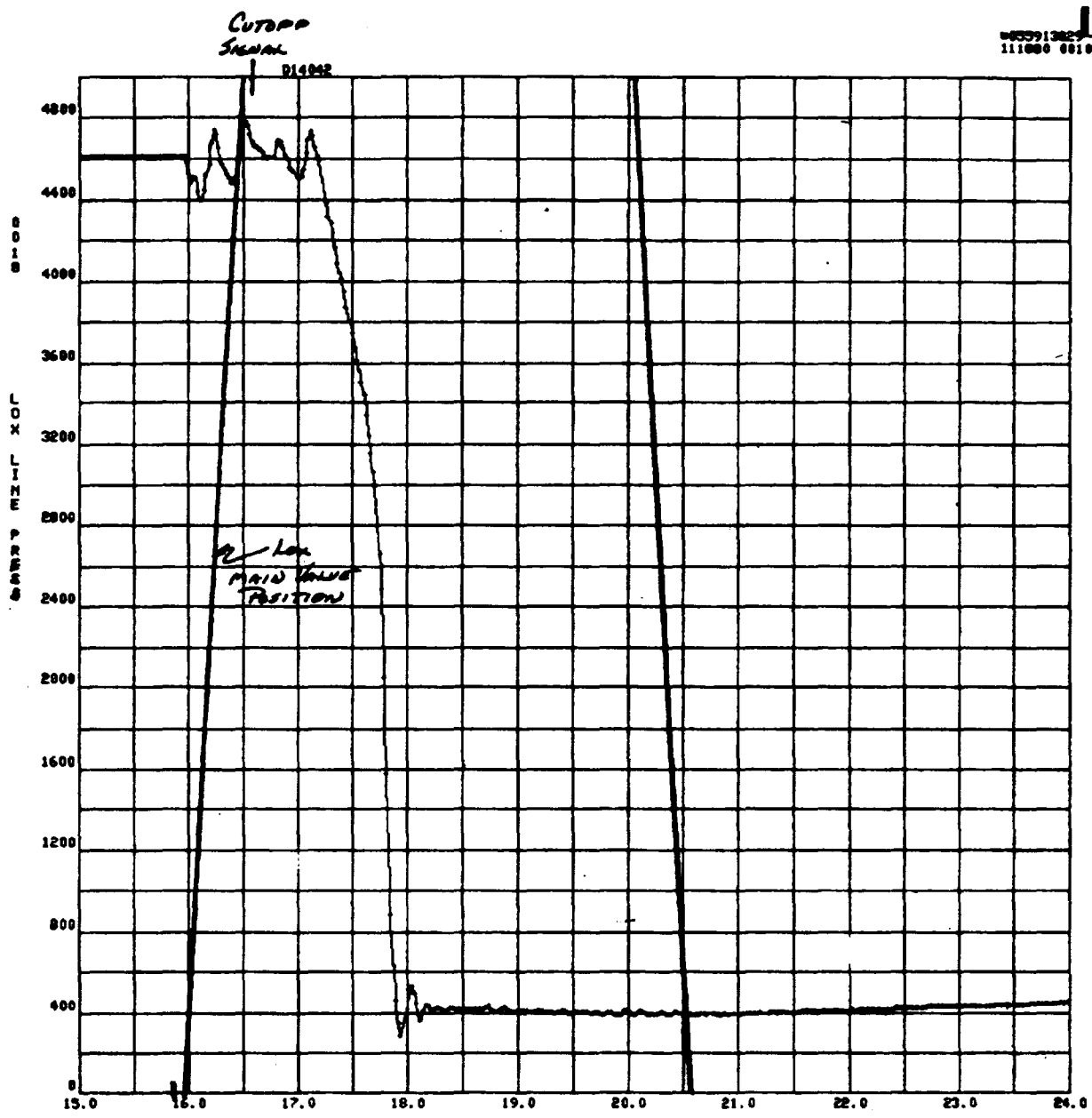


Figure 60. LOX Line Pressure vs Time

It is evident from the four test attempts conducted that limited technology was realized from this oxidizer-rich configuration. The configuration used would require major rework to permit satisfactory injector operation. With this knowledge, the NASA/MSFC program monitor chose to terminate the LOX/RP-1 oxidizer-rich small-scale testing and redirect the remainder of the program.

Cold-Flow Testing. The hot-fire testing of the injectors in this program seemed to indicate that the primary performance-limiting mechanism was mixing. This is suggested by the apparent lack of performance sensitivity to the various chamber lengths tested. The classic rocket combustion theory proposes that, while more complete vaporization is accomplished by increasing duration, (i.e. combustor length), mixing deficiencies at the primary flame front persist through large increases in chamber length unless significant efforts are expended to introduce turbulence in the entire chamber cross section.

For any extended injector development effort, cold-flow mixing tests would provide a reduced cost screening of proposed injector configurations prior to committing the designs to final fabrication or hot-fire testing. Cold-flow mixing tests can be conducted using models of the proposed configuration or, in many cases, using the actual hot-fire test hardware. The liquid/liquid systems can be evaluated using an existing collection grid system, which is more fully described below. The liquid/gas systems (LOX/CH₄, etc.) require a more elaborate, more restrictive facility, also more fully described in subsequent sections.

Both types of mixing tests are recommended for follow-on injection development effort. Properly utilized as a design screening and evaluation tool, the cold-flow testing will ensure higher performance and more uniform temperature distribution with fewer hot-fire tests. Although there are elements of "cut and try" in the cold-flow testing as well as hot-fire, the "cuts" and the "tries" are faster and cheaper and, in some ways, more quantitative than hot-fire testing.

The hot-fire test program did not indicate any significant vaporization limits within the envelope of the testing. For this reason, and with the present costs of dropsizes testing considered, a dropsizes cold-flow test program was not proposed. Special equipment, which would permit low-cost dropsizes measurement is being evaluated on another program, and this recommendation may be re-evaluated at a later date, based on these results.

Cleaning Procedure for Injectors. During attempts to conduct oxidizer-rich hot-fire tests, it was realized that using CTF, an oxidizer for an ignition source, was not satisfactory. The ignition occurred at off-design mixture ratio, and hardware over-heating and catastrophic failure were realized. A facility modification was made to permit the use of triethyl aluminum (TEA) for ignition. Although this system provided satisfactory ignition of the main propellants, injector orifice clogging was realized frequently when residual TEA trapped in plumbing and hardware joints hydrolyzed when exposed to air. The residue that formed through the hardware was more prevalent when the CH_4 was used. When using RP-1 fuel, the RP-1 "washed" and mixed/diluted the TEA.

To clean the copper injector bodies used in the LOX/hydrocarbon preburners, chemical, mechanical, and ultrasonic techniques were required. The fuel/oxidizer orifices were plugged/restricted with a residue from the hydrolyzed TEA. The following cleaning procedure was used:

1. Injector was immersed in 5% aqueous potassium hydroxide for 5 minutes, then rinsed with tap water.
2. Each fuel and oxidizer orifice was "pinned" with an appropriate-sized soft-wire gauge.
3. Injector body was immersed in an ultrasonic cleaner for 10 to 15 minutes, then rinsed with tap water.
4. Injector was flowed with tap water to verify that orifices were open.
5. After verification, the body was rinsed with deionized water, followed by reagent grade acetone, then blown dry with GN_2 .

Precautions were exercised to prevent the hydrolyzing of the TEA, but setup procedures required losing the inert environment for period of time. It was during this time that the residue deposition took place.

Gas Sampling Analysis. While conducting the 42 tests shown in data summary, four tests each for LOX/RP-1 and LOX/ CH_4 were run solely to attain hot-gas samples.

Each test had three sample locations, all in the same axial plane. It was apparent while sampling that the redundant samples could not be retained for each test. One sample each for three different LOX/RP-1 and LOX/CH₄ tests was analyzed thoroughly. The sample results are summarized in Tables 7 through 11. These recorded data are discussed in the subsequent text.

Tables 12 through 14 show the results of three different radial locations in test 010--a LOX/RP1 hot fire. The different radial positions are noted on the individual tables. Two positions are recorded for the LOX/CH₄ hot-fire test 025; these are shown in Tables 10 and 11. The results shown are based on a gas chromatography test and show relatively good correlation. The helium gas is realized from the pretest positive pressure introduced to the sample bottles. It can be seen from the sample pressure that one system could be more leak resistant than the others. The better sample was retained for analysis in all cases. Throughout the sampling, some samples were lost due to facility malfunctions or were contaminated during analysis. The subsequent text explains the technique used for obtaining the gas samples reported.

Six sample bottles for the high-pressure preburner tests were fabricated from 2-inch stainless-steel tubing with 0.120-inch wall thickness and a length of 12.6 inches. The ends were capped with standard AN fittings modified for 1/4-inch AN fittings. Copper seals were used for all flared joints. These sample bottles were fabricated, leak checked, proofed (2120 psig), and cleaned prior to each use. As shown in Fig.61, the bottles contain hand valves and a pressure gage (for transportation purposes).

A schematic of one of the sample systems is shown in Fig.61, and the installation of the sample main valve to the sample probe connection was as close as practical. Copper seals were used in the facility lines.

The sample procedure was to manually purge and pressure cycle the sample bottles in place with helium. During the hot-fire test, the sample main valve was sequenced open for a specified time to achieve a sample bottle pressure of less than 2000 psig. A relief valve was installed as safety protection for the sample bottles, which were rated at 2120 psig, and would open to chamber pressures of approximately

3500 psig. If the relief valve vented during the test, the sample of that particular line was invalid.

During the run, the remote sample valve was opened for a predetermined time to fill the bottle to approximately 1000 psig. Posttest, the sample bottle pressure was verified remotely using the line transducer, then the bottle was secured and removed from the system. However, if the bottle pressure exceeded the rating, the bottle was remotely vented using the sample main valve, and the sample was lost.

The sample bottles were labeled to establish the radial position in the chamber where the sample was taken. After the test was completed, the hand valve of the bottle was closed and the sample line broken. The samples taken were transported immediately to the SSFL chemical laboratory.

The minimum sample analysis consisted of:

1. An analysis of the gas phase by gas chromatography
2. The weight of the solid phase
3. The weight of the nonvolatiles separating aqueous matter from all others

TABLE 7. CHEMICAL ANALYSIS REPORT (TEST 014-010)

LOG NO. 0-5-39

SAMPLE IDENTIFICATION: TEST NO. 014-010
 SAMPLE NO. 2
 LOCATED AT 12 O'CLOCK; 0.33-INCH IMMERSION

DATA: P_c = 3620 PSIA
 \dot{w}_T = 17.7 LB/SEC
 T_c = 2155 R
 MR = 0.430
 c^*_{act} = 3469 FT/SEC
 PROBE DISTANCE = 15 INCHES

RESULTS:	WT %
H ₂	0.77
He	0.8
N ₂	0.4
CO	28.0
CO ₂	6.4
CH ₄	13.6
C ₂ H ₄	4.5
C ₂ H ₆	5.9
C ₃ H ₆	3.9
C ₃ H ₈	1.2
C ₄	1.1
C ₅	0.5
C ₆	0.7
C ₇	0.8
H ₂ O	7.7
CARBON	2.4
LIQUID HYDROCARBON	22.4

TABLE 8. CHEMICAL ANALYSIS REPORT (TEST 014-014)

LOG NO. 0-6-77

SAMPLE IDENTIFICATION: TEST NO. 014-014
 SAMPLE NO. 3
 LOCATED AT 9 O'CLOCK; 0.67-INCH IMMERSION

DATA: P_c = 3381 PSIA
 \dot{w}_T = 20.0 LB/SEC
 T_c = 2030 R
 MR = 0.366
 c^*_{act} = 2876 FT/SEC
 PROBE DISTANCE = 9 INCHES

RESULTS:	WT %
H ₂	1.07
He	0.8
N ₂	0.7
CO	31.2
CO ₂	6.9
CH ₄	13.1
C ₂ H ₄	5.7
C ₂ H ₆	4.7
C ₃ H ₆	4.5
C ₃ H ₈	1.1
C ₄	1.5
C ₅	0.4
C ₆	0.5
C ₇	-
H ₂ O	9.2
CARBON	2.6
LIQUID HYDROCARBON	16.1

TABLE 9. CHEMICAL ANALYSIS REPORT (TEST 014-015)

LOG NO. 0-6-79

SAMPLE IDENTIFICATION: TEST NO. 014-015
 SAMPLE NO. 3
 LOCATED AT 9 O'CLOCK; 0.67-INCH IMMERSION

DATA: P_c = 3353 PSIA
 \dot{w}_T = 20.6 LB/SEC
 T_c = 1856 R
 MR = 0.356
 c^*_{act} = 2771 FT/SEC
 PROBE DISTANCE = 9 INCHES

RESULTS:	WT %
H ₂	0.84
He	0.6
N ₂	0.4
CO	25.6
CO ₂	5.6
CH ₄	9.9
C ₂ H ₄	4.6
C ₂ H ₆	3.7
C ₃ H ₆	3.2
C ₃ H ₈	0.8
C ₄	2.1
C ₅	0.7
C ₆	0.5
C ₇	-
H ₂ O	9.4
CARBON	1.8
LIQUID HYDROCARBON	31.0

TABLE 10. CHEMICAL ANALYSIS REPORT (TEST 014-023)

LOG NO. 0-7-34

SAMPLE IDENTIFICATION: TEST NO. 014-023
 SAMPLE NO. 2
 LOCATED AT 12 O'CLOCK; 0.33-INCH IMMERSION

DATA: P_c = 3508 PSIA
 \dot{w}_T = 12.2 LB/SEC
 T_c = 2360 R
 MR = 0.805
 c^*_{act} = 4766 FT/SEC
 PROBE DISTANCE = 13 INCHES

RESULTS:	WT %	
H ₂	2.7	
He	-	
N ₂	-	
CO	28.6	
CO ₂	8.0	
CH ₄	40.9	
C ₂ H ₄	1.1	} TRACES
C ₂ H ₆	3.1	
C ₃ H ₆		
C ₃ H ₈		
C ₄		
C ₅		
C ₆		
C ₇		
H ₂ O	15.0	
CARBON	0.15	
LIQUID HYDROCARBON	0.5	

TABLE 11. CHEMICAL ANALYSIS REPORT (TEST 014-024)

LOG NO. 0-7-35

SAMPLE IDENTIFICATION: TEST NO. 014-024
 SAMPLE NO. 3
 LOCATED AT 9 O'CLOCK; 0.67-INCH IMMERSION

DATA: P_c = 3472 PSIA
 \dot{w}_T = 12.8 LB/SEC
 T_c = 2347 R
 MR = 0.759
 c^*_{act} = 4459 FT/SEC
 PROBE DISTANCE = 9 INCHES

RESULTS:	WT %
H ₂	2.7
He	-
N ₂	-
CO	27.7
CO ₂	7.5
CH ₄	43.0
C ₂ H ₄	1.1
C ₂ H ₆	3.3
C ₃ H ₆	} TRACES
C ₃ H ₈	
C ₄	
C ₅	
C ₆	
C ₇	
H ₂ O	14.1
CARBON	0.15
LIQUID HYDROCARBON	0.5

TABLE 12. CHEMICAL ANALYSIS REPORT (TEST 014-025)

LOG NO. 0-7-43

SAMPLE IDENTIFICATION: TEST NO. 014-025
 SAMPLE NO. 2
 LOCATED AT 12 O'CLOCK; 0.33-INCH IMMERSION

DATA: P_c = 3458 PSIA
 \dot{w}_T = 13.0 LB/SEC
 T_c = 2377 R
 MR = 0.735
 c^*_{act} = 4360 FT/SEC
 PROBE DISTANCE = 15 INCHES

RESULTS:	<u>WT %</u>
H ₂	8.2
He	-
N ₂	-
CO	27.9
CO ₂	7.8
CH ₄	37.3
C ₂ H ₄	0.9
C ₂ H ₆	2.3
C ₃ H ₆	} TRACES
C ₃ H ₈	
C ₄	
C ₅	
C ₆	
C ₇	
H ₂ O	14.2
CARBON	0.7
LIQUID HYDROCARBON	0.8

TABLE 13. CHEMICAL ANALYSIS REPORT (TEST 014-010)

LOG NO. 4-222-80 (21 MAY 1980)

SAMPLE IDENTIFICATION: TEST NO. 014-010; PRESSURE = 750 PSI
 SAMPLE NO. 1 (LOX/RP-1)
 LOCATED AT MIDPOINT, 1 INCH FROM WALL

DATA: P_c = 3620 PSIA
 \dot{w}_T = 17.7 LB/SEC
 T_c = 2155 R
 MR = 0.430
 c^*_{act} = 3469 FT/SEC
 CHAMBER LENGTH = 15 INCHES

RESULTS: (ON WATER-FREE BASIS)

	WT %	
H ₂	11.0	
He	7.3	
O ₂ /Ar	ND<0.5	
N ₂	0.9	
CO	31.0	
CO ₂	4.4	
CH ₄	34.0	
C ₂ H ₄	4.3	
C ₂ H ₆	4.2	
C ₃ H ₆	1.2	
C ₃ H ₈	0.2	
C-4	0.2	(6 COMPONENTS DETECTED)
C-5	0.03	(9 COMPONENTS DETECTED)
C-6	0.2	(5 COMPONENTS DETECTED)
C-7	0.02	(2 COMPONENTS DETECTED)

TABLE 14. CHEMICAL ANALYSIS REPORT (TEST 014-010)

LOG NO. 4-223-80 (21 MAY 1980)

SAMPLE IDENTIFICATION: TEST NO. 014-010 ; PRESSURE = 850 PSI
 SAMPLE NO. 2 (LOX/RP-1)
 LOCATED FARTHEST RADIALY, 0.33 INCH FROM
 WALL

DATA: P_c = 3620 PSIA
 \dot{w}_T = 17.7 LB/SEC
 T_c = 2155 R
 MR = 0.430
 c^*_{act} = 3469 FT/SEC
 CHAMBER LENGTH = 15 INCHES

RESULTS: (ON WATER-FREE BASIS)

	WT %	
H ₂	11.0	
He	6.3	
O ₂ /Ar	(C ₂ H ₄ INTERFERENCE)	
N ₂	0.7	
CO	32.0	
CO ₂	4.5	
CH ₄	33.0	
C ₂ H ₄	4.2	
C ₂ H ₆	4.7	
C ₃ H ₆	1.4	
C ₃ H ₈	0.3	
C-4	0.2	(8 COMPONENTS DETECTED)
C-5	0.08	(11 COMPONENTS DETECTED)
C-6	1.0	(8 COMPONENTS DETECTED)
C-7	0.2	(5 COMPONENTS DETECTED)

COMMENTS: CORRECTED RESULTS; SEE TABLE (LOG NO. 4-222-80, DATED
 21 MAY 1980) FOR EXPLANATION.

TABLE 15. CHEMICAL ANALYSIS REPORT (TEST 014-010)

LOG NO. 4-224-80 (21 MAY 1980)

SAMPLE IDENTIFICATION: TEST NO. 014-010; PRESSURE = 800 PSI
 SAMPLE NO. 3 (LOX/RP-1)
 LOCATED 1 AND 2 O'CLOCK, 0.67 INCH FROM WALL

DATA: P_c = 3620 PSIA
 \dot{w}_T = 17.7 LB/SEC
 T_c = 2155 R
 MR = 0.430
 c_{act}^* = 3469 FT/SEC
 CHAMBER LENGTH = 15 INCHES

RESULTS: (ON WATER-FREE BASIS)

	WT %	
H ₂	12.0	
He	6.5	
O ₂ /Ar	(C ₂ H ₄ INTERFERENCE)	
N ₂	0.5	
CO	32.0	
CO ₂	4.7	
CH ₄	27.0	
C ₂ H ₄	5.2	
C ₂ H ₆	6.3	
C ₃ H ₆	2.9	
C ₃ H ₈	0.9	
C-4	0.6	(8 COMPONENTS DETECTED)
C-5	0.2	(12 COMPONENTS DETECTED)
C-6	0.3	(10 COMPONENTS DETECTED)
C-7	0.02	(4 COMPONENTS DETECTED)

COMMENTS: CORRECTED RESULTS; SEE TABLE (LOG NO. 4-222-80, DATED
 21 MAY 1980) FOR EXPLANATION.

TABLE 16. CHEMICAL ANALYSIS REPORT (TEST NO. 014-025)

LOG NO. 7-31-80 (9 JULY 1980)

SAMPLE IDENTIFICATION: TEST NO. 014-025; PRESSURE = 950 PSI
 SAMPLE NO. 1 (LOX/CH₄)
 LOCATED AT MIDPOINT, 1 INCH FROM WALL

DATA: P_c = 3458 PSIA
 \dot{w}_T = 13 LB/SEC
 T_c = 2377 R
 MR = 0.735
 c^*_{act} = 4360 FT/SEC
 CHAMBER LENGTH = 15 INCHES

RESULTS: (ON WATER-FREE BASIS)

	<u>WT %</u>	
H ₂	23.0	
He	6.7	
O ₂ /Ar	ND<0.2	
N ₂	3.9	
CO	17.0	
CO ₂	3.2	
CH ₄	43.0	
C ₂ H ₄	0.7	
C ₂ H ₆	1.6	
C ₃ H ₆	ND<0.1	
C ₃ H ₈	ND<0.1	
C-4	0.01	(7 COMPONENTS DETECTED)
C-5	TR<0.01	(8 COMPONENTS DETECTED)
C-6	0.04	(2 COMPONENTS DETECTED)
C-7	ND<0.01	(0 COMPONENTS DETECTED)

PRESSURE = 903 PSIG AT 24 C

TABLE 17. CHEMICAL ANALYSIS REPORT (TEST 014-025)

LOG NO. 7-32-80 (9 JULY 1980)

SAMPLE IDENTIFICATION: TEST NO. 014-025; PRESSURE = 1075 PSI
 SAMPLE NO. 2 (LOX/CH₄)
 LOCATED AT MIDPOINT, 40.33 INCH FROM WALL

DATA: P_c = 3458 PSIA
 \dot{w}_T = 13 LB/SEC
 T_c = 2377 R
 MR = 0.735
 c^*_{act} = 4360 FT/SEC
 CHAMBER LENGTH = 15 INCHES

RESULTS: (ON WATER-FREE BASIS)

	<u>WT %</u>
H ₂	24.0
He	6.4
O ₂ /Ar	ND<0.2
N ₂	3.5
CO	18.0
CO ₂	3.2
CH ₄	42.0
C ₂ H ₄	0.6
C ₂ H ₆	1.4
C ₃ H ₆	ND<0.1
C ₃ H ₈	ND<0.1
C-4	TR<0.01 (7 COMPONENTS DETECTED)
C-5	TR<0.01 (5 COMPONENTS DETECTED)
C-6	0.04 (2 COMPONENTS DETECTED)
C-7	ND<0.01 (0 COMPONENTS DETECTED)

PRESSURE = 1041 PSIG AT 24 C

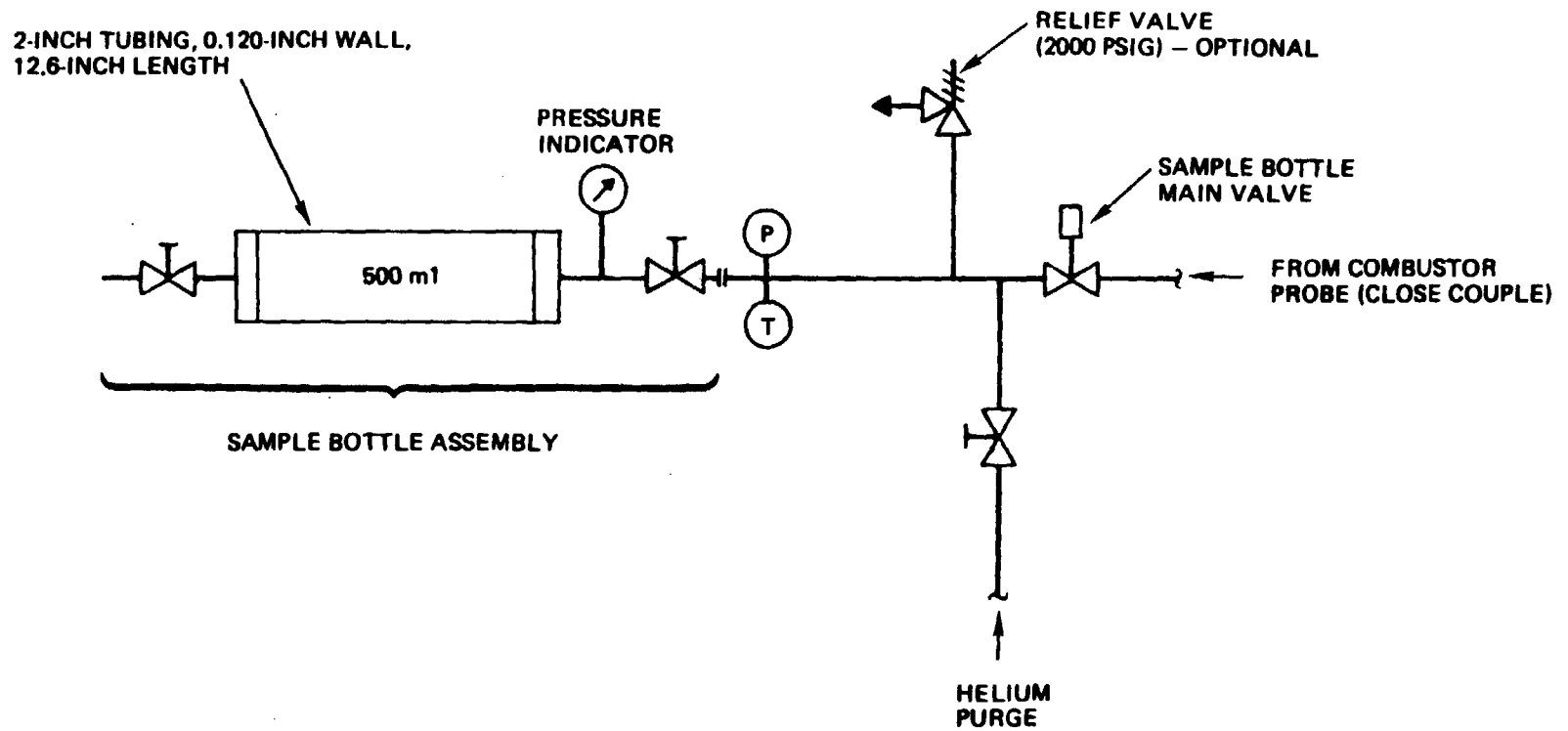


Figure 61. Schematic of Typical Sample Bottle System

Fuel-Rich LOX/RP-1. Plots of temperature and c^* versus mixture ratio are shown in Fig. 62 and 63, which also show equilibrium predictions as well as nonequilibrium based on: (1) C(s) excluded (simplified model), and (2) C(s) excluded and O_2 withheld (original model based on Atlas and Thor data, Table 18). From these figures it is concluded that, except in the three tests where a turbulator was used, equilibrium predictions are much too high but that excluding C(s) from the combustion products (both models) produces generally good agreement in relationship to experimental scatter. Withholding oxygen, according to the relation in Table 18, or not seems to be about equally favored in predicting temperature; that is, the experimental data are not sufficiently tight or biased to discriminate between the models. In the case of c^* prediction, withholding oxygen seems to be slightly favored. The effect of the turbulator to produce nearly equilibrium c^* but not equilibrium temperature is mysterious and seemingly a contradiction. The implication is that the turbulator caused thermoneutral reaction(s) ($\Delta H_T = 0$) to occur which formed products of lower molecular weight; examples of such reactions are not apparent. Gas samples, which might shed light on this anomaly, were not taken in these tests.

Six samples from fuel-rich LOX/RP-1 tests were analyzed, and the composition of the three with complete analysis are shown in Table 18 together with predictions according to equilibrium, simplified model, and the original model. The C(s) found ranged from 1.8 to 3.6 wt %; whereas, that predicted at equilibrium was 32.4 to 36.8 wt %, and that predicted by the nonequilibrium models was, of course, 0. The models predict about 6 to 21 and 12 to 31 wt % liquid hydrocarbon versus 16 to 31 experimental but 0 at equilibrium. There are a number of detailed differences in composition between the experimental, but with shifts in the amounts; for example, the models calculate more CH_4 but less liquid hydrocarbon than found experimentally. Detailed differences in composition between experimental compositions and model predictions are not viewed as critical or as a significant weakness in the models as long as temperature, c^* , and solid carbon are comparable. The fact that the model correlates the present data at 3500 psia and, the Atlas and Thor data from different hardware at 400 to 799 psia, is a strong verification that the model is good.

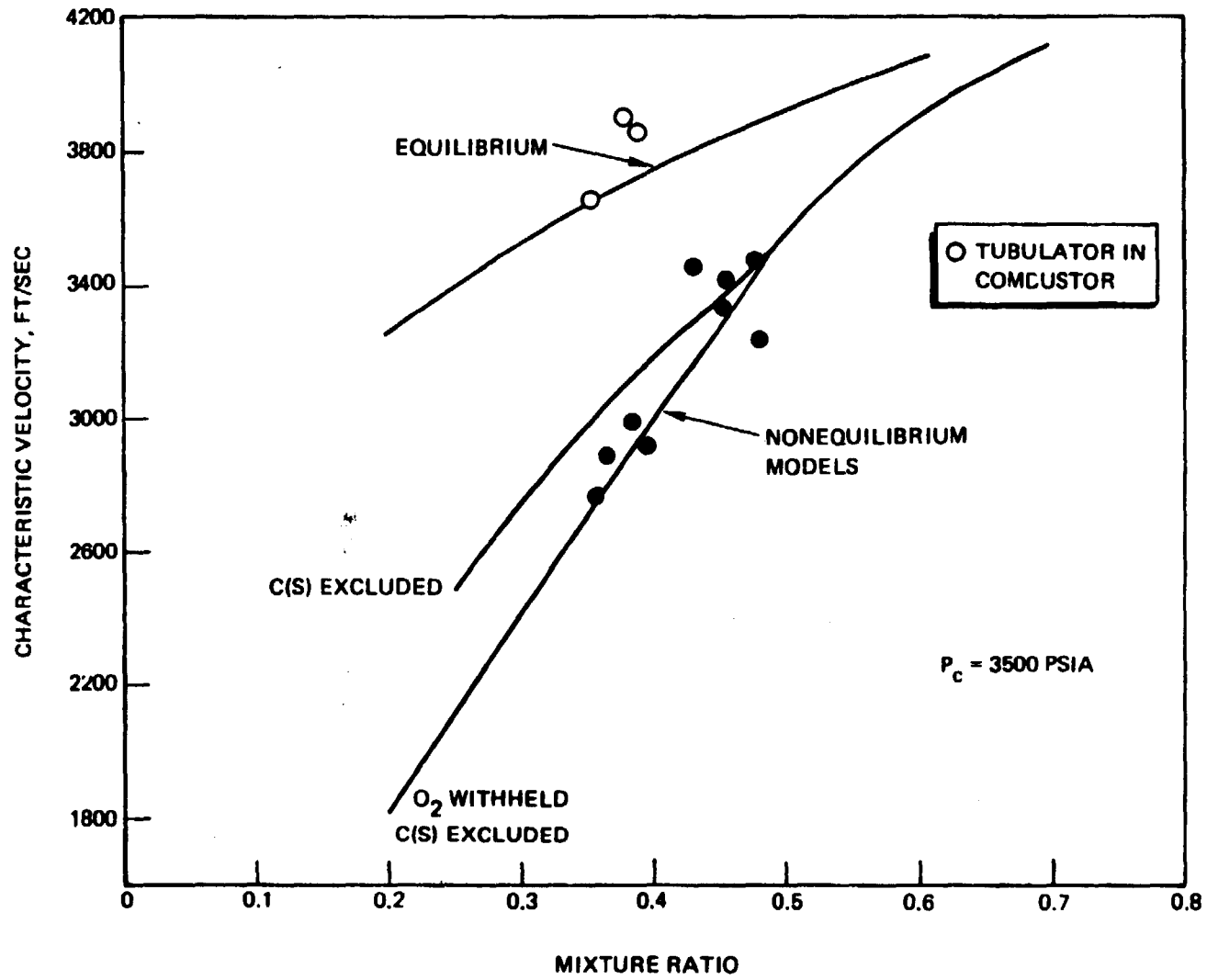


Figure 62. Theoretical Performance, LOX/RP-1

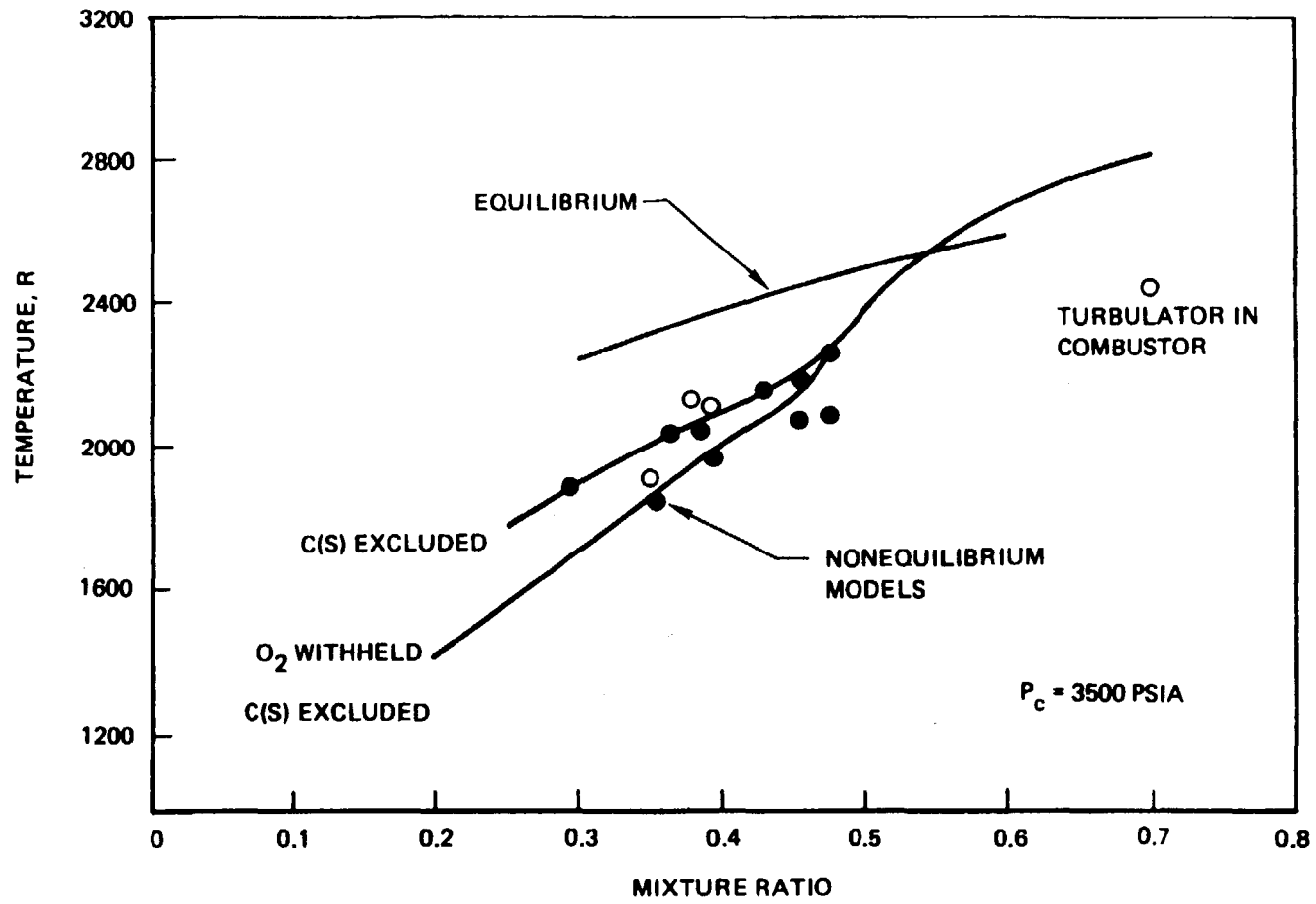


Figure 63. Theoretical Combustion Temperature, LOX/RP-1

TABLE 18. FUEL-RICH LOX/RP-1. GAS PROPERTIES AND COMPOSITION, EXPERIMENTAL AND THEORETICAL

TEST NO.	EXPERIMENTAL			EQUILIBRIUM			C(s) EXCLUDED			C(s) EXCLUDED O ₂ WITHHELD		
	10	14	15	10	14	15	10	14	15	10	14	15
MR	0.430	0.366	0.356	0.430	0.366	0.356	0.430	0.366	0.356	0.430	0.366	0.356
P _c , PSIA	3620	3381	3353	3620	3381	3353	3620	3381	3358	3620	3381	3353
T, R	2155	2030	1856	2444	2353	2339	2150	2033	2014	2089	1917	1887
c*, FT/S	3469	2876	2771	3846	3711	3688	3312	3049	3006	3173	2806	2748
COMPOSITION, wt %												
H ₂	0.8	1.1	0.8	4.1	3.8	3.8	0.1	0	0	0	0	0
CH ₄	13.5	13.2	9.9	18.2	20.8	21.3	26.6	23.7	23.2	24.7	20.6	19.9
C ₂ H ₄	4.5	5.7	4.6	0	0	0	10.5	7.1	6.5	8.4	3.6	3.0
C ₂ H ₆	5.8	4.6	3.7	0	0	0	3.0	2.7	2.7	2.8	2.3	2.2
C ₃ H ₆	3.8	4.5	3.2	-	-	-	-	-	-	-	-	-
C ₃ H ₈	1.2	1.1	0.8	0	0	0	0.3	0.3	0.3	0.3	0.3	0.2
OTHER HC	2.9	2.4	3.3	0	0	0	0.6	0.3	0.3	0.4	0.2	0.1
LIQUID HC	22.3	16.1	31.0	0	0	0	6.3	19.0	21.1	12.2	28.9	31.4
H ₂ O	7.6	9.2	9.4	10.2	11.1	11.2	0	0	0	0	0	0
CO	28.0	31.5	25.6	28.7	21.8	20.7	52.5	46.8	45.8	48.8	40.4	39.0
CO ₂	6.4	6.9	5.6	6.3	6.2	6.2	0.1	0.1	0.1	0.1	0.2	0.2
O ₂	0	0	0	0	0	0	0	0	0	2.1	3.6	3.8
C, SOLID	2.4	3.6	1.8	32.4	36.2	36.8	-	-	-	-	-	-

Following is a summary of important considerations in predicting properties in the fuel-rich LOX/RP-1 system:

1. Actual amounts of carbon found in samples from Atlas, Thor, F-1, and the present tests are around 2 wt %; the amounts calculated for equilibrium compositions are around 35 wt %. This difference was handled by causing the equilibrium solver to calculate 0% carbon, that is C(s) is simply deleted from the product file for these calculations. This resulted in a major improvement in predictions of temperature and c^* . It would be possible, with some difficulty, to cause the equilibrium solver to calculate a few percent carbon; however, any small improvement which may result from this would be completely hidden among the experimental scatter.
2. The other feature of the model is the withholding of a small amount of oxygen from combustion at MR below 0.5 according to the formula (% O₂ withheld) = 100 (0.5-MR). The reason for doing this is not that oxygen has been observed in the gas samples; it hasn't, although it would have been detected if present. The reason for withholding oxygen is that it simulates some kind of incomplete combustion which increases as mixture ratio is reduced. Another way to view this is that there may be some exothermic reactions, in the very complex combustion sequence, which go nearly to completion at MR >0.5, but which become excessively slow at the low temperatures attendant with low MR. At the present time, there is a case for withholding oxygen in the theoretical model; however, it is not a strong case. It is possible that future refinements in hardware design may lead to improved combustion efficiency at low mixture ratios so that withholding oxygen in the model will not be required.

Fuel-rich LOX/CH₄. Temperature and c^* 's are depicted in Fig. 64 and 65, and properties and compositions are summarized in Table 19. The most striking feature of this system is that predictions, according to equilibrium and by the special models, are quite close and are, overall, in good agreement with the experimental points. The nonequilibrium model, summarized in Table 19, assumes that C(s), CO₂, and all hydrocarbons except CH₄ are prohibited from forming.

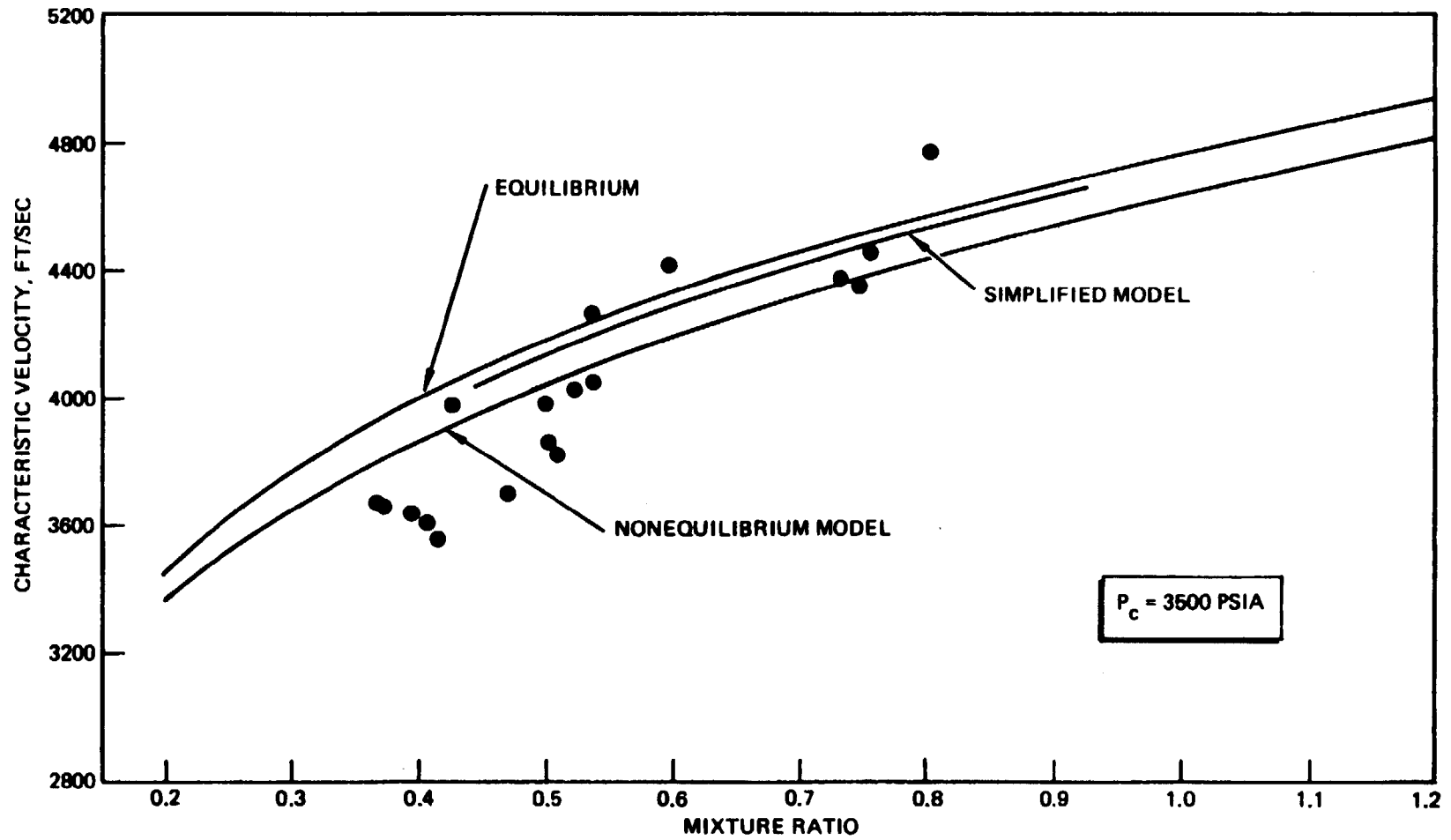


Figure 64. Theoretical Performance, LOX/CH₄ amb gas

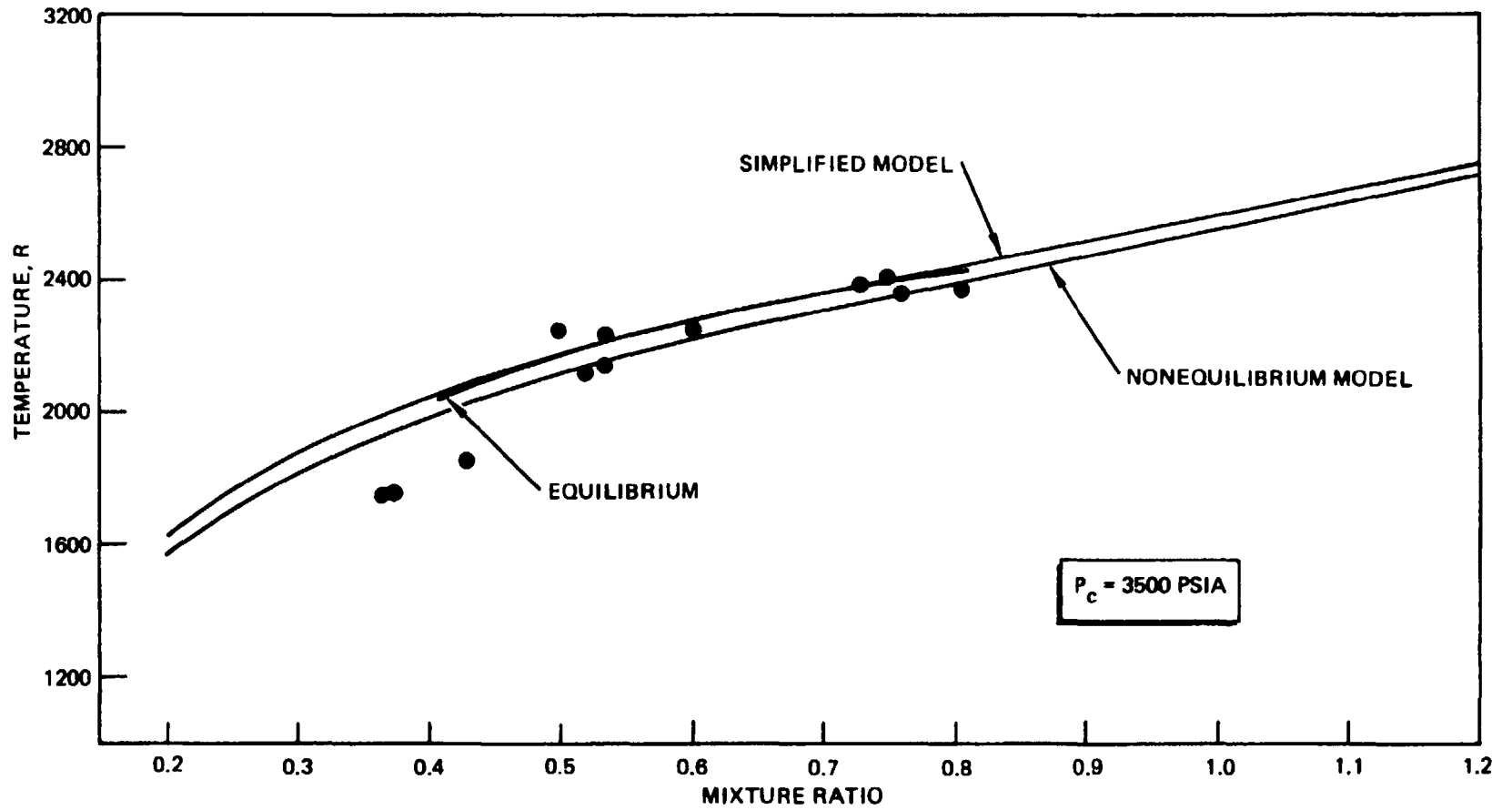


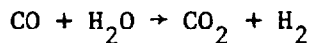
Figure 65. Theoretical Combustor Temperature, LOX/CH₄ amb gas

TABLE 19. FUEL-RICH LOX/CH₄. GAS PROPERTIES AND COMPOSITION, EXPERIMENTAL AND THEORETICAL

TEST NO	EXPERIMENTAL			EQUILIBRIUM			C(s) EXCLUDED			C(s) EXCLUDED CO ₂ WITHHELD		
	23	24	25	23	24	25	23	24	25	23	24	25
MR	0.805	0.759	0.735	0.805	0.759	0.735	0.805	0.759	0.735	0.805	0.759	0.735
P _c , PSIA	3805	3472	3458	3805	3472	3458	3805	3472	3458	3805	3472	3458
T _c , R	2360	2347	2377	2440	2405	2387	2436	2399	2379	2394	2356	2336
c*, FT/S	4766	4459	4360	4577	4526	4504	4549	4494	4464	4499	4442	4412
COMPOSITION, wt %												
H ₂	2.7	2.7	8.2	5.9	5.7	5.6	5.7	5.4	5.2	5.2	4.9	4.7
CH ₄	40.9	43.0	37.3	25.3	27.0	28.0	26.5	29.3	30.8	26.5	29.4	30.9
C ₂ H ₄	1.1	1.1	0.9	0	0	0	0	0	0	0	0	0
C ₂ H ₆	3.1	3.3	2.3	0.1	0.1	0.1	0.1	0.1	0.1	0	0	0
LIQUID HC	0.5	0.5	0.8	0	0	0	0	0	0	0	0	0
H ₂ O	15.0	14.1	14.2	14.9	15.7	16.0	13.9	13.7	13.6	17.8	17.7	17.7
CO	28.6	27.7	27.9	42.6	38.7	36.6	44.1	41.6	40.2	50.4	48.0	46.7
CO ₂	8.0	7.5	7.8	9.6	9.8	9.9	9.7	9.9	10.1	0	0	0
C(s)	0.2	0.2	0.7	1.5	3.0	3.7	0	0	0	0	0	0

The rationale for this model was that a portion of the CH₄ would burn (with all of the O₂) to form CO, H₂O, and H₂, and that the heat released would raise the temperature of the remaining CH₄, which would act as a working fluid. There were no experimental data to serve as a guide for this model.

The reason for excluding hydrocarbons other than CH₄ was that it was believed that there would not be sufficient time for the CH₄ to reform to higher hydrocarbons. Actually small amounts of ethylene and ethane were found in the samples, about 1 and 3 wt %, respectively. These undoubtedly result from combination of the fragments, CH₃ and CH₂, resulting from limited cracking of the CH₄. It is noteworthy that the amount of C(s) calculated at equilibrium, about 3 wt %, is much less than the amount calculated for RP-1--about 35 wt %. However, since the amount found in the samples from the CH₄ tests was about 0.3 wt %, it is considered desirable to suppress C(s) in modeling the CH₄ system. The reason for suppressing CO₂ in the original model was that it was feared that the amount of CO predicted would be low due to the theoretical thermodynamic instability of CO at lower temperatures, which tends to cause the following type of shift in composition:



Actually, the amount of CO predicted (without excluding CO₂) was quite high, and the amount of CO₂, about 10 wt %, was comparable to that in the samples--about 8 wt %. A significant discrepancy between the sample and calculated compositions is that the CH₄ and CO in the sample are approximately 40 and 28 wt %; whereas, they are about 28 and 42 wt % in the calculated compositions. Since the amounts of CO₂ and H₂O are comparable in the calculated and sample compositions, the discrepancy points to a shortage of oxygen in the samples. This would be explained by assuming nonuniform fuel/oxygen distribution and that sampling was done in a low MR zone. In spite of this, the samples serve as a valuable guide as to the kind of composition to be expected in this system.

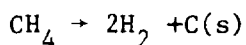
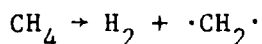
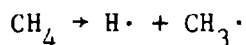
In view of the observations in the last paragraph, the simplified model is now recommended for property predictions in the fuel-rich LOX/CH₄ system. In this model, the only assumption made, distinguishing the model from equilibrium, is that the formation of C(s) is prohibited. Although the predictions of temperature and c* are quite close between the model and equilibrium, suppression of C(s), according to the model, is preferred because this aligns the model with reality that very little C(s) actually does form. Since the amount of hydrocarbons predicted by the simplified model is quite small, and since the relative amounts of CO₂, CO, and H₂O predicted are comparable to the amounts observed experimentally, suppression of CO₂ and higher hydrocarbons is not recommended.

The combustion process in off-mixture ratio gas generator regimes is believed to occur according to the following mechanism. In the case of fuel-rich LOX/RP-1, there are zones relatively abundant in oxygen, embedded in a matrix of fuel. Of course the exact mixture ratio will vary from point to point within the zones; however, the mixture ratios will be higher than the overall mixture ratio. Combustion occurs in these zones at relatively high temperatures, compared to the overall gas generator, leading to compositions essentially at equilibrium. The hot gases from these short zones then mix with the excess fuel in a very complex chemical process where each of the following occurs to some extent: (1) reactions of some species (mainly O₂, CO, and CO₂) in the hot gas with the fuel or its fragments; (2) pyrolysis (cracking) of the fuel to a very large variety of substances such as lower-molecular-weight olefins, hydrogen, some carbon, and free radicals; and (3) vaporizing and heating of excess fuel, unchanged.

The above mechanism is believed to be the major process in any fuel-rich gas generator; however, another process (minor) will also occur to some degree. Some oxygen will become entrained or mixed-in with fuel at low temperatures. As this mixture is heated, by the major process, the oxygen will react with the fuel or its fragments in a nonflamelike process. This process, similar to the "oxo-process" in the chemical industry can produce a wide variety of substances such as: alcohols, ketones, aldehydes, and carboxylic acids; subsequently, most of these compounds will decompose. The relative mix of the major and minor processes will depend on injector design and mixture ratios.

For example, conventional like-on-like oxidizer impingement probably will cause the major process to be quite dominant, with the minor process being negligible; whereas, unlike impingement would cause the minor process to play a more important role.

The mechanism for the fuel-rich LOX/CH₄ system is similar to the LOX/RP-1 system but is much simpler. Not only is methane the most stable hydrocarbon, in the temperature regime of interest here, but the possibilities for partial oxidation and cracking of CH₄ actually are enumerable. For example, cracking of CH₄ occurs mainly according to the following reactions:



The CH₃ and CH₂, in part react with like species to form C₂H₆ and C₂H₄ which, being less thermally stable than methane, will continue to decompose.

Oxidizer-Rich LOX/RP-1 and LOX/CH₄. The mechanisms for the oxidizer-rich gas generators are similar to the fuel-rich gas generators except that the roles of fuel and oxidizer are interchanged. In the oxidizer-rich systems, there will be zones relatively abundant in fuel surrounded by a matrix of oxygen. The fuel in these zones will be completely reacted to form products, not necessarily fully oxidized, in equilibrium at higher temperatures than the overall gas generator temperatures. As the hot gases from these zones mix with the surplus oxygen, complete oxidation will occur to form entirely CO₂ and H₂O. The fate of the excess oxygen can only be to emerge as oxygen. No reason can be found why equilibrium calculations should not be used to predict properties in the oxidizer-rich systems. The experimental data (Fig. 66 and 67) provide corroboration for use of equilibrium calculations, the deviations from the theoretical curves being attributed to experimental scatter and physical loss.

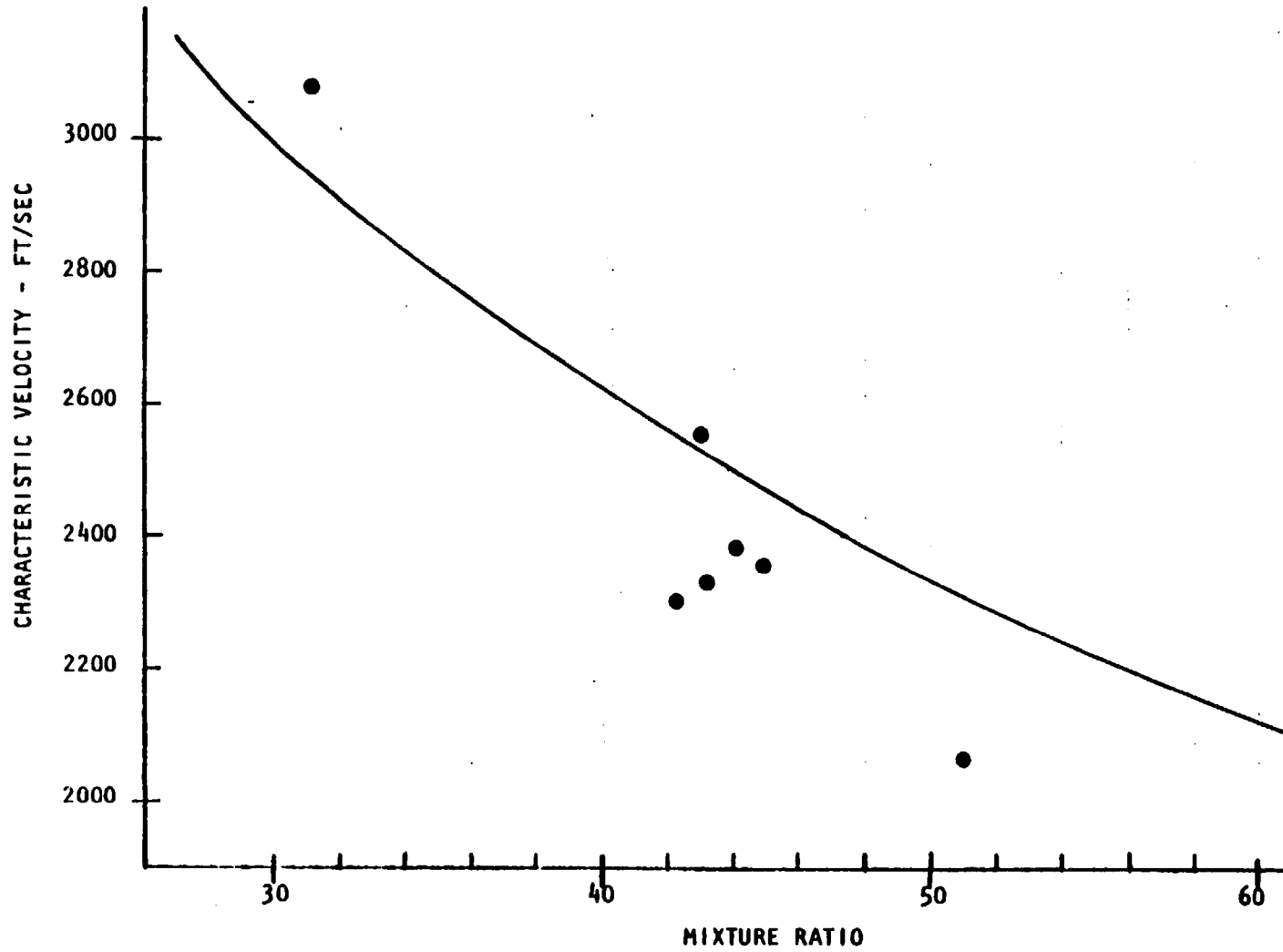


Figure 66. Theoretical Performance, LOX/CH₄

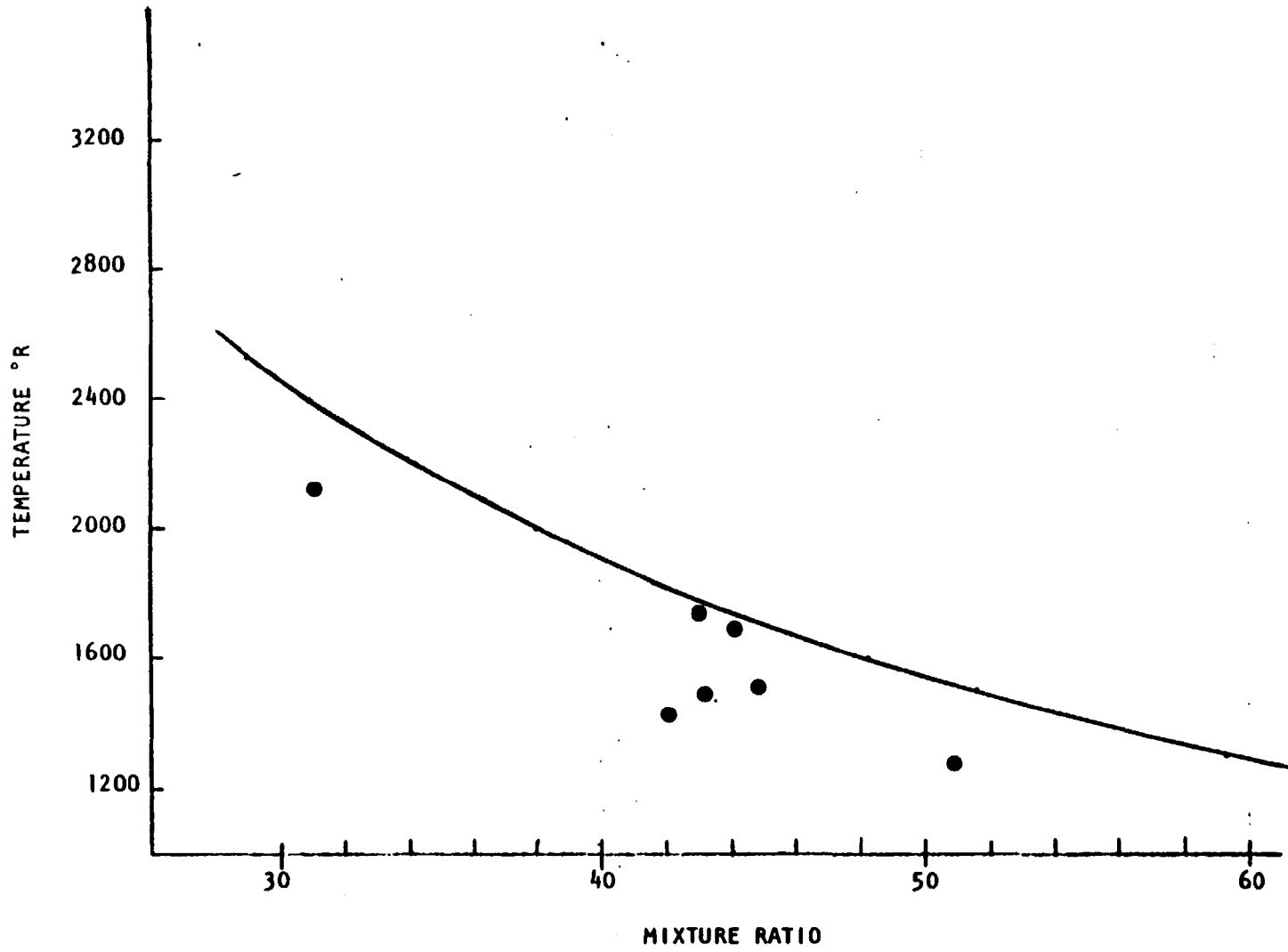


Figure 67. Theoretical Combustor Temperature, LOX/CH₄

Summary. It has long been recognized that theoretical equilibrium calculations are not appropriate for predicting flame temperatures and compositions for the low-temperature combustion systems typical in gas generators. Generally, the temperature predictions are high in the case of fuel-rich LOX/RP-1 and low in the case of hydrazine and some of its blends. For these reasons, three different models have been recommended for calculating theoretical gas properties and compositions in the four regimes covered in this program. The theoretical models recommended for property predictions in the LOX/RP-1 and LOX/CH₄ gas generator systems are summarized in Table 20.

Subtask 03300 - Models Modification

Modification to the basic injector design models is based on the analysis of the small-scale test data and its interpretation. A limited amount of experimental information is available to compare with the predicted results.

The goal of the program was to evaluate LOX/CH₄ and LOX/RP-1 preburner and gas generator performance and gas property methods for fuel- and oxidizer-rich operating conditions. The performance is defined as the product of the mixing efficiency and the vaporization efficiency. The requirements to know or predict gas properties derives from the uncertainty of the kinetic deficiency and the prevention of carbon depositon.

Rocketdyne has developed and established the use of two combustion performance models (SDER, CICM) and the gas equilibrium model for many of its engines. The latter is traditionally used to provide performance parameters (i.e., c^* , molecular weight, γ , etc.) as functions of pressure and mixture ratio. These values are used to design the injector and chamber. However, due to design limitations, complete mixing and vaporization are difficult to achieve. Consequently, the performance models are used to analyze the mixing, atomization, and vaporization processes to predict performance.

TABLE 20. SUMMARY OF MODEL FEATURES FOR LOX/RP-1 AND LOX/CH₄ GAS GENERATORS

MR REGION	SYSTEM	MODEL FEATURE
FUEL RICH	LOX/RP-1	1. C(s) SUPPRESSED IN EQUILIBRIUM CALCULATIONS 2. O ₂ WITHHELD ACCORDING TO WITHHELD = 100 (0.5 - MR) = 0 MR > 0.5
	LOX/CH ₄	1. C(s) SUPPRESSED IN EQUILIBRIUM CALCULATION
OXIDIZER-RICH	LOX/RP-1 LOX/CH ₄	1. EQUILIBRIUM CALCULATION

Based on experience and the high calculated instability mode frequencies of the small-scale hardware, injector stability was considered insignificant; therefore, the design task was to provide maximum performance.

It is recognized that reaction equilibrium can never be achieved in preburners or gas generators; therefore, the gas equilibrium model was modified to limit certain species production. To date, test results verify that the chamber pressure, flow-rates, and the characteristic velocity were as predicted. A general purpose kinetic model was utilized to simulate the LOX/CH₄ combustion process. The reaction rate constants are taken from published journals. The analysis showed that the reactions (CH₄ disassociation) were almost instantaneous, if sufficient thermal energy is provided to heat the methane gas to 1700 F. The radicals (i.e., CH₃^{*}) produced react with O₂ rapidly. These results encouraged the use of the limited/modified equilibrium gas properties in the performance model used to analyze the vaporization process.

The performance model uses empirical data to compute the mixing and the droplet size distribution for subsequent droplet vaporization computation. LOX as a cryogenic liquid is considered to be relatively easy to vaporize; therefore, the analysis focused on mixing performance.

To achieve excellent mixing, uniform flow distribution at the design mixture ratio must be considered during the design process; therefore, as many injection elements as possible were included.

The injection element configuration in rocket chambers generally is dictated by the chamber compatibility and the performance. Unlike impinging elements generally have good mixing, but may not be compatible with the chamber wall. The chamber thermal conditions for preburners or gas generators are not as severe as main chamber conditions; therefore, maximum mixing was a design criteria.

The combustion model (SDER) was constructed for liquid-liquid injection. For LOX/CH₄ (gas), the liquid-liquid correlation may not be valid, and new flow data are desirable. Extrapolation of the liquid data might be correlated with the hot-fire test results. The CH₄ gas properties were replaced with pseudo-"liquid" properties; i.e., low gas density, viscosity and zero surface tension. Other thermodynamic properties such as the specific heat, thermal conductivity, etc., of the gaseous CH₄ were used. The analysis showed excellent mixing (η_{c*} mixing - 100%) and extremely fine droplet size distribution for the LOX (~10 μ). There are some uncertainties in the resulting droplet size; therefore, a parametric study was performed. If the LOX droplet size increases to 50 μ , the vaporization performance is unchanged. It was concluded that the LOX/CH₄ injector design could achieve maximum performance. Quoted efficiencies are limited only by the c* values predicted by the gas equilibrium model. Comparing the data obtained from testing, the model prediction was within 2%. Using the data to date, there is no evidence to indicate that major modifications to the model is necessary.

The combustion instability occurring during the fuel-rich injector testing is unusual for this preburner combination. The injector face erosion and the chamber damage indicate that chamber compatibility cannot be overlooked. These areas are not included in the combustion performance model. Momentum ratios higher than realized with liquid-liquid injectors were used. The large momentum ratio used for the injection element designs is not unusual because:

1. Geometric element balance must be maintained or the imbalance minimized. The imbalance is caused by the mixture ratio and the large density difference. The geometric balance may become a dominating factor in determining the mixing performance. When smaller jets impinge on larger jets, a local momentum imbalance is realized. If secondary turbulent mixing is limited by chamber length, mixing performance will be degraded.
2. Injector compatibility is not considered as severe a requirement due to the assumption that "preburner equilibrium" can be achieved rapidly and the thermal loading realized is not as high as main chamber conditions.

The damages seen from the fuel-rich injectors were caused by combustion instability. Although the gas properties are unknown near the injector face, the gas temperature is sufficiently high to melt copper. The high temperature may be caused by local stoichiometric combustion due to recirculation brought about by the vigorous atomization process of the injection hydraulic coupling.

To investigate stability, both the Priem-type analysis and the engine hydraulic analysis should be used. Additional instrumentation may be necessary to provide better data correlation.

TASK IV: PREBURNER ANALYSIS AND PRELIMINARY DESIGN

The program original work statement required the delivery of four preburner assemblies: one each LOX/CH₄ fuel- and oxidizer-rich, and one each LOX/RP-1 fuel- and oxidizer-rich. During the subscale hot-fire evaluation tests, extensive effort was expended in an attempt to realize design criteria on the oxidizer-rich LOX/RP-1 injector configuration. Due to lack of adequate funds to eliminate the problems plaguing this test activity, all effort on the oxidizer-rich LOX/RP-1 injector was terminated. With a reduction in the scope of work, only three preburner assemblies remained to be analyzed and designed in this task.

Subtask 04100 - Analysis

The preliminary design effort and subsequent supporting analysis for the nominal 40K thrust chamber size preburner assemblies utilized the results of the Task III hot-fire test results and subsequent computer model improvements. Based on the test results, an injector element was selected for each of the propellant combinations. With this injector element configuration, a design was established with the maximum number of injection elements for each configuration that could reasonably be placed within the injector face limits, while maintaining a uniform mass flux distribution across the injector face. The appropriate performance models were used to optimize the element design parameters. A combustion stability analysis was conducted to determine if a stability aid was required.

Structural analysis of the preburner components was completed and all designs have been approved. The 12-inch combustor design selected results in a safety factor of 1.1 minimum on yield in the flange area. This factor is identical to that realized during the original analysis of the 40K SSME hardware. A maximum combustion gas temperature of 1540 F and a chamber pressure of 3500 psia resulted in a low-cycle fatigue life of 16 cycles with a safety factor of 4. This implies that 64 thermal cycles should be realized prior to surface cracking. The combustor wall is approximately 40% thicker than required so that the overall low-cycle fatigue life is far in excess of that predicted. Figure 68 illustrates the combustor wall temperature/time profile anticipated for a preburner operating

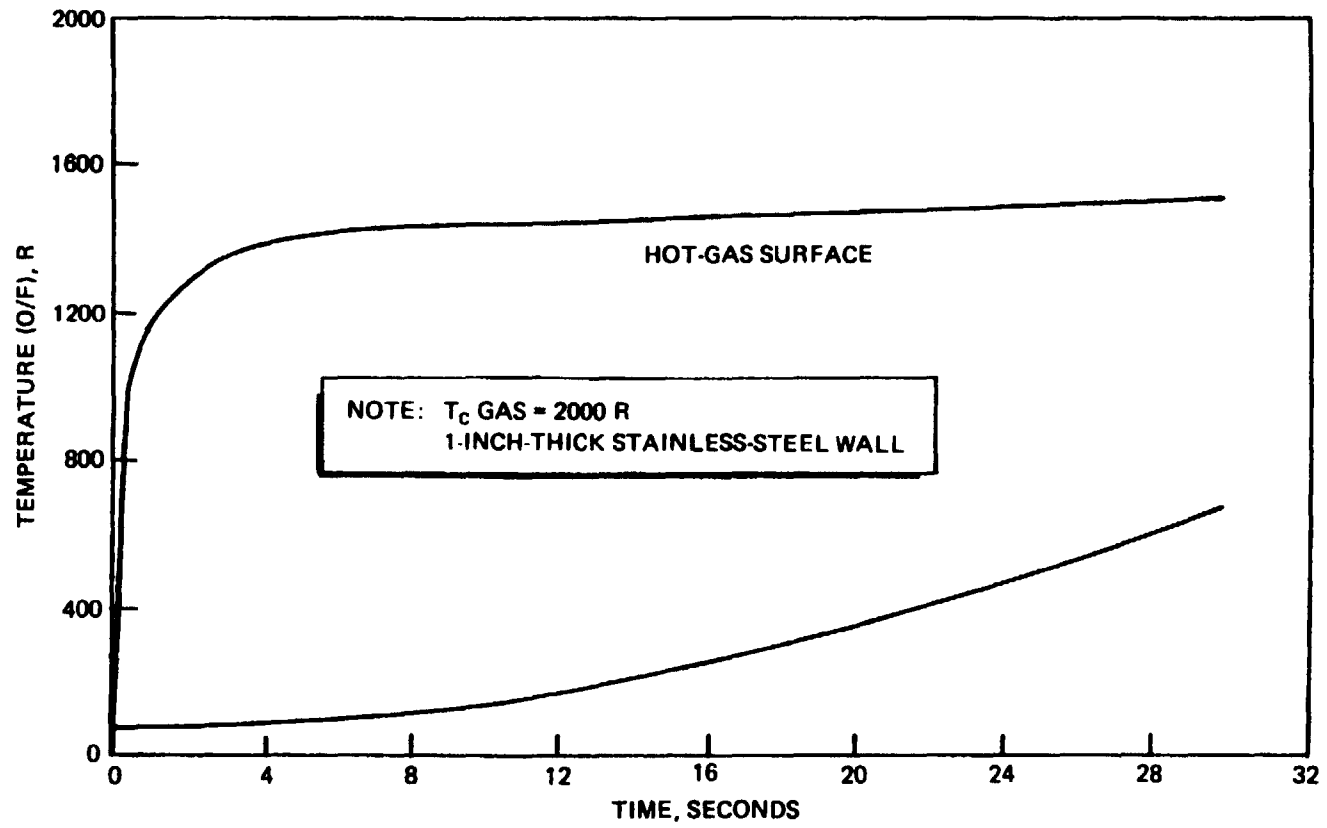


Figure 68. Material Operating Conditions

with a maximum gas temperature of 2000 R. A mean wall temperature of 1200 F was used in the structural analysis. This mean wall temperature limits the preburner operational time for a specific combustor gas temperature. Therefore, if the preburner assembly is hot-fired for 10 seconds, the mean wall temperature is only 800 F, two-thirds of that used for the analysis.

Table 21 itemizes the individual preburner components and lists the minimum safety factors as calculated based on the specified assumptions. In all cases, these values are for the weakest point of the component. Exceptions are discussed in the following paragraphs.

The structural analysis on the fuel manifold resulted in a minimum safety factor on yield of 5.2. No structural problems are anticipated with this design. When this manifold is used as an oxidizer manifold, i.e., during oxidizer-rich operation, the yield safety factor will be reduced to 1.29. This structural reduction is the result of the facility line shrinkage imposing a moment on the inlet flange.

The coaxial injector configuration was analyzed. Bending in the "Amzirc" face plate resulted in the minimum safety factor of 1.45 on yield. All other areas were considerably stronger.

In the triplet injector analysis, the braze joint that attaches the copper face to the stainless-steel ring is the weakest area of the design. At this point, the safety factor is reduced to 1.43 minimum on yield. All other areas of the injector are in excess of this safety factor.

Analysis of the oxidizer-rich pentad injector results in a minimum safety factor on yield of 1.24, also in the face plate. On this configuration, the minimum factor is established in the cross-sectional area of the post-braze joints in the second and third row of elements. Again, all other areas of the injector are considerably stronger per analysis. If the hardware is prechilled or the LOX posts are 150 F colder than the attachment points, the safety factor is reduced to 0.71. Under normal conditions this cannot occur if the ΔP limitations are upheld.

TABLE 21. PREBURNER ASSEMBLY - MINIMUM STRUCTURAL SUMMARY

ITEM	PART NO.	PRESSURE/ ΔP , PSI	ASSUMED TEMPERATURE, F	MINIMUM SAFETY FACTOR, YIELD	MINIMUM SAFETY FACTOR, ULTIMATE
LOX DOME	AP80-100-003	4675	-230	1.14	3.82
NOZZLE	AP80-097	3850	1580	1.11	2.86
FUEL MANIFOLD	AP80-096-001	4675	70	1.29	3.55
COMBUSTION CHAMBER	AP80-095-003	3850	1540	1.11	2.86
COAXIAL	AP80-103-011	ΔP 1200	300	1.45	3.25
TRIPLET	AP80-102-001	ΔP 1200	450	1.31	3.66
PENTAD					
OPERATION	AP80-105-001	ΔP 1200	450	1.24	5.30
OXIDIZER LEAD	AP80-105-001	--	$\Delta T = 150$	0.71	4.58

The triplet injector concept realized as a result of LOX/RP-1 hot-fire testing was adapted to the 40K injector configuration. Because the triplet injector configuration is a high performer, it is more prone to combustion instabilities. The vigorous burning in the combustor can drive an instability at the acoustic frequency of the chamber if insufficient damping exists. The damping can be the nozzle exhaust/contour, the wall compliance (acoustic absorber), or the injector stiffness. The primary contributor to high performance is the injector design. It was important, therefore, to analyze the injection dynamics of the injector to ensure that it would not respond to the combustion chamber pressure fluctuations. In an off-stoichiometric injector design, i.e., preburner/gas generators, this task becomes more significant because of limited knowledge of the combustion process. Assuming a pseudo-equilibrium condition (including kinetic effects), the chamber acoustic response, using an acoustic velocity of 2170 ft/sec, results in the first tangential mode being computed at 4360 Hz and the first longitudinal mode being 1085 Hz ($dia_c = 3.5$ inches and $L_c = 12$ inches). These values can change drastically if the injection rate of one of the propellants responds differently to the chamber disturbance. The resultant mixture ratio excursion can cause the gas temperature to vary dramatically. With this change, the chamber pressure will vary and, although the injector flow will respond, there will be a lag, causing further mixture ratio changes. The repetition of this process causes unstable combustion.

To avoid the instability, it is crucial not to have combustion processes coupled with the chamber acoustics. This is accomplished by analyzing the processes to ensure that the burning would not be influenced by the pressure oscillation at the chamber frequency. Based on chamber mode frequencies, combustion can be influenced if the burning time is within 1 msec, which experience indicates is highly unlikely for the LOX/RP-1 preburner injector. The injector injection orifices have even higher characteristic frequencies. First approximations show the organ modes for the fuel and the oxidizer orifices are at 40,000 and 84,000 Hz, respectively. Based on the combustion characteristics, the oscillatory component of the flowrate at high frequency would not affect the combustion.

Low-frequency instability, which generally is coupled with the bulk feed system, is called "chugging", which describes the chamber combustor as one element. It is characterized by the chamber break frequency which is the rate the chamber cycles the combustion products. If the upstream feed system responds to this frequency, instability will occur. Conversely, if the feed system is stiff and the flowrate does not fluctuate near that break frequency, the combustion oscillation cannot be maintained. Assuming an L_c^* of 36 inches and the characteristic velocity of 3200 ft/sec, the chamber break frequency is computed to be 70 Hz. Since the injector has calculated break frequencies at 2100 Hz and 2700 Hz for the fuel and oxidizer, respectively, the higher frequency and the low amplitude $\frac{\dot{w}}{\Delta P}$ resulting from the high injector resistance are positive factors in eliminating low-frequency 'chug'.

Subtask 04200 - Preliminary Design

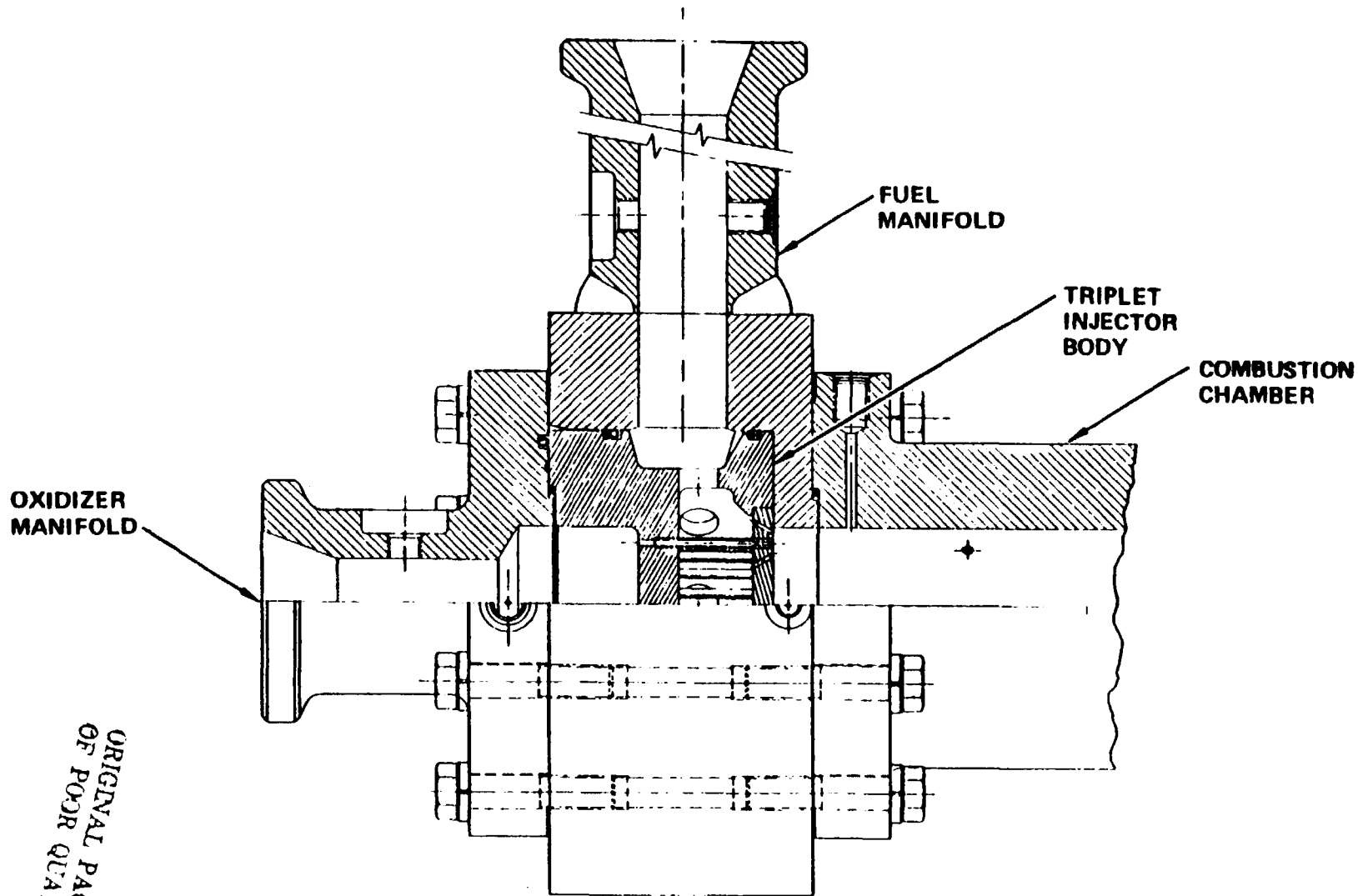
The layout, supplied under separate enclosure and identified as drawing number AP80-106L, shows the various preburner component identification and hardware required for complete assembly. The referenced dimensions locating the fuel and oxidizer inlets were taken from the original 40K configuration. This commonality will permit indiscriminate changing of the 40K preburner assemblies. The basic injector/manifold/dome composite is similar to that realized in the tested subscale configuration shown in Fig. 69. The injector is an insert isolated by redundant seals, resulting in maximum protection against interpropellant leakage.

Table 22 illustrates the nominal injector injection parameters realized during the subscale test activity. The velocities specified represent the individual orifice velocity in each case as compared to the 40K injector parameters. The momentum relationship is the ratio of the momentum of the outer orifices of an element to the core momentum. A thorough evaluation of the momentum relationship should be made to determine the significance of this factor vs geometric relationship (orifice diameters).

The triplet injector presently designed is a 66-element, 3-row injector. The injector design criteria for the LOX/CH₄ and LOX/RP-1 fuel-rich and oxidizer-rich propellants are presented in Table 23. The triplet design shown results in a relatively uniform face mass flux distribution.

The mass flux distribution realized for all injectors is shown in Table 24. The inertance of the triplet element was considered during the design and is reflected in the element geometry. The orifice area ratios and propellant injection velocities are virtually identical to the subscale triplet injector hot fire evaluated.

Unstable combustion was realized during the evaluation of the other injector configurations in fuel-rich LOX/RP-1. Therefore, the triplet subscale was never tested without an acoustic device. With this criteria, the design illustrated may require an absorber device to ensure stable operation.



ORIGINAL PAGE IS
OF POOR QUALITY

Figure 69. Injector Test Configuration

TABLE 22. INJECTOR INJECTION PARAMETERS

	SUBSCALE INJECTOR		40K INJECTOR	
	VELOCITY, FT/SEC	MOMENTUM RATIO	VELOCITY, FT/SEC	MOMENTUM RATIO
LOX/CH ₄ - FUEL RICH				
TRIPLET	590 FUEL 149 OXIDIZER	11.48		
PENTAD	570 FUEL 142 OXIDIZER	8.20		
COAX	634 FUEL 75 OXIDIZER	17.23	540 FUEL	16.98
LOX/CH ₄ - OXIDIZER RICH				
PENTAD	569 FUEL 248 OXIDIZER	17.47	616 FUEL 258 OXIDIZER	16.04
LOX/RP-1 - FUEL RICH				
TRIPLET	291 FUEL 282 OXIDIZER	2.34	283 FUEL 255 OXIDIZER	2.70
LIKE DOUBLET	288 FUEL 245 OXIDIZER	--		
FAN FORMER	383 FUEL 325 OXIDIZER	2.23		
LOX/RP-1 - OXIDIZER RICH				
LIKE DOUBLET/ SHOWERHEAD	293 FUEL 250 OXIDIZER	--		
NOTE: $m = \dot{w}V$				
*MOMENTUM RATIO = MOMENTUM OF THE OUTER ORIFICES OF AN ELEMENT TO THE CORE MOMENTUM				

TABLE 23. 40K PREBURNER INJECTOR DESIGN CRITERIA

ITEM	PROPELLANT		
	LOX/RP-1	LOX/CH ₄	LOX/CH ₄
INJECTOR	TRIPLET	COAX	PENTAD
\dot{w}_o LOX TEMPERATURE	13.34 LB/SEC ~200 R	10.66 LB/SEC ~200 R	58.29 LB/SEC ~200 R
\dot{w}_f FUEL TEMPERATURE	32.53 LB/SEC AMBIENT	24.8 LB/SEC AMBIENT	1.37 LB/SEC AMBIENT
MIXTURE RATIO	0.41	0.43	42.4
COMBUSTION TEMPERATURE, R	2045	2030	1300
INTERFACE PRESSURE, PSI	≤4200	≤4200	≤4200
CHAMBER PRESSURE, PSI	2000 TO 3500	2000 TO 3500	2000 TO 3500
ACOUSTIC DEVICE	HELMHOLTZ	PROVISIONAL	PROVISIONAL
COMBUSTOR DIAMETER, INCHES	3.5	3.5	3.5
CHAMBER LENGTH, INCHES	12	12	12

TABLE 24. MASS FLUX DENSITY*

	INJECTORS		
	COAXIAL	TRIPLET	PENTAD
CENTER	3.687	--	7.41
ROW 1	3.686	4.628	5.56
ROW 2	3.686	4.840	5.56
ROW 3	3.686	4.772	5.56
FILM COOLANT	--	--	+10% OXIDIZER TOTAL
ELEMENTS	49	66	37

*LB/SEC-IN.²

The face of the triplet injector design for the LOX/RP-1 preburner was analyzed to determine if the fuel orifices provide sufficient cooling at a chamber pressure of 3500 psia and a mixture ratio of 0.46 (gas temperature = 1740 F).

The triplet injector face initially analyzed has the following geometry:

2-inch diameter

0.25-inch-thick OFHC face

0.0577-inch-diameter fuel orifices (54)

0.0485-inch-diameter oxidizer orifices (27)

The element arrangement used was that of the Rocketdyne IR&D injector.

The injector face was analyzed for the following hot-gas conditions:

$P_c = 3500$ psia

MR = 0.46:1

$T_o = 1740$ F (2200 R)

$\dot{w}_g = 18.26$ lbm/sec

The oxidizer is cryogenic while the fuel is at ambient temperature.

Since no precise correlation exists for injector face heating rates, it was assumed that the face heat transfer coefficient is the same as the heat transfer coefficient on the preburner body at a distance 1 inch downstream of the face. This heat transfer coefficient is calculated using the following correlation for developing flow on a flat plate.

$$h_g = 0.0295 (k/x) Re^{0.8} Pr^{0.4}$$

The following values were used for the combustion gas properties

$$k = 1.84 \times 10^{-6} \text{ Btu/in.}\cdot\text{sec}\cdot\text{F}$$

$$\mu = 2.16 \times 10^{-6} \text{ lbm/in.}\cdot\text{sec}$$

$$Pr = 0.756$$

These values were interpolated from the Free Energy Program results at mixture ratios of 0.5:1 and 0.45:1. No carbon layer has been assumed in this analysis. The resulting hot-gas heat transfer coefficient is $0.0068 \text{ Btu/in.}^2\cdot\text{sec}\cdot\text{F}$.

The Rocketdyne-developed heat transfer correlation for RP-1, as given below, is utilized.

$$h_c = 0.0056 (k/D) Re^{0.95} Pr^{0.4}$$

A surface roughness of 8 uinches rms is assumed for the fuel passages.

For a passage this smooth there is no roughness enhancement to the coolant coefficient. The resulting coolant heat transfer coefficient is 0.016 Btu/in.²-sec-F. No entrance enhancement has been assumed.

A three-dimensional thermal model of a section of the injector was set up using the HEATING computer program. The cooling contribution from the oxidizer was ignored on the assumption that the thermal resistance through the oxidizer post (low thermal conductivity plus contact resistance) would be high. The cooling from the RP-1 on the backside of the face also was neglected. The only cooling considered was the RP-1 flowing through the orifices.

The face average temperature is 760 F, with a maximum temperature of 800 F. The heat flux to the face is 6.7 Btu/in.²-sec under the assumption that the face is exposed to the full gas temperature (1740 F). The heat load into the face causes the RP-1 to rise 3 F as it passes through the face. The maximum temperature of the RP-1 coolant surface is 700 F. This temperature is in the region where some coking of the fuel passage walls may occur. However, because of the conservatism in the analysis, this temperature probably will not be reached in actuality and no problem should exist.

Using this analysis, the 40K LOX/RP-1 triplet preburner was analyzed. Because of the assumptions made initially, the analysis also applies to the 40K preburner. The face temperature is a function of the fuel orifice length, as shown in Fig.70. Therefore, applying the same assumptions, the maximum face temperature realized for the triplet injector will not exceed 600 F.

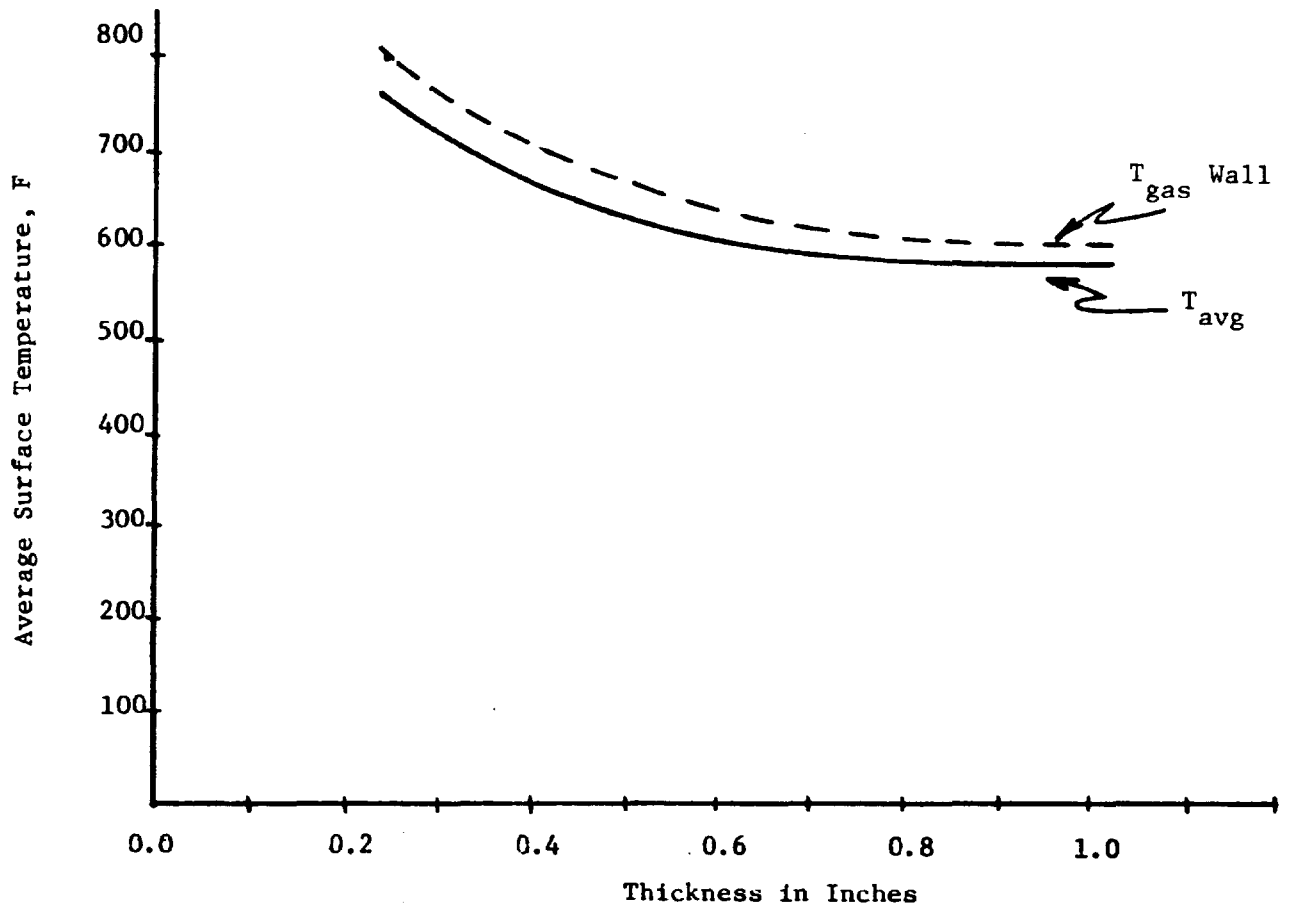


Figure 70. Injector Face Average Temperature

The fuel-rich LOX/CH₄ injector selected during the preliminary design was a solid-face coaxial injector capable of high performance and stable undamped operation. The injector has 49 elements and a uniform mass flux across the face. The inertance of the oxidizer element was considered during the design, and the resulting area ratios and injection velocities are virtually the same as the subscale coax injector utilized in hot-fire evaluation.

Very stable combustion was realized with the coax injectors evaluated; therefore, an acoustic device was not deemed necessary for the 40K configuration. Provisions have been made to accommodate an acoustic damping device if required, but the delivered configuration will have a blank ring installed for test. The ignition system to be used will be a CTF/CH₄/RP-1 igniter, similar to that presently used on the existing 40K hardware. Modification will be to the igniter inlet lines, but only because of location differences.

The oxidizer-rich LOX/CH₄ injector selected during the preliminary design phase was a modified pentad configuration with film coolant, similar in design to that successfully tested in subscale. The subscale configuration was high performing and operated in a stable regime in the areas investigated. The combustion model used to evaluate the stability factor showed the injector configuration to be stable over the range of interest. The pentad injector has 37 elements with 54 film coolant holes on the periphery, using 10% of the total oxidizer flow for combustion chamber wall compatibility. The addition of the film coolant holes was a necessity during the subscale hot-fire evaluation. The location of the coolant holes and the resultant wall impingement will provide an oxidizer-rich isolation boundary for the pentad elements.



TASK V: PREBURNER DETAIL DESIGN AND FABRICATION

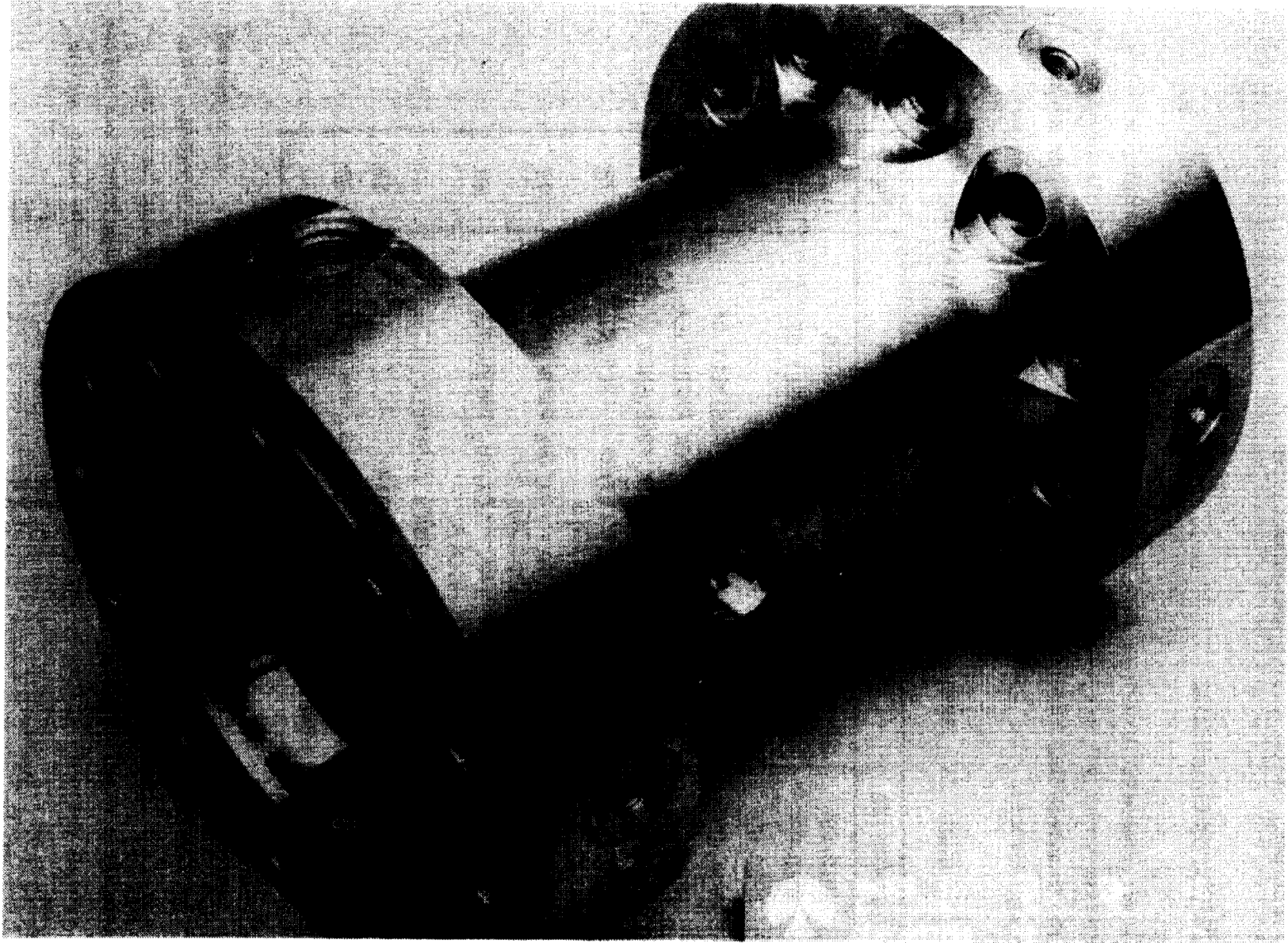
Subtask 05100 - Detail Design

The preburner component drawings were submitted to the NASA/MSFC program monitor under separate cover per contractual requirement. The following table presents a list of the drawings and identifying numbers compiled throughout the 40K preburner detail design effort. The listed figures in Table 25 show the completed part.

TABLE 25. PREBURNER COMPONENT DRAWING IDENTIFICATION

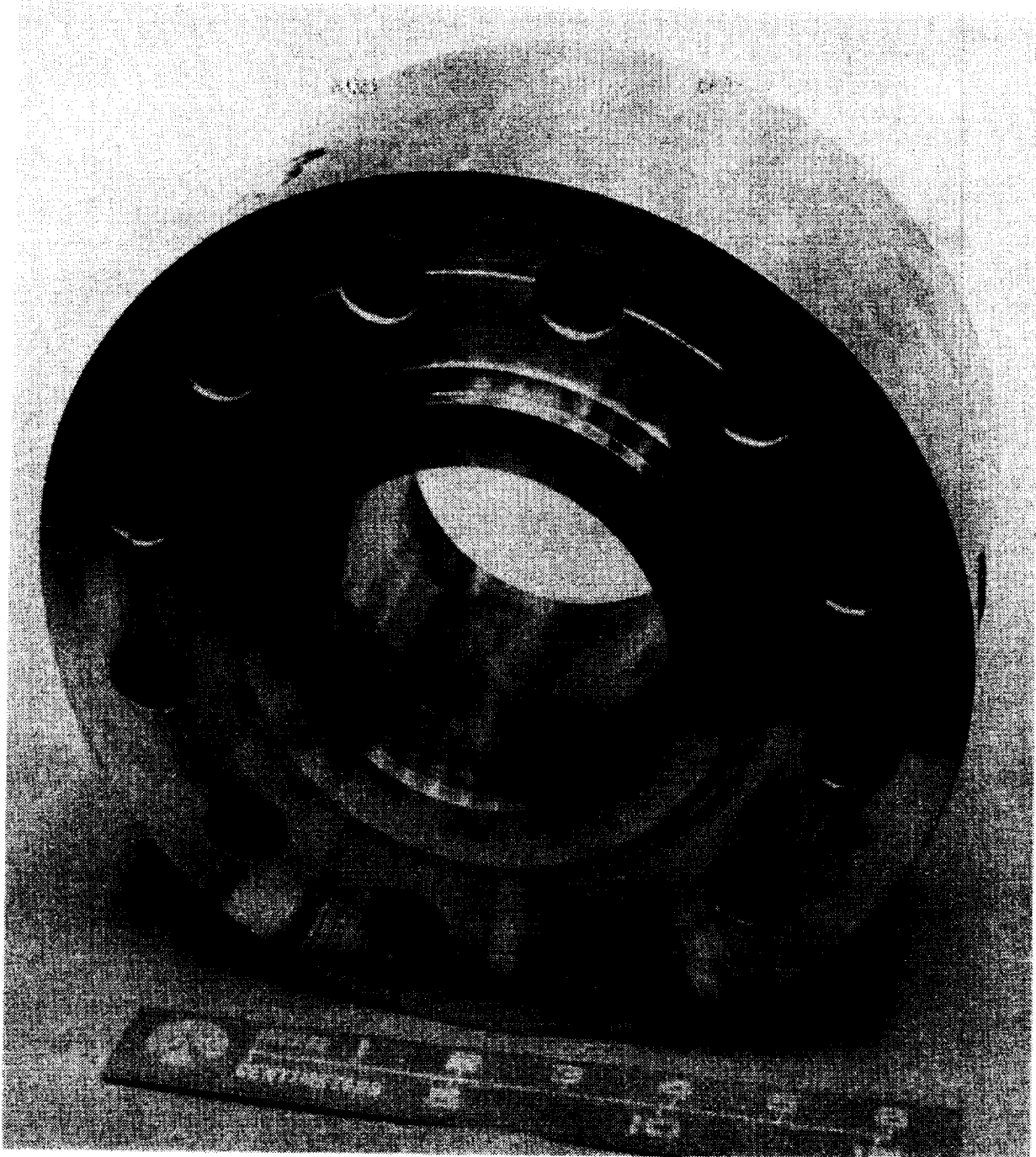
DRAWING NO.	TITLE	FIGURE
AP80-095	COMBUSTION CHAMBERS, 40K PREBURNER	71, 72
AP80-096	FUEL/OXIDIZER MANIFOLD, ASSEMBLY OF	73
AP80-097	NOZZLES, 40K PREBURNER	74
AP80-098	IGNITER - 40K PREBURNER, ASSEMBLY OF	75
AP80-099	PRESSURE TEST FIXTURE, 40K PREBURNER	76
AP80-100	OXIDIZER/FUEL DOME, 40K PREBURNER	77
AP80-102	INJECTOR, ASSEMBLY LOX/RP-1 PREBURNER (TRIPLET, FUEL-RICH)	78
AP80-103	INJECTOR, ASSEMBLY LOX/CH ₄ PREBURNER (COAXIAL, FUEL-RICH)	79
AP80-105	INJECTOR, ASSEMBLY LOX/CH ₄ PREBURNER (PENTAD, LOX-RICH)	80
AP80-106L	LAYOUT, 40K PREBURNER ASSEMBLY	--
AP80-107	ASSEMBLY, 40K PREBURNER	81
AP80-108	ACOUSTIC CAVITY/BLANK RING, 40K PREBURNER	82
AP80-109	STUD AND WASHER, 40K PREBURNER	--

A coaxial LOX/CH₄(g) injector, an unlike-triplet LOX/RP-1 injector, and a pentad oxidizer-rich LOX/CH₄ injector were designed for the 40K preburner program. The subscale hot-fire triplet injector specified Helmholtz-type acoustic cavities as the combustion stability aid. The item is provisional for the other two injectors. A design which is suitable for the triplet injector was made based on the damping effectiveness analysis.



1XZ25-2/17/81-C1D

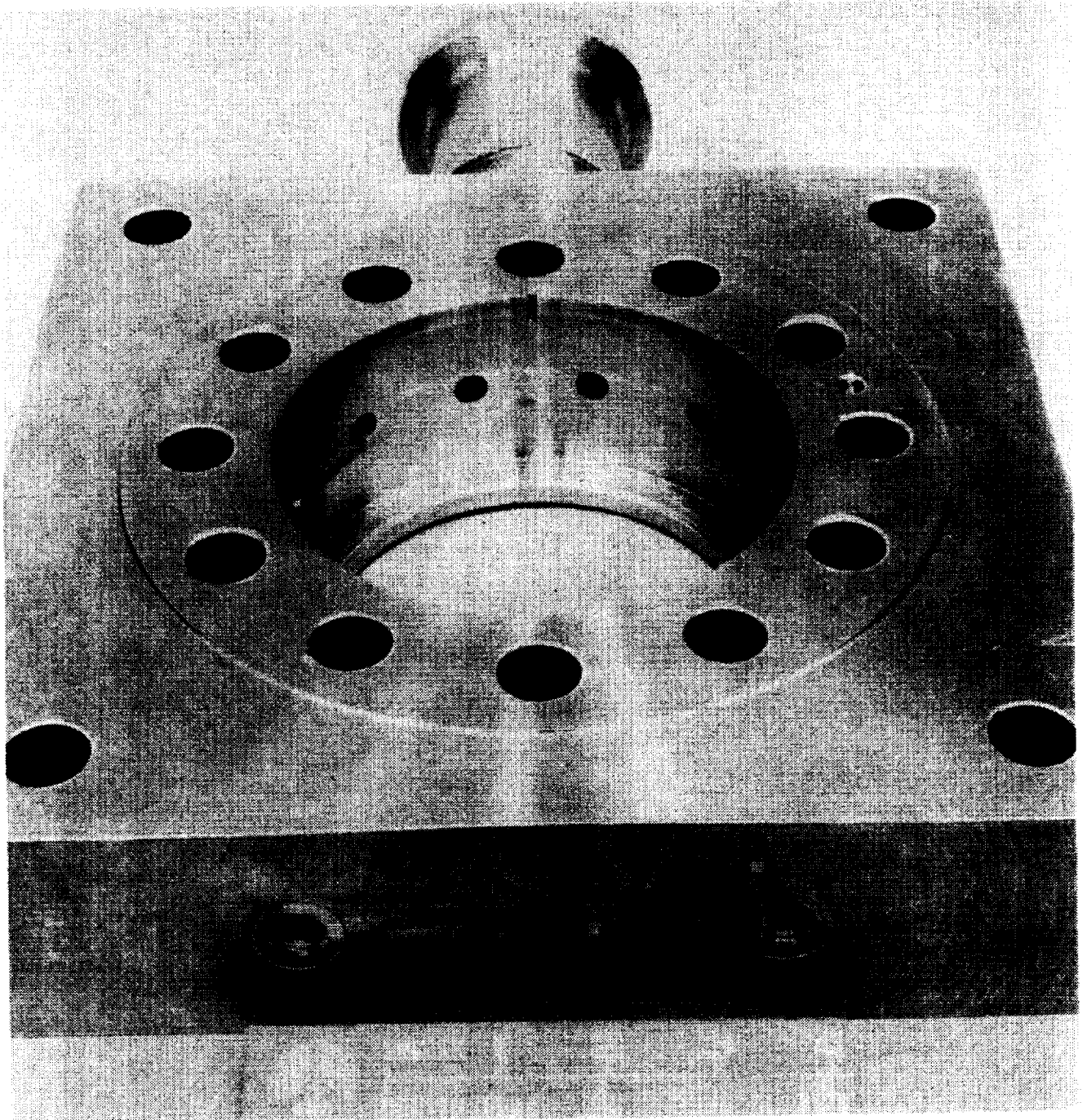
Figure 71. 12-Inch Combustion Chamber Section



1XZ25-2/17/81-C1L

Figure 72. 4-Inch Combustion Chamber Section

ORIGINAL PAGE IS
OF POOR QUALITY



1XZ25-2/17/81-C1K

Figure 73. Propellant Manifold - Fuel/Oxidizer

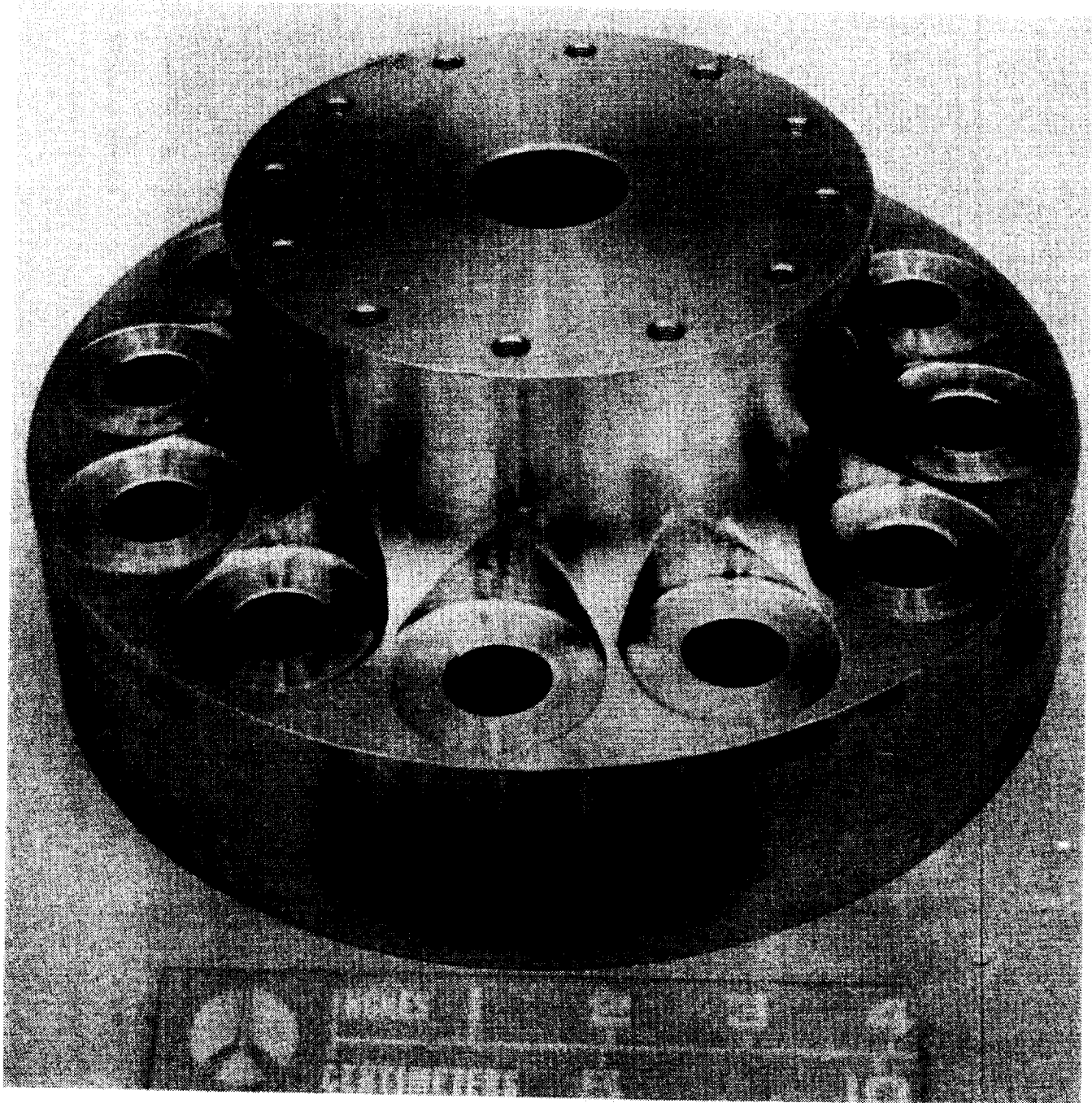


Figure 74. Nozzle

LXZ25-2/1/81-C1I

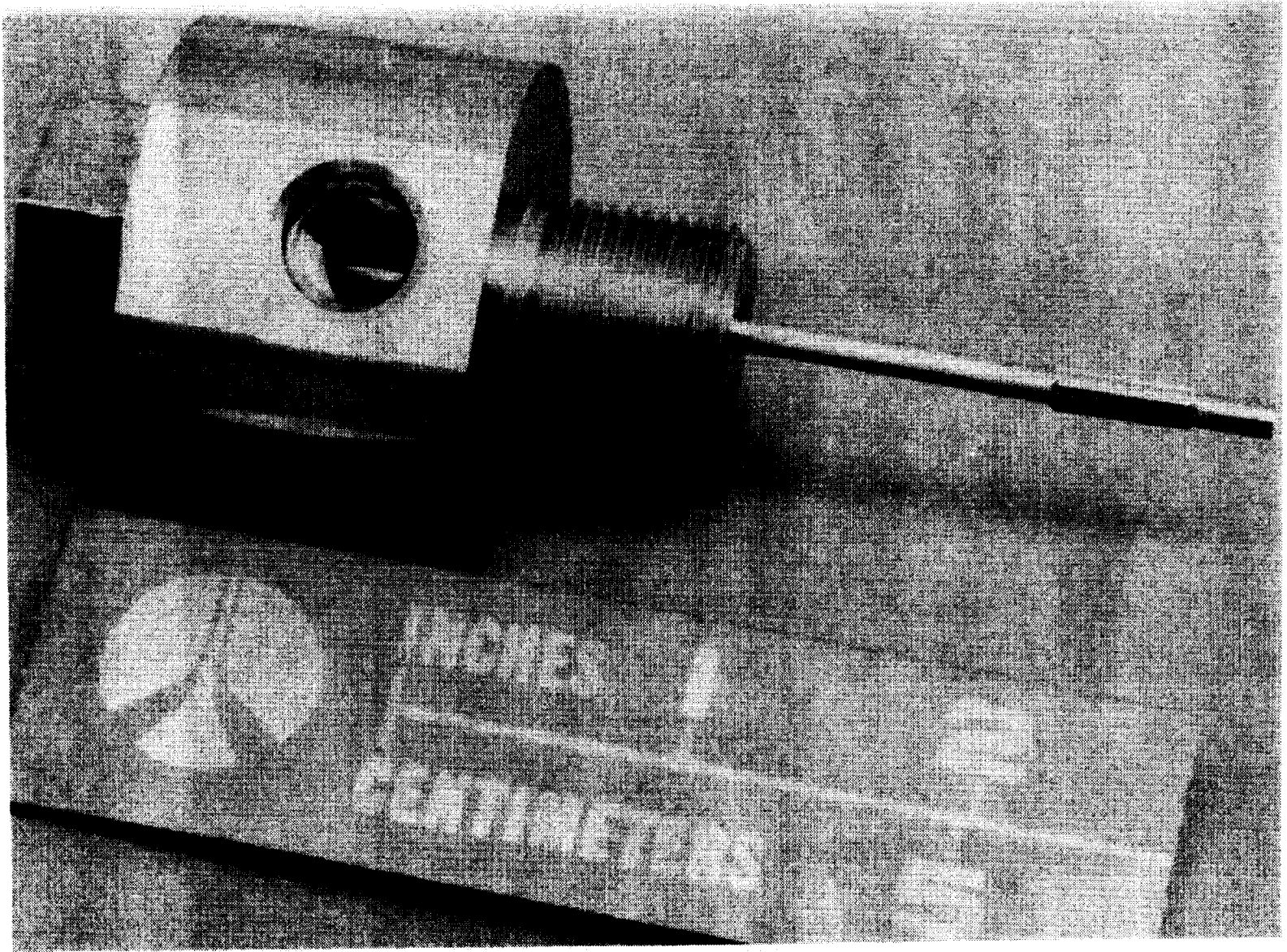


Figure 75. Igniter Assembly

LXZ25-2/17/81-C1Q

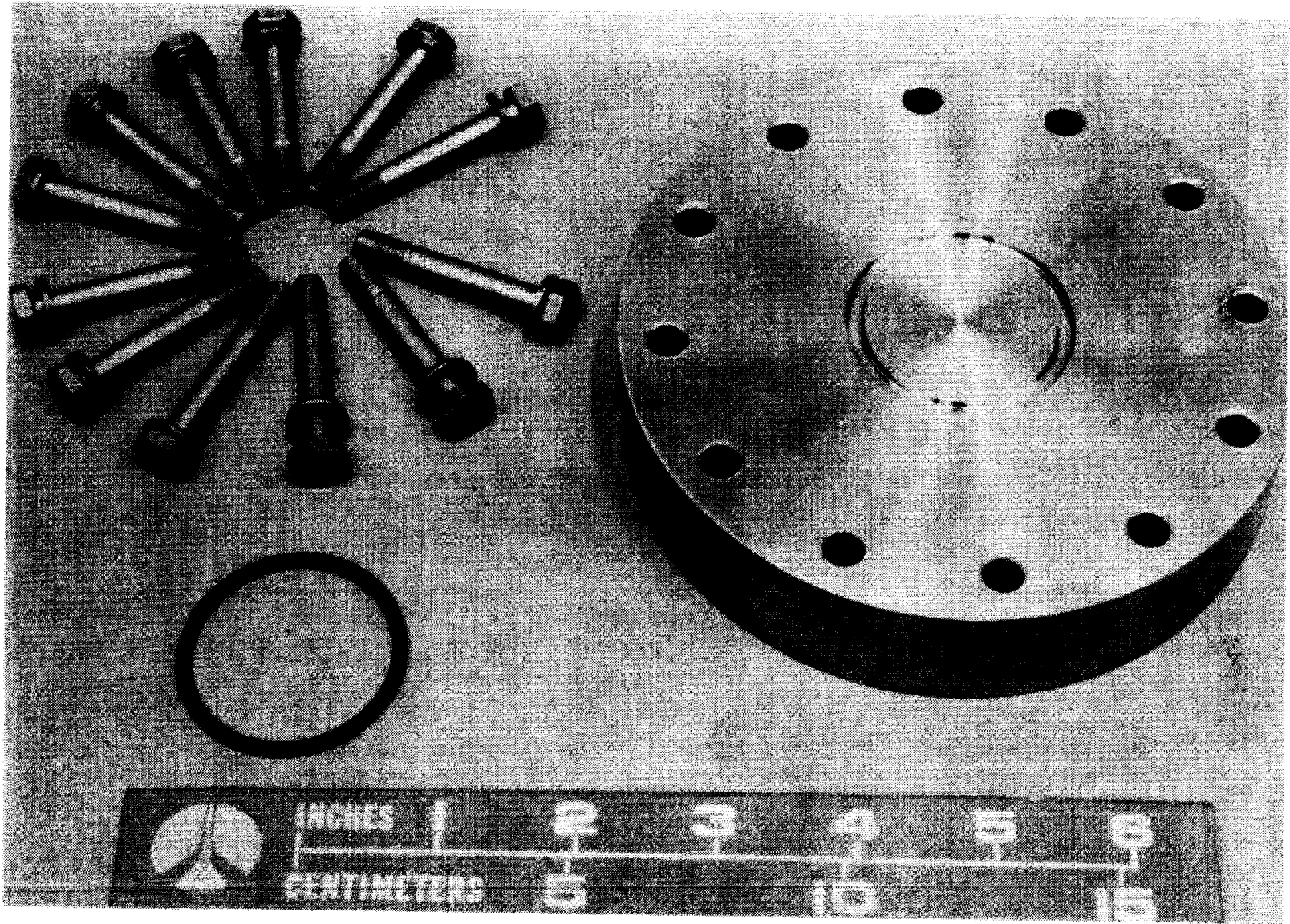


Figure 76. Pressure Test Plate

1XZ25-2/17/81-C1J

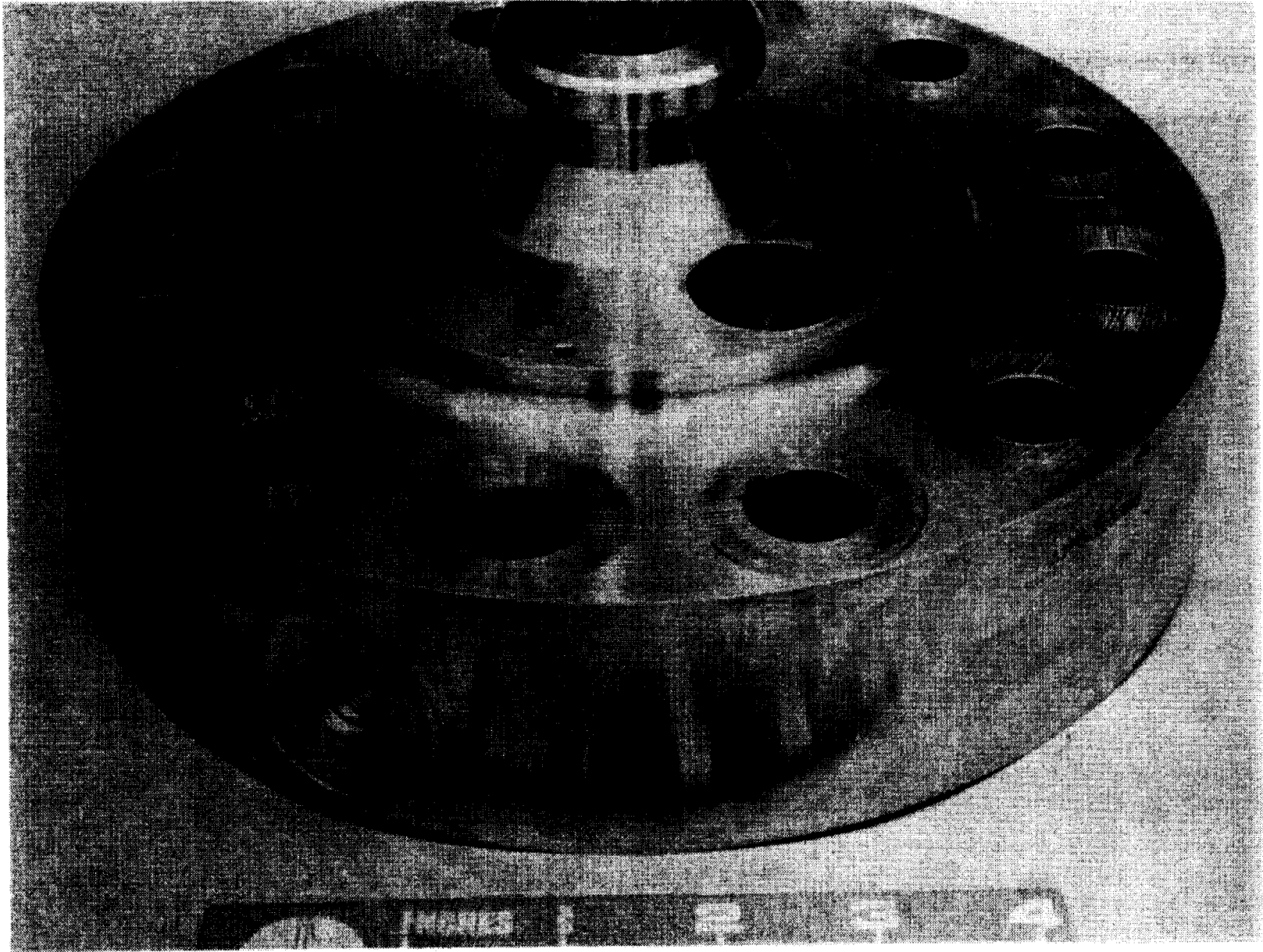
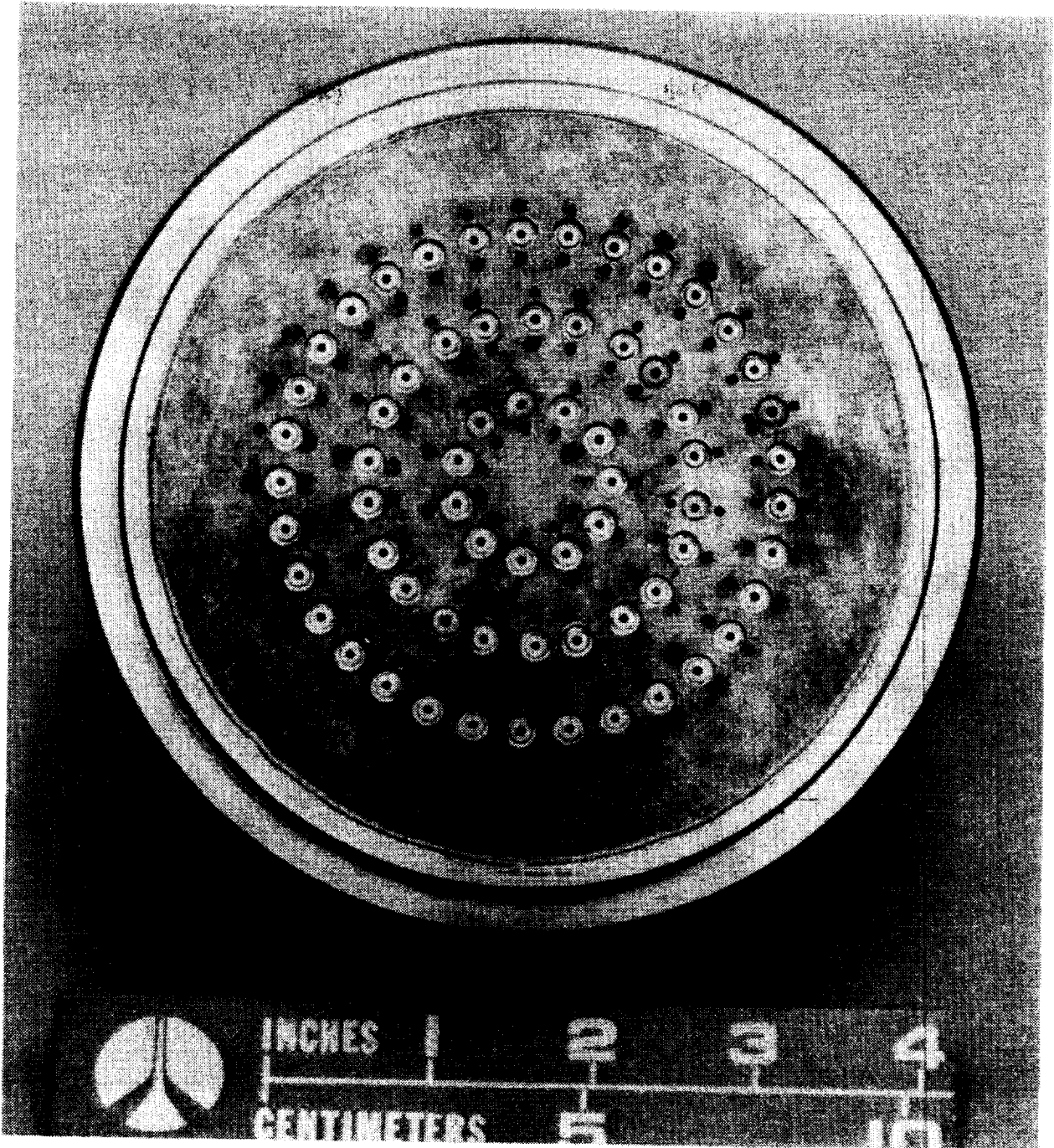


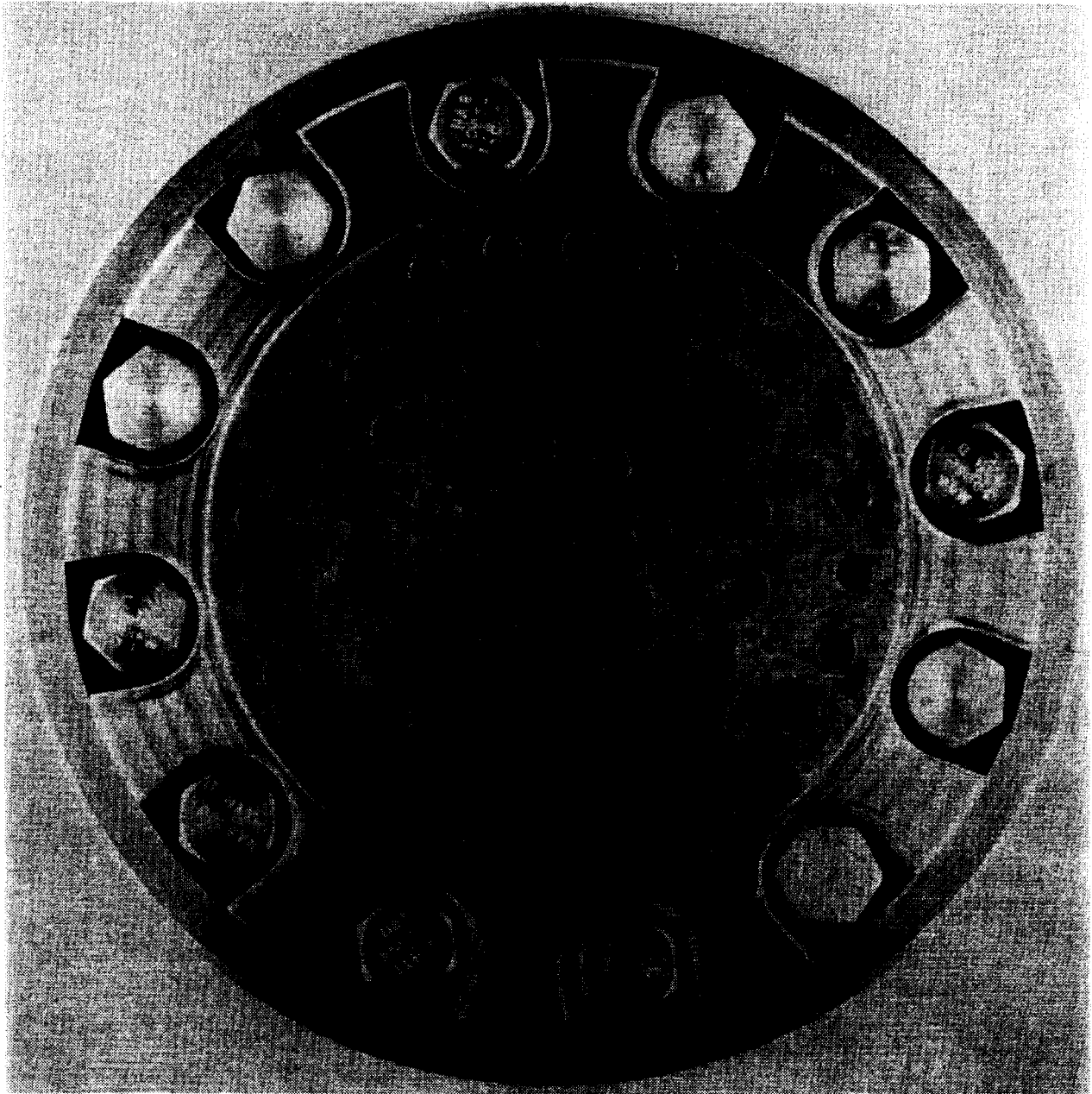
Figure 77. Propellant Dome - Fuel/Oxidizer

LXZ25-2/17/81-C1M



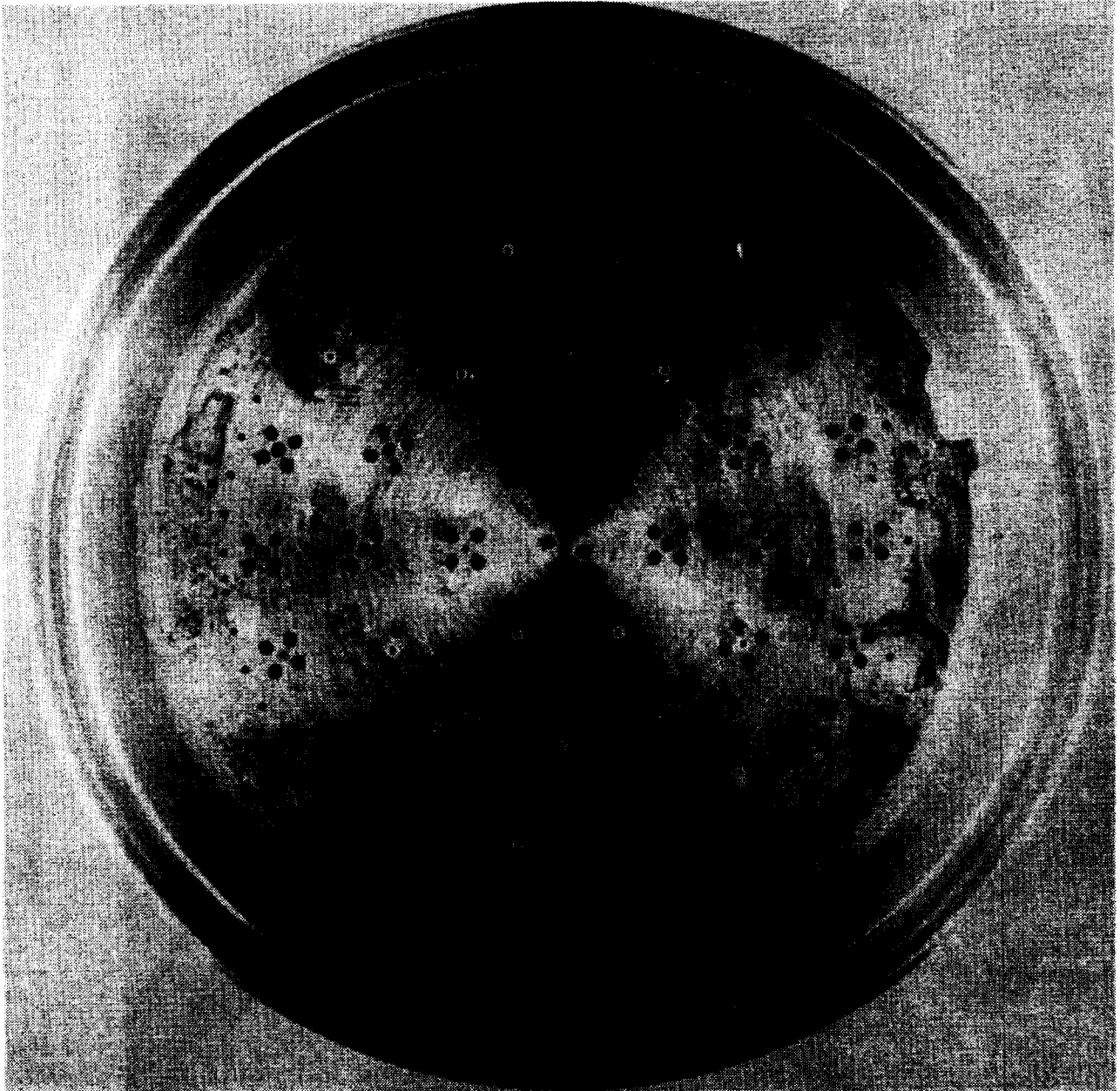
1X225-2/17/81-C1H

Figure 78. Fuel-Rich LOX/RP-1 Triplet Injector



1XZ41-3/6/81-CLD

Figure 79. Fuel-Rich LOX/CH₄ Coaxial Injector



LXZ41-3/6/81-C1C

Figure 80. Oxidizer-Rich LOX/CH₄ Pentad Injector

ORIGINAL PAGE IS
OF POOR QUALITY

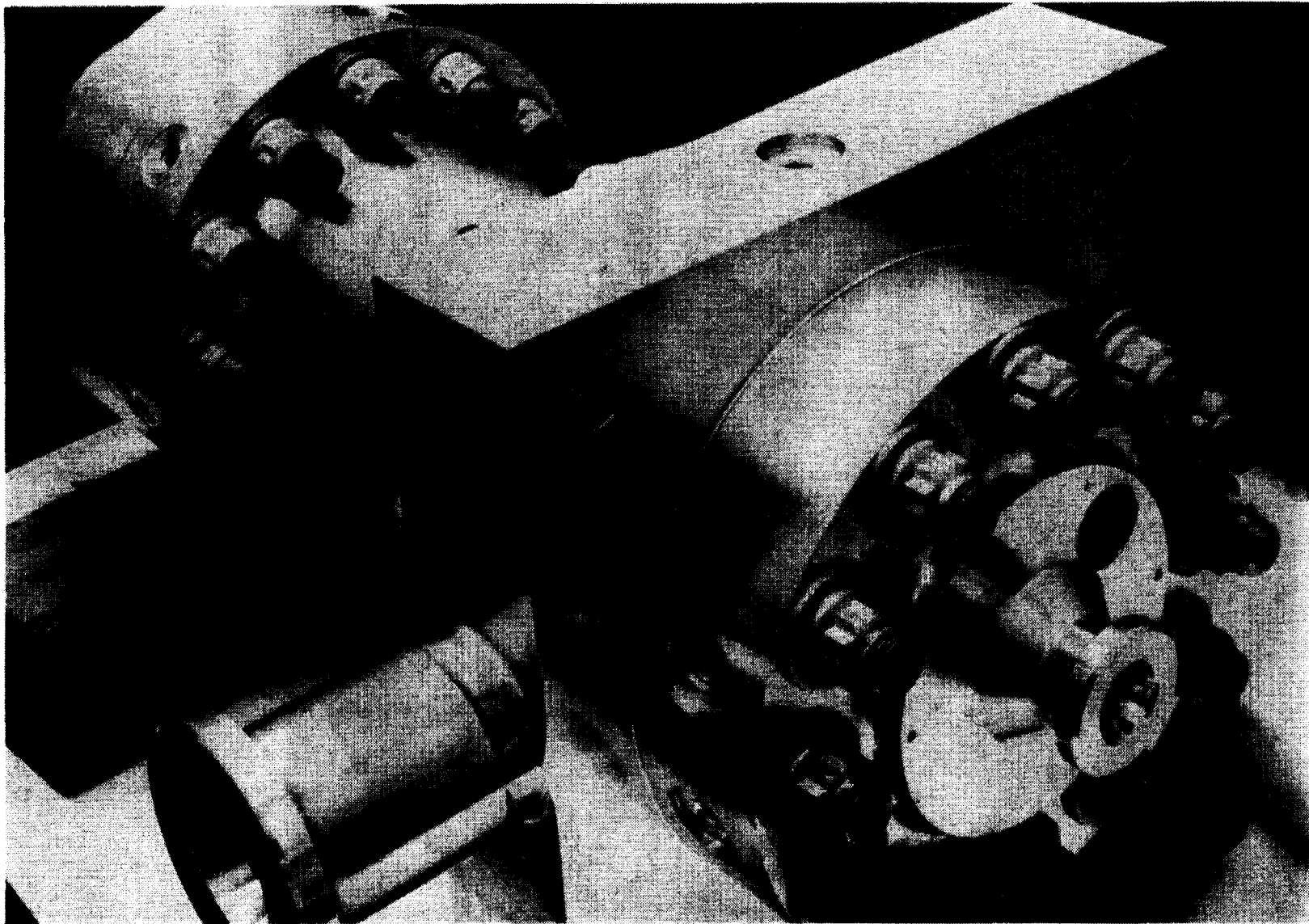
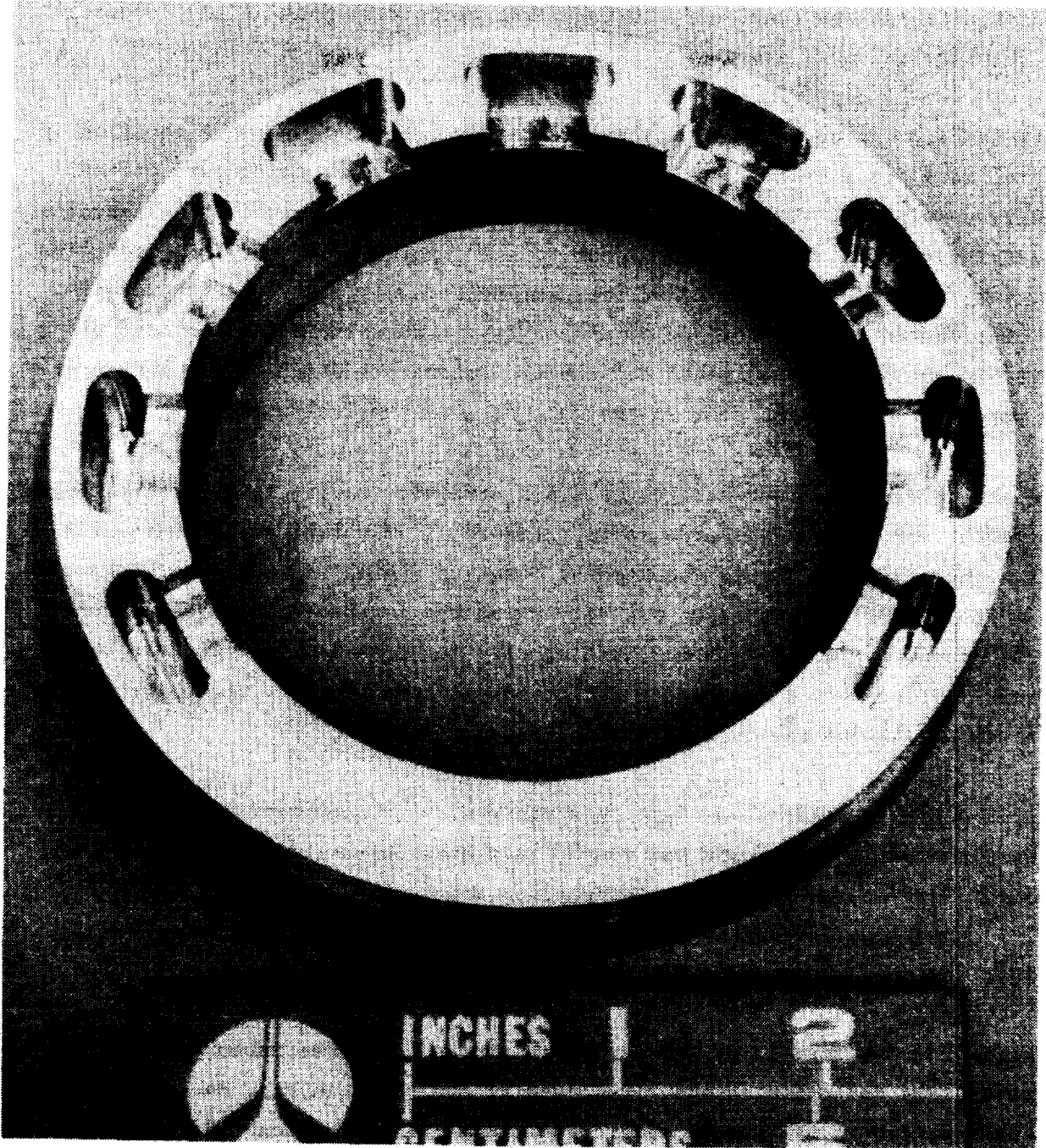


Figure 81. Preburner Assembly

1XZ25-2/17/81-C1A



1XZ25-2/17/81-C1R

Figure 82. LOX/RP-1 Acoustic Cavity

The cavity design was tuned only to the first tangential mode as this acoustic mode requires the most damping.

Cavity damping can be estimated by approximate solution of the wave equation in integral form for a cylindrical chamber with the cavity becoming part of the boundary conditions. The solution contains the complex frequency or eigenvalue. The damping coefficient is proportional to the imaginary part of the eigenvalue. Thus, the results really represent the damping or oscillatory energy dissipation contributed by the presence of the cavity. The formulation has been programmed to analyze a two-dimensional cavity (resonator) which can be interpreted as a partitioned straight slot in the wall of a cylindrical chamber.

There are in essence, four design variables studied: cavity length, slit length, slit width, and cavity/slit area ratio. Figure 83 illustrates the four parameters. The cavity open area requirement based on engine history determines the slit width. Currently, an open area of 10% of the injector face area is considered adequate. A value of 0.2 inch is used for the slit width. More open area will effectively decrease the cavity-to-slit area ratio. The upper design limit was a 1/4-wave cavity with narrow band damping.

The slit depth in general was kept to a minimum. For geometrically similar designs, the small slit depth can result in a more compact design with optimum damping. However, the thermal consideration imposed a limit as it determined the wall thickness for the L-shaped cavity. A value of 0.2 inch was selected for this purpose.

The remaining two variables, the cavity length and the area ratio, then become the parameters for optimization. The results are shown in Fig. 84. Insignificant differences in maximum damping coefficient existed between the two area ratios. Therefore, the smaller ARAT value (5.5) was chosen for the design. This selection minimized the impact on the performance due to the stability device.

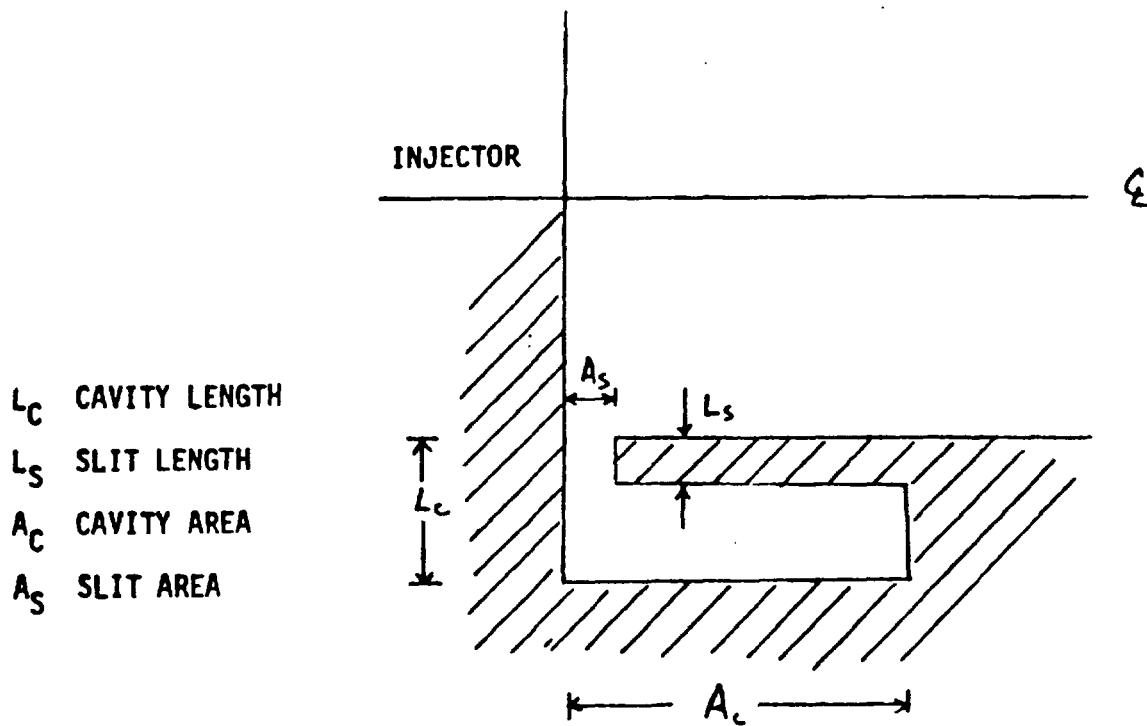


Figure 83. L-Shaped Acoustic Cavity

The damping characteristics for the two fuel-rich injectors were very similar. They differ only by the magnitude of the damping coefficient. If required, a single design could be utilized for both injectors.

The damping effectiveness from the analysis was limited to the damping contributed by the cavities alone. The stability characteristics are drastically different for the two combustion processes. The cavity design and the analysis provide a measure of the temporal damping, if the first tangential mode does occur, and is independent of the combustion processes.

Using this analysis, the acoustic cavity designed is illustrated in AP80-108. This drawing also shows the blank rings which are used in place of the acoustic cavity ring.

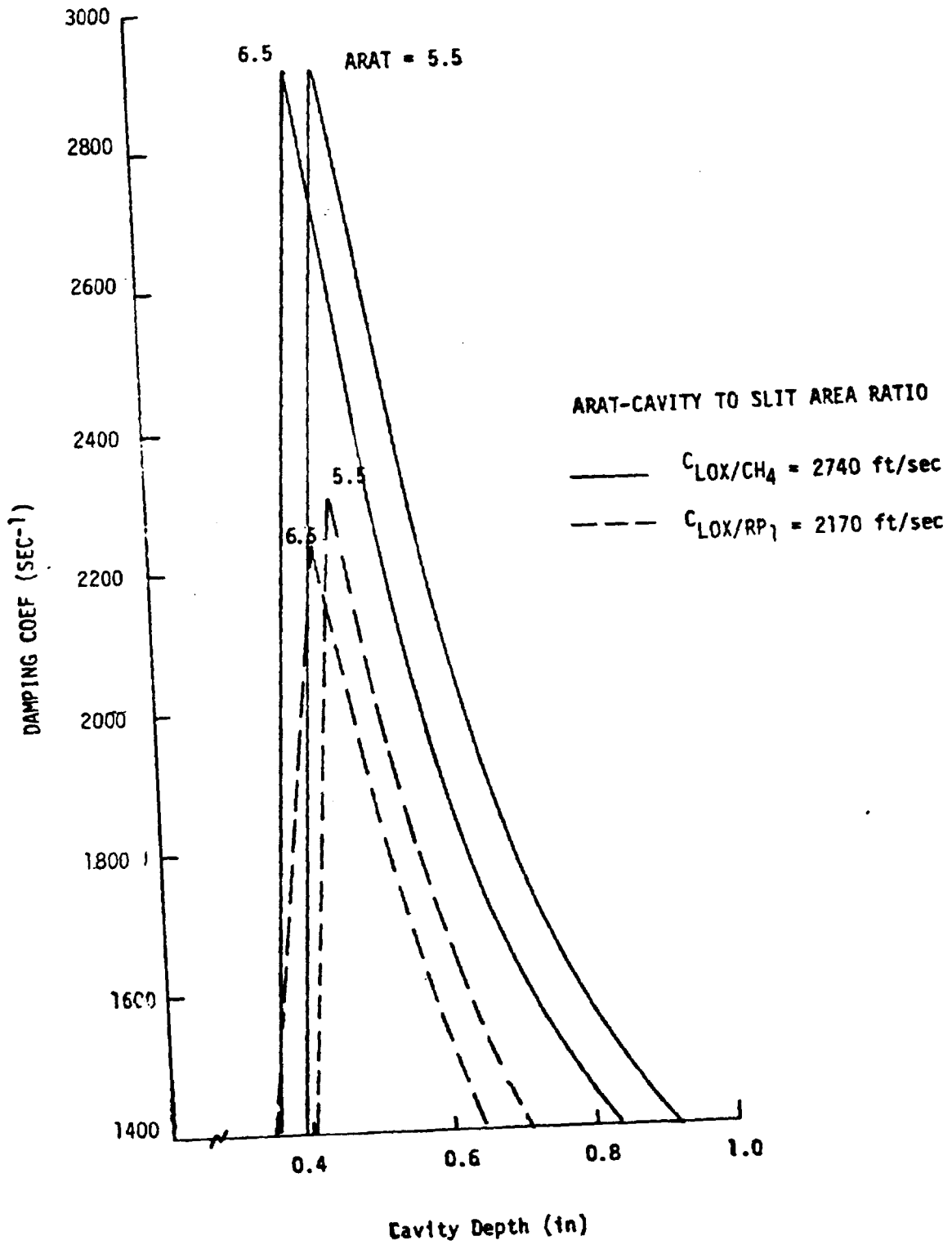


Figure 84. Cavity Design Damping Coefficient

Subtask 05200 - Fabrication

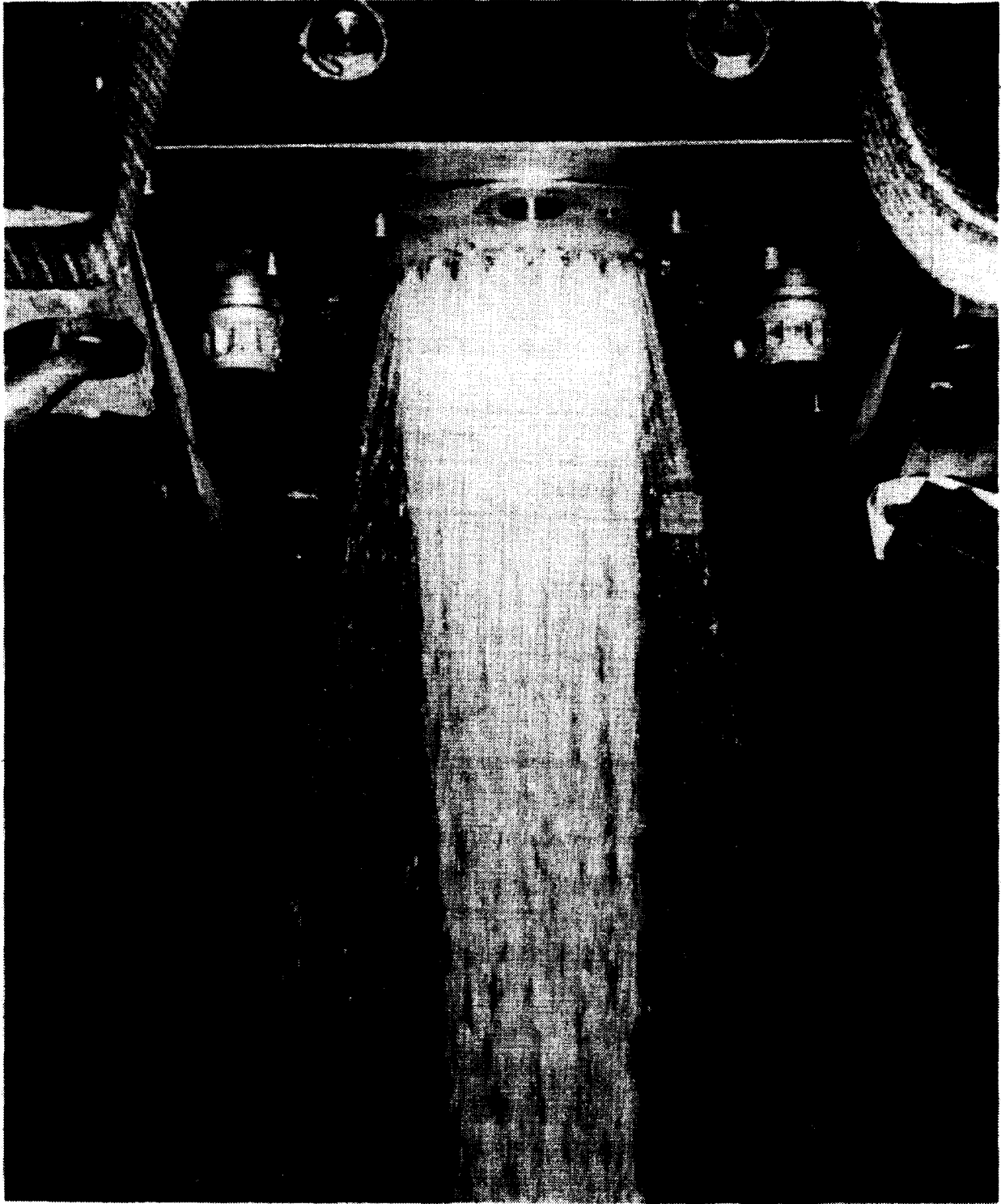
The two fuel-rich preburner assemblies (LOX/CH₄ and LOX/RP-1) and one oxidizer-rich preburner assembly (LOX/CH₄) have been fabricated. On completion of fabrication, the injector assemblies were cold-flow calibrated using the combustor and a nozzle restriction as a back-pressure device. The resultant flow C_DA's are presented in Table 26.

TABLE 26. FLOW COEFFICIENTS

	Injector		
	Coaxial	Triplet	Pentad
C _D A Average			
Fuel	0.31237	0.23297	0.01811
Oxidizer	0.06770	0.09368	0.33697

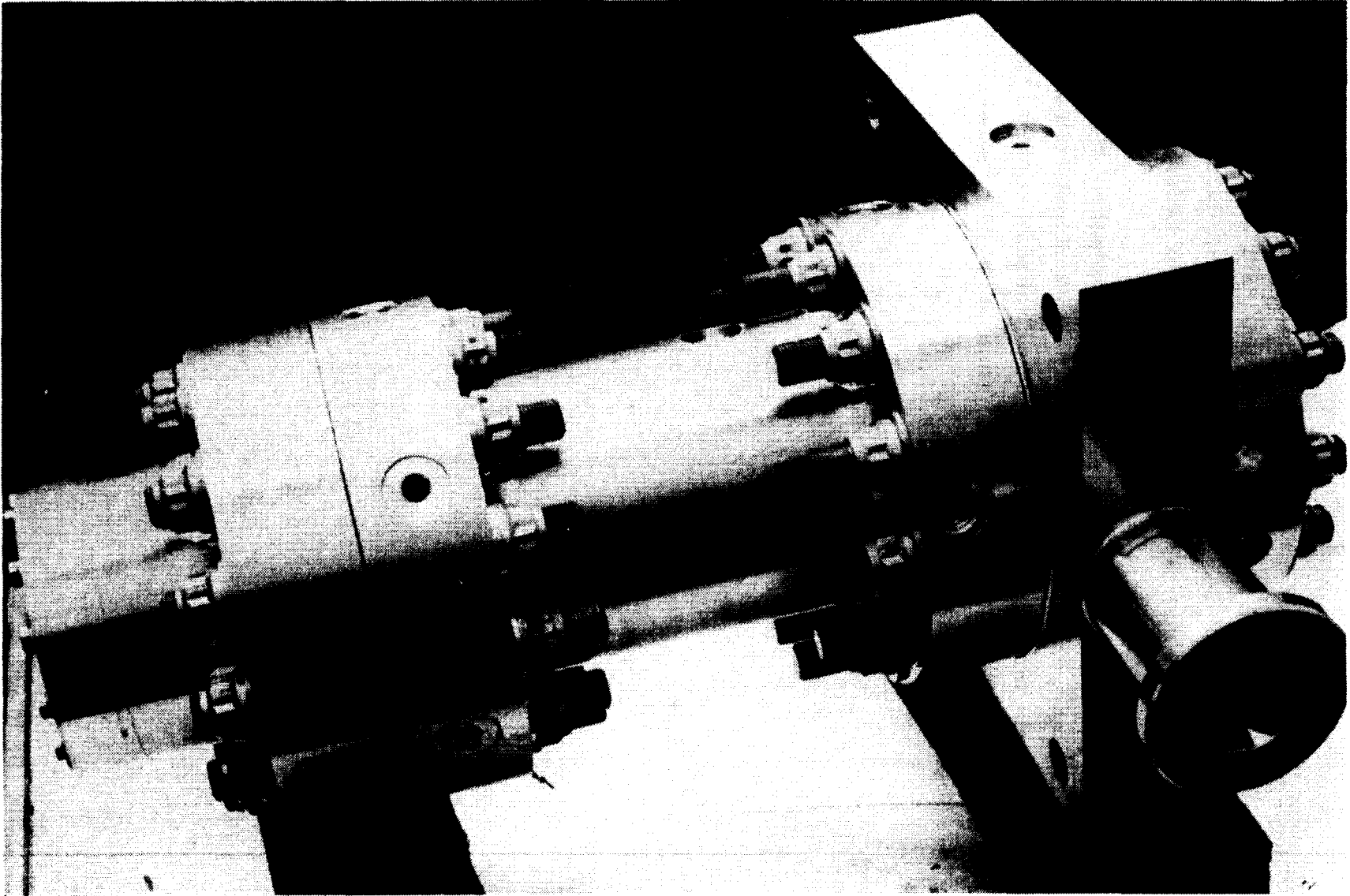
The coax injector oxidizer elements were sampled randomly and the flow results showed a maximum element deviation of ±5%. In the case of other injectors it was not feasible to determine or obtain an individual element sample. Figure 85 illustrates an open-face flow check of the pentad injector conducted to observe the symmetry of the flow pattern and the uniformity and wall protection offered by the film coolant holes shown in the figure.

On completion of the flow sampling, the preburner assembly illustrated in Fig. 86 was subjected to a proof test. The proof test consisted of 5 cycles of 6300 psi for 30 seconds at each plateau. The completion of this requirement demonstrated the satisfactory structural integrity of the assembly for use in hot fire at the 3500-psi chamber pressures scheduled. The minimum safety factors of the individual components were itemized in a previous section.



1XZ41-3/6/81-C1G

Figure 85. Oxidizer-Rich Pentad Cold Flow



1XZ25-2/17/81-C1C

Figure 86. Preburner Assembly Pressure Check

Figure 87 shows the preburner assembly in the final assembled condition. Outward appearance of this hardware is similar to the original SSME 40K LOX/LH₂ preburner assembly. This configuration was designed externally to fit the interfaces previously determined for the NASA/MSFC hot-fire test position on stand 116.

Figures 88 and 89 show the LOX/RP-1, fuel-rich triplet injector. Figure 19 illustrates the LOX dome seal areas, a redundant seal with an external vent line separating the two seals. This assembly was designed to minimize injector costs and to simplify rework/replacement. The injector insert slips into the manifold assembly, sealing axially with two seals.

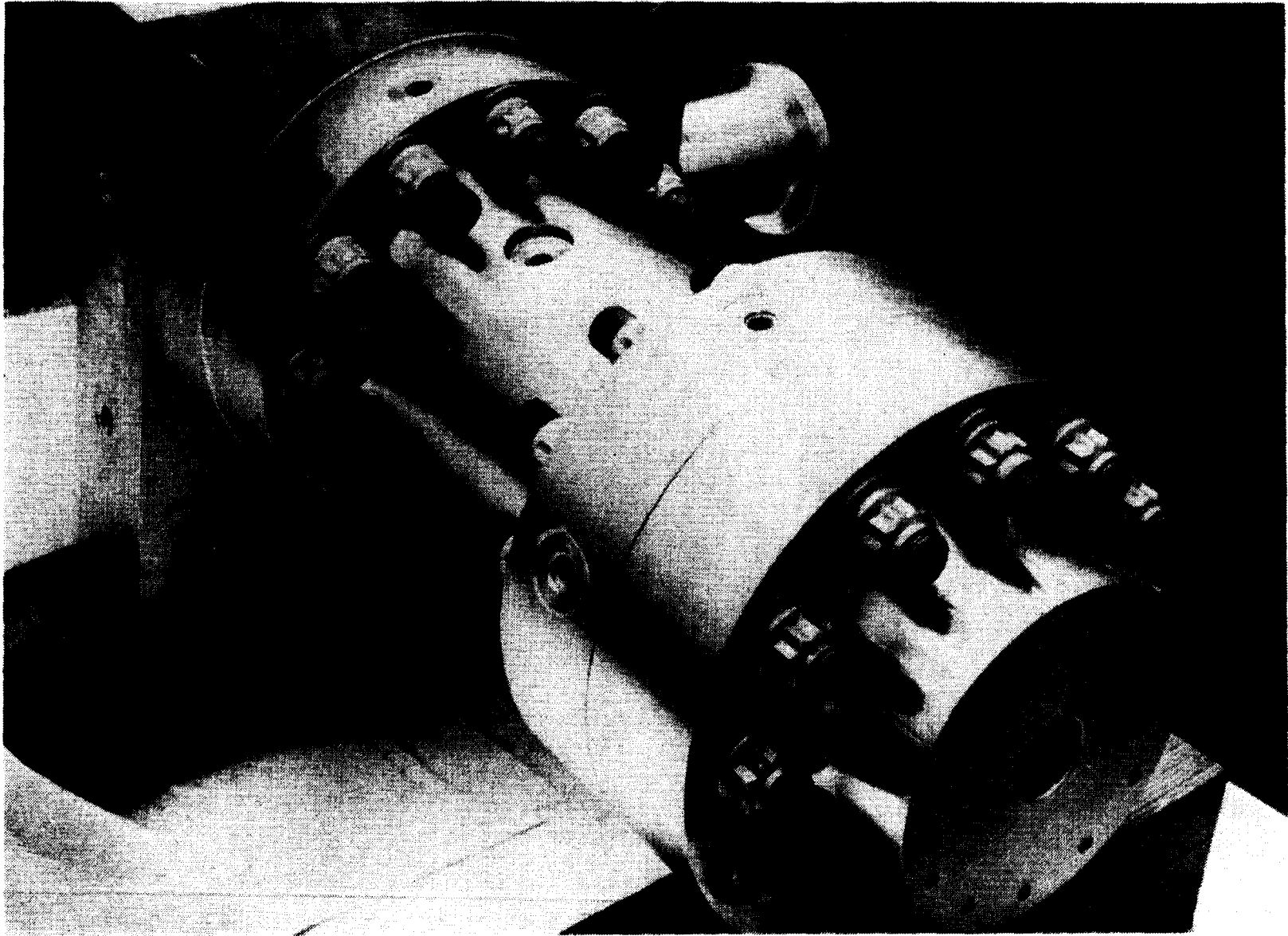
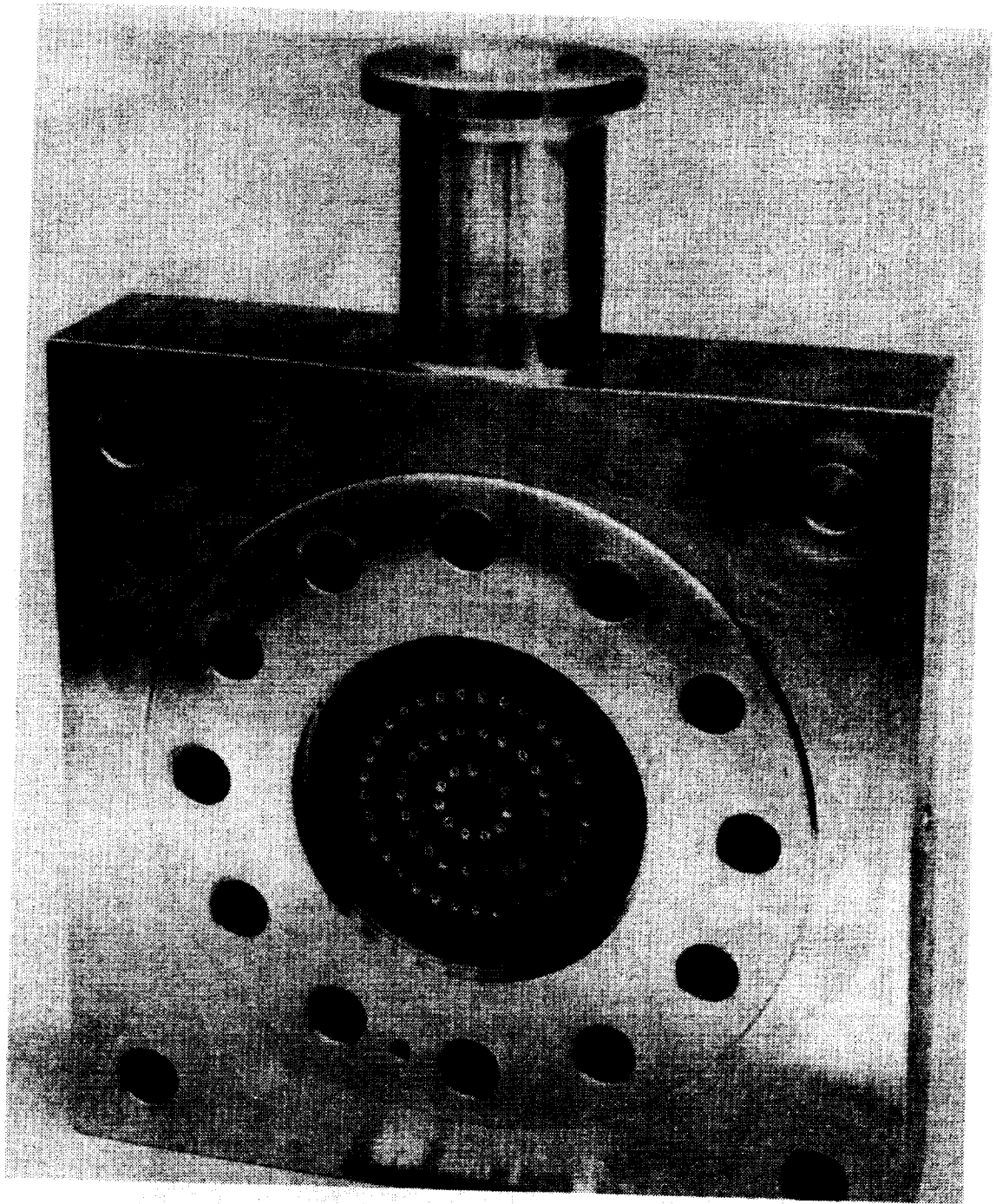


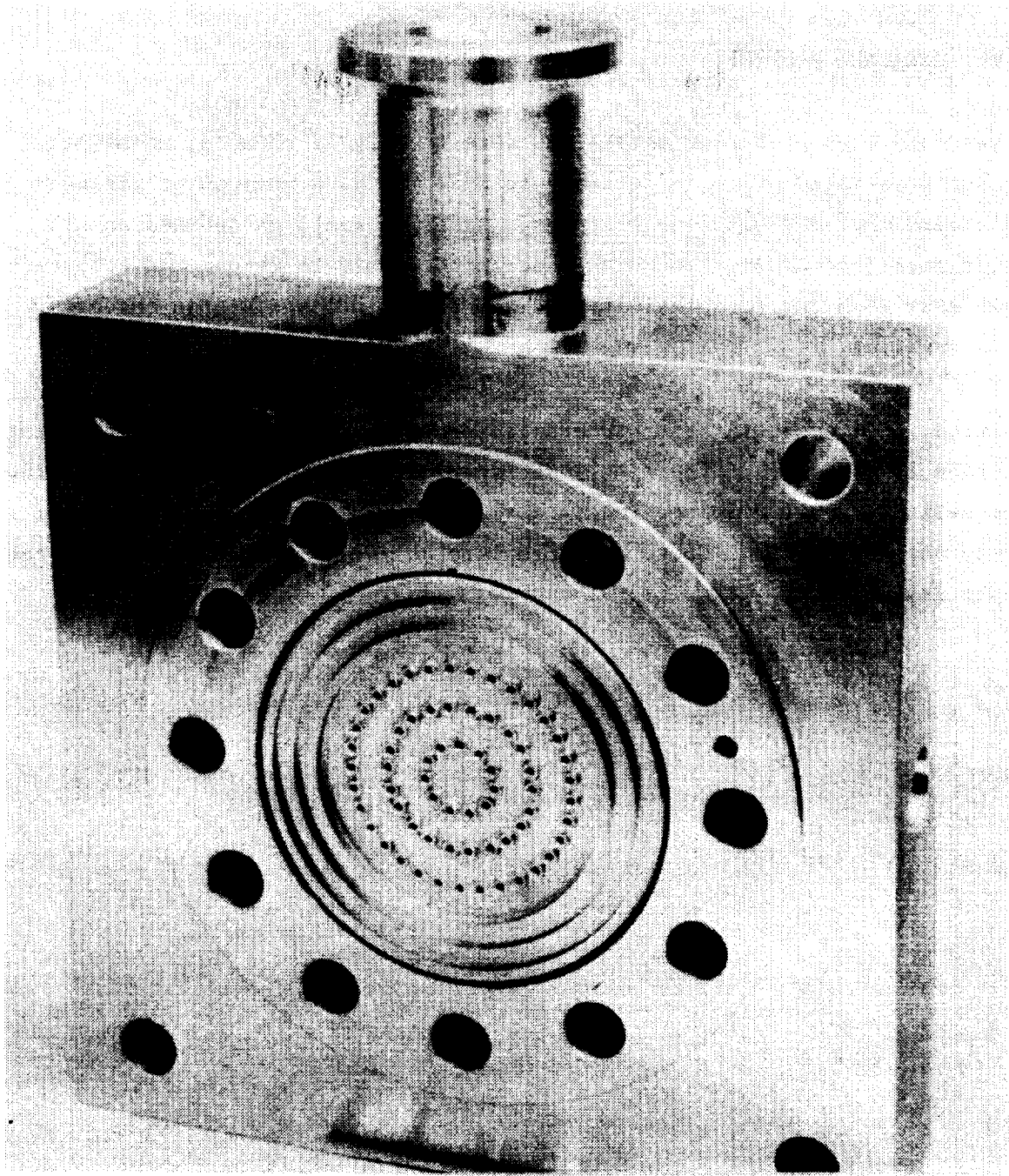
Figure 87. Preburner Assembly

1XZ25-2/17/81-C1B



1XZ25-2/17/81-C10

Figure 88. Triplet Injector/Fuel Manifold Assembly



1XZ25-2/17/81-C1P

Figure 89. Rear View - Triplet Injector Assembly

ORIGINAL PAGE IS
OF POOR QUALITY

TASK VI: HARDWARE DELIVERY

The three completed preburner assemblies were thoroughly cleaned, inspected, and properly packaged prior to delivery to NASA/MSFC. A minimum of six sets of seals were included with the shipment. A set of seals is defined as all preburner interface connections or all seals necessary to remove and replace the preburner from the test facility and any seals included within the preburner assemblies.

In addition, five complete sets of detailed drawings were furnished, including one reproducible master of the final preburner design. A complete set of drawings is defined as all drawings required and produced for the fabrication of the preburner assemblies. These drawings were delivered to NASA/MSFC with the preburner assemblies.